ROLE OF mTOR IN SALIVARY GLAND ATROPHY AND REGENERATION

Bozorgi, Sophie Shaghayegh

Awarding institution:
King's College London

ROLE OF mTOR IN SALIVARY GLAND ATROPHY AND REGENERATION

Thesis submitted for degree of
DOCTOR OF PHILOSOPHY
By

SOPHIE SHAGHAYEGH BOZORGI

SEPTEMBER 2015

Supervisors: Dr Guy Carpenter & Prof Gordon Proctor

ABSTRACT

The mammalian target of rapamycin (mTOR) is a protein kinase whose dysfunction has been identified in many diseases ranging from cancer to Down's syndrome. Previous studies have examined salivary gland atrophy and observed the submandibular gland's ability to regenerate from atrophy, however the mechanism underlying this process is still unknown. The current study aims to investigate the effects of blocking mTOR signaling in atrophic salivary glands and blocking mTOR signalling in submandibular glands regenerating from atrophy.

The first part of the study revealed that inhibition of mTOR delays ligation-induced atrophy of salivary glands and that furthermore, mTOR could only be inhibited for shorter periods of 3 days, whereas 5 or 7 days of ligation and rapamycin treatment cause glands to re-express active mTOR and show considerable signs of atrophy.

The second part of the study aimed to find out the reasoning behind the reactivation of mTOR following 5 or 7 days, despite the presence of mTOR inhibitors. It concluded that 2nd generation mTOR inhibitors also failed to block mTOR activation following 7 days of atrophy. Proteomic

and microarray analysis were performed and gave rise to possible future enquiries.

This study then exposed the role of mTOR in salivary gland regeneration following atrophy, revealing that mTORC1, specifically its substrates, are needed for a full regeneration. Inhibiting mTOR during periods of atrophy and allowing phosphorylation of mTORC1 substrates during periods of regeneration, is a treatment method which could be of importance.

The final part of the study observed samples of atrophic human salivary glands in order to find evidence of aberrant mTOR activity. It caused three realisations, firstly that mTOR is one of the driving forces of atrophic processes as once atrophy is severe, most acinar cells are lost and mTOR is no longer as active. Secondly, that autophagy coincides with salivary gland atrophy in humans. And thirdly, that some salivary gland functions might possibly be intrinsically linked to ageing.

This leads to the suggestion that the future of treating salivary gland atrophy in humans could lie in using mTOR inhibitors, whether they be localised treatment in the form of intraductal injection of rapamycin

loaded nanoparticles to get localised targeting whilst reducing whole body toxicity or in the form of combination therapies that combine mTOR inhbitiors with the addition of another drug that inhibits autophagy and counteracts any toxic effects of mTOR inhibition.

ACKNOWLEDGEMENTS

First and foremost, my heartfelt gratitude goes to my first supervisor Dr Guy Carpenter for guiding me throughout my doctorate. I am most grateful for the opportunities you have given me, the inspiration you provided as well as your unfailing and unconditional counsel, encouragement and support. My sincere thanks also go to my second supervisor, Prof Gordon Proctor, for his enriching advice, help and support throughout my time at King's College.

My sincere gratitude to my postgraduate coordinator, Prof Lucy Di Silvio, for her unceasing support, encouragement and friendship, always extended especially when I needed it the most. I would also like to thank all the members of the Salivary Research Lab. You have all made my time at King's College enriching, inspiring and truly memorable, as well as enabling me to make lifelong friends!

Last but not least, I would like to thank my family, my mum, dad and sister, for their patience, love and their belief in me. Finally a special thanks to my brother Alborz, without whom the stars would fade.

PUBLICATIONS AND PRESENTATIONS

Peer-reviewed journal publications:

- Bozorgi, S. S., Proctor, G. B. & Carpenter, G. H., (2014). Rapamycin Delays Salivary Gland Atrophy Following Ductal Ligation. Cell Death & Disease. Volume 5, issue 3. doi:10.1038/cddis.2014.108

Conference presentations:

- Evidence of mTOR Activity During Human Salivary Gland Atrophy. IADR/AADR/CADR General Session. International Association for Dental Resarch, Boston (2015).

- Persistence of mTOR Activity Despite *in vivo* Rapamycin Application. Talks about TORCs. Biochemical Society, London (2013).

- Role of mTOR in Salivary Gland Atrophy. 15th Annual Dental Institute Postgraduate Research Day. King's College London, London (2013).

- mTOR and Salivary Gland Atrophy. King's-Taiwan Workshop on Stem Cell and Cancer Research. King's College London, London (2012).

- mTOR Mediates Salivary Acinar, but not Ductal, Atrophy during Ligation. PER/IADR Congress. International Association for Dental Resarch, Helsinki (2012).

- mTOR Mediates Salivary Gland Atrophy. 3rd International Congress on Salivary Gland Diseases. International Sialendoscopy Society, Geneva (2012).

TABLE OF CONTENTS

TABLE OF FIGURES

TABLE OF TABLES

TABLES OF ABBREVIATIONS

4E-BP1	Eukaryotic Translation Initiation Factor 4e–Bi3nding Protein 1
AB/PAS	Alcian Blue/Periodic Acid-Schiff's
ANOVA	Analysis Of Variance
ATG3	Autophagocytosis Associated Protein 3
ATG5	Autophagocytosis Associated Protein 5
BEZ	Nvp-Bez235
CA VI	Carbonic Anhydrase VI
CQ	Chloroquine
DMAB	Para-Dimethylaminobenzaldehyde
DTT	Dithiothreitol
H&E	Hematoxylin And Eosin
HRP	Horseradish Peroxidase
LC3	Microtubule-Associated Protein 1a/1b-Light Chain 3
mTOR	Mamallian Target Of Rapamycin
mTORC1	Mamallian Target Of Rapamycin Complex 1
mTORC2	Mamallian Target Of Rapamycin Complex 2
OCT	Optimal Cutting Temperature
PAS	Periodic Acid-Schiff's
PBS	Phosphate Buffered Saline
PBS-T	1% Tween With Pbs
PI3K	Phosphatidylinositide 3-Kinase
PIP	Prolactin-Induced Protein
S6K	P70-S6 Kinase 1
S6RP	Ribosomal S6 Kinase 1
SCC	Squamous Cell Carcinoma
SDS-PAGE	Sodium Dodecyl Sulphate – Polyacrylamide Gel Electrophoresis
SS	Sjögren's Syndrome
TBS	Tris Buffered Saline
TBS-T	1% Tween With Tbs
TC1	Transcobalamin I

CHAPTER 1

INTRODUCTION

1.1 Human Salivary Glands

Salivary glands are exocrine glands that secrete saliva into the oral cavity. They are classified into two categories: major and minor. About 90% of total salivary secretion is from the major salivary glands (Brosky, 2007), with most mammals having three paired sets of major salivary glands: the parotid, sublingual and submandibular salivary glands, situated at a distance from the oral mucosa (Figure 1.1).

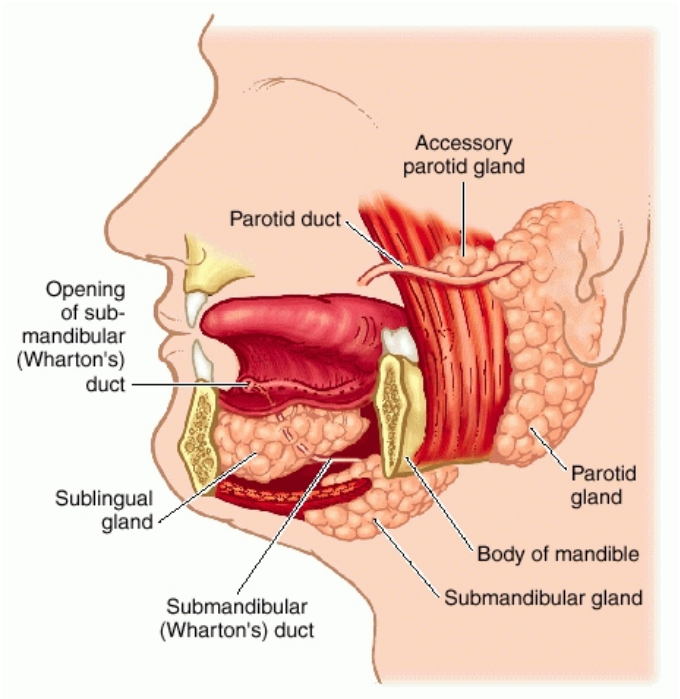

Figure 1.1 The major salivary glands in humans (Dorland, 2007).

1.1.1 Parotid Glands

The parotid glands are the largest salivary glands in humans, weighing around 20 - 30 g and dominating the parotid fascial space. Parotid glands have three major surfaces: the lateral, the anteromedial and the posterior medial, and four borders: the superior, the anterior, the posterior and the medial. In humans, they overlay the mandibular ramus and anterior and inferior to the external ears on each side of the head. Saliva is excreted from the parotid glands via the Stensen's duct into the oral cavity. The Stensen's duct arises from the anterior border and is 4 - 6 cm in length and 5 mm in diameter and opens opposite the second upper molar crown (Myers and Ferris, 2007).

1.1.2 Sublingual Glands

The sublingual glands are the smallest of the three major glands, weighing 2 - 4 g and are situated just deep of the oral muscosa on the floor of the mouth, beneath the tongue, between the mandible and genioglossus muscle.

Unlike the other major glands, sublingual glands have no true fascial capsule and lack a single dominant duct comparable to the other glands.

Instead saliva is excreted via 8 - 20 small excretory ducts, known as the ducts of Rivinus, that depart the superior aspect of the gland and open under the tongue along the sublingual fold. The rest of the small sublingual ducts open into the mouth on the *plica fimbriata*, a mucous membrane formed on either side of the frenulum of the tongue (Darby, 2013).

1.1.3 Submandibular Glands

Submandibular glands are located on the medial surface of the mandible, intermediate to the lower jaws and digastric muscles. The glands weigh half as much as parotid glands, are lobular and compact in shape, with two lobes: the superficial lobe and deep lobe. Submandibular gland saliva is excreted via its main excretory ducts, known as Wharton's ducts, that are approximately 4 – 5 cm long and run from the submandibular papillae across the floor of the mouth to excrete into the oral cavity at the sublingual caruncles.

1.1.4 Minor Salivary Glands

Aside from them, approximately a thousand minor salivary glands, ranging in size from 1 to 5mm, are situated throughout the oral cavity

as well as in the lips, pharynx, nasal cavity and paranasal sinuses (McKenna, 1984). They are classified according to their site into labial, zygomatic, palatine and lingual glands. Minor salivary glands only contribute to a small portion of total salivary secretion (Dawes, 2008). However they are clinically important as they can also be a source for glandular tumours (Hollinshead, 1982).

1.2 Mouse Salivary Glands

In mice, the 3 pairs of major salivary glands are located in the subcutaneous tissue of the ventral neck area and are closely associated (Figure 1.2). In fact, rodent sublingual glands share a common connective tissue with submandibular glands, however this connection is not shared in humans. Mouse parotid glands are not the largest salivary gland, unlike in humans, as they extend from the base of the ears, across the exorbital lacrimal glands and posterior to the clavicle. The sublingual salivary glands are smaller and narrowly associated with the anterolateral surface of the submandibular glands. Mouse submandibular glands are the largest lobulated glands and extend posteriorly to the sternum and clavicle, anteriorly to the hyoid bone and overlap marginally on the median line. These glands are larger and more opaque in male mice than those of females (Raynaud, 1964).

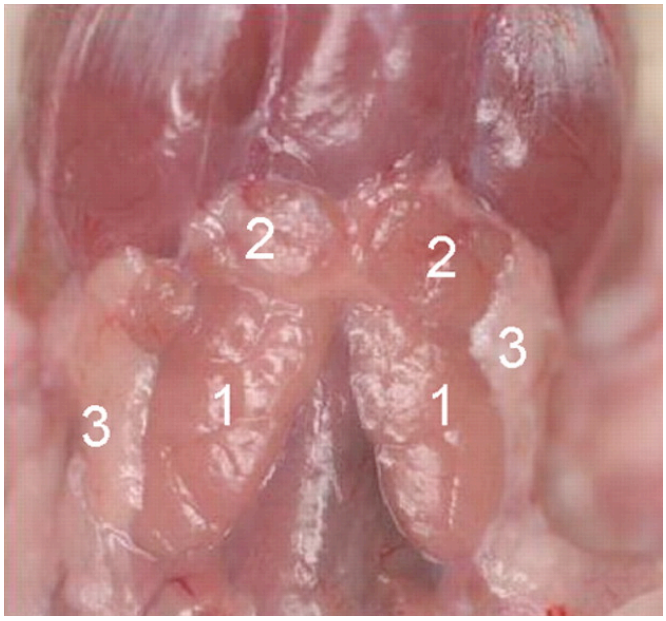

Figure 1.2 A ventral dissection of the neck of rodents
1- Submandibular glands; 2- Sublingual glands; 3- Parotid glands (Pfestroff et al., 2010).

1.3 Human Salivary Gland Micro-Structure

All the major glands encompass parenchymas that consist of the secretory unit along with ducts. Their nerve and blood supply are supported by a connective tissue stroma that divide glands into lobules. The secretory products of the salivary glands (e.g. Secretory IgAs) are mostly synthesised intracellularly and subsequently released from secretory granules through a ductal system (Myers and Ferris, 2007). The ductal system is categorised as: intercalated ducts, excretory ducts and striated ducts (Figure 1.3).

The intercalated ducts have low cuboidal epithelium with a narrow lumen and are where the salivary fluid first passes through to enter the striated ducts. Columnar cells with numerous mitochondria line the striated ducts. Then the salivary fluid passes through the excretory ducts, which are lined with cuboidal cells until the terminal part, which is lined with stratified squamous epithelium (Myers and Ferris, 2007).

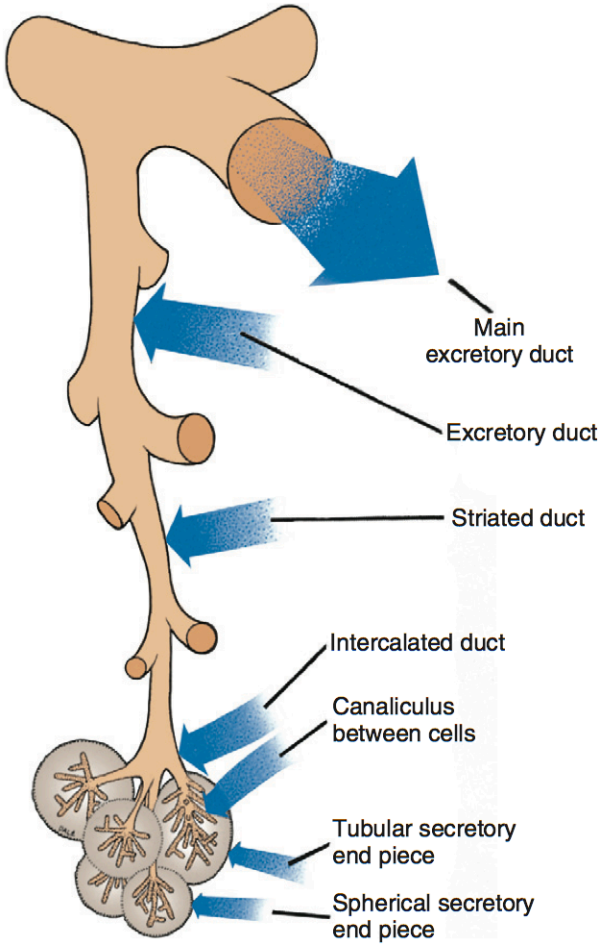

Figure 1.3 Diagrammatic illustration of the ductal system of salivary glands (Nanci and Ten Cate, 2012).

This secretory structure's terminal unit is the salivary acinus that produces saliva and each gland has distinct histological structures and functions in relation to their acini. Parotid glands are purely serous in nature, sublingual glands are primarily mucous and submandibular glands are mainly serous (Munger, 1964).

In serous glands, the acini are arranged in a roughly spherical form and secrete a watery fluid rich in amylase, other salivary enzymes and electrolytes, via exocytosis (Humphrey and Williamson, 2001).

Mucous cells, which also form the most of the minor salivary glands (Witt, 2005), secrete viscous glycoproteins, mucins, that when released forms mucus, which serous cells lack (Pinkstaff, 1993).

1.4 Mouse Salivary Gland Micro-Structure

Similar to human glands, the mouse parotids are serous, the sublingual are predominantly mocous and the submandibular glands are mixed but primarily serous (Figure 1.4). However unlike humans, the duct system of all rodents, including mice, has a separation between the striated and intercalated ducts via a granular convoluted tubule (Gresik, 1994).

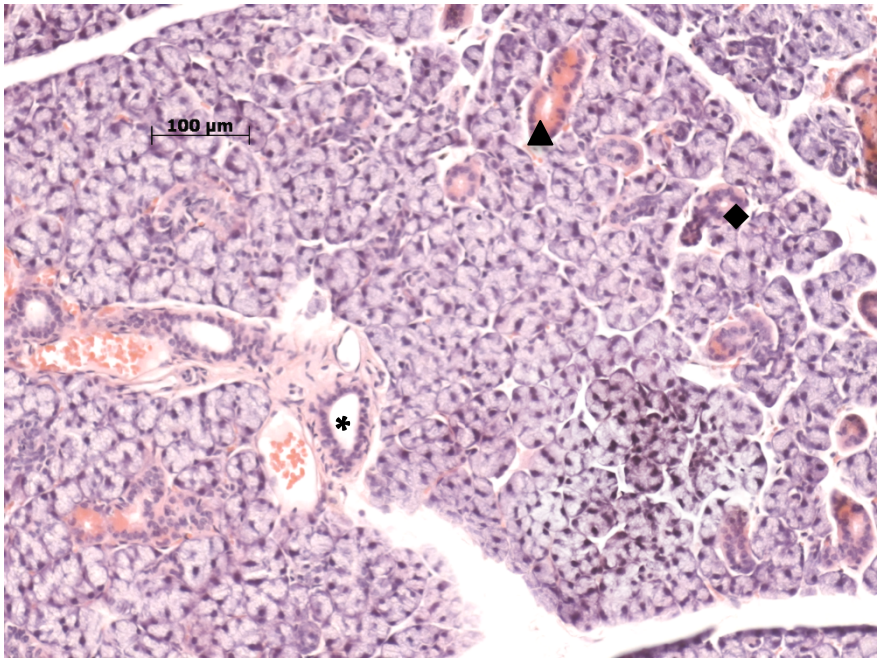

Figure 1.4 Histological (H&E) appearance of mice submandibular tissues showing excretory duct (star), striated duct (diamond) and granular convoluted tubule (arrowhead). Scale bar represents 100 µm.

Furthermore, histologically there are sex differences in mouse submandibular glands – in male mice, the granular ducts are approximately 50% larger in diameter and vastly superior in quantity, whereas in female mice the acinar cells predominate the histological appearance (Fekete, 1941, Gresik and MacRae, 1975, Chai et al., 1993).

Nerve growth factor and epidermal growth factor, which are synthesized by granular duct cells, are produced in greater quantities in males than in females (Levi-Montalcini and Angeletti, 1964, Byyny et al., 1972). In studies of 3H-thymidine incorporation during testosterone-induced granular duct development, hypertrophy has been found to be the main factor responsible for the increased presence of granular ducts, in male mice (Chretien, 1977).

A further histological difference in the mouse submandibular glands is the presence of granular intercalated duct cells in females and their absence in males (Caramia, 1966, Gresik and MacRae, 1975). These cells are located at the junction of intercalated ducts and acini, and they have been suggested as an intermediatory in the conversion of terminal intercalated duct cells to acini cells (Qwarnström and Hand, 1983) and

the localized low levels of mucin in the granular intercalated duct cells supports this supposition (Denny et al., 1988).

1.5 Saliva

The main physiological function of the salivary glands is saliva production. Saliva, which consists of over 99% water (Engelen et al., 2007), is crucial in the digestion process and mouth lubrication, among other functions (Figure 1.5). The secretions of each of the salivary glands may vary at any given time and thus it can be difficult to account for the precise composition of saliva. Generally in unstimulated saliva, about 25% of saliva is secreted from the parotid glands, 5% from sublingual glands and 60% comes from submandibular glands (Edgar et al., 2004), however this can vary according to how stimulated each gland is. In recognition of this variability, the term whole mouth saliva (WMS) is used to describe the oral cavity fluid.

1.5.1 Salivary Proteins

WMS gets its physical properties from salivary proteins (Gibbins and Carpenter, 2013), including proline-rich proteins (PRPs), statherin, histatin, carbonic anhydrase VI (CA VI) and amylase, among others.

1.5.2 Salivary Mucins

The salivary mucins, produced by sublingual and submandibular glands, are essential for the lubricating properties of saliva (Inoue et al., 2008, Boze et al., 2010). The most important glycoproteins found in saliva are the secreted salivary mucins, MUC5B and MUC7 (Gibbins et al., 2014). MUC5B has a high molecular weight (>1000kDa) and is composed of highly glycosylated covalently linked subunits. MUC7, with a lower molecular weight (200-300kDa), is a single glycosylated peptide chain.

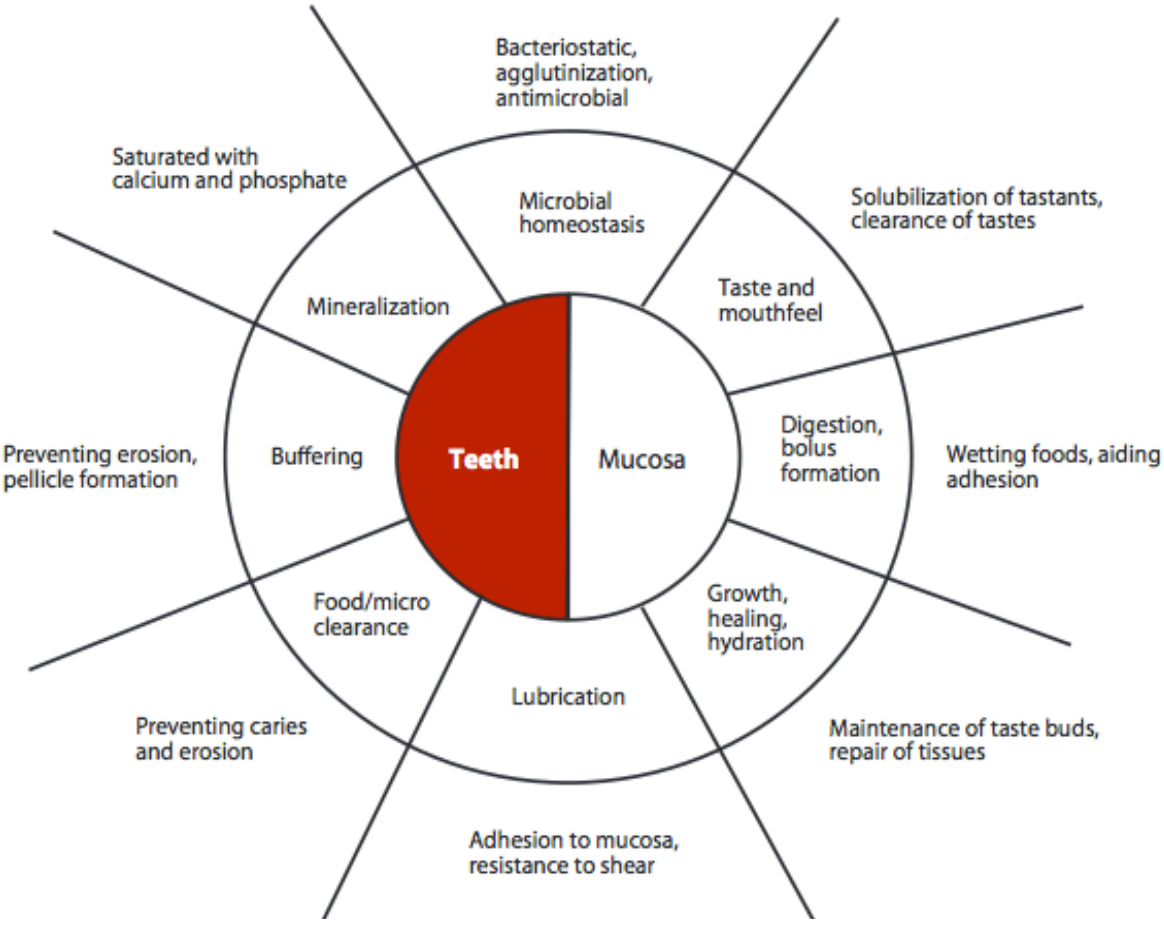

Figure 1.5 Summary of salivary functions according to the surface (Carpenter, 2013).

1.6 Salivary Gland Innervation

Salivary secretions are regulated, either directly or indirectly, by the parasympathetic and sympathetic nervous systems. Parasympathetic innervation to the salivary glands is provided by the cholinergic parasympathetic nerves which release acetylcholine that binds to muscarinic 3 (M3) receptors and, to a lesser extent, muscarinic 1 (M1) receptors (Proctor and Carpenter, 2007), promoting the fluid secretion of saliva. Sympathetic innervation regulates salivary gland secretions through several ways including vasoconstriction, whereby increased sympathetic activity reduces glandular bloodflow causing a decrease to the volume of fluid in salivary secretions (Guyton and Hall, 2006). It is believed that the primary sympathetic salivary centres, which are located somewhere in the upper thoracic segments of the spinal cord although it remains unclear precisely where in this region (Garrett et al., 1999, Bradley et al., 2005), are responsible for the dry mouth associated with anxiety (Proctor and Carpenter, 2007).

1.7 Salivary Gland Function

Although salivary glands are innervated and may increase their secretory rate in response to nerve activity, they are also influenced by

other exogenous regulators including androgens, growth hormones and the thyroid gland (Hosoi et al., 1978, Boyer et al., 1991, Hiramatsu et al., 1994).

Within saliva, potassium (K+) concentration is always high while sodium (Na+) concentration is low, compared to that found in plasma. Saliva synthesis begins with an efflux of chloride (Cl-) and K+ that generates transepithelial potential difference, causing a drive of Na+ between epithelial cells and the production of isotonic saliva in the acinus' lumen. The primary isotonic saliva formed in the acini then becomes more hypotonic during its transport through the ducts, as sodium and chloride are reabsorbed, while K+ and bicarbonate ($HCO3^-$) are secreted into the fluid. Whilst the permeability of the duct system may increase under certain conditions, such as physical exercise, generally the final saliva that enters the mouth is hypotonic with a lower salivary sodium concentration than the primary saliva, allowing for taste buds to be able to detect salt in the mouth.

Apart from their saliva secretory functions, salivary glands are also thought to be involved in the growth regulation of other tissues by means of EGF (Lambotte et al., 1997), as well as neuronal and

immunological pathways by means of NGF (Boyer et al., 1991, Mathison et al., 1994).

1.8 Salivary Gland Dysfunction

Although tissue morphology may be associated with age, the secretory function of salivary glands in healthy individuals is not thought to be affected by age (Pedersen et al., 1999, Nagler, 2004), with age generally considered to only cause insignificant increases in the prevalence of dry mouth, also known as xerostomia (Edgar et al., 2004). In fact, the most relatively quotidian reason for salivary gland dysfunction in humans is dry mouth induced by prescription medication (Sreebny and Schwartz, 1997), with a wide range of drugs having been identified as xerogenic (associative of xerostomia). However, dry mouth has been proven not to be a reliable, objective indicator of glandular hypofunction (Fox, 1998), this is because most human studies concerning oral dryness are based on the perceived sensation of dryness, with relatively few studies actually taking an objective assessment of the rate of saliva production (Carpenter, 2014).

Salivary calculi (or salivary stones) can cause obstruction of the ducts and swelling, leading to dysfunction. Whilst the cause of salivary calculi in many instances is idiopathic, it is known that continued ductal obstructions can cause glandular atrophy (Sumi et al., 1999). Salivary gland atrophy is characterised by morphological and functional changes of the glands (Takahashi et al., 2004), including reduced glandular weight (Harrison and Garrett, 1976), shrunken acinar cells (Osailan et al., 2006b) and partial loss of acinar cells (Takahashi et al., 2000); with the remaining acini thought to be in a quiescent, non-functional state (Cotroneo et al., 2008).

Salivary gland atrophy can take place as a result of many diseases and medical treatments, including but not limited to, Sjögren's syndrome (an autoimmune disease in which lymphocytic infiltration occurs in the salivary and lacrimal glands) (McCartney-Francis et al., 1996), autonomic denervation in salivary glands (Raz et al., 2013), salivary gland tumours (Hollinshead, 1982), chronic-sialadenitis (Burgess and Dardick, 1998) and GVHD (Nagler et al., 1996). Although chemotherapy only results in temporary salivary gland impairment (Epstein and Huhmann, 2011), radiotherapy to the head and neck region continues to present multiple significant clinical problems (Fox, 1998). With over

550,000 people worldwide diagnosed with head and neck cancer every year (Jemal et al., 2011), the effects of head and neck radiation therapy on the salivary glands and the oral cavity have only become more pronounced, such as the irreversible hypofunction resulting following X-ray irradiation (Fox, 1998). Consequently the loss of normal salivary gland functionality can seriously affect the quality of life in patients and remains difficult to manage (Atkinson and Fox, 1992, Jansma et al., 1992, Atkinson and Wu, 1994, Vissink et al., 2003).

Previous rodent studies have suggested that glandular hypofunction, in response to irradiation, is induced over four phases (Coppes et al., 2001). The first phase is characterised by a declined flow rate, the second by a reduction in acinar cell count, the third by stabilisation of the flow rate and acinar cell count and the fourth phase by an increase in acini, albeit with poor tissue morphology (Coppes et al., 2001).

Such findings are divergent from rodent studies based on atrophy of denervation, which caused secretions to vary according to different routes of protein secretion (Proctor and Carpenter, 2007), for example amylase secretion increased following 1 week of symphathectomy (Asking and Emmelin, 1989)

Furthermore certain studies of salivary gland atrophy in mice, specifically those based on diabetes (Nashida et al., 2013) or gland ligation (Takai et al., 1986), have produced histologically similar results to human patients with salivary gland dysfunction, and thus serve as a useful model for salivary gland atrophy.

1.9 Duct Ligation Induced Atrophy

Duct ligation surgery on patients has been carried out previously and found to carry many risks such as sialadenitis of the parotid glands (Witt, 2005) or even irreversible atrophy (Baron and Ober, 1962). However the animal ligation model, whether intra-oral duct ligation or extra-oral duct ligation, is reversible, due the gland's ability to recover its functionality following de-ligation (Osailan et al., 2006a, Carpenter et al., 2009).

Duct ligation-induced atrophy in animals is caused by a ligation of excretory ducts at the hilum. The resultant atrophy causes morphological and functional changes of the glands (Takahashi et al., 2004), as exampled in Figure 1.6, including changes such as reduced

glandular weight (Harrison and Garrett, 1976), shrunken acinar cells (Osailan et al., 2006b) and partial loss of acinar cells (Takahashi et al., 2000); with the remaining acini thought to be in a quiescent, non-functional state (Cotroneo et al., 2008).

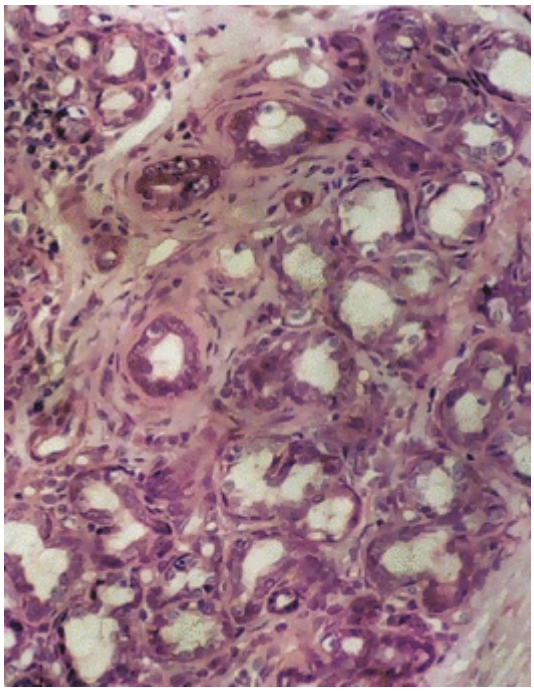

Figure 1.6 Hematoxylin and eosin staining of ligation induced atrophy exhibiting a reduction in acini and the appearance of duct-like structures as well as fibrosis of stromal connective tissue (Miguel et al., 2002).

Additionally, Alcian Blue and Periodic acid–Schiff (AB/PAS) staining of ligated tissue sections has shown localised loss of secretory granules (Correia et al., 2008) and striated duct lumena appear dilated due to the degranulation (Norberg et al., 1988). Hematoxylin and eosin (H&E) staining showed large amounts of infiltrating inflammatory cells

(mainly neutrophils and macrophages) (Carpenter et al., 2007) and an increased extracellular space (Correia et al., 2008). Ligation-induced atrophy also results in necrosis (Harrison et al., 2000), whilst a previous study in our group has found activation of autophagy during ligation-induced atrophy via immunoblotting of Microtubule-associated protein 1A/1B-light chain 3 (LC3) protein (Silver et al., 2010). In terms of gland functionality, ligated glands secrete a vastly reduced quantity of saliva (Shiba et al., 1972), with the remaining saliva rich in Na+ (Martinez et al., 1982). This impairment has been linked to the loss of acinar cells due to apoptosis (Takahashi et al., 2000, Takahashi et al., 2007). As well as apoptosis, there is evidence that prolonged atrophy can also cause necrosis and autophagy in submandibular, sublingual and parotid salivary glands (Harrison et al., 2000, Harrison et al., 2001).

In contrast to the loss of acini during prolonged atrophy, myoepithelial cells persist in the gland, however they developed a bizarre shape which protrudes into the interstitial space (Emmelin et al., 1974). Takahashi et al., found in immunohistochemical studies of rat duct ligation-induced atrophy that myoepithelial cells are able to proliferate in submandibular and sublingual glands, with apoptosis of myoepithelial cells occurring in the early stages of atrophy in submandibular glands

(Takahashi et al., 2001) and the transition of myoepithelial cells from the small to large ducts in sublingual glands (Takahashi et al., 2003). A study on mice found similar histopathological changes on myoepithelial cells in mice, whilst they were more pronounced in rats than in mice (Takai et al., 1986). Proliferation of myoepithelial cells has also been shown in parotid glands during atrophy (Burgess et al., 1996).

1.10 Salivary Gland Regeneration

Currently there are several treatment strategies that aim to dissipate or regenerate the damage caused to salivary glands from radiotherapy or the xerostomia induced by prescription medication.

Intensity-modulated radiation therapy (IMRT) is a high-precision radiation technique that introduces the ability to conform the treatment volume to concave tumor shapes (Pazdur et al., 2010), allowing for a more accurate delivery of radiation whilst sparing the surrounding tissues, for example major salivary glands (Jensen et al., 2010, Nutting et al., 2011). Recent trials have supported this theory by showing that parotid sparing IMRT significantly reduces the risk of severe hyposalivation, in comparison with traditional 3-dimensional

conformal radiation therapy (3D-CRT) (Nutting et al., 2011). However this procedure has raised concerns regarding an increased potential for secondary cancer induction (Hall and Wuu, 2003, Curtis et al., 2006). Current treatments for improving quality of oral health following dry mouth, which is most commonly induced by prescription medication, involve the substitution of saliva for artificial saliva, usually in the form of a gel or spray (Matsuo et al., 1997, Davies, 2000). An alternative approach involves medicating to increase overall secretory output from residual salivary gland cells, such as the use of cevimeline (Suzuki et al., 2005), however these treatments are often accompanied by unendurable side effects (Fox, 2003).

Preclinical studies have also shown that salivary gland progenitor and stem cell biology (Figure 1.7) provides a rationale for therapeutic salivary gland regeneration (Lombaert et al., 2011). These findings have shown that stem cell transplants can differentiate into salivary epithelial cells and restore salivary gland function in hyposalivatory glands (Sumita et al., 2011), and furthermore they restore tissue homeostasis within irradiated glands, which is critical for long term maintenance of the tissue (Imanguli et al., 2007). *In vitro* studies have been capable of exhibiting self-renewal and differentiation capabilities

from stem cell–containing salispheres cultured from human parotid and submandibular salivary glands (Lombaert et al., 2008), bringing human clinical applications closer within reach.

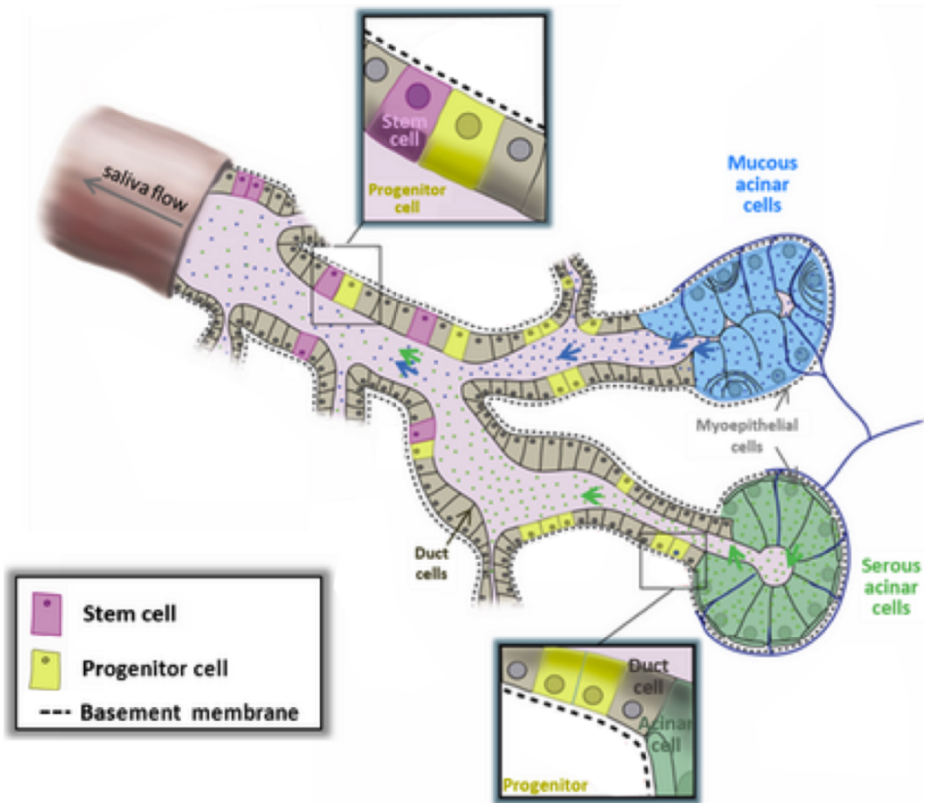

Figure 1.7 Schematic representation of salivary glands with stem cell and progenitor cells
(Pringle et al., 2013)

Alternatively, adipose-derived stromal cell transplantation (Kojima et al., 2011), bone marrow-derived clonal mesenchymal stem cells transplantation (Lim et al., 2013) and human amniotic epithelial cell transplantation (Zhang et al., 2013) have all been successfully applied in

rodents, proving their potential use as a source of cell-based therapy for restoration of salivary gland function.

1.11 Duct De-ligation Induced Regeneration

The process of glandular regeneration follow de-ligation of the ducts of salivary glands in mice has previously been investigated by our group (Osailan et al., 2006a, Carpenter et al., 2007). In terms of glandular functionality, it has been shown that de-ligated glands possess the ability to recover their function by secreting normal amounts of saliva with conventional quantities of ions and proteins (Osailan et al., 2006a, Carpenter et al., 2007).

On a cellular level, both mitosis and apoptosis occur during regeneration, however they occur at different stages of regeneration in each major salivary gland (Takahashi et al., 1998, Takahashi et al., 2004, Takahashi et al., 2005).

In terms of tissue morphology, it was found that de-ligation of excretory ducts starts a process of glandular regeneration with a proportional increase of acini volume in comparison with normal glands, although there is a higher duct-to-acinar ratio (Scott et al., 1999). In submandibular glands, myoepithelial cells actively proliferate during regeneration around the newly formed acini, suggesting a possible role for myoepithelial cells in glandular regeneration (Cutler and Chaudhry, 1973, Takahashi et al., 2004). Similarly, they may have an active role following de-ligation in parotid glands as indicated by their change of location from the newly formed acini to the intercalated duct (Takahashi et al., 1999). However the method for their relocation to the ducts remains unclear; whether they move onto the ducts (Takahashi et al., 1999) or whether they differentiate from the basal cells located in the duct-like structures (Takahashi et al., 1997).

Furthermore, in glands regenerated following ligation, it is thought that differentiation of the newly formed acini from the ductal compartment accounts for most of the observed glandular recovery (Tamarin, 1971a, Takahashi et al., 2004). This is because acinar cells, more specifically the self-duplication of acinar cells, are responsible for salivary gland homeostasis (Aure et al., 2015). However, the acini that are newly

formed from ducts differentiate from unique branched structures present in the tissue, by expressing positive immunoreactivity for the perinatal proteins known as submandibular gland protein A (SMG-A) (23.5 kDa), SMG-B1 (26 kDa), and B2 (27.5 kDa) (Cotroneo et al., 2008, Cotroneo et al., 2010). Whereas typically in adult glands the SMG proteins are no longer present in the acini (Cotroneo et al., 2010), suggesting that regenerating glands enter embryonic-like state of development in order to regenerate their acini secretory function.

1.12 Salivary Gland Development

Salivary gland development in mammals arises in the embryo and progresses through successive stages before reaching their distinct and independent identities by adulthood. The submandibular gland is the first major salivary gland to develop in the embryo, followed by the proximate sublingual gland and the parotid (Tucker, 2007), and salivary glands continue to develop postnatally until they reach full maturity at puberty (Patel et al., 2006).

Mammalian salivary glands are generated during embryonic development by the process of branching morphogenesis, a process that

turns a single epithelial bud into an array of epithelial branches. Branching morphogenesis is a fundamental mechanism employed to generate the functionally efficient, multifaceted and systematic tissue architecture of mammalian development of salivary glands as well as lungs, mammary glands, pancreas, kidney (Hogan, 1999).

The three major salivary glands share a common mechanism in their embryonic branching morphogenesis (Denny et al., 1997); a set of repetitive bifurcations leading to the formation of new epithelial outgrowths, which generates the branching structures (Tucker, 2007). The stages of salivary glands development have been described using the mouse submandibular glands for over 50 years, as it shows classic branching morphogenesis (Borghese, 1950).

The mouse submandibular gland development undergoes a series of reciprocal interactions among the oral epithelium covering the first branchial arch, and a population of mesenchymal cells derived from the cranial neural crest (Jaskoll et al., 2002). The five embryonic stages of salivary gland development (Figure 1.8) begins with the Prebud stage at gestation day 11 (E11.5) with the thickening of the epithelium in the floor of the mouth, at the back of the first mandibular molar and

adjacent to the developing tongue. This thickening develops at the bottom of the alveolo-lingual sulcus, in the floor of the mouth as a consequence of the upward growth of the tongue rudiment.

The thickening protrudes into the underlying mesenchyme at the Initial bud stage from E12.5 and the epithelium invaginates to form a bud linked to the oral surface by a duct. As the epithelial cells proliferate continuously in a downward direction, they lead to the formation of a dense solid epithelial stalk ending in a bulge constituting the initial bud stage of salivary gland development.

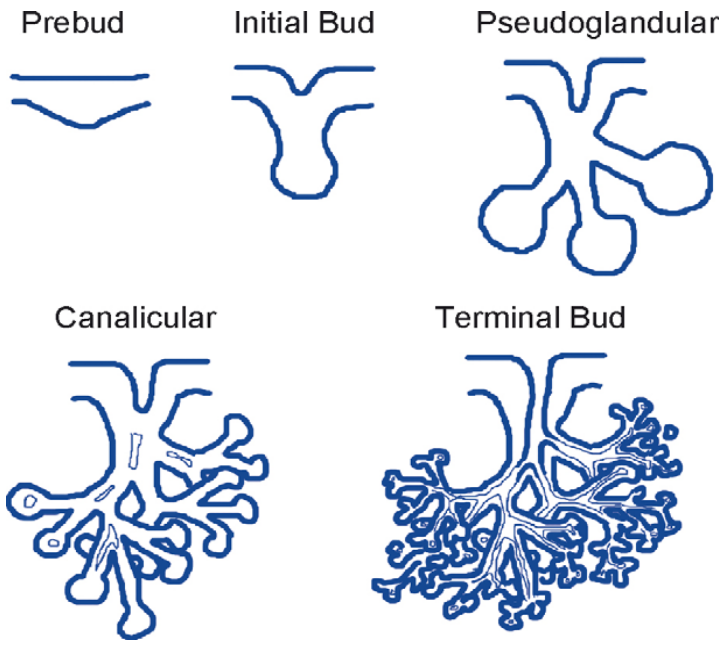

Figure 1.8 Schematic diagram of embryonic development of the SMG in the mouse (Tucker, 2007).

The capsular character of the submandibular gland is due to the mesenchymal cells condensing around the submandibular primordium. The initial bud, surrounded by the mass of connective tissue, will form the parenchyma of the SMG, while the excretory duct formed by closure, in a rostal direction of the alveolo-lingual sulcus (Hamilton et al., 1945).

The pseudoglandular stage is reached as the epithelium and mesenchymal cells expand in volume, which later produces a cluster of branches and buds as it undergoes branching, known as the pseudoglandular stages at E13.5. As the epithelium undergoes branching morphogenesis with 4-5 buds it continues branching and so produces a multi-lobed gland by E14.5.

The majority of the ducts develop lumen around E15.5 known as the canalicular stages, as the ducts need to undergo cavitation for allowing access between acinar cells (saliva producing) and the oral cavity (glands are initially formed from a solid core of epithelium). The epithelium around the forming lumen actively proliferates and the epithelium at the centre of the presumptive lumen undergoes apoptosis. The branches and terminal buds are hollowed out forming the presumptive ducts and acini (Jaskoll et al., 2002). At E17.5, the

terminal bud stage, well-developed lumena are visible in the terminal end buds and in the presumptive ducts (Tucker, 2007). Development and differentiation of the SMG continues postnatally with further morphological changes in the granular convoluted tubule (GCT) cells of the submandibular gland taking place at puberty (Gresik, 1994).

1.12.1 Branching Morphogenesis Regulating Factors

Signalling involving fibroblast growth factors (FGFs) and fibroblast growth factor receptors (FGFRs) has been shown in numerous studies to be highly important in the regulation of submandibular gland development (Patel et al., 2006). FGFs bind to heparin-sulphate (HS) on the cell surface and extracellular matrix (ECM) proteoglycans and glycolipids (Davies, 2002, Patel et al., 2006), increasing their affinity for FGFRs (Mohammadi et al., 1996). FGF10 knockout and FGFR2b knockout mice do not develop salivary glands due to transient bud degeneration prior to branching morphogenesis by E13.5 (De Moerlooze et al., 2000, Jaskoll et al., 2005). Similarly in humans, mutations of FGF10 cause aplasia of the lacrimal and salivary glands (ALSG) syndrome (Entesarian et al., 2005).

Histological analysis of heterozygous FGF10 and FGFR2b mouse embryos has indicated hypoplastic submandibular glands, portrayed by less terminal buds (Jaskoll et al., 2005) and an addition of soluble recombinant FGFR2b or decreasing FGFR1 expression, all resulted in reduced branching morphogenesis in E12 mouse submandibular glands (Hoffman et al., 2002, Steinberg et al., 2005).

Furthermore, Sonic hedgehog (Shh), TGFβ, bone morphogenic proteins (BMPs), hepatocyte growth factor (HGF), activins, the tumor suppressor p63, transcription factor Six1 and Pitx1, TNF pathway and IL-6 are amongst other molecules that play a role in the branching morphogenesis of SMGs either from phenotypes described in genetically modified mice or organ culture experiments (Patel et al., 2006).

1.13 mTOR

The mammalian target of rapamycin (mTOR), also known as the mechanistic target of rapamycin, is a serine/threonine protein kinase belonging to the phosphatidylinositol 3-kinase (PI3K)-related kinase protein family. mTOR plays a critical role in regulating cell growth, cell

proliferation, cell motility, cell survival, protein synthesis and transcription (Hay and Sonenberg, 2004), by forming two distinct complexes named mTOR complex 1 (mTORC1) and mTOR complex 2 (mTORC2) that differ in their subunit composition (Laplante and Sabatini, 2012).

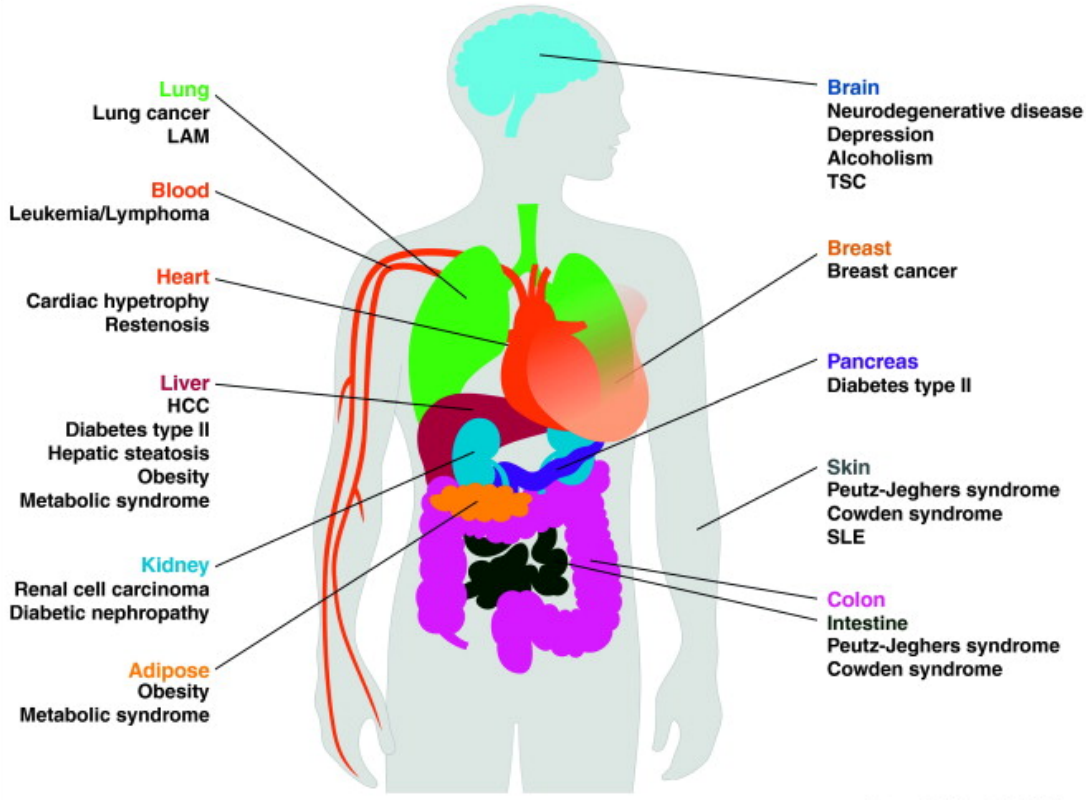

Figure 1.9 Diseases (and their corresponding organs) that are linked to dysregulation of mTOR (Dazert and Hall, 2011).

Dysregulation of mTOR has been found to occur in many diseases (Figure 1.9), including cancer (Guertin and Sabatini, 2007), diabetes (Zoncu et al., 2011), ageing (Johnson et al., 2013), or even Down's

syndrome (Antonio Troca-Marin et al., 2014). Therefore there are significant ongoing efforts in pharmacologically targeting the mTOR pathway (Laplante and Sabatini, 2012). This section of the chapter will review our current understanding of the mTOR pathway, mTOR mediated cellular processes, the protein's role in health and disease, as well as pharmacological approaches of inhibiting mTOR activity.

The mTOR pathway, and mTORC1 more explicitly, is the target of a molecule named rapamycin or sirolimus – a macrolide known for its potent immunosuppressive and antiproliferative properties. Upstream regulators such as nutrients, growth factors, energy and stress can activate mTOR and magnify its activity, as shown for mTORC1 (Figure1.10).

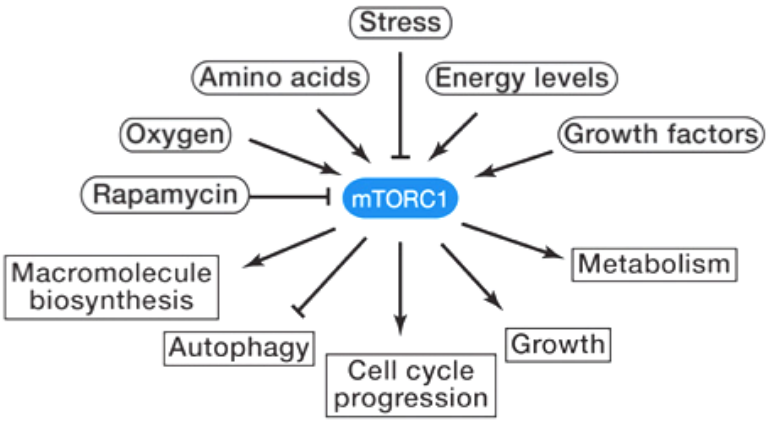

Figure 1.10 Cloud diagram of the mTORC1 signalling network. mTORC1 responds to amino acids, oxygen, energy levels, stress as well as growth factors, whilst being acutely sensitive to rapamycin. It promotes cell growth, cell cycle progression, induces anabolic processes and also inhibits catabolic processes such as autophagy (Laplante and Sabatini, 2012)

The mTOR signalling network in mammalian cells (Figure 1.11) is activated by growth factors and hormones, such as Insulin, and mediated through the PI3-Kinase pathway that leads to the phosphorylation and activation of Akt (Wang and Proud, 2006). In turn, Akt phosphorylates a protein called tuberous sclerosis 2 (TSC2) (Inoki et al., 2002).

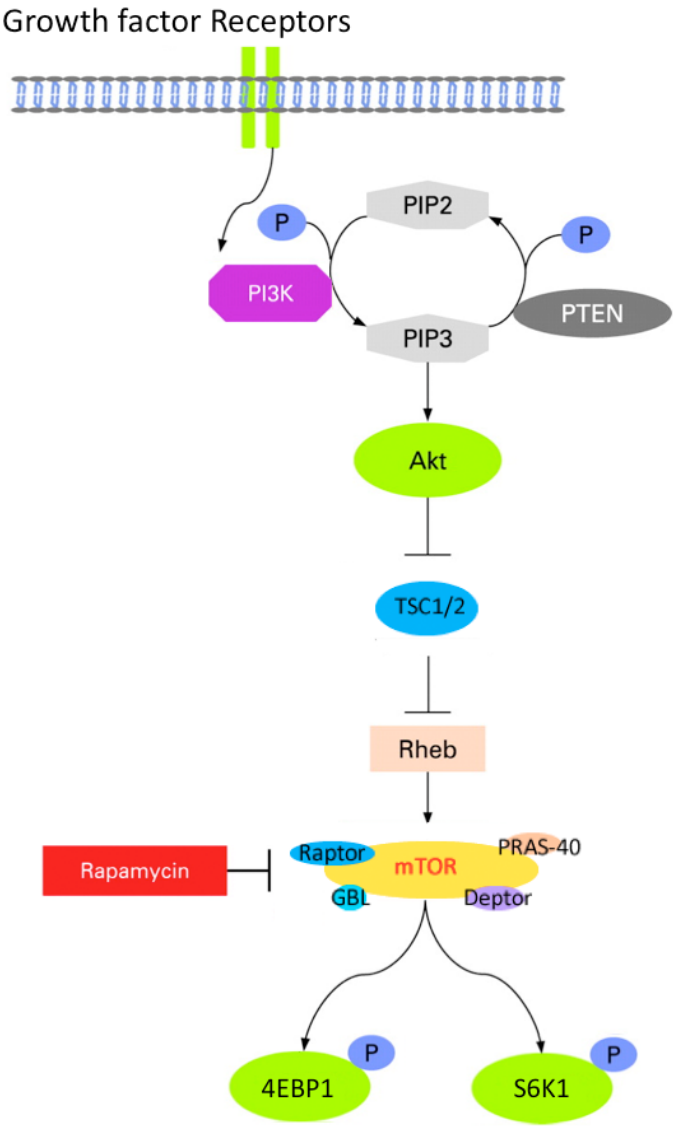

Figure 1.11 A schematic diagram of the mTORC1 signalling network
The upstream signals that affect mTORC1, including growth factors and cellular energy levels, are transmitted through phosphatidylinositol 3-kinase (PI3K) and Ras pathways that phosphorylate AKT. This inactivates TSC1/2, allowing RHEB to accumulate in its inactive GTP-bound form and switch on mTORC1. The mTORC1 subunits of 4E-BP1 and S6 kinases can then be phosphorylated by Raptor. Rapamycin inhibits mTORC1 activity and PTEN can also impair mTOR signalling by inhibiting PIP2 → PIP3 conversion.

The TSC1 & TSC2 heterodimer is a key upstream regulator and functions as a GTPase-activating protein (GAP) for Ras homolog enriched in brain (RHEB) (Laplante and Sabatini, 2012). RHEB, Ras-related GTPase, is thought to be necessary for mTORC1 activation regardless of upstream signals (Avruch et al., 2009). Phosphorylation of TSC2 is thought to inhibit its GAP activity (Wang and Proud, 2006), thus TSC1/2 negatively regulates mTORC1 by converting RHEB into its inactive GDP-bound state (Inoki et al., 2003, Tee et al., 2003). Phosphatase and tensin homolog (PTEN) also negatively regulates the mTOR pathway (Diegel et al., 2010). Low cellular ATP levels can also cause phosphorylation and activation of TSC2 via the AMP-activated protein kinase (AMPK) (Wang and Proud, 2006). Canonical Wnt signalling can also activate the mTOR pathway, either by directly activating β-catenin-dependent transcription (Laplante and Sabatini, 2012) or via inhibiting GSK3 without involving β-catenin-dependent transcription (Inoki et al., 2006) and comparably, inhibition of mTOR by rapamycin blocks activated Wnt signalling (Inoki et al., 2006).

1.13.1 mTOR Structure

The crystal structure of mTOR has not yet been determined, however the protein is believed to consist of mainly helical structures (Perry and Kleckner, 2003) and the protein is primarily localised in the cytosol of two multi-protein complexes, mTORC1 & mTORC2. However, it has also been associated with the membranes of several organelles, such as Golgi, endoplasmic reticulum, mitochondria and nucleus (Withers et al., 1997, Sabatini et al., 1999, Desai et al., 2002, Tirado et al., 2003, Drenan et al., 2004, Liu and Zheng, 2007).

mTORC1 is composed of the mTOR subunit, mammalian lethal with sec-13 protein 8 (mLST8/GβL), regulatory-associated protein of mTOR (Raptor), DEP domain containing mTOR-interacting protein (DEPTOR), proline-rich Akt substrate 40 kDa (PRAS40) (Laplante and Sabatini, 2012) and the recently identified Tti1/Tel2 complex (Kaizuka et al., 2010). mTORC2 is composed of the mTOR subunit, mLST8/GβL, DEPTOR, rapamycin-insensitive companion of mTOR (Rictor), mammalian stress-activated protein kinase interacting protein 1 (mSIN1) and protein observed with Rictor 1 and 2 (Protor 1 & 2) (Laplante and Sabatini, 2012).

Both mTOR complexes has different sensitivities to rapamycin and different downstream signalling. mTORC1 activates transcription and translation through its interactions with p70-S6 Kinase 1 (S6K1) and the eukaryotic initiation factor 4E-binding protein 1 (4E-BP1) (Hay and Sonenberg, 2004) and is thought to be critical during development as mTOR knockout mice die *in utero* shortly after implantation (Gangloff et al., 2004, Murakami et al., 2004), with evidence of multiple developmental abnormalities as embryonic development halts at E5.5 (Wang and Proud, 2006)

The S6K1 serine/threonine kinase is also directly phosphorylated by mTORC1 and in turn, S6K1 activates the 40S ribosomal S6 protein to selectively increase the translation of a class of around 90 transcripts known as TOP mRNAs that encode ribosomal proteins and other translation regulators (Hannan et al., 2003). However recent evidence suggests that S6Ks may not be key mediators in how mTOR regulates TOP mRNA translation (Brian et al., 2012), such as the Patursky-Polischuk et al study which found that rapamycin was not thoroughly effective in inhibiting top mRNA translation through mTOR (Patursky-Polischuk et al., 2009).

4E-BP1 is a protein that in its unphosphorylated state binds to the eukaryotic translation initiation factor 4E (eIF4E), repressing eIF4E activity in the initiation of protein synthesis (Gingras et al., 1999b). mTORC1 positively mediates eIF4E activity by directly phosphorylating 4E-BP1, leading to its release from eIF4E (Hands et al., 2009) to allow eIF4E to bind the 5'-cap structure of cytoplasmic mRNA (Wang and Proud, 2006).

eIF4E also interacts with other proteins such as the multidomain scaffold protein eIF4G to circularize the mRNA (Pause et al., 1994), markedly enhancing its translation. eIF4E:eIF4G interaction is therefore considered to be influential in the initiation of mRNA translation (Hands et al., 2009).

mTORC2 is a rapamycin-insensitive entity (Sarbassov et al., 2005) which encourages cellular survival by activating Akt to phosphorylate FOXO1 & FOXO3 (downstream of Akt) (Guertin et al., 2006, Guertin et al., 2009) . Alpha serine/threonine-protein kinase (Akt or PKB), plays a critical role in multiple cellular processes including glucose metabolism, apoptosis, cell proliferation, transcription and cell migration (Sarbassov et al., 2005, Guertin and Sabatini, 2005, Lee et al., 2005, Yang et al., 2006, Guertin and Sabatini, 2007).

Recently, mTORC2 activity has been implicated in the regulation of autophagy too (Datan et al., 2014). Complex 2 also functions as an important regulator of the cytoskeleton, via its organisation and stimulation of F-actin stress fibres, by the addition of GTP to RhoA, Rac1 and Cdc42 (Sarbassov et al., 2004).

1.13.2 mTOR Functions

The mTOR pathway coordinates cell growth, cell cycle progression, cellular survival and translation (Fingar and Blenis, 2004) and has been shown to interact, directly or indirectly, with targets that are responsible for many functions including cell-mediated immunity (Thomson et al., 2009), programmed cell death (PCD) (Gharagozloo et al., 2013), protein synthesis (Davoodi et al., 2012), lipid synthesis (Laplante and Sabatini, 2009) and autophagy (Silver et al., 2010). Furthermore mTOR is thought to be critical during embryonic development as mTOR knockout mice die *in utero* shortly after implantation (Gangloff et al., 2004, Murakami et al., 2004), with evidence of multiple developmental abnormalities as embryonic development halts at E5.5 (Wang and Proud, 2006).

mTOR signalling controls cell growth and survival primarily through 4E-BP1 and S6K. Unphosphorylated 4E-BP1 binds to the eukaryotic translation initiation factor 4E (eIF4E), preventing it from performing translation initiation. mTORC1 has been shown to phosphorylate two sites in the translation inhibitor 4E-BP1 *in vitro* (Brunn et al., 1997, Burnett et al., 1998) and also phosphorylates at least 4 known residues of 4E-BP1 (Gingras et al., 1999a, Mothe-Satney et al., 2000, Huang and Houghton, 2001). This phosphorylation allows 4E-BP1 to unbind from eIF4E (Martelli et al., 2011) to join the eukaryotic translation initiation factor 4G (eIF4G) and the eukaryotic translation initiation factor 4A (eIF4A) to initiate translation (Wang et al., 2012).

S6K regulates cell growth (Shima et al., 1998) and mTORC1 phosphorylates S6K to make it active. mTORC1 can do this on at least two residues, with the most studied phosphorylation occurring on the hydrophobic-motif residue Thr^{389} (Saitoh et al., 2002), which subsequently stimulates the phosphorylation of S6K1 by Phosphoinositide-dependent kinase-1 (PDK1) (Pullen et al., 1998). Activated S6K can initiate its functions via the stimulation of S6 Ribosomal protein and the eukaryotic translation initiation factor 4B (eIF4B) (Peterson and Schreiber, 1998). Furthermore S6K is a part of a

negative feedback loop that involves the inhibition of Akt by mTORC1. Active S6K inhibits insulin receptor substrate 1 (IRS-1) by phosphorylating it at multiple sites, which in turn induces its degradation, dampening Akt activation (Takano et al., 2001, Hartley and Cooper, 2002, Harrington et al., 2004). This loop is relevant in clinical applications as it is known to play a role in Type 2 diabetes (Um et al., 2004). A functionally similar loop is the S6K1-mediated inhibition of platelet-derived growth factor receptor (PDGFR), that also signals through Akt (Zhang et al., 2007).

1.14 Rapamycin

The mTOR pathway, or to be more specific the protein complex mTORC1, is the target of a molecule named rapamycin. Rapamycin is a macrolide known for its potent immunosuppressive and anti-proliferative properties, which works through a gain-of-function mechanism where it binds with the intracellular peptidyl-prolyl cis-trans isomerase FKBP12. The newly created Rapamycin - FKBP12 complex then binds and interacts with mTOR's FKBP-rapamycin-binding (FRB) domain to inhibit the kinase activity of mTORC1, however Rapamycin - FKBP12 does not bind to mTORC2 (Sarbassov et

al., 2006, Leone et al., 2006). Although mTORC1 is able to bind with the Rapamycin - FKBP12 complex, it is unable to bind to FKBP12 individually and rapamycin can only bind to the FRB domain individually with a much lower affinity (Banaszynski et al., 2005). In addition to rapamycin, other rapamycin analogs (rapalogs) such as temsirolimus, everolimus and deforolimus are also used, because rapalogs have the same mechanism of action as rapamycin – binding to FKBP12 and interfering with the FRB domain (Ballou and Lin, 2008).

The inhibition of mTORC1 activity via the Rapamycin - FKBP12 complex suppresses mTOR mediated translation and synthesis, eventually resulting in anticancer effects (Dancey, 2005) and therefore rapamycin has been studied for use as an anti-cancer agent in a large variety of cancer cell lines in culture and syngeneic and xenogeneic tumours in mice (Neshat et al., 2001, Wu et al., 2005, Mosley et al., 2007). However as with all immunosuppressive medications, in theory, rapamycin could decrease a patient's naturally anticancer activity and allow some cancers that would have been naturally destroyed to proliferate (Gallagher et al., 2010).

1.15 Autophagy

Autophagy is a catabolic process involving the controlled self-degradation of cellular components, varying from individual proteins (microautophagy) to entire organelles (macroautophagy). Autophagy arbitrates recycling of damaged or redundant cellular materials to provide an important source of substrates for energy production during periods of nutrient stress (He and Klionsky, 2009). It is essential for cell degradation in mammalian cells as cells degrade incompletely when autophagy is inhibited (Berry and Baehrecke, 2008), however a recent study suggests that autophagy might also cause cell death (Denton et al., 2012). The autophagic pathway can be activated in mammalian cells by growth factor deprivation, nutrient starvation, hypoxia, DNA damage, protein aggregation or damaged organelles (Kroemer et al., 2010) and it can also be activated as part of the process of Type I programmed cell death (apoptosis) (Shintani and Klionsky, 2004). In the salivary glands, autophagy is necessary for efficient salivary gland protein secretion (Anding and Baehrecke, 2015).

The primary morphological difference between the three types of autophagy is the site of sequestration. The macroautophagy process works by sequestering and delivering cargo, such as unused long-lived

proteins, in a double membrane vesicle called an autophagosome to the lysosomes (the primary organelle for degradation in eukaryotic cells) (Hands et al., 2009). Autophagosome formation is initiated by the PI3K signalling pathway and the autophagy-related gene (Atg) (Baehrecke, 2005). The outer membrane of the autophagosome fuses in the cytoplasm with a lysosome to form an autophagolysosome, where the organelle contents are degraded via the lysosome's acidic hydrolases (Ohsaki et al., 2010).

The microautophagy process, on the other hand, does not involve an intermediate transport vesicle; rather divisions of cytosol or entire organelles are sequestered directly at the surface of the degradative organelle, with the lysosome directly engulfing cytoplasm either by invagination of the limiting membrane, protrusion of arm-like structures or by septation (Klionsky, 2003).

A third form of autophagy, chaperone-mediated autophagy (CMA), functions via lysosomes that target a soluble pool of cytosolic proteins for selective degradation (Majeski and Dice, 2004). Cytosolic proteins with a CMA-targeting motif bind to a receptor protein, the lysosome-associated membrane protein type-2A (LAMP-2A). Following protein

unfolding and translocation across the lysosome membrane, the proteins are degraded within the hydrolase-rich lumen. In CMA, the substrate/chaperone complex is translocated across the lysosome membrane singularly, as opposed to the sequestration/engulfment of substrates in bulk during macroautophagy and microautophagy (Hands et al., 2009).

1.16 mTOR and Autophagy

Autophagosomes are continuously formed and destroyed within the body, this is known as autophagic flux (Shen et al., 2011). mTOR can mediate this process because inhibition of mTORC1 strongly induces autophagosome formation (Noda and Ohsumi, 1998), as derived from the observation that rapamycin treatment induces autophagy in cells with mTOR already activated (Kamada et al., 2004). This is because mTORC1 is a known inhibitor of macroautophagy, from hereon referred to as autophagy, (Jung et al., 2010). Two recent studies, showed that mTORC1 negatively regulates autophagy by acting on Atg13 and Atg1 homologues (Jung et al., 2009, Hosokawa et al., 2009), which are responsible for the induction of autophagy initiation (Chen and Klionsky, 2011). In the salivary glands, autophagy is necessary for

efficient salivary gland protein secretion (Anding and Baehrecke, 2015) exhibited in Figure 1.12.

The inhibition of mTOR to induce autophagy has been used in irradiated glands to restore salivary gland function and reestablish glandular homeostasis (Morgan-Bathke et al., 2014). In such autophagic processes, vesicle elongation and completion is mediated by the conjugation of LC3 (mammalian Atg8) to phosphatidylethanolamine (PE) (Denton et al., 2012).

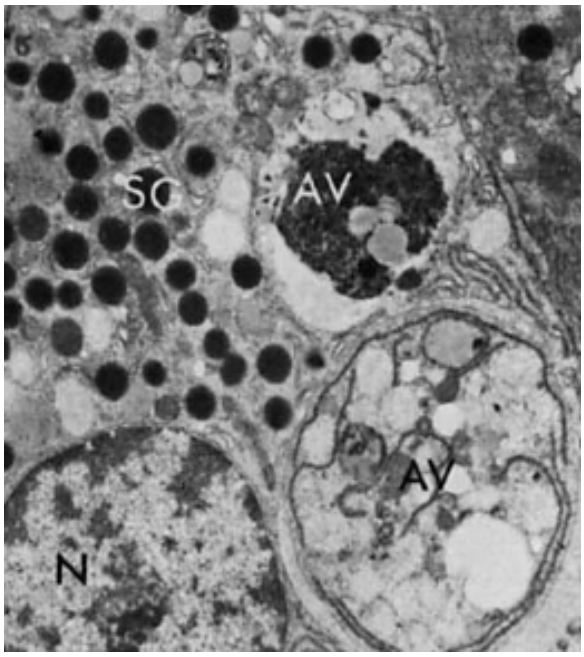

Figure 1.12 Electron Microscope image of autophagy in parotid glands. The nucleus (N) is present, whilst numerous secretory granules have filled the cytoplasm (SG) and large autophagic vacuoles have appeared (AV). X5900 (photograph from (Oliver et al., 1979))

LC3 is cleaved at its C terminus by Atg4 to form LC3-I, which is conjugated by Atg3 to PE to form LC3-II. LC3-II is correlated with the number of autophagosomes at any given time (Tanida et al., 2008) as the half of life LC3-II is short because LC3-II itself is degraded by autophagy. Therefore tracking the conversion of LC3-I to LC3-II by Atg3 is useful to monitor autophagic activity in salivary glands (Silver et al., 2010).

1.17 mTOR in Salivary Glands

As stated earlier, rapalogs have been used to induce autophagy in irradiated mice to restore salivary gland function and reestablish glandular homeostasis, (Morgan-Bathke et al., 2014). But there has also been extensive research into the functions of mTOR in the salivary glands by our group, such as the finding that activation of mTOR coincides with autophagy during salivary gland atrophy (Silver et al., 2010). Irradiated salivary gland tissues also exhibit activation of mTOR (Iglesias-Bartolome et al., 2012, Finkel, 2012), however inhibition of mTOR in salivary glands has been found to reduce angiogenesis - a complex biological process involved in tumorigenesis and tumour progression (Yu et al., 2014).

Diegel et al found that, in the mouse model, the inactivation of tumour suppressing genes adenomatous polyposis coli (negative regulator of Wnt signalling) and Pten (negative regulator of the mTOR pathway) caused the development of carcinomas in the salivary glands, with 100% penetrance and an extraordinary morphological similarity to human acinar cell tumours (Diegel et al., 2010). Furthermore, analysis of all tumour types revealed increases in PI3K, Akt and mTOR expression in comparison with normal salivary gland control tissue (Ettl et al., 2012), concluding that mTOR signalling is active in salivary gland cancers (Ettl et al., 2012) and that the mTOR pathway is not normally active in healthy salivary glands. However, inhibiting mTOR in human salivary duct carcinomas has not yet produced prolific results as a treatment method, suggesting that additional studies of mTOR inhibition-based treatments in salivary glands are warranted (Piha-Paul et al., 2011).

1.18 Aims

Despite some initial studies finding a bridge between mTOR expression and salivary gland cancers (Ettl et al., 2012, Iglesias-Bartolome et al., 2012, Finkel, 2012), the role of mTOR in atrophic salivary glands, or during their regeneration, remains unclear. Therefore the overall aim of this project is to observe and possibly identify the role of mTOR in salivary gland atrophy and regeneration.

Our group has previously established a baseline for this study by observing such mechanisms, whereby the activation of mTOR correlated with the loss of protein translation and autophagic consumption (Silver et al., 2010). Therefore the first objective of this study will be to further build upon these previous findings and characterise the functions of mTOR in duct ligation induced salivary gland atrophy by examining the effects of blocking mTOR activation during ligation-induced atrophy in mice, to determine whether mTOR activation helps prevent atrophy or exacerbates atrophic processes.

Once these characteristics are established, the purported regenerative effects of blocking mTOR will be observed in salivary glands. Therefore the second objective will be to examine the effects of mTOR inhibition,

via several schedules of rapamycin administration, during ductal deligation induced regeneration of the salivary glands in mice.

Determining the effects of mTOR, and its inhibition, are important in mice as they allow us to discover the role of mTOR in enabling gland regeneration. The findings can then be used as a baseline to compare to humans to assess if mTOR activation occurs in human salivary tissues and whether it is an important pathway in human salivary gland atrophy and regeneration. Therefore the third, and final, objective of this project will be to determine the relevance of mTOR activity in human salivary gland disease / atrophy.

CHAPTER 2

MATERIALS AND METHODS

2.1 Animals

All experimental procedures were conducted on adult female ICR mice that were obtained from Charles Rivers Laboratories (Margate, UK), weighing an average of 20-25g.

On arrival mice were housed in groups of eight, with food and water provided ad libitum. A 12 hour light- dark cycle was maintained and a constant temperature of 20-22°C. Environmental enrichments (tunnels, chewing sticks & nesting material) were provided in each cage. Animals were allowed to acclimatize to their new environment for 1 week prior to experimental procedures.

All animal studies and procedures were conducted in accordance with UK Home Office Animal (Scientific Procedures) Act 1986.

2.2 Experimental Design

The mice were designated in to three labels: The control groups, the ligation groups and the de-ligation groups (Figure 2.1). The control groups were either unoperated controls, receiving drug vehicle for 3 days or receiving only drug injections for 3 days.

The ligation groups underwent unilateral submandibular excretory duct ligation surgery under recovery anaesthesia for either 3, 5 or 7 days, or underwent surgery whilst also receiving mTOR inhibiting drugs for 3, 5 or 7 days post surgery.

The de-ligation groups underwent ductal de-ligation under recovery anaesthesia for 7 days following unilateral submandibular excretory duct ligation surgery for 7 days, or underwent de-ligation whilst also receiving mTOR inhibiting drugs during either ligation, de-ligation or throughout.

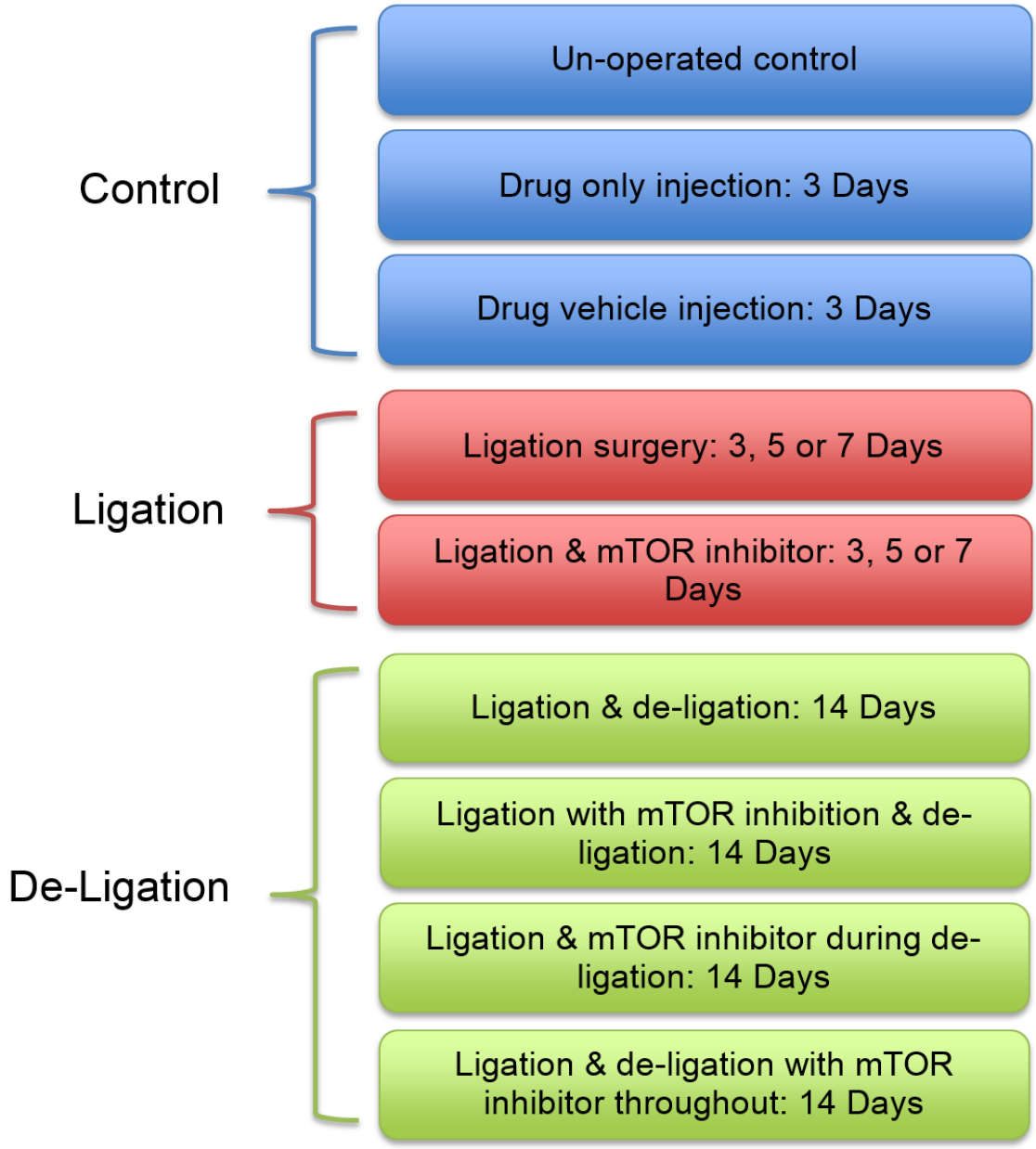

Figure 2.1 The experimental design branched into control, ligation and de-ligation groups.

2.3 Submandibular Duct Ligation & De-ligation Surgery

The mice were weighed and anaesthetized with xylazine (5mg/Kg) /ketamine (25mg/Kg) i.p injections, and placed on a controlled heating pad to maintain the body temperature. The depth of anaesthesia was assessed by pedal reflex.

Held in the supine position with the neck extended, a skin incision ~0.5 cm long was made in the midline of the neck (on the medial side of the angle of the mandible), the fat surrounding the salivary glands was cleared via blunt dissection and subsequently the left submandibular gland duct was isolated (Figure 2.2). The left submandibular excretory duct was ligated using a 6-0 Ethicon suture (Johnson and Johnson Intl, Brussels, Belgium). For de-ligation surgery, the submandibular glands were de-ligated (under recovery anaesthesia).

After surgery on the main secretory duct, the neck was sutured. The mice were allowed to recover from anaesthesia in a cage maintained in a warm room and were administered analgesics (buprenorphine, 10 μg/kg) post surgery.

Aseptic conditions were used throughout the surgical procedure of duct ligation and de-ligation to reduce the risk of infection. Animal body weights were recorded daily. Mice were sacrificed by an overdose of pentobarbitone and cervical dislocation.

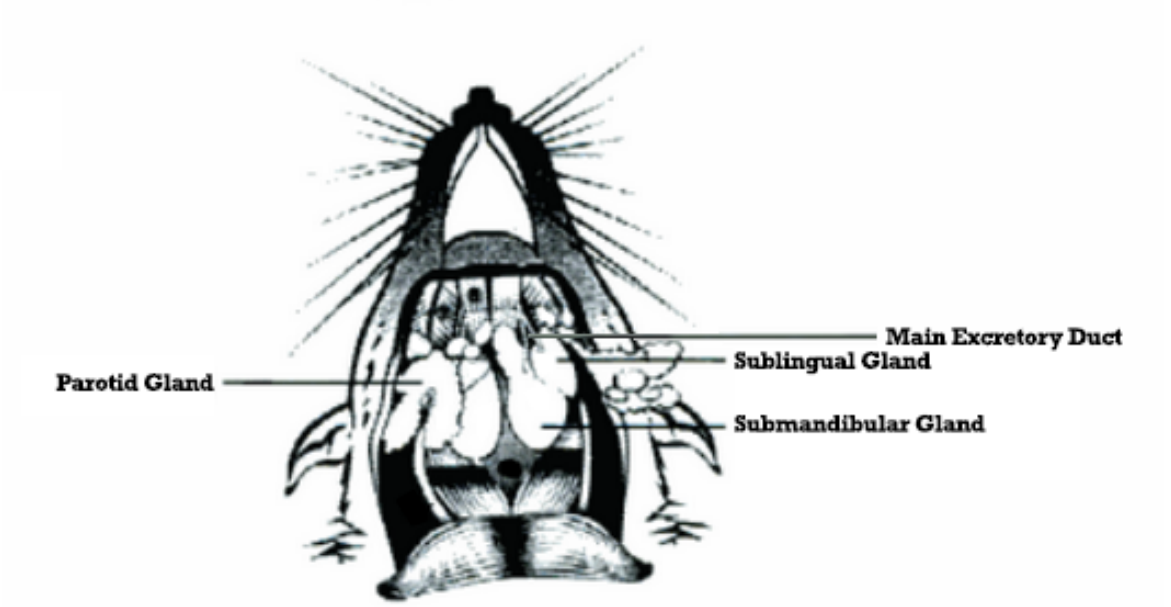

Figure 2.2 Animated diagram depicting salivary glands in mice showing positions of major salivary glands after dissection of surrounding connective tissue (Adapted from Van Valckenborgh, 2005).

2.4 Rapamycin treatment

Rapamycin was resuspended in a stock solution at 20 mg/ml in DMSO and stored at -20 °C until used. For vehicle controls, animals were

injected (*s.c.*) with 200 μl of rapamycin injection vehicle (10 % polyethylene glycol 400 and 17 % tween-80).

The experimental groups received *subcutaneous (s.c.)* injections, each injection consisted of 5 mg/kg/day of Rapamycin diluted in 200 μl of injection vehicle (10 % polyethylene glycol 400 and 17 % tween-80), all as previously demonstrated by (Liu et al., 2007). This particular dose was chosen because of the efficacy and comparative effectiveness of the inhibition of mTOR signaling by rapamycin shown in previous studies (Hu et al., 2011, Shillingford et al., 2010), furthermore, in preparatory undertakings for this study, this was found to be the maximum dose without seeing significant body weight loss.

No toxicity or adverse effects of the compound were identified in this experiment, in accordance with previous rapamycin studies (Banerjee et al., 2011, Shillingford et al., 2010).

2.5 Tissue Collection

At the end of experiments, the submandibular glands were removed, weighed and cut into two sections. One section was snap frozen in

liquid nitrogen and stored in -80°C freezer for biochemical measurements and the other section of gland was fixed in 4% formalin.

Contralateral submandibular glands from the experimental mice were not collected as standard of control, as they experience compensative hyperplasia when the other gland is extirpated or ligated (Walker and Gobe, 1987, Schwartz-Arad et al., 1991).

2.6 Histochemical Staining of Tissue Sections

Submandibular gland tissues were fixed in 4% formalin for 24 hours, then processed in ascending alcohols and then embedded in paraffin wax. Sections at 5 μm thick were cut and mounted on super-frost plus-coated slides.

Following overnight incubation at 37°C, slides underwent the following de-waxing procedures: 5 minutes incubation in xylene followed by a second xylene incubation for 10 minutes, 3 incubations (3 minutes each) in 100% industrial methylated spirit, and a final 5 minutes rinsing in running water.

2.6.1 Haematoxylin and Eosin Staining

General morphology of the tissue sections was assessed by haematoxylin and eosin (H&E) staining. For this method, tissue sections were stained with Mayer's Haematoxylin (Thermo Fisher Scientific, Leicestershire, UK) for 3-5 minutes, washed in running water (2 minutes), differentiated (de-stain) with 1% acid alcohol and then stained with 1% Eosin solution (VWR International, Leicestershire, UK) for 1-3 minutes (H& E staining). Then the slides were dehydrated, air-dried, cleared and mounted.

2.6.2 Alcian Blue Periodic Acid Schiff's Staining

The secretory granules inside the acinar cells were demonstrated by Alcian Blue/periodic acid Schiff's reagent (AB/PAS) staining.

Following de-waxing slides were washed in distilled water and placed into a 0.05% Alcian Blue solution for 10 minutes then washed in running tap water for 2 minutes. Slides were then briefly rinsed in

distilled water, oxidised with 1% Periodic Acid (Sigma-Aldrich, Gillingham, UK) for 10 minutes, and then incubated with Schiff's reagent (VWR International, Leicestershire, UK) for 30 minutes. AB/PAS stained the acidic mucins blue and the neutral mucins magenta. The nuclei were stained with haematoxylin for 2 minutes then washed with running water for 2 minutes and differentiated with 1% acid alcohol. Rinsed in warm water, then cold water. Then the slides were dehydrated, air dried for 15 minutes, cleared and mounted.

2.6.3 DMAB Staining

Granular ductal kallikreins were stained using dimethylaminobenzaldehyde (DMAB) nitrite reaction for tryptophane (DMAB) staining, as previously demonstrated by (Silver et al., 2010). Freshly cut samples were incubated on a hot plate for 30 minutes and underwent the de-waxing procedure as described above. Samples were treated in DMAB- HCl solution for 1 minute, drained for 1 minute, then transferred to the sodium nitrite- HCl for 1 minute with continuous agitation, washed in water for 30 seconds, de-stained in 1% acid alcohol for 15 seconds and counter stained in neutral red solution for 5

minutes. Using blotting paper, sections were blotted. Dehydrated, air dried for 15 minutes, cleared and mounted.

2.7 Immunohistochemistry

Prior to the immunohistochemical staining, tissue sections were de-waxed, dehydrated in absolute xylene and then through Industrial Methylated Spirits (IMS) solutions. Sections were rehydrated with distilled water and treated with 3% hydrogen peroxide, to quench the endogenous peroxidase, for 10 minutes. Preheated citric acid buffer solution (pH 6.0) was used as an antigen retriever to unmask formalin meshwork covering antigens of interest. Sections were allowed to cool down in cold tap water and incubated with 2% bovine serum albumin (BSA) to avoid nonspecific binding and incubated with the primary antibody of interest, to investigate the localisation of mTOR substrates, at room temperature overnight.

5 minute washes with 1% tween tris buffer saline (TBS-T) were applied before incubating sections with secondary biotinylated antibodies for 30 minutes (Dako UK). Sections were incubated with streptavidin biotin complex horseradish peroxidase (StreptABC-HRP; Vector Laboratories.

UK) for a further 30 minutes. The peroxidase activity was visualized with diaminobenzidine tetrahydrochloride (DAB; Sigma-Aldrich, Gillingham, UK) (0.5 mg / ml) after 10 minutes of DAB incubation, counter stained with Mayer's haemotoxylin and eosin (nuclear counterstain) for 30 seconds.

2.8 Morphometric Analysis

From the submandibular gland samples prepared for histochemical staining, 20 acini per sample were selected and the mean area (μm^2) measured using Leica TCS SP2 confocal microscope software version 2.1 (Leica Microsystems Heidelberg).

2.9 Gland Homogenates

Approximately 0.01mg of previously frozen (-80°C) gland tissues were homogenized in the homogenizing buffer solution (1 % Triton X-100, 1 mM EDTA, and a 1 % v/v dilution of protease inhibitor cocktail set 1 (Merck Chemicals Ltd, Nottingham, UK) using an Ultra-Thurrax homogenizer (IKA Labortechnik, Staufen, Germany).

Samples were centrifuged and the supernatants were collected. Tissue lysates were prepared under reducing condition (Dithiothreitol (DTT) 0.5 M, 1:10) and NUPAGE® LDS (Invitrogen, Paisley, UK) at a 1:4 ratio of final volume.

Tissue lysates were then boiled at 100°C for 5 minutes and electrophoresed in order to allow cellular proteins to be separated based on their molecular weight on a 4-12% SDS-PAGE gel (NUPAGE Novex Bis-Tris 4-12 % gel; Life technologies, Paisley, UK) according to manufacturer's protocol.

Proteins resolved by electrophoresis were then electroblotted onto 0.45 μm nitrocellulose membranes (Anderman and Co., Kingston-Upon-Thames, UK).

2.10 Protein concentration assay

Submandibular gland tissue homogenates protein concentrations were determined using BCA Assay (Thermo Scientific, IL, USA) in 96 multiwell plate according to manufacturer's instructions. Homogenates were assessed at a dilution of 1 : 100. Results were derived from a

standard curve generated using Bovine Serum Albumin (BSA) serial dilution incubated at the same time and protein concentrations were determined.

2.11 Periodic Acid Schiff Staining

Periodic acid Schiff (PAS) technique was used to detect and assess glycoproteins (Nerve Growth Factors and Epidermal Growth Factors). After electrophoreses the gel was fixed in 25 % methanol and 10 % glacial acetic acid for 60 minutes, washed in water for 20 minutes, incubated in 2% periodic acid for 15 minutes, rinsed with double distilled water. Schiff reagent (VWR, Leicestershire, UK) was incubated in the dark with gentle agitation for up to 60 minutes or until pink stained bands appeared.

2.12 Immunoblotting

The proteins were transferred from the gel on to nitrocellulose membrane in NUPAGE® transfer buffer (Invitrogen, Paisley, UK) plus 10% methanol according to manufacturer's protocol, they were stained with Fluorescein Isothiocyanate (Sigma-Aldrich, Missouri, USA) (0.1mg/ml), to check whether the protein transfer was achieved.

The membranes to be probed for specific proteins were either blocked overnight in PBS with 10% milk power (pH 7.2; Marvel, Spalding, UK) at 4°C or blocked for 60 minutes in tween tris buffered saline (TBS-T) (20mM TRIS, 150mM NaCI, .1% Tween-20, pH 7.6), in order to minimise the non-specific binding of the antibodies to the membrane. The membranes were washed three times (5 minutes each) in TBS-T or 0.05% tween 20 in PBS (PBS-T). Primary antibodies, which are specified in Table 2.1, were diluted according to manufacturer's guidelines in TBS-T or 1% skimmed milk in PBS. The membranes were then allowed to incubate in the primary antibody for 60 minutes at room temperature or overnight at 4°C. The following morning, the membranes were washed 3 times (5 minutes each) in TBS-T or Phosphate Buffered Saline with 0.05% Tween 20 (PBS-T). The membranes were then incubated for 60 minutes at room temperature with the relevant HRP-linked secondary antibody. Secondary antibodies included polyclonal goat anti-mouse immunoglobulin-HRP (P0447) and polyclonal goat anti-rabbit immunoglobulin-HRP (P0448) from Dako Ltd (Ely, UK). The membranes were washed more three times (5 minutes each) in TBS-T or PBS-T prior to development by enhanced chemiluminescence.

The substrate for developing colour reaction were added to membranes, which were then placed in the ChemiDoc ™ Imaging System (BIORAD Laboratories Ltd, Hertfordshire, UK) to obtain images of the protein bands, utilising optimised exposure times and the ChemiDoc ™ Imaging System's built-in high-sensitivity blot detection which highlights over-saturated pixels, in order to obtain ideal exposure in images of the protein bands. Band intensity from immunoblots were quantified using the image analysis software ImageJ version 1.46 (NIH, Maryland, USA), with each bar representing the mean normalized from the ratio of β-actin ±SEM.

Table 2.1 Primary antibodies used in immunoblotting protocol.

Antibody	Dilution	Source
Rabbit Anti-human / mouse p4E-BP1	1 : 1000	Cell Signaling Technology (Hertfordshire, UK)
Rabbit Anti-human / mouse pS6RP	1 : 1000	Cell Signaling Technology (Hertfordshire, UK)
Rabbit Anti-human / mouse mTOR	1 : 1000	Cell Signaling Technology (Hertfordshire, UK)
Mouse Anti-human / mouse β-actin	1 : 4000	Sigma –Aldrich (MO, USA)
Rabbit Anti-human LC3	1 : 1000	MBL International (MA, USA)
Rabbit Anti-human / mouse ATG3	1 : 1000	MBL International (MA, USA)
Rabbit Anti-human / mouse ATG5	1 : 1000	MBL International (MA, USA)

2.13 Densitometry

Immunoblot images were imported into the image analysis software Image J version 1.46 (NIH, MD, USA) for quantification of the band intensity, as per the Image J software guide (Ferreira and Rasband, 2012). Bands were from 3 to 5 animals per treatment group and the time points were normalised to their loading control, as a precursor to being displayed as a ratio to the loading control (β-actin) ±SEM.

2.14 Statistical Analysis

Results were expressed as mean ± standard error of the mean (SEM), and n represents the number of mice per experiment. Statistical comparisons were student's t-test; whereby $p<0.05$ was considered statistically significant. Data analysis was performed with Microsoft Excel 2011 (Microsoft, Redmond, WA).

Citation: Cell Death and Disease (2014) 5, e1146; doi:10.1038/cddis.2014.108

www.nature.com/cddis

CHAPTER 3

RAPAMYCIN DELAYS SALIVARY GLAND ATROPHY FOLLOWING DUCTAL LIGATION

S S Bozorgi, G B Proctor and G H Carpenter

3.1 Foreword

The authors would like to acknowledge that this chapter has been previously published in Cell Death & Disease, in issue 3 of volume 5, from the Nature Publishing Group. Sophie Bozorgi, as first author, wrote the manuscript, collected and assembled data, performed data analysis and interpretation, as well as final approval of manuscript. Gordon Proctor contributed with conception and design, as well as final approval of manuscript. Guy Carpenter contributed with conception and design, provision of study material, data analysis and interpretation, and final approval of manuscript. Furthermore the authors would like to gratefully acknowledge the support of the Newland Pedley Studentship in Dental Research for financial support.

For the purposes of maintaining the original publishing's integrity and for copyright reasons, this chapter has been added to this PhD thesis with minimal editing and retains the same formatting, as edited by Dr Anastasis Stephanou from Cell Death & Disease.

3.2 Abstract

Salivary gland atrophy is a frequent consequence of head and neck cancer irradiation therapy but can potentially be regulated through the mammalian target of rapamycin (mTOR). Excretory duct ligation of the mouse submandibular gland provokes severe glandular atrophy causing activation of mTOR. This study aims to discover the effects of blocking mTOR signaling in ligation-induced atrophic salivary glands. Following 1 week of unilateral submandibular excretory duct ligation: gland weights were significantly reduced, 4E-BP1 and S6rp were activated, and tissue morphology revealed typical signs of atrophy. However, 3 days following ligation with rapamycin treatment, a selective mTOR inhibitor, gland weights were maintained, 4E-BP1 and S6rp phosphorylation was inhibited, and there were morphological signs of recovery from atrophy. However, following 5 and 7 days of ligation and rapamycin treatment, glands expressed active mTOR and showed signs of considerable atrophy. This evidence suggests that inhibition of mTOR by rapamycin delays ligation-induced atrophy of salivary glands.

Published in Cell Death and Disease (2014), Volume 5 on 27 March 2014.

3.3 Introduction

Approximately 500 000 people worldwide are diagnosed with head and neck cancer every year (Jemal et al, 2009). Radiation therapy to the head and neck is a common treatment for such malignancies and salivary glands in the radiation field are severely damaged. Atrophy of the salivary glands is inevitable post radiation therapy and can also occur in autoimmune sialadenitis (Sjögren's syndrome) and obstructive sialadenitis. Patients experience reduced salivary flow, xerostomia, dental caries, mucosal infection, dysphagia, considerable discomfort and pain (Nagler et al, 2003, Vissink et al, 2003).

Salivary gland atrophy can be recreated experimentally in rodents via ligation of the main excretory duct of the submandibular gland, which creates a histological appearance comparable with that which occurs in humans (Cummins et al, 1994), which involves deletion of acinar cells through apoptosis (Takahashi et al, 2000) and autophagy (Harrison et al, 2000), as well as mitotic proliferation of ductal cells (Takahashi et al, 2000).

One potentially important mechanism of regulating atrophy in salivary gland and other tissues is through the mammalian target of rapamycin

(Mieulet et al, 2007); a highly conserved serine/threonine protein kinase which integrates cues from nutrients and growth factors, acting as a nexus point for cellular signals to control growth, metabolism and longevity. Activated mTOR regulates protein synthesis by phosphorylating ribosomal S6 kinase 1 (S6K1) and eukaryotic translation initiation factor 4E–binding protein 1 (4E-BP1) (Ma et al, 2009) at multiple sites (Herbert et al, 2002). Although in normal circumstances, mTOR is switched on in some tissues such as muscle and liver, it is normally switched off in salivary glands. mTOR is potentially instrumental in controlling acinar and ductal atrophy as it gets switched on after duct ligation-induced atrophy in the animal model (Silver et al, 2010), however the role of mTOR in ligation-induced atrophy of salivary glands is still not fully clear.

Rapamycin is a specific inhibitor of mTOR signaling that binds directly to the mTOR complex 1 (mTORC1) and suppresses mTOR-mediated phosphorylation of S6K1 and 4E-BP1 (Ma et al, 2009).

In the present study, rapamycin was used to study the effects of mTOR inhibition on duct ligation-induced salivary gland atrophy.

3.4 Methods and Materials

3.4.1 Submandibular duct ligation surgery

A total of 37 adult female ICR mice were obtained from Charles Rivers Laboratories (Margate, UK); weighing an average of 20–25 g upon arrival. On arrival mice were housed in groups of four, with food and water provided ad libitum. A 12 h light-dark cycle was maintained at a constant temperature of 20–22 °C. Environmental enrichments (tunnels and nesting material) were provided in each cage. Animals were allowed to acclimatize to their new environment for 1 week before experimental procedures. All animal studies and procedures were conducted in accordance with UK Home Office Animal (Scientific Procedures) Act 1986. The mice were weighed and anaesthetized with xylazine (5 mg/Kg) /ketamine (25 mg/Kg) i.p. injections, and placed on a controlled heating pad to maintain the body temperature. The depth of anesthesia was assessed by pedal reflex. Held in the supine position with the neck extended, a skin incision ~0.5 cm long was made in the midline of the neck (on the medial side of the angle of the mandible), the fat surrounding the salivary glands was cleared via blunt dissection and subsequently the left submandibular gland duct was isolated. The left

submandibular excretory duct was ligated using a 6-0 Ethicon suture (Johnson and Johnson Intl, Brussels, Belgium).

After ligation of the main secretory duct, the neck was sutured. The mice were allowed to recover from anaesthesia in a cage maintained in a warm room and were administered analgeics (buprenorphine, 10 μg/kg) post surgery. Aseptic conditions were used throughout the surgical procedure of duct ligation to reduce the risk of infection.

Submandibular gland samples were collected for analysis. The samples were designated in to groups: the control and experimental groups. The control groups were either unoperated controls (n=4), receiving drug vehicle for 3 days (n=4) or receiving rapamycin injections for 3 days (n=4). The experimental groups underwent unilateral submandibular excretory duct ligation surgery under recovery anaesthesia for either 3 (n=3), 5 (n=3) or 7 days (n=4), or they underwent surgery whilst also receiving 5 mg/kg per day of rapamycin (subcutaneous (s.c.)) for 3 (n=4), 5 (n=4) or 7 days (n=7) post surgery.

At the end of experiments, submandibular glands were removed, weighed and tissues were either fixed in 4% formalin overnight or snap frozen in liquid nitrogen for biochemical analysis.

Contralateral submandibular glands from the experimental mice were not collected as controls, as they experience compensative hyperplasia when the other gland is extirpated or ligated (Walker et al, 1987, Schwartz-Arad et al, 1991).

Animal body weights were recorded daily. Mice were sacrificed by an overdose of pentobarbitone.

3.4.2 Rapamycin treatment

Rapamycin was resuspended in a stock solution at 20 mg/ml in DMSO and stored at −20 °C until used. For vehicle controls, animals were injected (s.c.) with 200 µl of rapamycin injection vehicle (10% polyethylene glycol 400 and 17% tween-80). The experimental groups received s.c. injections, each injection consisted of 5 mg/kg per day of Rapamycin diluted in 200 µl of injection vehicle (10% polyethylene glycol 400 and 17% tween-80), all as previously demonstrated (Liu et al, 2007). This particular dose was chosen because of the efficacy and comparative effectiveness of the inhibition of mTOR signaling by rapamycin as shown in previous studies (Hu et al, 2011, Shillingford et

al, 2010), furthermore, in preparatory undertakings for this study, this was found to be the maximum dose without seeing significant body weight loss. No toxicity or adverse effects of the compound were identified in this experiment, in accordance with the previous rapamycin studies (Shillingford et al, 2010, Banerjee et al, 2011).

3.4.3 Histochemical staining of tissue samples

Submandibular glands were embedded in wax and 5 μm thick sections were cut and mounted on super-frost plus-coated slides.

General morphology of the tissue sections was assessed by H&E staining. The secretory granules inside acinar cells were identified by AB/PAS staining. Granular ductal kallikreins were stained using DMAB, as previously demonstrated (Silver et al, 2010).

3.4.4 Morphometric analysis

From the submandibular gland samples prepared for histochemical staining, 20 acini per sample were randomly selected and the mean area

(μm2) was measured using Leica TCS SP2 confocal microscope software version 2.1 (Leica Microsystems, Heidelberg, Germany).

3.4.5 Tissue preparation and immunoblotting

Tissue specimens stored at −80 °C were homogenized in 19 volumes (wt/vol) of ice-cold homogenization buffer (1% Triton X-100, 1 mM EDTA, and a 1% v/v dilution of protease inhibitor cocktail set 1 (Merck Chemicals Ltd, Nottingham, UK) using an Ultra-Thurrax homogenizer (IKA Labortechnik, Staufen, Germany).

SDS-PAGE of samples was carried out (NUPAGE Novex Bis-Tris 4–12% gel; Life technologies, Paisley, UK). Proteins resolved by electrophoresis were then electroblotted onto 0.45 μm nitrocellulose membranes (Anderman and Co., Kingston-Upon-Thames, UK).

The procedure followed for immunoblotting is that which has been previously established (Carpenter et al, 2004). Membranes were imaged in a ChemiDoc Imaging System (BIORAD Laboratories Ltd, Hertfordshire, UK), with optimized exposure times and the built-in

high-sensitivity blot detection which highlights over-saturated pixels, to obtain ideal exposure in images of the protein bands.

Band intensity from immunoblots were quantified using the image analysis software ImageJ version 1.46 (NIH, Maryland, MD, USA), with each bar representing the mean normalized from the ratio of β-actin ±S.E.M.

3.4.6 Antibodies

Anti-phospho-4E-BP1 (1 : 1000 for western blotting), anti-phospho-S6 ribosomal protein (1 : 1000 for western blotting), anti-mTOR (1 : 1000 for western blotting) were obtained from Cell Signaling Technology (Hertfordshire, UK) and anti-β-actin was from Sigma–Aldrich (St. Louis, MO, USA). Secondary antibodies included polyclonal goat anti-mouse immunoglobulin-HRP (P0447) and polyclonal goat anti-rabbit immunoglobulin-HRP (P0448) from Dako Ltd (Ely, UK).

3.4.7 Periodic acid-Schiff's staining

PAS of glandular homogenates was used to assess glycoproteins. After electrophoreses the gel was fixed in methanol and acetic acid, incubated

in 1% periodic acid for 15 min, rinsed with double distilled water and stained with Schiff's reagent for up to 60 min.

3.4.8 Statistical analysis

Results were expressed as means±S.E.M., and were statistically compared by ANOVA followed by student's t-test; $P<0.05$ was considered statistically significant.

3.5 Results

3.5.1 Gland Weights

Mean submandibular gland weight was significantly reduced in the 3 day ligation group (0.040±0.001 g, n=3), compared with nonligated control mice (0.055±0.003 g, n=4). Following rapamycin treatment (0.056±0.002 g, n=4), mean gland weight was significantly (P=0.0008) greater compared with the ligation only group and was not different to unoperated controls. However, 5 day (0.040±0.005 g, n=3) and 7 day ligation (0.035±0.003 g, n=4) groups experienced a significant reduction compared with unoperated controls, which was not affected by rapamycin treatment (Figure 3.1).

All control groups showed similar gland weight measurements, with unoperated controls, rapamycin only and rapamycin vehicle-treated groups all showing no statistically significant difference.

By the end of the experiment, there was no statistically significant difference in body weight between experimental mice and the controls. For example, neither the 7 day ligation only (28.52±0.80 g, n=4) nor 7 day ligation with rapamycin treatment (31.47±1.18 g, n=7) differed

significantly (P=0.22) from unoperated control (31.20±1.49 g, n=4) mice body weights.

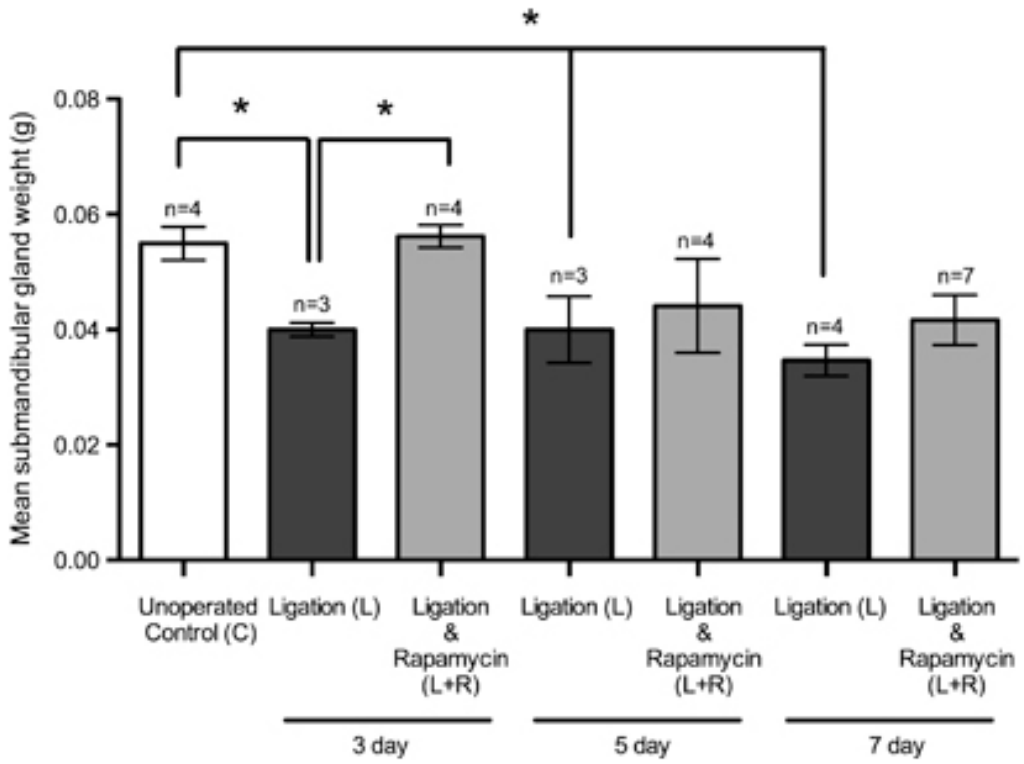

Figure 3.1 Mean Submandibular gland weights.
Mean submandibular gland weights were significantly (*P<0.05) reduced at 3, 5 and 7 day ligation only groups in comparison with unoperated controls. Post ligation surgery and 3 days of rapamycin treatment, the gland weights increased 40% greater than the ligation only group. Five days and seven days of rapamycin treatment post ligation did not significantly alter gland weights in comparison with their respective ligation only groups. Data is expressed as mean±S.E.M.

3.5.2 Complete inhibition of mTOR after 3 days of rapamycin treatment

Immunoblotting of phospho-S6 ribosomal protein, a downstream component of the mTOR substrate S6K1 in glandular homogenates revealed activation of S6K1 (and therefore activation of mTOR) in only the ligated state in the 3 day group. However, rapamycin treatment abolished this activation (Figure 3.2a and quantified in Figure 3.2c).

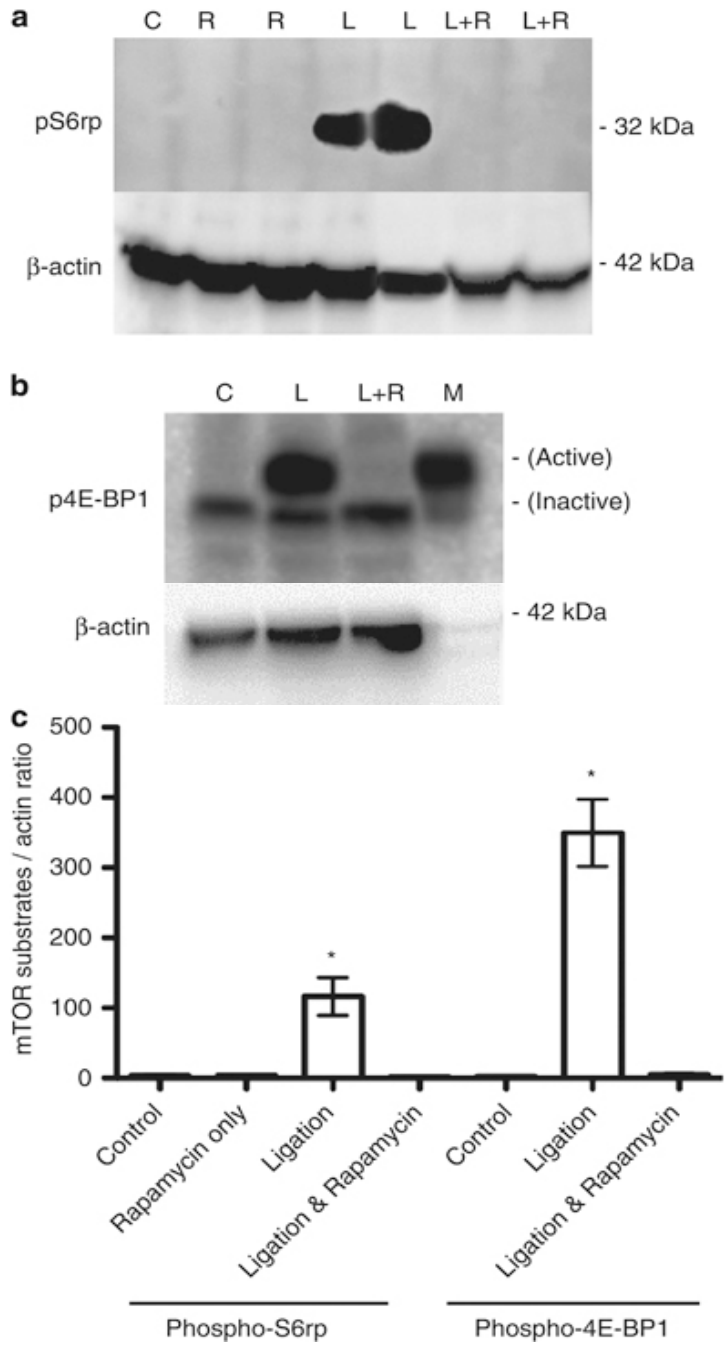

Figure 3.2 Immunoblotting of phospho-S6 ribosomal protein (pS6rp) (a) and phospho-4E-BP1 protein (b) expression in submandibular glands of 3 day groups. pS6rp showed no expression in controls (c) and rapamycin only (R). Presence of pS6rp indicates activation of mTOR in the ligated state (L) but rapamycin treatment post ligation (L+R) abolished this activation. Phospho-4E-BP1 protein expression in controls (c) showed an inactive isoform of 4E-BP1, whereas ligation (L) increased 4E-BP1 phosphorylation and therefore activation, indicating mTOR phosphorylation. Rapamycin treatment following ductal ligation (L+R) abolished this activation, as represented by a visible reduction back to the inactive isoform. Muscle homogenates (M) were used as a positive control. Beta actin (β-actin) was used as a loading control, however muscle homogenates showed absence of beta actin (β-actin) as muscle expresses α-smooth muscle actin (α-SMA). Densitometric analysis from the 3 day experiments (c) show pS6rp and p4E-BP1 phosphorylation as a ratio of β-actin, *P<0.05 in comparison with controls. The bars represent the mean±S.E.M., ANOVA (*P<0.05) data represents results from at least three different experiments.

Low expression of 4E-BP1 occurred, as the inactive isoform, in unoperated controls. Ligation revealed an increase in 4E-BP1 phosphorylation (and therefore activation of mTOR) in 3 day groups, as shown by the presence of a higher molecular weight band. Rapamycin treatment following ductal ligation abolished this activation, as represented by a visible reduction of isoforms (Figure 3.2b and quantified in Figure 3.2c). Rapamycin only treated glands showed no expression of mTOR activity, identical to unoperated controls.

3.5.3 Incomplete inhibition of mTOR during long term rapamycin treatment

Immunoprobing of phospho-S6 ribosomal protein expression on 3, 5 and 7 day samples indicated mTOR activation in the ligated state. However, whilst rapamycin treatment abolished this activation after 3 days; a small protein band remained visible following rapamycin treatment after longer periods of ductal ligation (Figure 3.3a and quantified in Figures 3.3c and 3.3d).

Duct ligation at 5 and 7 days increased 4E-BP1 protein expression and increased phosphorylation status compared with control, suggesting

mTOR activation. Following ligation and rapamycin treatment for 5 days glandular homogenates revealed incomplete reduction of hyperphosphorylated status in all four mice examined. Seven day glandular homogenates also showed a visible increase in 4E-BP1 in ligation and a reduction of all isoforms post rapamycin treatment, however the upper isoform was only slightly reduced following rapamycin treatment (Figure 3.3b and quantified in Figures 3.3c and 3.3d). Rapamycin only treated glands showed no expression of mTOR substrate activity, identical to unoperated controls.

Western blotting of total mTOR in submandibular glands (Figure 3.3e and quantified in Figure 3.3f) showed a marked increase in mTOR presence in ligated glands at all time points in comparison with controls. Rapamycin treatment greatly reduced total mTOR protein expression, but did not completely inhibit the presence of mTOR.

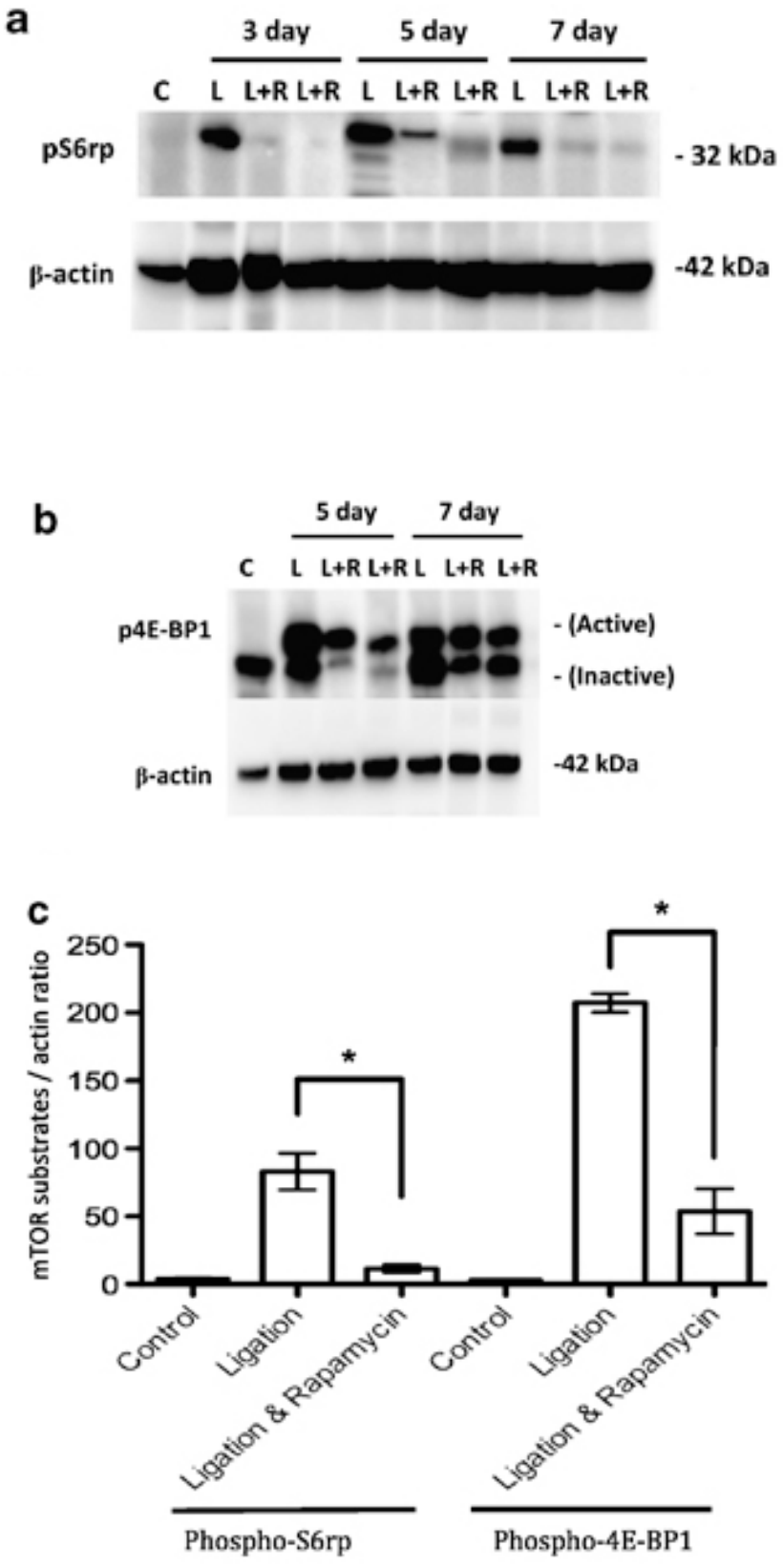

Figure 3.3 continues on the following page

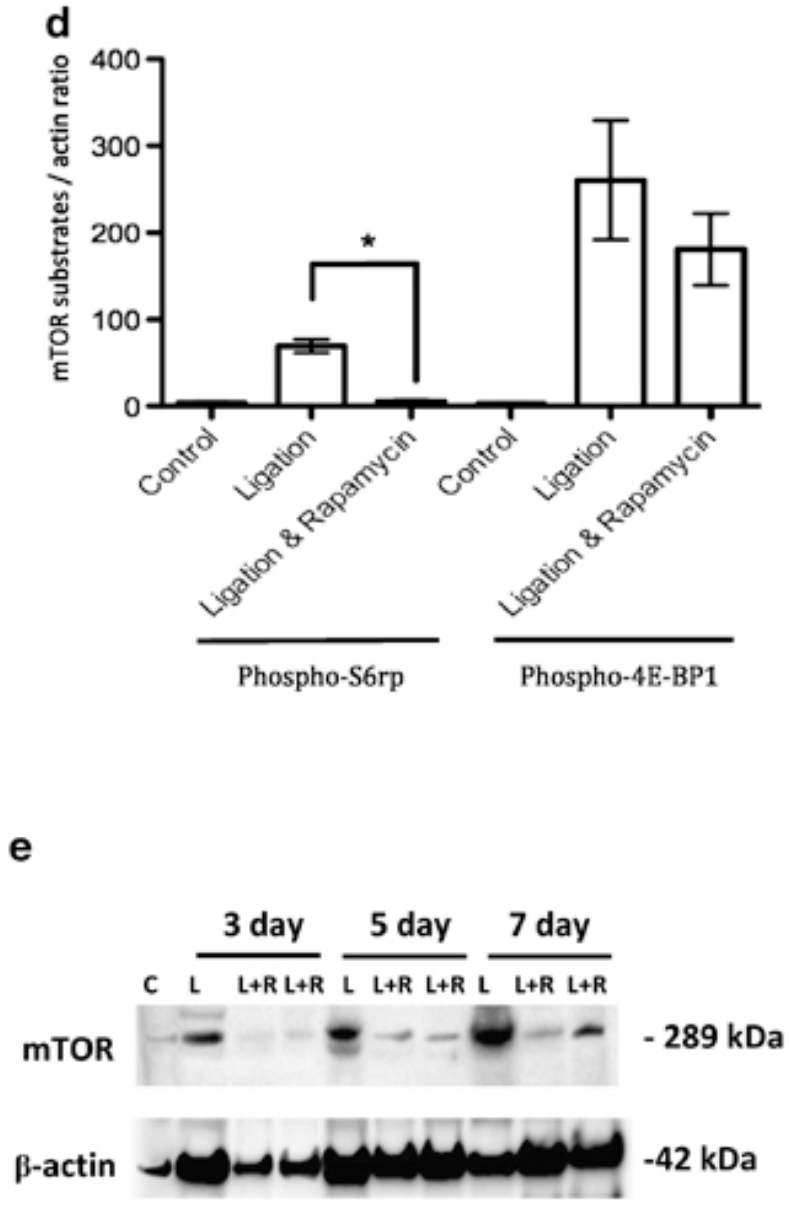

Figure 3.3 continues on the following page

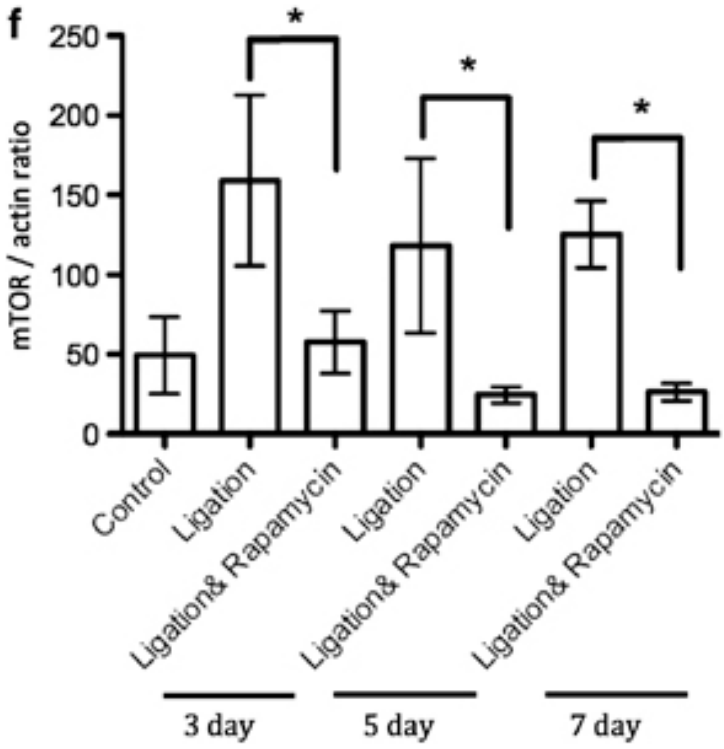

Figure 3.3 Immunoblotting of phospho-S6 ribosomal protein (pS6rp) (a) and phospho-4E-BP1 protein (b) expression in submandibular glands during the longer 5 and 7 day periods of ligation and ligation with rapamycin treatment. pS6rp expression was abolished after 3 day rapamycin treatment post ductal ligation (L+R) hence inhibiting mTOR expression. Five and seven day ligated (L) glandular homogenates revealed increased pS6r-protein expression. Rapamycin treatment during ductal ligation showed a visible reduction but not complete abolishment of expression at 5 and 7 days, indicating incomplete inhibition of mTOR. Phospho-4E-BP1 protein expression experienced a marked increase (the activated isoform bands), after ligation (L) for 5 and 7 days, indicating phosphorylation of mTOR. Rapamycin treatment following ductal ligation (L+R) on 5 day showed a visible reduction of isoforms but not complete return to inactive isoform bands, indicating incomplete inhibition of mTOR, whereas 7 day ligation with rapamycin treatment revealed no visible reduction of 4E-BP1 protein expression. Densitometric analysis from the 5 (c) and 7 day experiments (d) show pS6rp and p4E-BP1 phosphorylation as a ratio of β-actin (*P<0.05). Protein expression of total mTOR in submandibular glands (e) in unoperated control, ligated and ligated with rapamycin-treated mice at increasing time points. Rapamycin treatment reduces total mTOR protein expression but does not completely inhibit mTOR, correlating with the pS6rp and 4E-BP1 protein expressions. Densitometric analysis showing mTOR expression as a ratio of β-actin (f) (*P<0.05). The bars represent the mean±S.E.M. Beta actin (β-actin) was used as a loading control. Data represents results from at least three independent experiments.

3.5.4 Short term rapamycin treatment rescues acinar atrophy

Periodic acid-Schiff's (PAS) staining of glandular homogenates indicated significant loss of acinar mucin with ligation at all time points (Figure 3.4). The 3 day ligation with rapamycin group showed only partial loss of mucin. Whereas 7 day rapamycin and ligation groups experienced complete loss of mucin, even post rapamycin treatment (Figure 3.4a). Five day groups experienced variable results with partial loss of mucin in some animals (Figure 3.4b) and a complete loss in other animals.

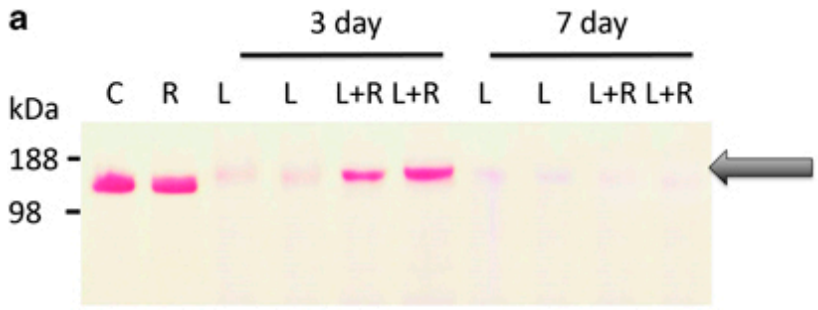

Figure 3.4 continues on the following page

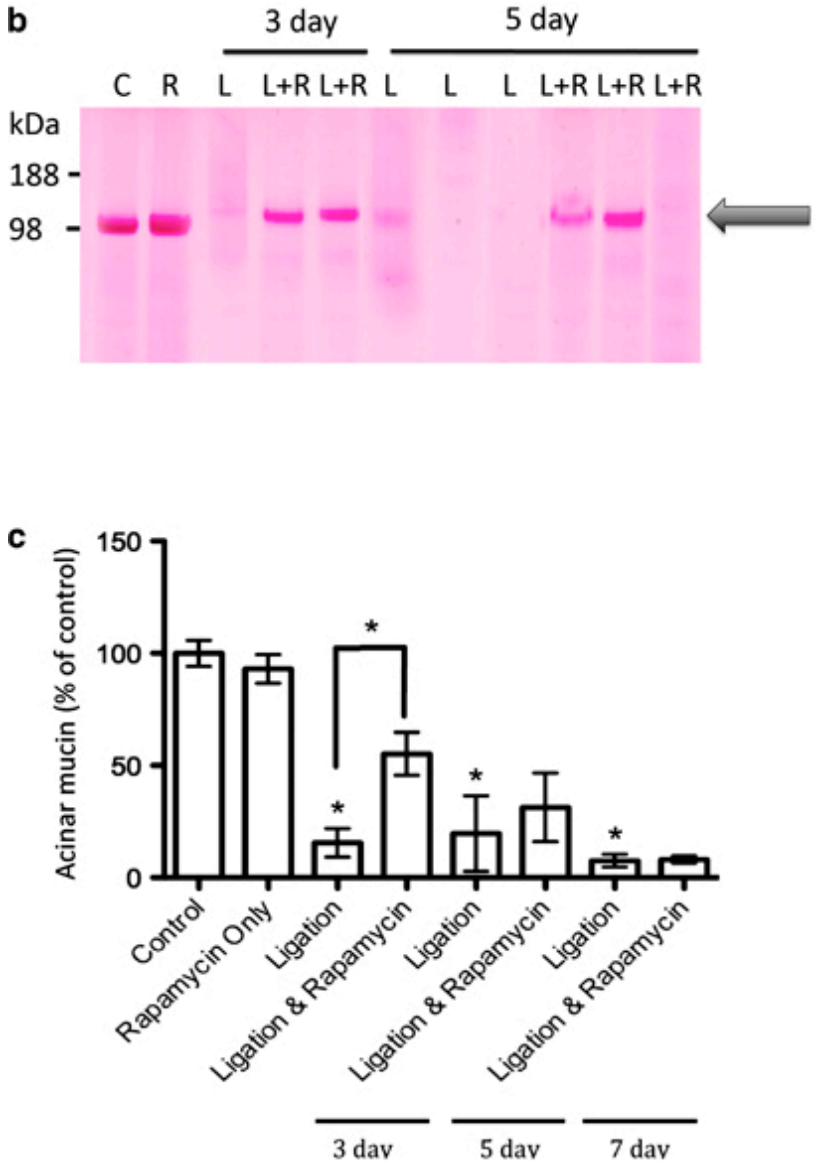

Figure 3.4 Periodic acid-Schiff's staining of glandular homogenates of 3 and 7 day (a) and 3 and 5 day (b). PAS staining of all ligation only (L) groups marked a significant loss of acinar mucin. The 3 day ligation with rapamycin group (L+R) showed only partial loss of mucin (indicated by arrow), suggesting rapamycin reduced acinar loss of mucin. Five days of rapamycin treatment following ductal ligation revealed transitional results between a partial loss or a complete loss of mucin. No staining was seen after 7 days of rapamycin treatment following ligation. Densiometric analysis of submandibular acinar mucin (c) as a ratio of control (*P<0.05), shows that increased acinar mucin in 3 days of ligation with rapamycin treatment was significantly higher in comparison with ligation only. The bars represent the mean±S.E.M. Data represent results from at least three independent experiments.

3.5.5 Histological assessments

The haematoxylin and eosin staining (H&E) of both the ligation (Figure 3.5b) and the ligation with rapamycin treatment (Figure 3.5c) groups showed the presence of inflammatory cell infiltration, which were composed mainly of neutrophils and macrophages (as previously mentioned) (Silver et al, 2010, Correia et al, 2008) in the connective tissue between the lobules and among the parenchymal elements after 3 days in comparison with controls (Figure 3.5a). Three day ligation groups also revealed shrunken acinar cells with loss of secretory granules and duct luminal dilation as they underwent degranulation, similar to previous findings (Cotroneo et al, 2008). Rapamycin-treated ligated glands didn't appear to affect inflammatory cell infiltrates, but showed intact acinar cells and some larger than normal acinar cells.

Morphometric analysis of H&E-stained samples revealed the mean area±Standard Error of the Mean (S.E.M.) of the acini from the 3 day ligation samples (227.40±30.72μm2, n=60) significantly decreased ($P<0.0001$) in comparison with the control glands (469.90±17.35μm2, n=80). Rapamycin treatment following ligation rescued the acini size (541.90±47.56μm2, n=80) significantly ($P<0.0001$) from the ligated state (Figure 3.5d).

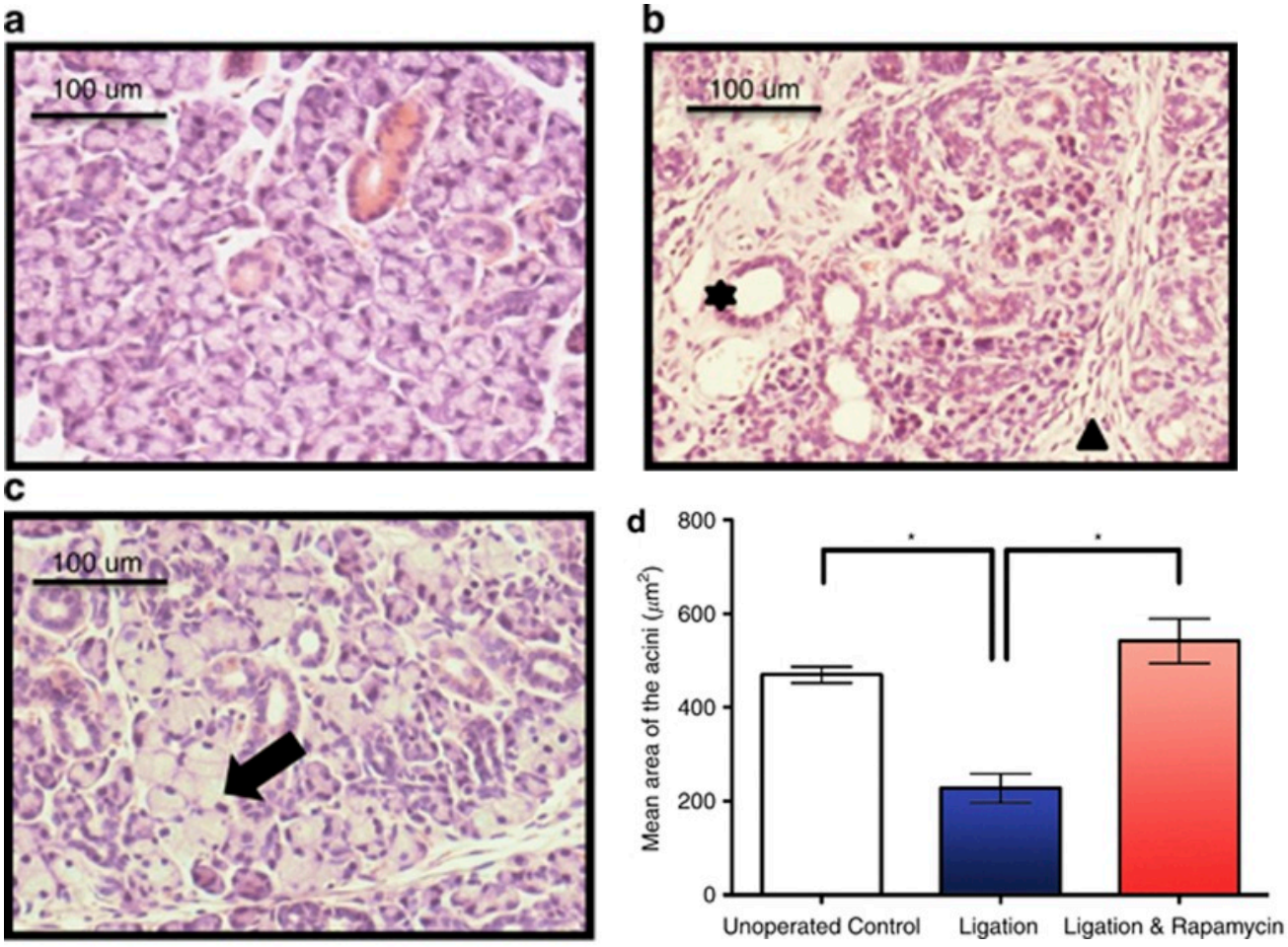

Figure 3.5 Haematoxylin and Eosin (H&E) staining of submandibular glands in control (a), following 3 day periods of ligation (b) and ligation with rapamycin treatment (c). The unoperated submandibular gland indicates a conventional appearance of acini and ductal cells. Ligation revealed infiltration of a large number of inflammatory cells (mostly neutrophils and macrophages; arrowhead) and duct luminal dilation (star), exemplary of the atrophic state. Ligation with rapamycin treatment, revealed lack of atrophy in intact acinar cells (arrow). Morphometric analysis of the H&E-stained samples indicated the mean area of acini (d) from the control, 3 day ligation and 3 day ligation with rapamycin treatment. Ligation significantly decreased the size of the acini (*P<0.0001) in comparison with control. Rapamycin treatment post ligation showed a significant increase in acini area (*P<0.0001). Data is expressed as mean±S.E.M.

Histological assessments of alcian blue/periodic acid-Schiff's (AB/PAS)-stained adult female submandibular gland sections after 3 day rapamycin treatment following ductal ligation (Figure 3.6b) revealed enlarged acinar cells as shown in H&E staining that are strongly stained by alcian blue, when compared with ligation only (Figure 3.6a).

The H&E staining of the 7 days ligation and the 7 days ligation with rapamycin treatment, the 5 days ligation and the 5 days ligation with rapamycin treatment groups all revealed very similar results as ligation only glands with very little, to no differences.

Histomorphometric analysis indicated that the area of acini from ligated glands was significantly reduced at longer time periods, in both ligated and rapamycin-treated ligated samples, compared with unoperated control samples.

The histochemical staining of granular ducts by DMAB-nitrite showed loss of kallikrein, which is a marker for ductal function (Gresik et al, 1980), secretory granules of granular tubule cells 3 days post duct ligation (Figure 3.6d) in comparison with unoperated controls (Figure 3.6c), rapamycin treatment following ligation did not rescue the

reduction of stored tissue secretory granules containing kallikreins (Figure 3.6e). All 5 and 7 day experimental groups (ligation only and the ligation with rapamycin groups) indicated a complete loss of DMAB in comparison with unoperated controls.

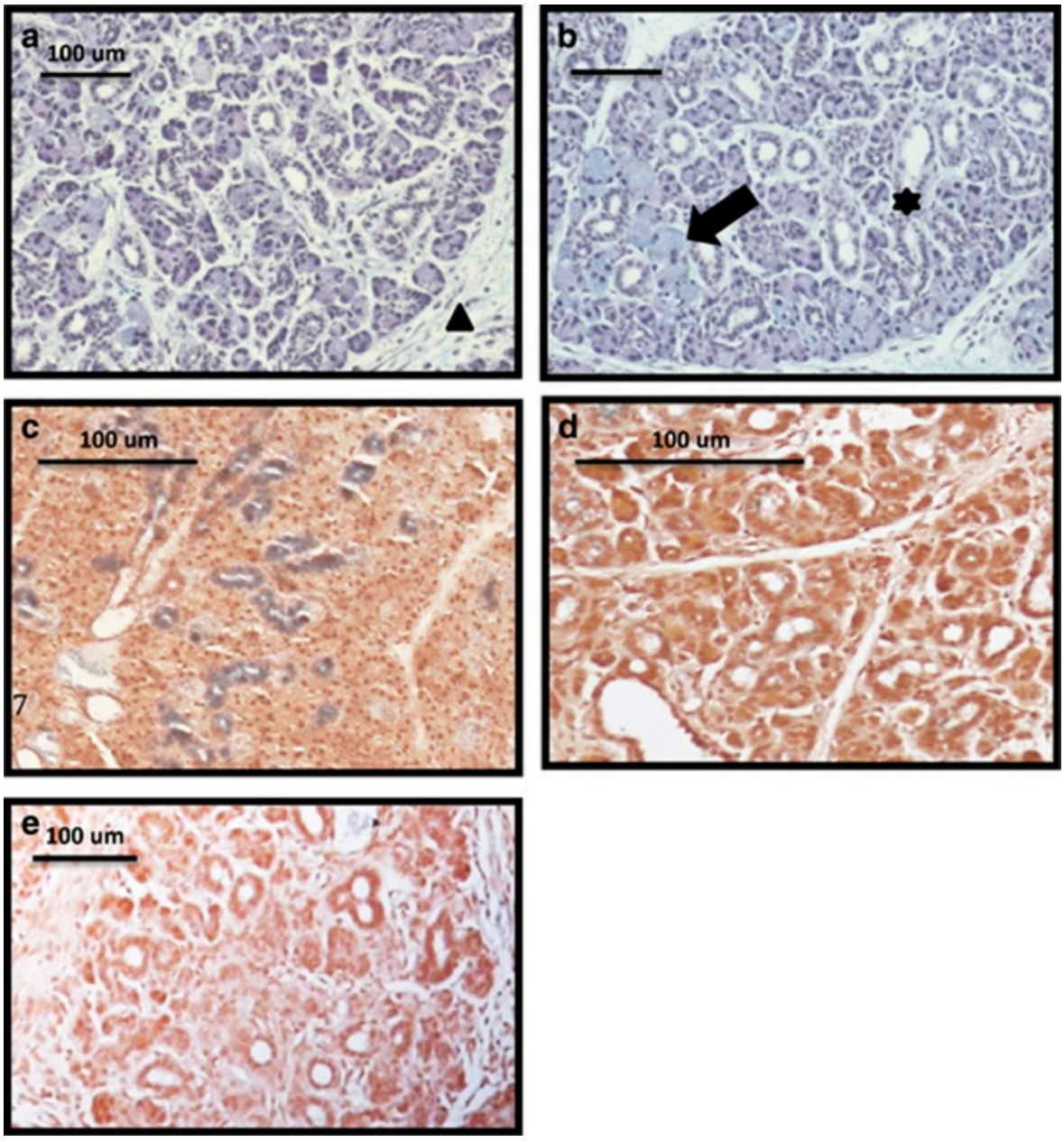

Figure 3.6 Alcian blue/PAS staining of submandibular glands after 3 days of ligation (a) and ligation with rapamycin treatment (b). The ligated state revealed signs of atrophy such as shrunken acinar cells with no secretory granules, duct luminal dilation and presence of inflammatory cells (mostly neutrophils and macrophages; arrowhead). Rapamycin treatment following ductal ligation, showed intact acinar cells (arrow) and although the ducts displayed larger lumena (star), not all acinar cells appeared enlarged. Histochemical staining of granular ducts by DMAB-nitrite on unoperated controls (c), 3 day ligation (d) and 3 day ligation and rapamycin (e). Lack of blue DMAB on ligation and ligation with rapamycin treatment, shows a loss of blue DMAB staining indicating loss of kallikrein-containing secretory granules in ductal cells.

3.6 Discussion

Our previous study suggested that mTOR was associated with the atrophic process during submandibular duct ligation. This study provides further evidence that mTOR is required for an autophagy-like process. However this study underlines the complexity of the *in vivo* regulation of mTOR and hints at its interaction with other pathways.

The ligation of the main excretory duct of the submandibular gland to study atrophy of the salivary glands has been well characterized in rats (Takahashi et al, 2004, Carpenter et al, 2007).

As the first study of it's kind to use mice, this study found that the ligation of the excretory duct of the submandibular gland led to glandular atrophy as the gland underwent morphological, cellular and microscopic changes.

One such change is that mean submandibular gland weight was significantly reduced in all ligation groups in comparison with controls. Decreased volume and size of acinar cells with acinar and ductal degranulation may explain the significant decrease of glandular

weights, although the increase of inflammatory cells infiltrating may have added to the gland weight initially.

Tissue morphology indicated that the glands of the 3 day ductal ligation group had shrunken acinar cells with loss of secretory granules, duct luminal dilation as they underwent degranulation and a general loss of cytoplasm in the duct cells. Similarly at 5 and 7 days of ligation most acinar cells had disappeared, ductal lumena were dilated with little cytoplasm left and there was an increased amount of connective tissue filled with inflammatory cell infiltrates.

The DMAB staining specific for stored tissue kallikrein of the granular convoluted ducts (Shori et al, 1997) of submandibular gland tissues at all time points post ligation indicated loss of kallikrein-containing secretory granules, corresponding with PAS staining of glandular homogenates, which showed a complete loss of mucin with ligation as previously demonstrated in duct-ligated submandibular gland of rats (Cotroneo et al, 2010). The absence of secretory glycoproteins indicates a lack of acinar cell synthetic activity.

Immunoprobing of the phospho-S6 ribosomal protein, which is

phosphorylated at several sites by S6K1 (Burnett et al, 1998, Isotani et al, 1999) and 4E-BP1 (another mTORC1 substrate) confirmed that mTOR is activated during ligation-induced atrophy of the salivary glands, which corresponds with the start of autophagic processes during ligation-induced atrophy (Silver et al, 2010).

Three days of rapamycin treatment following duct ligation showed a complete inhibition of mTOR, as shown by the immunoprobing of mTOR substrates S6rp and 4E-BP1. Tissue morphology revealed intact acinar cells, although the ducts displayed larger lumena compared with control mice with the presence of inflammatory cells suggesting ductal atrophy. The preservation of mucin-content post treatment suggests that rapamycin maintains synthesis or prevents degradation of secretory glycoproteins by fully inhibiting the activity of mTOR. Therefore, inhibition of mTOR can delay ligation-induced atrophy of salivary glands, however only affecting acinar, but not ductal, atrophic processes.

However, longer periods of rapamycin treatment post ligation surgery showed a loss of efficacy as gland weights were reduced, with morphological changes similar to ligation only and phosphorylation of

S6rp and 4E-BP1 showing an incomplete inhibition of mTOR. Based on the results obtained in this experiment, rapamycin treatment is not believed to be effective in longer periods of administration and that rapamycin treatment only delays salivary gland atrophy following ductal ligation, as rapamycin is not a full inhibitor of mTOR, owing to the PI3K-negative feedback mechanism (which re-activates mTORC1 via the TSC1/2 complex) (Guertin et al, 2009). It is possible rapamycin is ineffective against the negative feedback mechanism because rapamycin only inhibits mTORC1 (Zaytseva et al, 2012), although there has been some evidence to suggest that the prolonged rapamycin treatment inhibits mTORC2 assembly (Sarbassov et al, 2006), which may be relevant to the changes observed from day 3 to day 5 in our study. Using a second generation mTOR inhibitor, Torin1, which is thought to inhibit all kinase-dependent functions of mTOR (Thoreen et al, 2009), we obtained essentially identical results to rapamycin. It is possible that rapamycin had been effective in mTOR inhibition, yet S6K1 and 4E-BP1 were activated via mTOR-independent phosphorylation of S6K1 and 4E-BP1, a mechanism suggested by other studies (Liu et al, 2013).

Evidence from this study leads to the conclusion that inhibition of mTOR can delay ligation-induced atrophy of salivary glands, however only affecting acinar, but not ductal, atrophic processes.

CHAPTER 4

TORIN1 & NVP-BEZ235 EFFICACY AS ALTERNATIVES TO RAPAMYCIN IN SALIVARY GLAND ATROPHY

4.1 Introduction

The mammalian target of rapamycin (mTOR) pathway, also known as the mechanistic target of rapamycin, is a prime regulator of cell growth and its serine/threonine kinase, as the key component of the pathway, is formed of two functionally distinct protein complexes, mTORC1 and mTORC2, that differ in their subunit composition (Thoreen et al., 2009, Silver et al., 2010, Laplante and Sabatini, 2012). Many of the insights that have been gained into mTOR signalling have came through investigating the mechanism of action of rapamycin, a macrolide immunosuppressant drug that has an inhibitory effect on mTORC1 (Santos et al., 2011).

Conversely, mTORC2 is considered to be unaffected by rapamycin, although its assembly can be inhibited by prolonged rapamycin treatment in certain cell types (Sarbassov et al., 2006). Because of its perceived potency (Feldman et al., 2009), rapamycin is commonly used in research experiments as a test of the involvement of mTOR in a particular process, such as in the previous chapter of this thesis where the role of mTOR in morphological changes and biochemical changes during salivary gland atrophy were investigated.

However rapamycin has been shown to be ineffective for long-term administration, as it does not completely inhibit mTOR *in-vivo* (Feldman et al., 2009, Bozorgi et al., 2014, Takayama et al., 2014).

Table 4.1 Comprehensive listing of mTOR inhibitors. It should be noted that for comparative purposes, the Rapamycin category includes the rapalogs of temsirolimus, everolimus and deforolimusalan.

Drug	Structure	Mechanism	mTORC1 (IC_{50})	mTORC2 (IC_{50})	PI3K (IC_{50})	Reference
Rapamycin	Macrolide ester	mTORC1 inhibitor	<10nM	N/A	N/A	(Laplante and Sabatini, 2012)
Torin1	Pyridinonequinoline	mTOR kinase inhibitor	<10nM	<10nM	1.8M	(Thoreen et al., 2009)
PP242	Pyrazolopyrimidines	mTOR kinase inhibitor	<10nM	<10nM	1.96M	(Feldman et al., 2009)
PP30	Pyrazolopyrimidines	mTOR kinase inhibitor	<100nM	<100nM	3M	(Feldman et al., 2009)
NVP-BEZ235	Imidazoquinazoline	mTORC1 and PI3K inhibitor	<10nM	<10nM	<10nM	(Maira et al., 2008a)

This is believed to be due to the PI3K-negative feedback mechanism that re-activates mTORC1 via the TSC1/2 complex (Guertin and Sabatini, 2009). As discussed in the previous chapter, it is possible rapamycin is ineffective against the negative feedback mechanism because rapamycin only inhibits mTORC1 (Zaytseva et al., 2012). Therefore this chapter will utilise second generation mTOR inhibitors, specifically Torin1 and NVP-BEZ235 (BEZ), which are believed to inhibit all kinase-dependent functions of mTOR (Table 4.1), in an experiment to fully

inhibit mTOR to allow for the observation of the underlying mechanisms of the mTOR pathway during atrophy in the salivary glands and to analyse whether or not the full inhibition of mTOR, rather than a delay, can have restorative effect similar to the results seen when mTOR was inhibited in the previous chapter.

4.2 Materials & Methods

4.2.1 Experimental Procedure

The mice were designated into two labels: control and ligation groups, as previously explained in Chapter 2.2.

Control groups consisted of unoperated controls (n=4) or non-ligated mice treated with NVP-BEZ235 (n=1). With the ligation groups, either untreated for 3 days (n=3) or 7 days (n=4) for comparative purposes, or receiving the mTOR inhibiting drugs NVP-BEZ235 for 3 days (n=6) or Torin1 post ligation for 3 days (n=7) or 7 days (n=5).

Surgical and sacrificial procedures were performed as previously described in Chapter 2.3. Submandibular gland tissue sections were

collected from the glands subsequent to gland weighing and either fixed in 4% formalin overnight for histochemical staining or snap frozen in liquid nitrogen for immunoblotting.

4.2.2 Torin1 Treatment

Torin1 (Tocris Bioscience, Bristol, UK) was suspended with a stock solution of 25 mg / ml in 100% N-methyl-2-pyrrolidone (NMP) made fresh daily and diluted in 1:4 concentration of 50% polyethylene glycol 400 (PEG400). Leading to a final concentration of 5 mg / ml. The mice, following ligation, received *i.p.* injections that consisted of 20 mg / kg / day. This particular dose was chosen because of the efficacy and comparative effectiveness of the inhibition of mTOR signaling by Torin1 shown in previous studies (Liu et al., 2010).

4.2.3 NVP-BEZ235 (BEZ) Treatment

NVP-BEZ235 (BEZ) was formulated at 4 mg / ml in N-methyl-2-pyrrolidone (NMP) / polyethylene glycol (PEG) (10% / 90%, v/v). These solutions were prepared fresh each day of dosing. The BEZ powder was dissolved in NMP upon sonification, with the remaining volume of PEG

added thereafter. This method of preparation was used in accordance with previous BEZ treatment studies (Maira et al., 2008b). The final application volume of 10 ml / kg was administered *p.o.* once every 24 hours. This particular dose was chosen because of the efficacy and comparative effectiveness of NVP-BEZ235 as shown previously (Serra et al., 2008, Yasumizu et al., 2014). Furthermore, in preparatory undertakings for this study, this was found to be the maximum dose without seeing significant body swelling, particularly across the abdomen, similar to the significant abdominal swelling found in a previous PI3K inhibition study (Hu et al., 2002). NVP-BEZ235 treatment could not be attempted for 7 days of ligation-induced atrophy as during preparatory undertakings for this study, toxicity was observed from the use of the compound, similar to the common toxicities of mTOR inhibitors (Soefje et al., 2011).

4.2.4 Histochemical Staining

The formalin-fixed tissues were processed through a series of ascending IMS and then stained. For the assessment of general morphology, haematoxylin and eosin (H&E) staining was performed. The secretory granules inside acini cells were identified by alcian blue/periodic acid

Schiff's (AB/PAS) staining, all according to procedures previously described in chapter 2.6.

4.2.5 Immunohistochemistry

Formalin-fixed paraffin-embedded sections were de-waxed, dehydrated in absolute xylene and then rehydrated with distilled water and treated with 3% hydrogen peroxide. Inhibition of endogenous peroxidase along with treatment for prevention of non-specific binding of the primary antibody was carried out as previously described in chapter 2.7. The primary antibody used was Rabbit Anti-Mouse PS6 (Cell Signalling Technology, Hertfordshire, UK), at 1:100 and secondary HRP polyclonal antibodies at 1:250 dilution (DAKO, Ely, Uk). The sections were subjected to DAB detection kit (Sigma-Aldrich, Gillingham, UK), according to the manufacturer's instructions, and counterstained with Mayer's haemotoxylin.

4.2.6 Morphometric Analysis

H&E stained samples were also used for measuring the mean acini area (μm^2) using a Leica TCS SP2 confocal microscope, version 2.1 (Leica systems, Heidelberg GmBH).

4.2.7 Statistical analysis

Results were expressed as means±S.E.M., and were statistically compared by ANOVA followed by Bonferroni Correction; $P<0.05$ was considered statistically significant.

4.2.8 Protein Detection

The tissue samples were homogenised, loaded protein samples were normalised using BCA Assay (Thermo Scientific, IL, USA), as detailed in chapter 2.10. SDS-PAGE was performed on tissue homogenates, in preparation for protein detection, as described in chapter 2.12.

Immunoprobing of membranes were performed to visually analyse the specific proteins of mTOR and autophagy status using the antibodies shown in Table 4.2. PAS of glandular homogenates was used to assess glycoproteins, as previously described in chapter 2.11.

Table 4.2 Antibody concentrations in Immunoblotting protocol

Primary Antibodies	Concentration
Rabbit Anti-human / mouse p4E-BP1	1 : 1000
Rabbit Anti-human / mouse pS6RP	1 : 1000
Rabbit Anti-human / mouse mTOR	1 : 1000
Rabbit Anti-human / mouse ATG5	1 : 1000
Rabbit Anti-human / mouse ATG3	1 : 1000
Mouse Anti-human / mouse β-actin	1 : 4000

Secondary Antibodies	Concentration
Horseradish peroxide (HRP) labelled Goat Anti-rabbit	1 : 2000
Horseradish peroxide (HRP) labelled Goat Anti-mouse	1 : 1000
Horseradish peroxide (HRP) labelled Mouse Anti-goat	1 : 1000

4.2.9 Glandular Densitometry

The intensity of the western blots were quantified and displayed as a ratio of β-actin using Image J version 1.46 (NIH, MD, USA), as previously explained in 2.13.

4.2.10 Proteomic Analysis

Two female adult mice were used for the proteomics experiment. One mouse was ligated for 7 days (Sample A), whilst the other was ligated for 7 days with rapamycin treatment (Sample B). The liquid chromatography – mass spectrometry (LC-MS/MS) protein identification was performed by The Centre of Excellence for Mass

Spectrometry at King's College London, following the well established protocols (Xi et al., 2011, Rauniyar et al., 2013, Das et al., 2014). In brief, 100μg of each sample had its proteins separated using SDS-PAGE and then samples were in-gel digested with trypsin, as almost all large-scale projects in mass spectrometry-based proteomics use trypsin to convert protein mixtures into more readily analysable peptide populations (Olsen et al., 2004). Following digestion, samples were isobarically labelled and then desalted using C18 columns. The samples were then divided for total peptide analysis and a phosphopeptide-enriched sample for LC-MS/MS analysis.

Samples that were to be subjected to total peptide analysis had their raw protein and raw peptide fold changes calculated using Proteome Discoverer (Thermo Fisher Scientific, MA, USA). The acquired raw data was then identified using the mouse proteins database (Uniprot, Cambridge, United Kingdom) and fold change measurements were analysed using Excel (Microsoft, WA,USA).

The second sample underwent phosphopeptide enrichment and clean up before analysis, using a titanium dioxide kit (Thermo Fisher Scientific, MA, USA), according to manufacturers protocol. This is because naturally low abundances of phosphopeptides and low degrees

of phosphorylation, make the isolation and concentration of phosphopeptides essential prior to analysis (Dunn et al., 2010). The phosphopeptide-enriched sample was then subjected to data analysis using the PhosphoRS node in Proteome Discoverer (Thermo Fisher Scientific, MA, USA). The obtained data was further analysed to determine molecular function, cellular compartment and protein information using the Pfam database (Finn et al., 2014). Fold change measurements were analysed using Excel (Microsoft, WA, USA).

4.2.11 DNA Microarray Analysis

Two female adult mice were used for the DNA microarray experiment. One mouse was ligated for 7 days (Sample A), whilst the other was ligated for 7 days with rapamycin treatment (Sample B). The generation of gene expression microarray data using Affymetrix genechip probe arrays follows a simple procedure consisting of six major steps (Downey, 2004). This procedure for the genomic analysis of the genechip for the DNA Microarray was performed by FWB Genomics Centre at King's College London, following the well established protocols (Carpenter and Cotroneo, 2010, Silver et al., 2010)

In brief, 30mg of frozen tissue from each sample was homogenised and then cleaned using affinity column, this is because the single most important step in ensuring a successful genechip experiment is the preparation of a clean, intact RNA sample (Zhang and Rokosh, 2007). RNA was extracted using a RNeasy Mini Kit (Qiagen, Venlo, Netherlands), according to manufacturer's instruction. The sample labelling protocol was then followed for Affymetrix DNA microarray analysis (Affymetrix, High Wycombe, UK), according to manufacturer's instructions. The labelled RNA was purified and then underwent fragmentation using heat and Mg^{2+}, in order to create shorter sequences. This is because longer RNA fragments are very susceptible to degradation (Fasold and Binder, 2012), whereas shorter sequences of about 100 to 200 base fragments are more suitable to be hybridised with the probes on a genechip (Li and Wong, 2001).

Mouse genome genechip 430 2.0 arrays (Affymetrix, High Wycombe, UK) were used in this study, covering over 39,000 transcripts and variants on each single array. The sequences that this genechip array probes for are derived from selected sequence clusters that were created from the UniGene database (NCBI, MD, USA). The previously extracted RNA fragments were hybridised on the genechip and left overnight in

an oven at 45°C. Following hybridisation, the genechip was washed and stained using a genechip fluidics station (Affymetrix, High Wycombe, UK), according to the manufacturer's instructions. Raw microarray data were scanned from the genechip arrays using a genechip scanner and the resulting data was analysed using the GeneChip Operating Software (GCOS) (version 3.2) (Affymetrix, High Wycombe, UK) in order to summarise probe sets, with the genes absent from both experimental samples dismissed. The remaining gene results were further analysed to determine gene family/sub-family and protein class using The Panther Classification System Version 9.0 (Thomas lab, CA, USA), and ascertain gene pathway and pathway components using Kyoto Encyclopedia of Genes and Genomes (KEGG) (Kyoto, Japan).

4.3 Results

4.3.1 Gland weights

Mean submandibular gland weight was significantly (p=0.0008) reduced in the 3 day ligation group (0.040±0.001 g, n=3) and also significantly reduced (p=0.002) in the 7 day ligation group (0.035±0.003 g, n=4), all in comparison to non-ligated control mice (0.055±0.003 g, n=4). Following Torin1 treatment (0.048±0.003 g, n=7), mean submandibular gland weight was greater than 3 day ligation only group, however this change was not to a significant extent (p=0.146). NVP-BEZ treatment (0.064±0.003 g, n=6) did however cause a significant (p=0.001) increase in comparison to 3 day ligation only. 7 days of Torin1 treatment post ligation (0.034±0.003 g, n=5) displayed similar results to 7 day ligation only.

By the end of the experiment, there were no statistically significant differences in body weight between 3 day Torin1 experimental mice (29.25±1.71 g, n=7) and the controls (31.20±1.49 g, n=4), however BEZ treated mice (34.0±3.10 g, n=6) had a 9% increase in comparison to

controls due to swelling across the body.

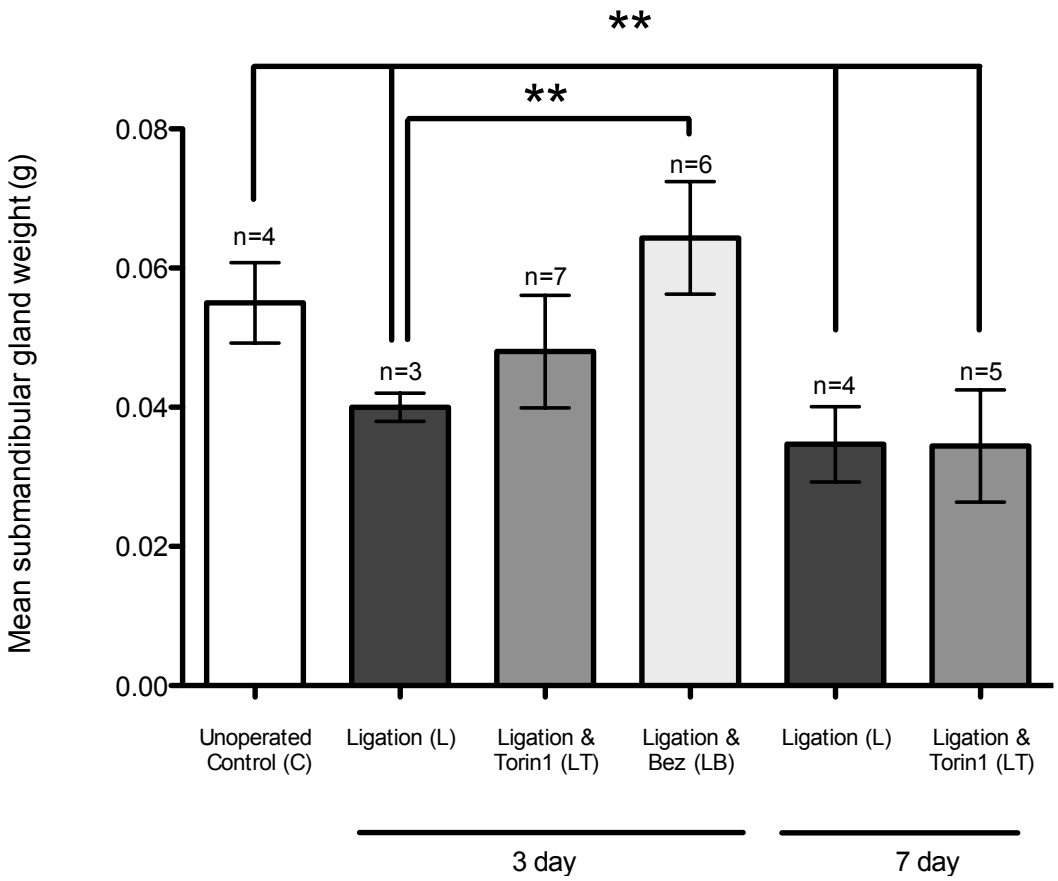

Figure 4.1 Mean submandibular gland weights for Unoperated Control, Ligation only, Ligation & Torin1 and Ligation & BEZ for either 3 or 7 days. Mean submandibular gland weights were reduced after 3 days (p=0.0008) and 7 days (p=0.0002) ligation in comparison to unoperated controls. Post ligation surgery and 3 days of Torin1 treatment, the gland weights were 20% greater than the ligation only group, whereas 3 days of BEZ treatment increased mean gland weights significantly by 60% (p=0.001). 7 days of Torin1 treatment post ligation did not significantly alter gland weights in comparison to the respective ligation only group. Data from ANOVA, Bonferonni's post-test, is expressed as mean ± SEM.

4.3.2 Torin1 Treatment

4.3.2.1 mTOR status

Western blots of the mTOR substrates, pS6rp and p4E-BP1 in unoperated controls, 3 day ligation, 3 day ligation & Torin1, 7 day ligation only and 7 day ligation & Torin1 treatment, showed that unoperated controls displayed a small inactivate state of the p4E-BP1 protein. Whereas 3 days of ligation caused the phospho-4E-BP1 protein to activate it's second isoform.

Torin1 treatment following ligation inactivated the higher isoform, however the total 4E-BP1 protein expression (as a ratio of b-actin) remained greater than control (Figure 4.2 A).

Ligation displayed a presence of pS6rp, however 3 days of Torin1 treatment caused a complete inhibition of the pS6r protein to bring in line with unoperated controls (Figure 4.2 B). This suggests that Torin1 treatment caused a complete inhibition of mTOR activity after 3 days of treatment.

With regards to 7 days treatment of Torin1, ligation alone displayed a relatively small activation of the p4E-BP1 protein (2^{nd} isoform).

However the treatment of Torin1 for 7 days following ligation, had no inhibitory effects on mTOR as indicated by the phosphorylated (active) upper isoforms of p4E-BP1 that are present (Figure 4.3 A).

Similar results were present when observing pS6rp after 7 days treatment of Torin1 following ligation (Figure 4.4 A), as the visible pS6rp bands indicate lack of mTOR inhibition.

The densitometry of the western blots quantified the 3 & 7 day p4E-BP1 results (Figure 4.3 B), revealing a statistically significant difference between the control & ligation only glands ($p = 0.0007$) when analysing p4E-BP1 as a ratio of actin. A similar significance can be found when comparing control & ligation with 7 days Torin1 treatment ($p < 0.0001$), indicating no inhibition of mTOR after 7 days of Torin1 treatment.

Densitometric analysis of the western blot findings for 3 & 7 day pS6rp treatment (Figure 4.4 B) indicated that ligation caused a significant increase of pS6rp phosphorylation in comparison to controls, however this increase was statistically significantly reduced ($p = 0.0002$)

following 3 days of Torin1 treatment. 7 days of Torin1 treatment however, caused a recovery of pS6rp phosphorylation once again.

Total mTOR protein expression in submandibular glands was visible in ligated glands (Figure 4.5), however 3 days of Torin1 treatment reduced total mTOR protein expression to very faint, almost imperceptible bands. Nevertheless the resistance of the total mTOR protein was quite prominent as expression of total mTOR returned following 7 days of ligation & Torin1 treatment, indicating that 7days of Torin1 treatment had little or no inhibition on total mTOR. This can be further evidenced by quantifying these results using densitometric analysis to reveal the statistically significant difference between ligation exclusively and 3 days of Torin1 treatment following ligation ($p < 0.0001$), as well as the statistically significant difference between ligation exclusively and 7 days of Torin1 treatment following ligation ($p = 0.0001$).

A

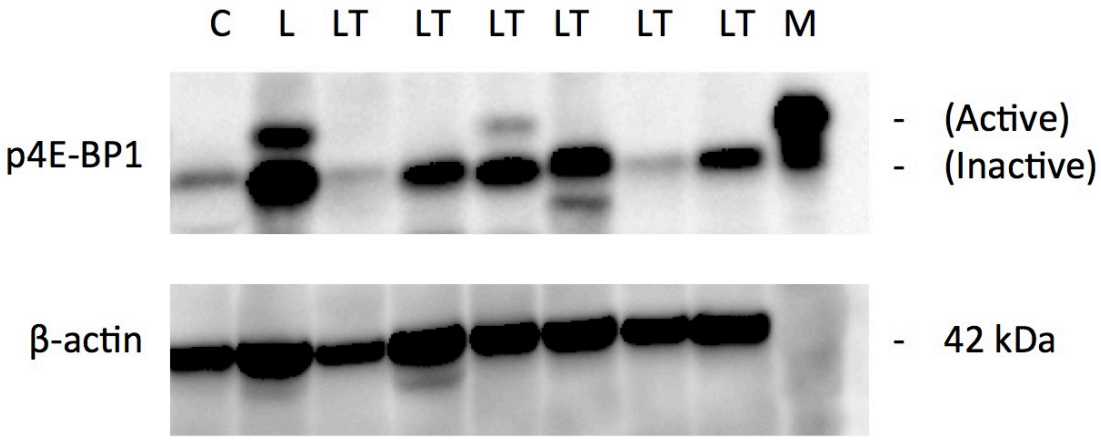

B

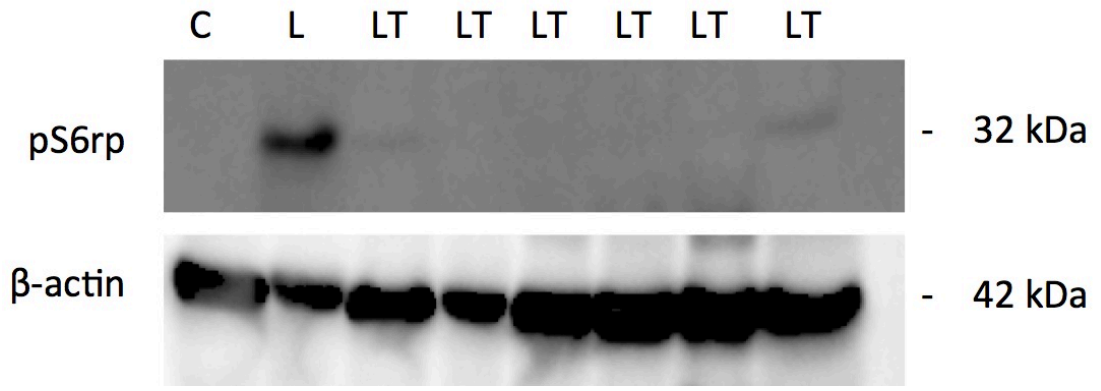

Figure 4.2 Immunoblotting of phospho-4E-BP1 protein expression (A) and phospho-S6 ribosomal protein expression (B) in adult mouse submandibular glands after 3 days of ligation (L) or 3 days of Torin1 treatment following ligation (LT). The submandibular gland homogenates appear to exhibit a high responsiveness to Torin1 treatment, as can be seen via the inhibition of p4E-BP1 indicated by the (active) band following Torin1 administration and the inhibition of pS6rp following Torin1 treatment. Beta actin (β-actin) was used as a loading control for both blots. Mouse muscle tissue (M) was used as positive control for p4E-BP1, however muscle homogenates show absence of β-actin, as muscle expresses α-smooth muscle actin (α-SMA). Data is indicative of results from at least three independent experiments.

A

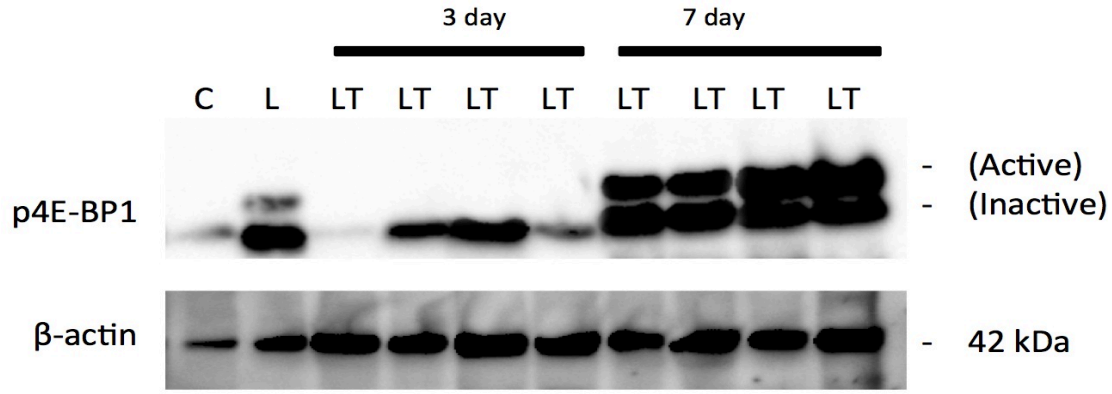

B

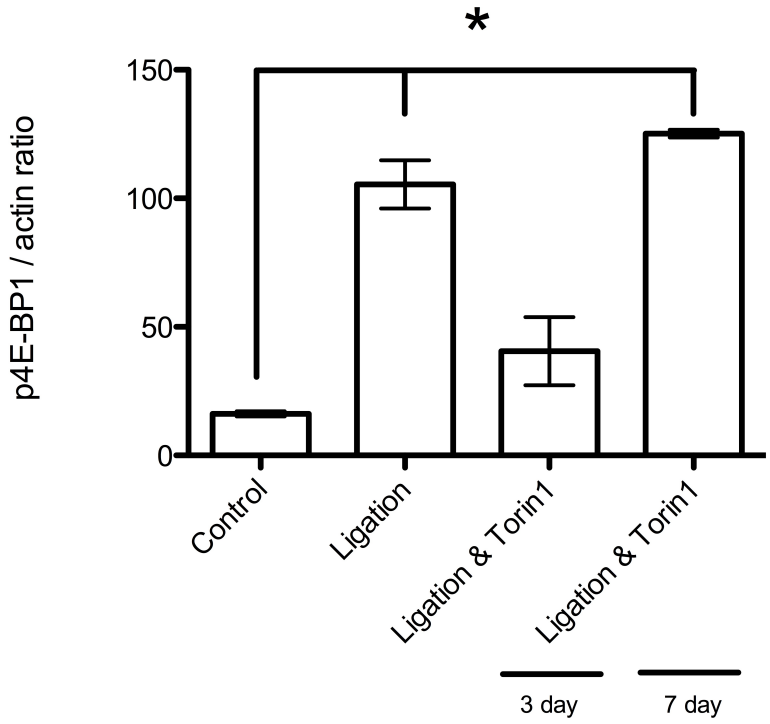

Figure 4.3 Immunoblotting of phospho-4E-BP1 protein expression (A) in adult mouse submandibular glands after ligation exclusively, 3 days of Torin1 treatment following ligation and 7 days of Torin1 treatment following ligation. 3 day ligation & Torin1 exhibited a visible reduction in p4E-BP1 phosphorylation indicated by the lack of a (active) band following Torin1 administration. However, 7 days of Torin1 treatment following ligation reactivated p4E-BP1, with protein expression returning to levels similar to ligation only. Densitometric analysis showing p4E-BP1 expression as a ratio of its actin (B) show a statistically significant increase following ligation in comparison to control ($p = 0.0007$) and following 7 days of Torin1 treatment in comparison to control ($p < 0.0001$). The bars represent mean + SEM. Beta actin (β-actin) was used as a loading control. Data is indicative of results from at least three independent experiments.

A

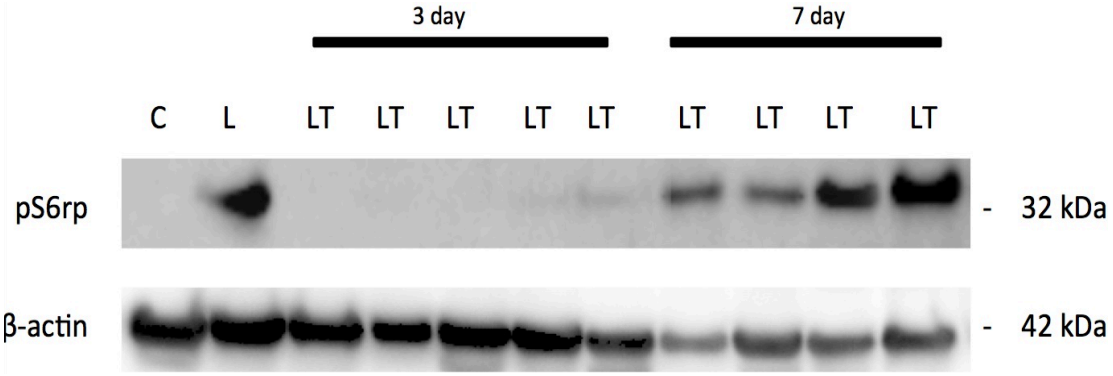

B

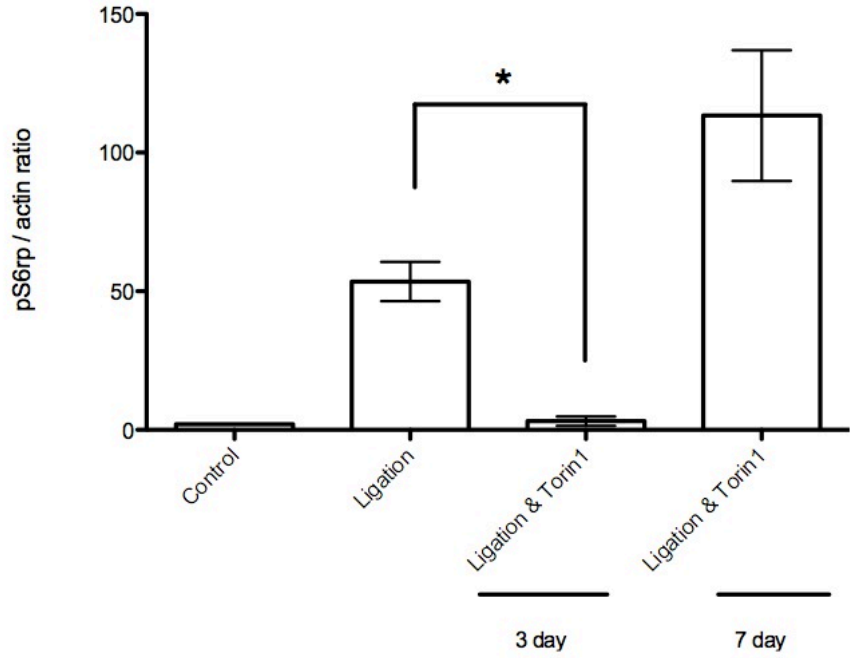

Figure 4.4 Immunoblotting of phospho-S6 ribosomal protein expression (A) in adult mouse submandibular glands after ligation exclusively, 3 days of Torin1 treatment following ligation and 7 days of Torin1 treatment following ligation. Ligation displayed a noticeable presence of pS6rp. But this presence was visibly reduced following 3 day ligation & Torin1 administration. However, 7 days of Torin1 treatment following ligation demonstrated an activation of pS6rp, with protein expression increasing to levels beyond that of even just ligation only. Densitometric analysis of pS6rp expression as a ratio of its actin (B) showed a statistically significant difference of pS6rp to actin ratio between ligation and 3 days of Torin1 treatment ($p = 0.0002$). The bars represent mean + SEM. Beta actin (β-actin) was used as a loading control. Data is indicative of results from at least three independent experiments.

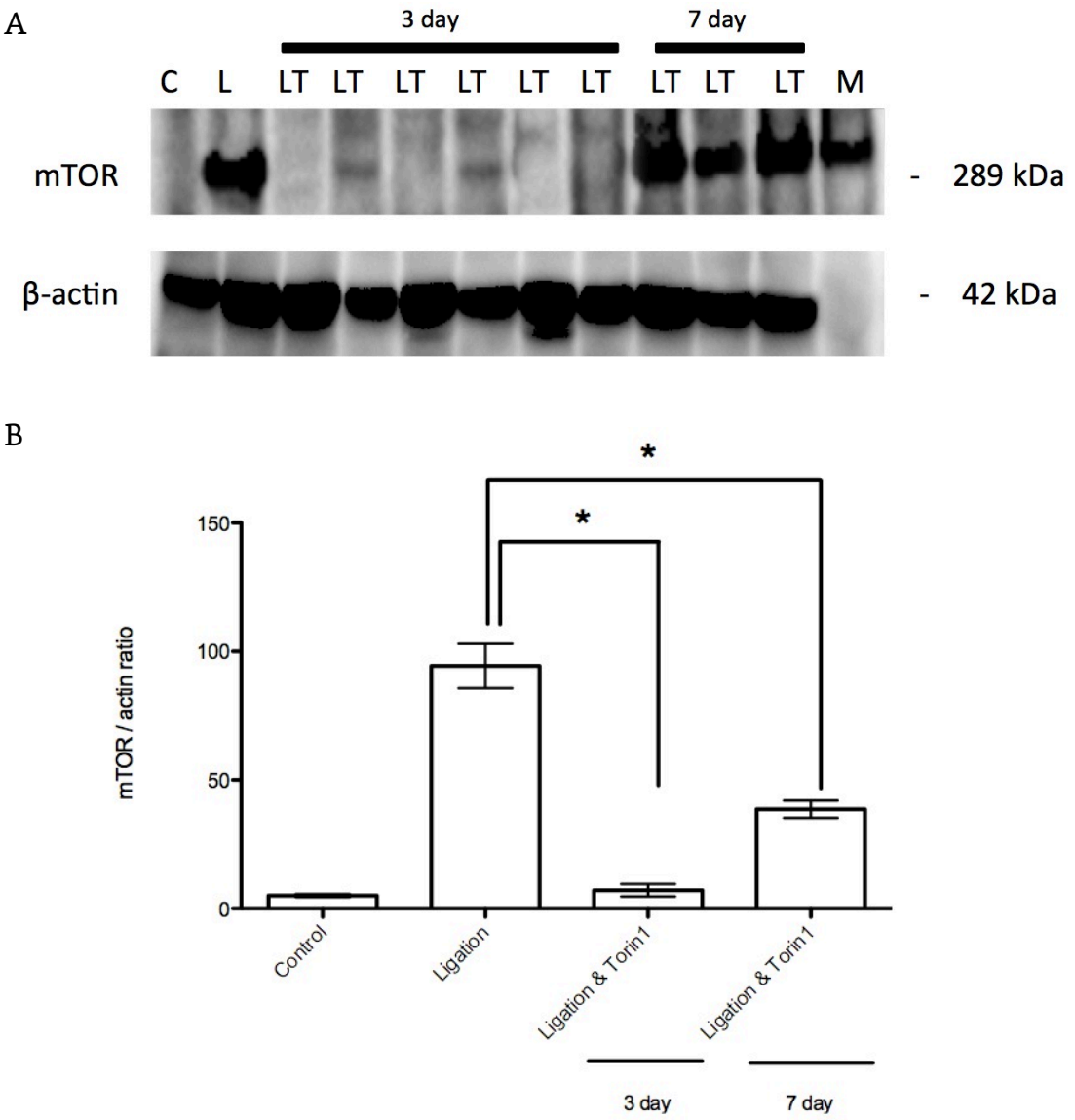

Figure 4.5 Immunoblotting of total mTOR protein kinase expression (A) in adult mouse submandibular glands after 3 & 7 days of Torin1 treatment following ligation. Total mTOR protein kinase expression was increased following ligation but visibly reduced following 3 days of Torin1 administration. However, 7 days of Torin1 treatment following ligation appeared to reactivate the mTOR pathway as total mTOR protein expression increased. Densitometric analysis of total mTOR expression as a ratio of its actin (B) showed a statistically significant difference in mTOR to actin ratio between ligation and 3 days of Torin1 treatment ($p < 0.0001$) as well as between 7 days of Torin1 treatment and ligation ($p = 0.0001$). The bars represent mean + SEM. Beta actin (β-actin) was used as a loading control for both blots. Mouse muscle tissue was used as positive control for mTOR, however muscle homogenates show absence of β-actin, as muscle expresses α-smooth muscle actin (α-SMA). Data is indicative of results from at least three independent experiments.

4.3.2.2 Biochemical Analysis of Glycoprotein Content

Levels of acinar secretory glycoproteins in 3 day ligated and ligated with Torin1 treatment (Figure 4.6 A) and 7 day ligated and ligated with Torin1 treatment (Figure 4.6 B) glands' homogenates were assessed by means of PAS gel staining.

Periodic acid-Schiff's staining in all ligated only glands revealed that the low molecular weight acinar mucins (98 – 188 kDa), that were typical of unoperated controls, had been completely lost due to ligation-induced atrophy. The recovery of acinar secretory gylcoproteins, as exhibited by PAS gel staining, following 3 days of Torin1 treatment subsequent to ligation was significant ($p < 0.05$) in comparison to ligated only glands. However such results could not be replicated in gland homogenates with 7 days of Torin1 administration post submandibular gland ligation, whereby these gland homogenates displayed a significantly ($p=0.01$) lower expression of glycoprotein content in comparison to 3 days of Torin1 treatment subsequent to ligation. Moreover, 7 days of Torin1 administration post ligation had no recovery effects of the submandibular gland glycoprotein content to the extent that 7 day Torin1 treated glands were not statistically significantly divergent to ligated only glands.

A

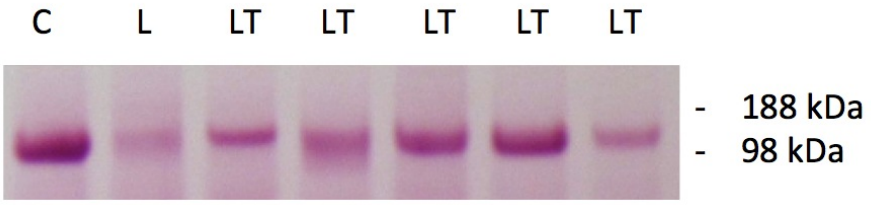

B

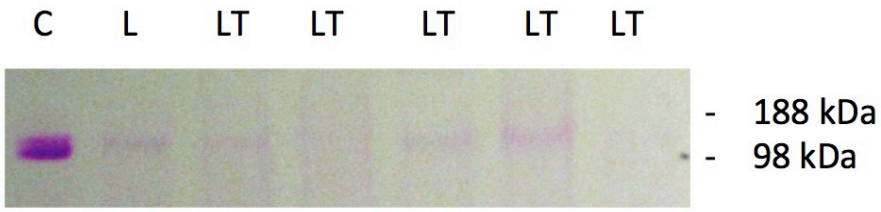

C

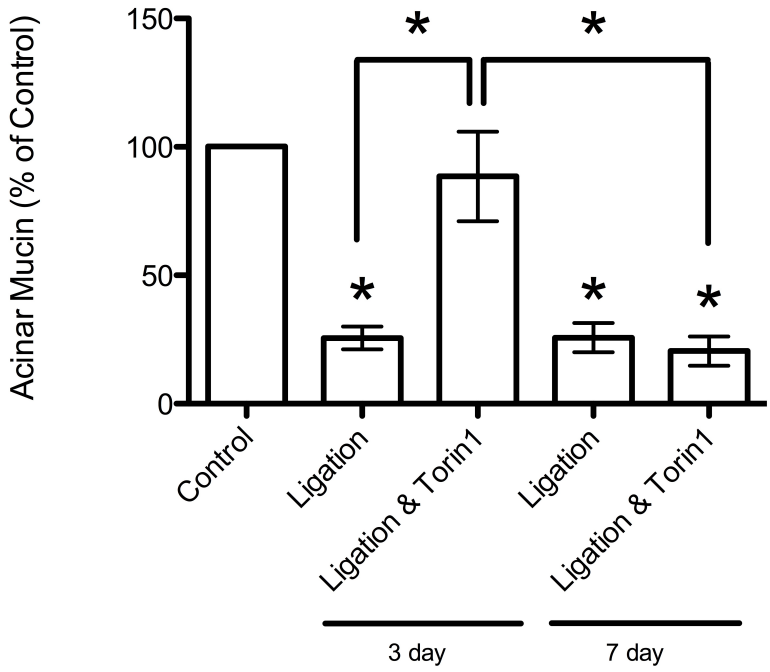

Figure 4.6 Periodic acid-Schiff's staining of glandular homogenates of 3 day ligated and ligated with Torin1 treatment (A) and 7 day ligated and ligated with Torin1 treatment (B) glands' homogenates. Ligation resulted in significant loss of mucins, 3 days treatment showed a visible recovery, yet this recovery was not carried through 7 days of Torin1 treatment. Densiometric analysis of submandibular acinar mucin as a ratio of control (C), showed that both 3 and 7 day ligation only, as well as 7 days ligation and torin1 treatment, were all significantly lower than control (indicated by star). The bars represent the mean + SEM. Data represents results from at least three independent experiments.

4.3.2.3 Biochemical analysis of autophagy

In order to determine presence of autophagy, immunoblotting analysis was performed on ligated mouse submandibular glands and ligated glands with Torin1 treatment for 3 or 7 days, probing for the autophagy markers Atg5, Atg3 and LC3.

The Atg5 immunoblots (Figure 4.7) indicated that autophagic activity was present in ligated glands. However 3 days of Torin1 treatment, appeared to give the visual appearance of a reduction in autophagic activity, whilst 7 days of Torin1 treatment limited the visual appearance of autophagic activity even further.

The immunoblots showing upregulation of Atg3 protein (Figure 4.7) indicated that the autophagy marker was present in all experimental groups to varying degrees. Unlike Atg5 immunoblots, Torin1 treatment did not appear to reduce the expression of Atg3.

Levels of the autophagy markers LC3-I (18 kDa) and LC3-II (16 kDa) showed that autophagy was greatest in ligated only tissue samples and 3 days of Torin1 treatment following ligation, represented by a 50% increase of LC3-I to LC3-II ratio in 3day ligated glands and 63% increase

of LC3-I to LC3-II following Torin1 treatment. However 7 days of Torin1 treatment reduced the presence of autophagy markers, to the extent that some blots only revealed a very faint isoform of LC3-II (Figure 4.7).

Statistical analysis of the band intensity using densitometric analysis (Figure 4.8), revealed that levels of the autophagy market Atg5 were significantly greater in ligation only, whether in comparison to control, 3 or 7 days ligation with Torin1 (all $p<0.005$). The levels of Atg3 were high throughout in comparison to control (all $p<0.01$), but 7 days of ligation and Torin1 was significantly ($p=0.005$) greater than ligation only samples, suggesting autophagy had not stopped following 7 days of Torin1 treatment.

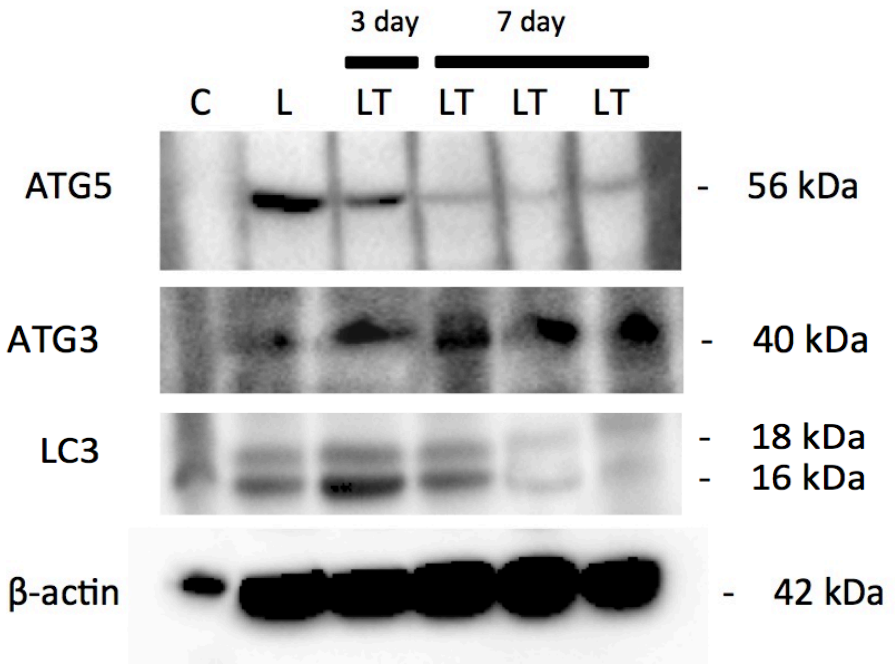

Figure 4.7 Immunoblotting of autophagy markers Atg3, Atg5 and LC3 in ligated, ligated with 3 days Torin1 or ligated with 7days Torin1, as well as their β-actin in mouse submandibular gland homogenates. Levels of the autophagy markers were greatest in ligated only glands, with a visible reduction following Torin1 which progressed further from 3 days to 7 days, with the least autophagic activity in control samples. Beta actin (β-actin) was used as a loading control. Data represent results from at least three different experiments.

A

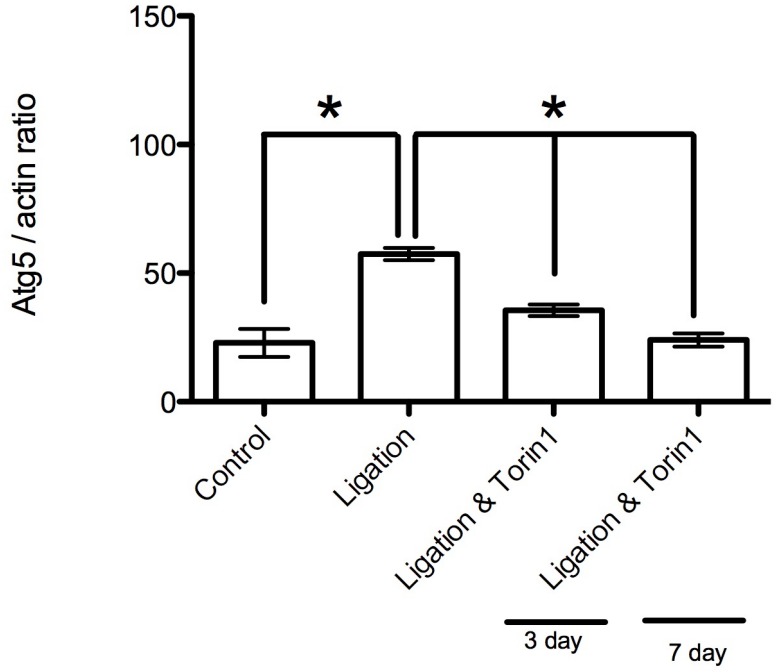

B

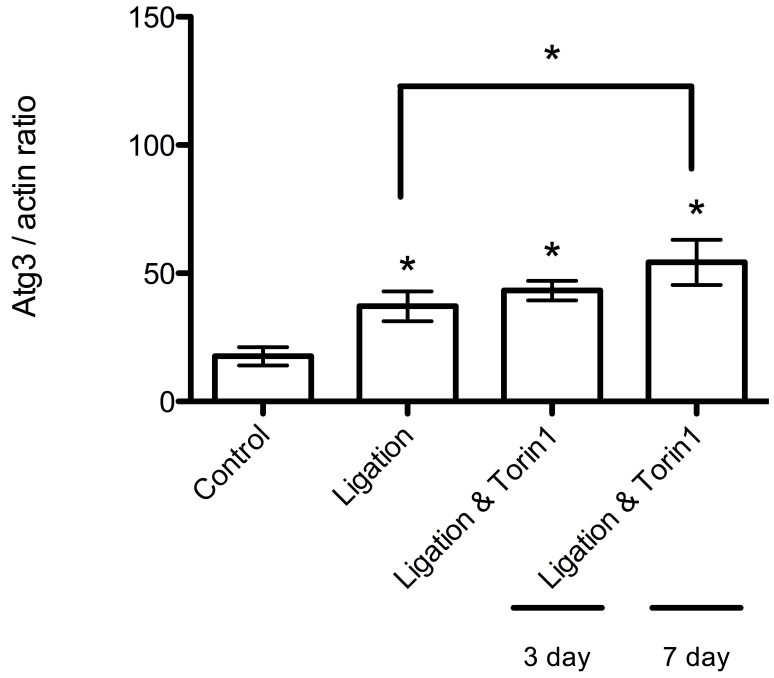

Figure 4.8 Densitometric comparisons of autophagy markers, Atg5 (A) and Atg3 (B), expression in comparison to β-actin in mouse submandibular gland homogenates. Atg5 revealed that its expression was at its greatest in ligated only glands, which were significant to all other experimental groups. Atg3 expression was significant in all groups in comparison to control (asterisks), and furthermore 7 days of Torin1 treatment following ligation was significantly more than ligation only. Data represent results from at least three different experiments. Data is expressed as mean+SEM.

4.3.3 BEZ Treatment

4.3.3.1 mTOR status

Western blots of the mTOR substrates, pS6rp and p4E-BP1 in unoperated controls, 3 day ligation and 3 day ligation & BEZ treatment showed that 3 days of ligation caused the phospho-4E-BP1 protein to activate its second isoform. BEZ treatment following ligation completely inactivated the higher isoform (Figure 4.9 A).

Unoperated controls displayed a small inactivate state of the p4E-BP1 protein. Rapamycin treated ligated glands were also used for comparative purposes to reveal a visibly reduced the higher isoform showing a much lower protein expression than ligated only glands.

Densitometric analysis of the p4E-BP1 western blot findings (Figure 4.9 B) indicated that ligation caused a significant ($p<0.005$) increase of p4E-BP1 phosphorylation in comparison to controls, however this increase was reduced to a statistically ($p<0.005$) significantly lower quantity following 3 days of BEZ treatment.

Ligation displayed a presence of pS6rp antibody. 3 days of BEZ treatment caused inhibition of the pS6r protein, however this inhibition

varied greatly from being with unoperated controls to being almost identical to ligated only glands (Figure 4.9 C). Suggesting that BEZ treatment may not have caused a complete inhibition of mTOR activity after 3 days of treatment. For comparison, rapamycin treated ligated submandibular glands were also used and these samples revealed much lower protein expression than ligated glands with BEZ treatment.

Densitometry of the western blots quantified the 3 day pS6rp results (Figure 4.9 C), revealing that there were statistically significant differences between the control & ligation only glands when analysing pS6rp as a ratio of actin. A similar significance can be observed when comparing ligated only glands & ligation with 3 days of BEZ treatment ($p < 0.005$), indicating partial inhibition of mTOR after 3 days of BEZ treatment.

A

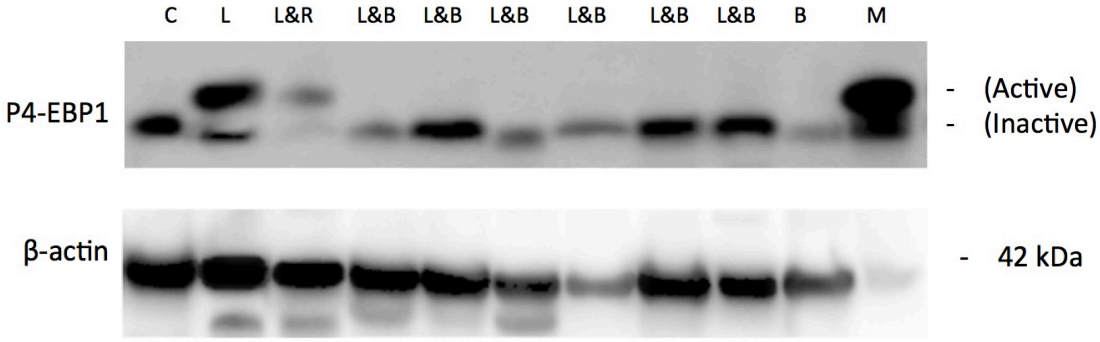
C
L
L&R
L&B
L&B
L&B
L&B
L&B
L&B
B
M
P4-EBP1
- (Active)
- (Inactive)
β-actin
- 42 kDa

B

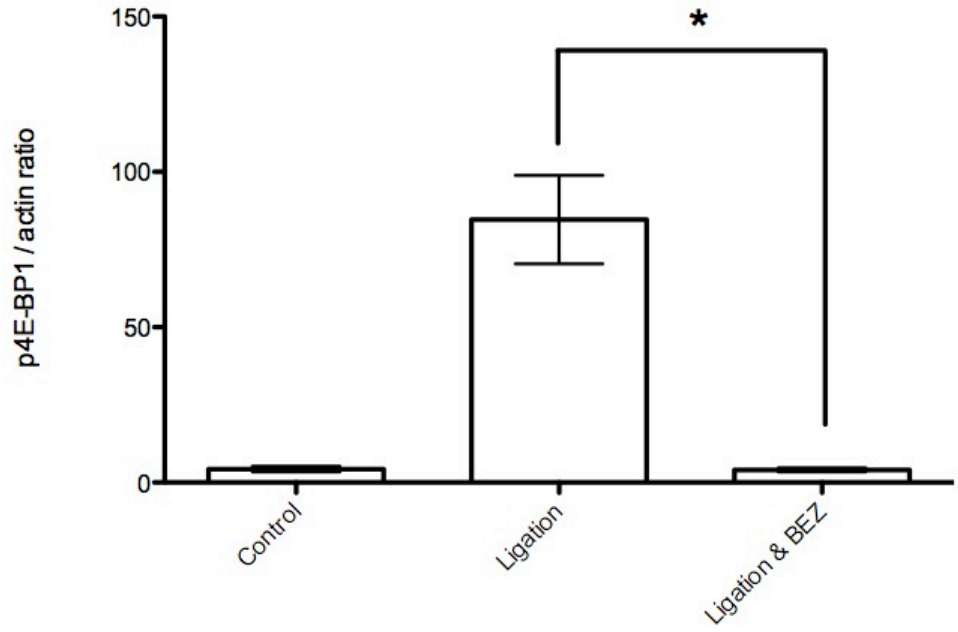
150
100
50
0
p4E-BP1 / actin ratio
*
Control
Ligation
Ligation & BEZ

C

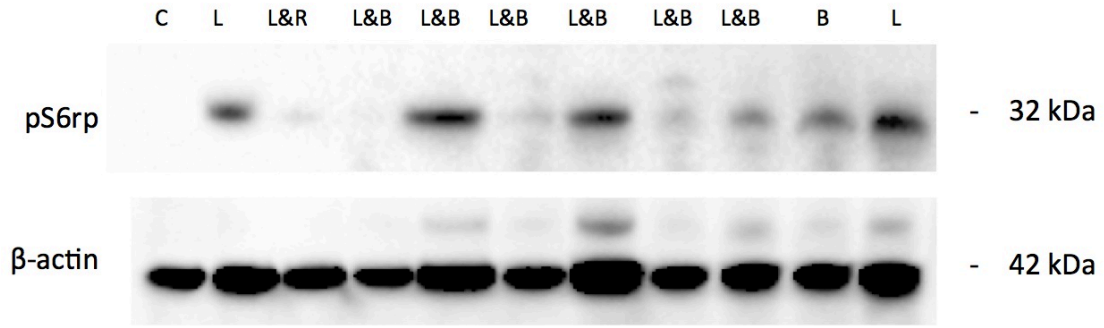

D

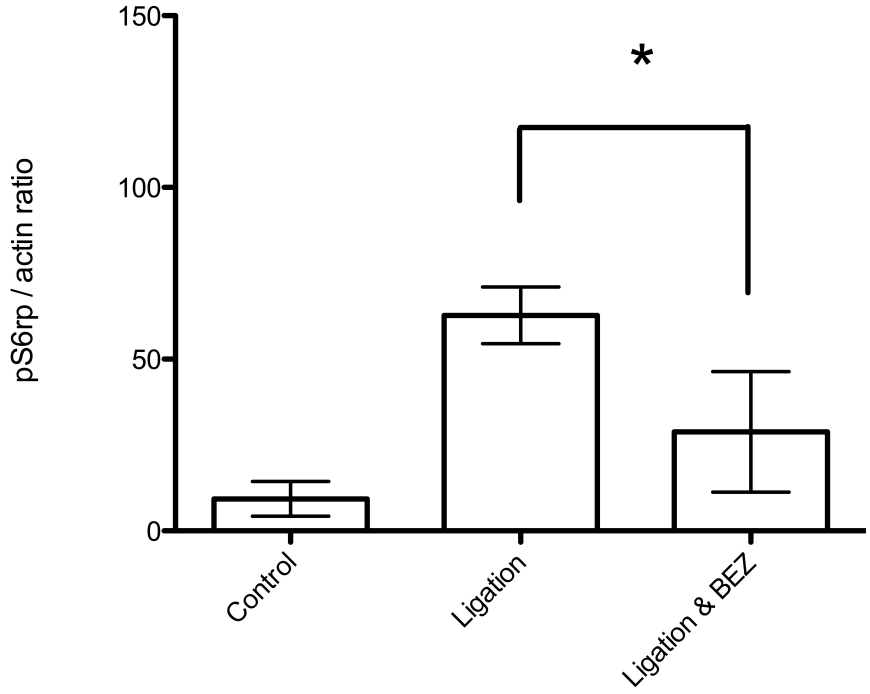

Figure 4.9 Immunoblotting of phospho-4E-BP1 protein expression (A) and phospho-S6 ribosomal protein expression (C) in adult mice submandibular glands after ligation exclusively (L), 3 days of Rapamycin treatment following ligation (L&R) or after 3 days of BEZ treatment following ligation (L&B). Ligation displayed a noticeable presence of both p4E-BP1 & pS6rp. But their presence was visibly reduced following 3 day ligation & BEZ administration. Densitometric analysis of p4E-BP1 (C) and pS6rp expression (D) as a ratio of their actin showed a statistically significant difference of protein to actin ratio between ligation and 3 days of BEZ treatment. The bars represent mean + SEM. Beta actin (β-actin) was used as a loading control. Mouse muscle tissue was used as positive control for p4E-BP1, however muscle homogenates show absence of β-actin, as muscle expresses α-smooth muscle actin (α-SMA). Data is indicative of results from at least three independent experiments.

4.3.3.2 Biochemical Analysis of Glycoprotein Content

Periodic acid-Schiff's staining demonstrated presence of acinar secretory glycoproteins in mice submandibular glands that were ligated or ligated and treated with 3 days of BEZ administration (Figure 4.10 A).

Unoperated controls demonstrated a visible presence of mucins, however 3 days of ligation eliminated this presence, as assessed by PAS gel staining. On the other hand, PAS gel staining of acinar mucins in ligated glands with 3 days of BEZ treatment revealed a recovery of acinar secretory glycoproteins, as exhibited by the presence of the low molecular weight acinar mucins (98 – 188 kDa), similar to those from the unoperated controls.

Statistical analysis of the band intensity of the stains as a percentage of controls (Figure 4.10 B), revealed that in fact ligated glands with 3 days of BEZ treatment were not statistically significantly different from unoperated controls. However, submandibular glands which had been exclusively ligated were significantly ($p<0.0001$) lower than unoperated controls, suggesting all glycoprotein content had been lost due to ligation onset atrophy. Moreover, the recovery of acinar secretory

glycoproteins following 3 days of Torin1 treatment during ligation was significant ($p < 0.05$) in comparison to ligated only glands.

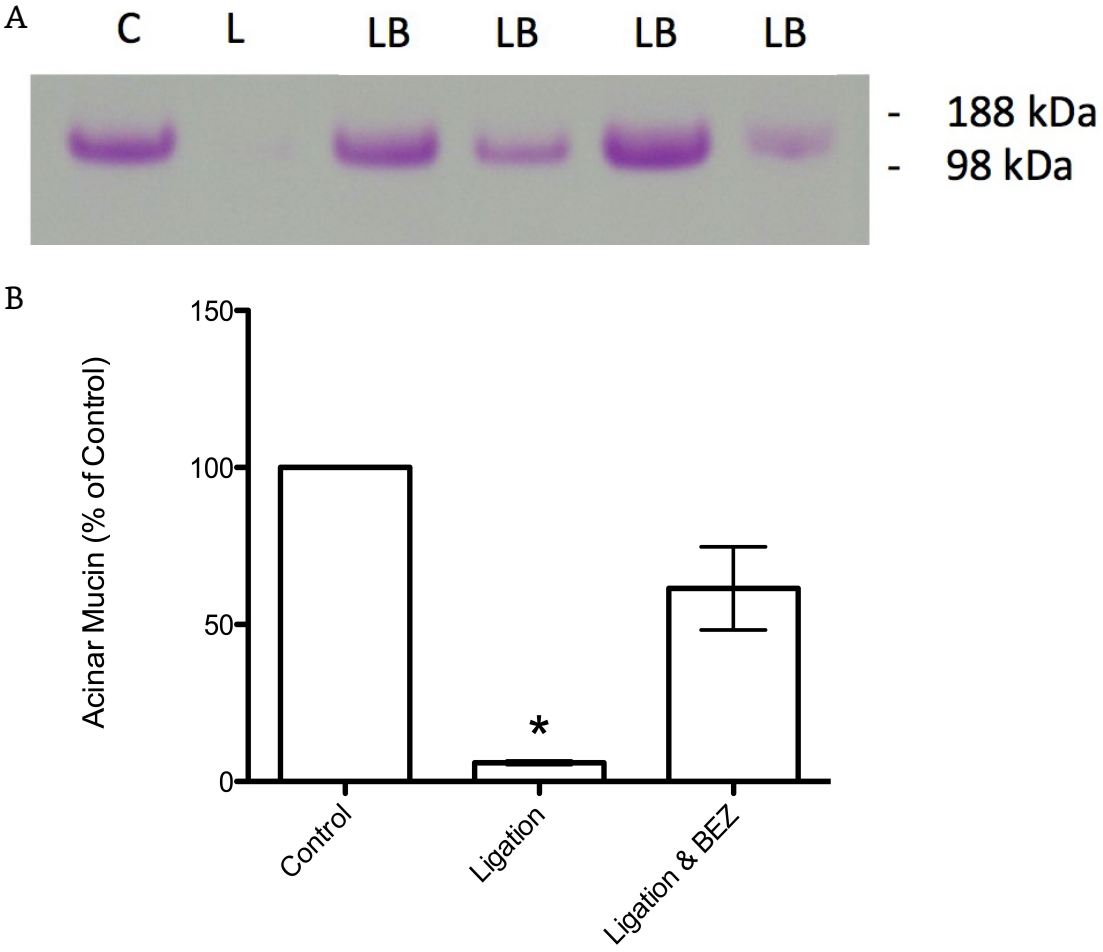

Figure 4.10 Periodic acid-Schiff's staining of glandular homogenates of 3 day ligated and ligated with BEZ treatment (A) glandular homogenates. Ligation resulted in significant loss of mucins, 3 days of BEZ treatment showed a visible recovery. Densiometric analysis of submandibular acinar mucin as a ratio of control (B), showed that 3 day ligation only was significantly lower than control (indicated by star), however 3 days ligation with BEZ treatment was not significantly different from control. The bars represent the mean + SEM. Data represents results from at least three independent experiments.

4.3.4 Histological Assessment

4.3.4.1 Torin1 Treatment

In order to judge the general tissue morphology for ligated glands, H&E staining (Figures 4.11 A) and AB/PAS staining (Figure 4.11 B) were used, demonstrating that 3 day ligation samples demonstrated a reduction in the size of acinar cells with loss of secretory granules, however an increase in the size of ducts and their lumen. In contrast, 7 day ligation samples experienced an almost complete loss of recognisable acini, but the presence of duct-like structures remained. The residual duct-like structures displayed considerable ductal luminal dilation in comparison to control, presumably as a result of degranulation. These morphological results also showed that in intense atrophy, cells appeared less densely packed as the volume of interlobular space increased. In addition, both groups showed the presence of inflammatory cell infiltration, which were composed mainly of neutrophils and macrophages in the connective tissue between the lobules and among the parenchymal elements.

3 days of Torin1 treatment following ligation induced atrophy H&E staining (Figure 4.11 C) showed that the extensive inflammatory cell

infiltration, adipose tissue displacement and increased extracellular space remained despite Torin1 administration. Ducts appeared very similar to ligated only glands, with very large lumena and AB/PAS staining (Figure 4.11 D) revealed no granular ducts left. AB/PAS findings also indicated that acini glycoproteins were localised to mucous cells, despite submandibular glands typically being predominantly serous.

After 7 days of Torin1 treatment following ligation, H&E results (Figure 4.11) showed signs of severe atrophy such as a complete loss of serous and mucous cells and glandular morphology which no longer resembled a submandibular gland. Fat cells had infiltrated between where the serous and mucous acinar cells had previously resided. Only duct-like structures had abided and surrounded by fibrous tissue. AB/PAS revealed a complete lack of secretory granules, as shown by no pink staining amongst the blue in Figure 4.11 F.

Control glands (Figure 4.11 G) were used to show normal glandular morphology and for comparison to atrophic tissues.

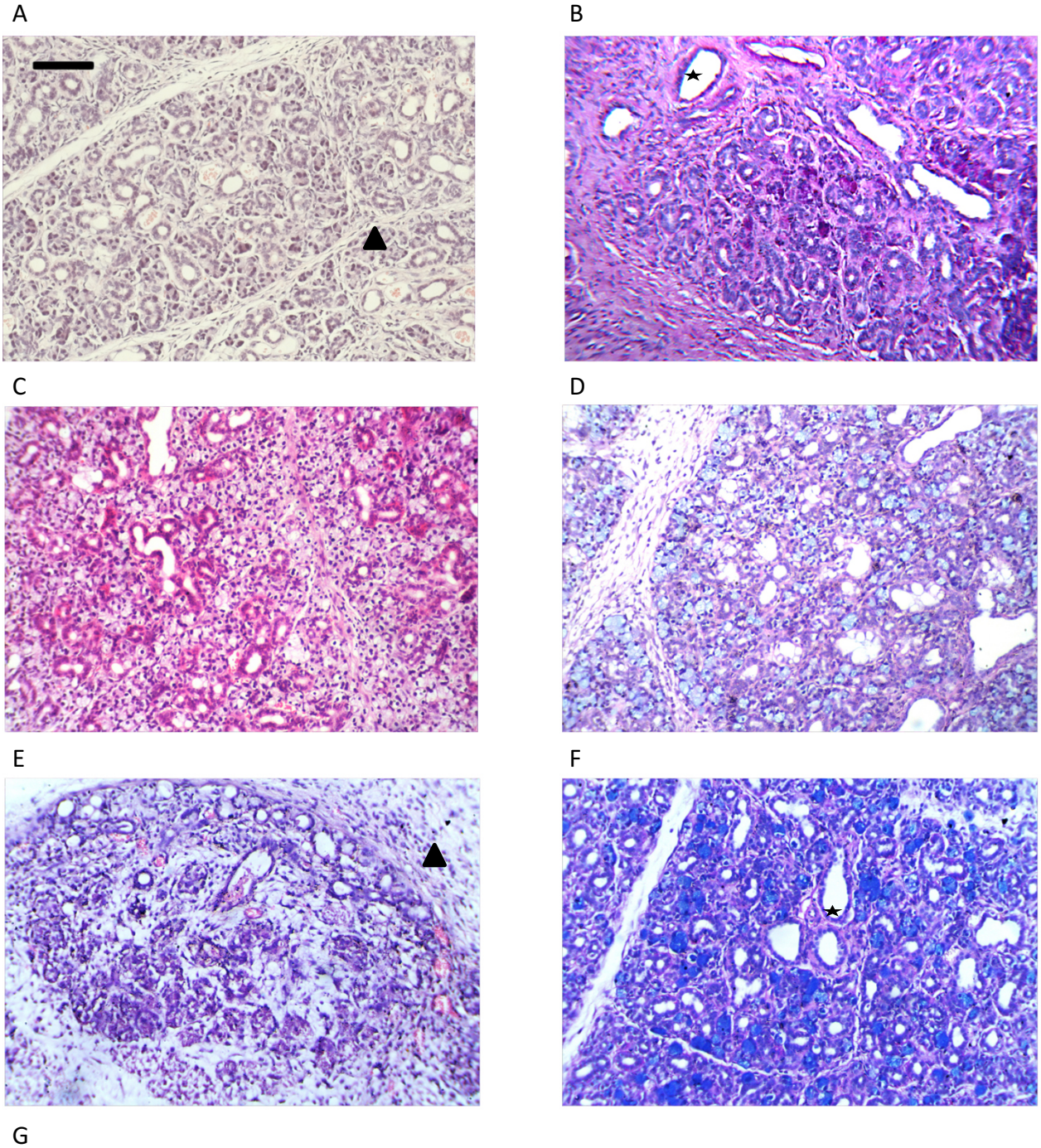

Figure 4.11 Histology of 3 day ligated (A), 7 day ligated (B), 3 day ligated with Torin1 treatment (C)(D), 7 day ligated with Torin1 treatment (E)(F), and control (G) glands. Ligation showed signs of atrophy including reduced acini, fat displacement, dilated ducts (star) & inflammatory infiltrates (arrowhead). 3 days of Torin1 alleviated some of these signs, however this could not be sustained for 7 days of treatment. Images are representative of samples from independent experiments. Scale *bar* represents 100 μm.

4.3.4.2 BEZ Treatment

The tissue morphology of BEZ treated ligated glands, shown via H&E staining, revealed that inflammatory cells had infiltrated along with adipose tissue displacement (Figure 4.12 A). Ductal structures experienced an apparent increase in quantity as well as increased ductal lumena, whereas acini remained intact, all in comparison to controls (Figure 4.11 G). Very large vacuoles and intraductal vacuolation were also present. AB/PAS staining (Figure 4.12 B) revealed that acini were intact and retained secretory granules.

4.3.5 Morphometric Analysis

In order to be able to quantify the results of tissue morphology, the mean area of the acini was measured (Figure 4.13). The morphometric analysis of samples revealed the mean area ± S.E.M. of the acini from the 3 day ligation samples (140.40±10.12μm^2, n=60) significantly decreased (P<0.005) in comparison with the control glands (422.90±39.02μm^2, n=80). Torin1 treatment following ligation could not rescue the acini size, whether it was administered for 3 days (179.09±12.18μm^2, n=140) or for 7 days (130.30±8.68μm^2, n=100). However BEZ treatment following ligation for 3 days did significantly (P=0.006) increase the mean acini area (305.69±29.65μm^2, n=120) from the ligated state and also in comparison to 3days Torin1 treatment (p=0.01).

A

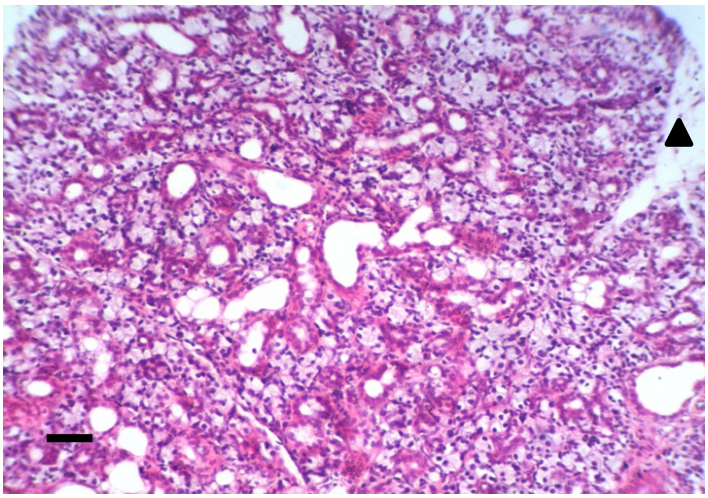

B

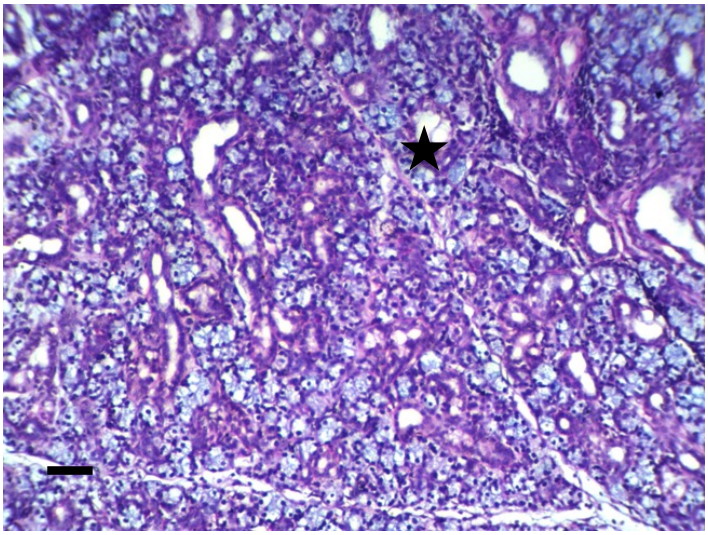

Figure 4.12 H&E staining (A) of submandibular glands following 3 days of ligation along with BEZ administration. The infiltration of a varying quantity of inflammatory cells was visible (arrowhead), along with duct luminal dilation (star), exemplary of the atrophic state. However, AB/PAS staining (B) of submandibular glands following 3 days of ligation along with BEZ administration, showed that not only are acini present, but they retain secretory granules, which is not typical for atrophic glands. Scale bar represents 100 μm.

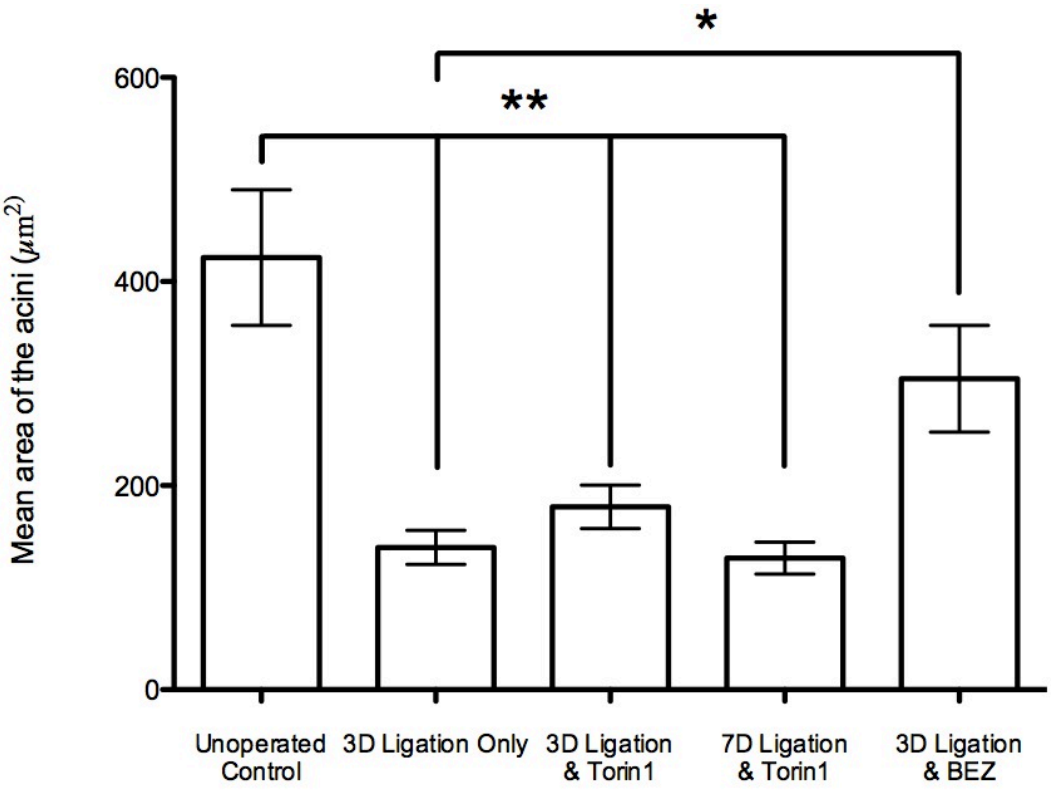

Figure 4.13 Morphometric analysis of the mean acini area from the H&E Stained samples of unoperated control, ligation only, 3 days of Torin1 following ligation, 7 days of Torin1 following ligation and 3 days of BEZ following ligation. Ligation significantly ($p<0.005$) the mean size of the acini in comparison with control. Torin1 treatment post ligation did not significantly increase the acini area from ligation only. However 3 days of BEZ treatment following ligation showed a significant increase in acini area ($p=0.006$). Data is expressed as mean+S.E.M.

4.3.6 Immunohistochemical Assessment

The localisation of mTOR during atrophy (and treatment with Torin1) was evaluated using anti-pS6rp immunohistochemistry (Figure 4.14). The immunohistochemical assessments revealed that pS6rp was present in the acini, but with little ductal staining, in atrophic glands following 3 days of duct ligation (Figure 4.14 A). Atrophic glands also showed that most of the acini, which were positively stained, were shrunk.

3 days of Torin1 treatment post ductal ligation revealed that mTOR was inhibited as pS6rp presence was minimal. Localisation of pS6rp revealed very little presence in the shrunken acini that had degranulated, whereas ducts were negative (Figure 4.14 B).

7 days of Torin1 treatment post ductal ligation in mice, however, revealed that mTOR had returned. pS6rp positive staining was visible in the shrunken acini as well as some ducts, alongside the presence of abnormal branched entities characterised by short duct like structures ending with smaller acini. (Figure 4.14 B).

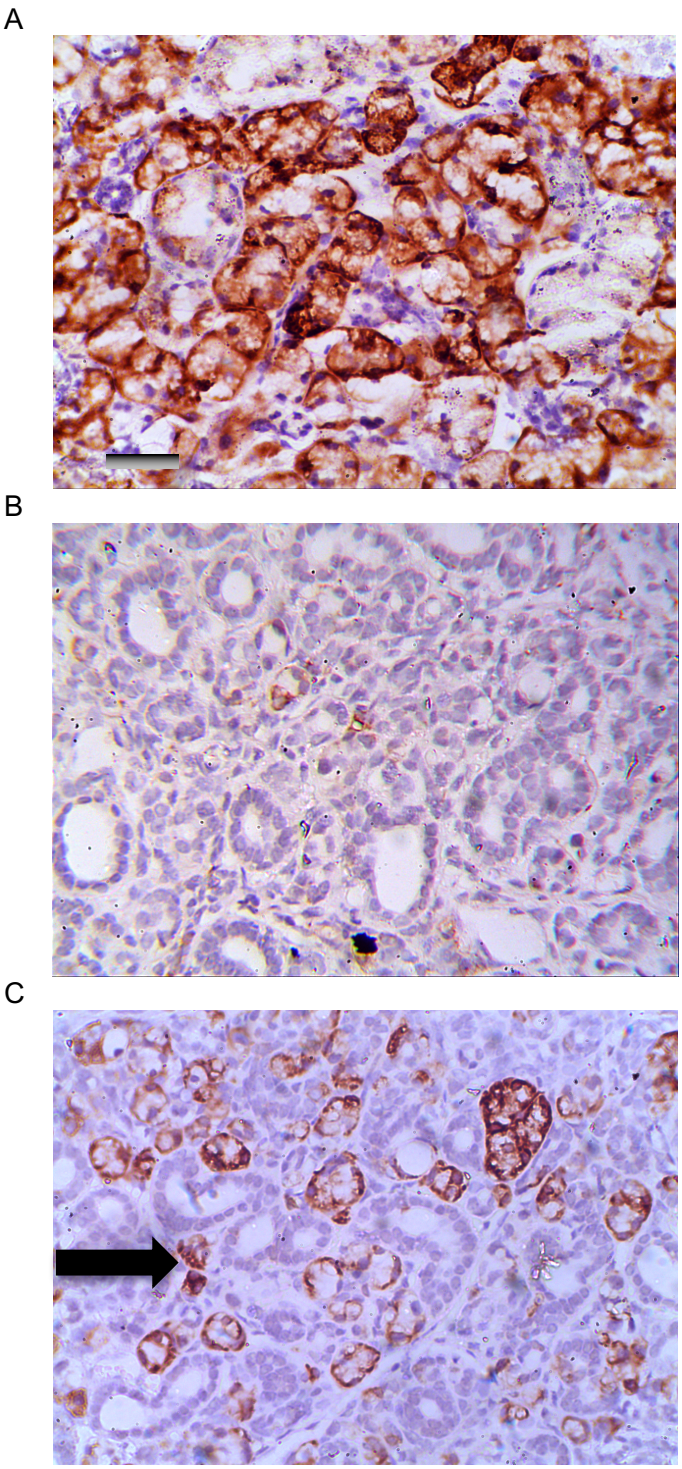

Figure 4.14 Immunostaining of pS6rp, counter-stained with H&E, in 3 day ligated mice (A), 3 day ligated with Torin1 treatment (B) and 7 day ligated with Torin1 treatment (C). mTOR expression was clearly evident in ligated only glands, however 3 days of Torin1 treatment reduced localisation to a barely visible presence (arrow) with residual staining in some shrunken acini. 7 days of Torin1 treatment had a return of mTOR to acini as well as some duct-like structures. Scale bar represents 100 µm.

4.3.7 Detection of rapamycin-induced alterations in protein & phospho-protein expression

In order to discover what kinase or pathway is protecting mTOR from becoming fully inhibited despite the presence of mTOR inhibitors, proteomic analysis of differentially expressed proteins among ligated glands (Sample A) and ligated with rapamycin treated glands (Sample B) was performed. In order to identify the different factors between the two samples, peptide mass fingerprinting and LC-MS/MS were used to monitor changes in the abundance of proteins. A total of 303 protein quantity alterations were identified in rapamycin treated ligated mice, in comparison to ligated only submandibular glands. From these, 45 had a significant ($p<0.005$) increase in their normalised values, calculated as fold change. Moreover, 5 protein chains were differentially expressed >5-fold between the ligated with rapamycin treatment and ligated only samples (Table 4.3).

Analysis of phosphopeptide-enriched samples, in order to identify the changes in abundance of phosphorylated proteins between ligated

glands and ligated with rapamycin treated glands. A total of 132 phosphorylated proteins changes were identified in rapamycin treated ligated mice submandibular glands, in comparison to ligated only submandibular glands. From these, 32 had a significant ($p<0.005$) increase in their normalised values, calculated as fold change. Furthermore, 5 phosphorylated protein chains experienced a >5-fold increase between the ligated with rapamycin treatment and ligated only samples (Table 4.4).

Table 4.3 Total proteins up-regulated in Sample B compared to Sample A

Accession	Name	MW (kDa)	Fold Change
P15945	Kallikrein 1-related peptidase b5	28.7	24
Q61754	Kallikrein 1-related peptidase b24	28.4	18
Q6JHY2	Submandibular gland protein C	74.3	16
P15947	Kallikrein-1	28.8	12
Q9D0F3	Lectin mannose-binding 1	57.8	8

Table 4.4 Phospho-proteins up-regulated in Sample B compared to Sample A

Accession	Name	MW (kDa)	Fold Change
Q8CCJ3	E3 Ubiquitin-like modifier protein ligase 1	89.5	8
Q99PL5	Ribosome-binding protein 1	172.8	6
Q9CRA5	Golgi phosphoprotein 3	33.7	6
O55028	Bckdk kinase, mitochondrial	46.6	5
Q61823	Programmed cell death protein 4	51.7	5

4.3.8 Detection of rapamycin-induced alterations in gene expression

Microarray experimentation revealed that rapamycin treatment following ligation had induced a total of 22690 gene changes in Sample B, compared to Sample A. Following statistical analysis, a list of 2430 genes that had significantly ($p<0.05$) increased in Sample B, was generated. Within the up-regulated genes, 598 genes showed an increase in expression above 5 fold changes (Table 4.5).

Table 4.5 Gene changes in Sample B compared to Sample A

	Quantity	% of total
Total changed genes	22690	100%
Total upregulated genes	10549	46%
Total downregulated genes	12141	53%
Significantly upregulated genes	2430	11%
Significantly downregulated genes	3902	17%
More than 5 fold upregulated	598	2%
More than 5 fold downregulated	1049	4%

Among these 2430 significantly upregulated genes, attention was mainly focused on genes relating to the mTOR pathway, regenerating salivary glands or atrophic salivary glands. A selection of genes of interest were identified among the significantly upregulated genes (Table 4.6) and therefore the roles of these particular genes and their pathways were chosen for further discussion.

Table 4.6 Genes of interest

Gene Name	Symbol	Fold Increase	Reason of Interest
GLI-Kruppel family member 2	GLI2	9.37	Activates Sonic hedgehog transcription (Pan et al., 2006)
Solute carrier family 18 member 1	SLC18A1	4.99	Interacts with mTOR pathway in Rats (Asante and Dickenson, 2010)
5'-AMP-activated protein kinase subunit gamma-2	PRKAG2	13.60	Increases TSC2 function (Inoki et al., 2005)
Fibroblast growth factor receptor 4	FGFR4	7.57	Interacts with FGFR1 (Loo et al., 2000)
Fibroblast growth factor receptor 1	FGFR1	2.55	Regulates branching morphogenesis and salivary gland development (Hoffman et al., 2002)
Target of rapamycin complex subunit LST8	MLST8	4.46	Gene for encoding a subunit of both mTORC1 and mTORC2 (Montero et al., 2012)
DEP domain containing MTOR-interacting protein	Deptor	2.13	Inhibits mTORC1, but conversely overexpression activates mTORC2 and Akt (Lamming and Sabatini, 2010)
Late endosomal / Lysosomal adaptor and MTOR activator 2	Lamtor2	2.08	Activator of mTORC1 (Scheffler et al., 2014)
Carcinoembryonic antigen-related cell adhesion molecule 1	CEACAM1	2.44	Influences Wnt pathway (Chen et al., 2009)
cAMP responsive element binding protein 1	CREB1	5.34	Downstream target of Akt (Du and Montminy, 1998)
Mitogen activated protein kinase 6	Map2k6	10.00	Activates MAPK in response to inflammatory cytokines or environmental stress (Koffel et al., 2014)
Phosphodiesterase 6G subunit gamma	PDE6G	5.39	Activates MAPK activity (Wan et al., 2001)
Mitogen-activated protein kinase 7	Mapk7	6.01	MAPK subunit that activates SGK1 (Hayashi et al., 2001)
Serum and glucocorticoid-regulated kinase 1	SGK1	2.40	Kinase that interacts with MAPK and is also phosphorylated by mTORC2 (Roux and Topisirovic, 2012)
TIP41-like protein	TIPRL	2.47	Regulates mTORC1 (Nakashima et al., 2013)

4.4 Discussion

Although atrophy of salivary glands due to the ligation of the main excretory duct of the submandibular gland has been well characterized in rats (Takahashi et al., 2004, Carpenter et al., 2007), our previous study was the first study of it's kind to use mice (Bozorgi et al., 2014). The results obtained demonstrated that rapamycin could not induce substantial regression of atrophy and could only delay atrophy, whilst hinting at mTOR's interactions with other pathways.

There are numerous factors that could account for the limited efficacy of rapamycin, including the PI3K-negative feedback mechanism (which re-activates mTORC1 via the TSC1/2 complex) (Guertin and Sabatini, 2009) or the theory that a significant subset of mTORC1's functionality is resistant to inhibition by rapamycin (Thoreen and Sabatini, 2009). Therefore inorder to counteract to the complex mechanisms of the PI3K–PTEN–AKT pathway (Figure 4.15), this study attempted to use mTOR complex inhibitors that inhibit both mTORC1 and mTORC2, as a method to induce substantial limiting of salivary gland atrophy, rather than a delay of atrophy, following duct ligation.

Torin1, an ATP-competitive small molecule inhibitor that inhibits both mTOR complexes, mTORC1 and mTORC2, equally (Thoreen and Sabatini, 2009) and BEZ, an orally administered imidazaoquanazoline derivative that binds to ATP-binding pockets, thus inhibiting mTOR kinases as well as PI3K isoforms (Tang and Ling, 2014), were chosen due to their pre-clinical studies that demonstrated stronger inhibitory activity of mTOR, suggesting they may have more promise as atrophy prevention agents.

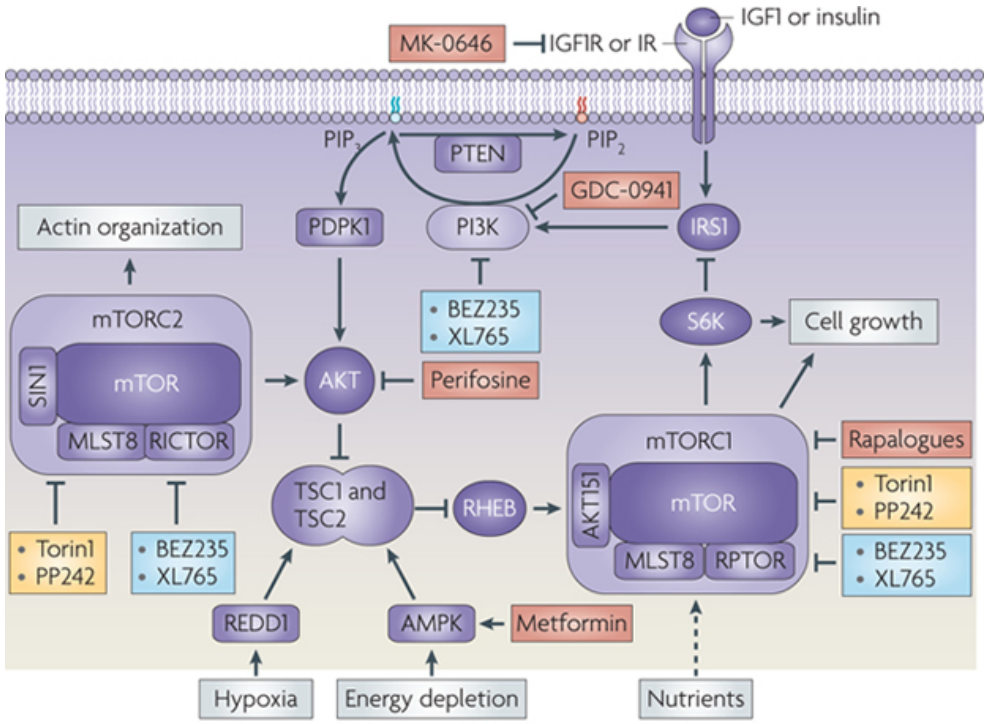

Figure 4.15 Schematic diagram of the PI3K–PTEN–AKT pathway showing inhibitors and activators in red, dual inhibitors of mTORC1 & mTORC2 in yellow, and triple inhibitors of mTORC1, mTORC2 & PI3K are highlighted in blue (Tennant et al., 2010).

Furthermore, it has been reported that one limitation of rapamycin administration in mammalians is that it appears to only exert partial effects of inhibition, at least with respect to autophagy induction and 4E-BP1 dephosphorylation (Thoreen et al., 2009), among many other reported limitations. This study also attempted to analyse the factors behind these partial inhibitory effects, in order to be able to further understand the mTOR pathway during atrophy, by performing a DNA microarray examination and a proteomic analysis of proteins and phosphorylated-proteins of changes that occur following rapamycin administration during ligation induced salivary gland atrophy.

One such change that occurred is that mean submandibular gland weight was significantly reduced in all ligation only groups in comparison with controls. This decrease was maintained even despite 3 days or 7 days of Torin1 treatment. Decreased volume and size of acinar cells with acinar and ductal degranulation may explain the significant decrease of glandular weights, although the increase of inflammatory cells infiltrating may have added to the gland weight initially (Correia et al., 2008). However, BEZ treatment following ligation did significantly increase the mean submandibular gland weights by 60% in comparison to ligation only, to an extent where their mean weight was slightly

above unoperated control's mean gland weight. This may be possibly due to glandular hyperplasia or even the swelling of the glands, as the BEZ treated mice did have some bodily swelling, causing their mean body weights to be 9% higher than unoperated controls. Whereas, there were no noticeable differences in body weight between any Torin1 experimental mice and unoperated controls. Furthermore, in preparatory undertakings for this study, this particular dose of BEZ administration was found to be the maximum dose without seeing significant levels of body swelling, particularly across the abdomen, similar to the significant abdominal swelling found in a previous PI3K inhibition study (Hu et al., 2002).

Another change from the previous study is that although previously rapamycin was safely administered for 7 days, and shown to delay salivary gland atrophy (Bozorgi et al., 2014), here BEZ treatment could not be attempted for 7 days of ligation-induced atrophy as during preparatory undertakings for this study, toxicity was observed from the long term use of the compound, similar to the common toxicities of mTOR inhibitors (Soefje et al., 2011). A previous study that observed the cytotoxic effects of BEZ, recommends the addition of CQ, a common

clinical anti-cancer drug, that inhibits autophagy and counteracts the cytotoxic effect of BEZ (Li et al., 2013).

Immunoprobing of the phospho-S6 ribosomal protein, which is phosphorylated at several sites by S6K1 (Burnett et al., 1998, Isotani et al., 1999) and 4E-BP1 (another mTORC1 substrate) confirmed that mTOR is activated during ligation-induced atrophy of the salivary glands, which corresponds with the start of autophagic processes during ligation-induced atrophy (Silver et al., 2010).

Immunoblots revealed that 3 days of Torin1 administration after ligation had completely inhibited mTOR, as western blots of p4E-BP1, pS6rp and total mTOR, were all visibly absent. However one point of mention is that total 4E-BP1 protein abundance, predominantly in its lower isoform, is still more visible in ligated and Torin1 treated samples in comparison with unoperated controls.

7 days of Torin1 treatment following ligation, however, appeared to have lost all inhibitory effects on mTOR, as western blots of p4E-BP1, pS6rp and mTOR, were all significantly increased in comparison to 3 days of Torin1 treatment. This suggests that Torin1, similar to

rapamycin, could not fully inhibit mTOR for longer periods, as mTOR activity had returned by 7 days. It should also be noted that both mTORC1 substrates, 4E-BP1 and S6k, were actually more present in western blots of 7day Torin1 treated ligated glands rather than in ligated only glands, this could be because mTORC1 substrates may be increasing their total kinase quantity via PI3K in order to compensate for mTOR inhibition (Mendoza et al., 2011, Fruman and Rommel, 2014), which can accumulate across the 7days as Torin1 has been suggested to only have a limited ability to affect the long term accumulation of early or immediate proteins (Moorman and Shenk, 2010).

Western blots of the mTOR substrates, pS6rp and p4E-BP1, for BEZ treatment for 3 days after ligation revealed that mTOR had been inhibited in submandibular gland tissues. The densitometry of the western blots, revealed that after 3 days of BEZ treatment both pS6rp and p4E-BP1 were significantly lower than ligated only glands. Furthermore, BEZ treatment had reduced latent 4E-BP1 levels to that which is comparable to unoperated controls, unlike 3 days of Torin1 treatment which had left total 4E-BP1 protein abundance, predominantly in its lower isoform, more visible than in unoperated controls. This may be because the phosphorylation of mTORC1

downstream targets is differentially sensitive to mTOR complex inhibition (Kudchodkar et al., 2004, Walsh et al., 2005, Moorman and Shenk, 2010). While the mTORC1 phosphorylation of S6 kinase is inhibited by rapamycin and other mTOR inhibitors, during times of biological stress (Johnson et al., 2001, Moorman and Shenk, 2010), the phosphorylation of 4E-BP1 is slightly resistant to mTOR complex inhibition (Nyfeler et al., 2011, Thoreen et al., 2012).

It has been suggested that this differential effect of inhibition on mTOR targets could indicate that a kinase other than mTOR is responsible for 4E-BP1 phosphorylation during periods of stress, such as atrophy or infection (Moorman and Shenk, 2010), such as the PI3K dependent phosphorylation of 4E-BP1 (Pham et al., 2000, Gingras et al., 2001). This theory is further supported because BEZ, which is a triple inhibitor of PI3K as well as both mTOR complexes, fully inhibited 4E-BP1 phosphorylation and returned it to levels which were similar to unoperated controls, in contrast to Rapamycin and Torin1. These results demonstrate that the mTOR inhibitory-resistant phosphorylation of 4E-BP1 during ligation induced atrophy is dependent on BEZ-sensitive mTOR and PI3K activity. This suggests that were it not for the BEZ-induced toxicity and bodily swelling that

prevented a 7 day experiment of BEZ treatment following ligation, BEZ might have been able to fully inhibit mTOR even after 7 days of treatment following ligation unlike Torin1 or Rapamycin treatment, which had both lost efficacy at 7 days of treatment.

Immunoblotting for pS6rp antibody after 3 days of BEZ treatment following ligation did also express significantly lower band intensity than ligated only, however results were still higher than unoperated controls and with more variance between the highest and lowest expression levels. The reasoning for this could be that suboptimal doses of BEZ induce a disruption of the S6K to IRS-1 negative feedback loop (Harrington et al., 2004, Serra et al., 2008). During short term exposure to BEZ, this loop can be completely supressed regardless of the dose level used (Serra et al., 2008), on the contrary, longer term exposures of over 48 hours result in an increase of P-Akt (Serra et al., 2008), which can re-activate mTORC1 substrates. Whereas higher dose concentrations of BEZ are required to completely block Akt phosphorylation (Serra et al., 2008), however this was unmanageable in this experiment, as in preparatory undertakings for this study, such high doses were found to result in significant body swelling, particularly across the abdomen, similar to the significant abdominal swelling found in a previous PI3K

inhibition study (Hu et al., 2002), alongside the BEZ-induced toxicity as discussed earlier.

The immunoblotting of autophagy markers Atg3, Atg5 and LC3 were used in amalgamation to identify the status of autophagy during duct-ligation induced atrophy and also whether or not autophagy was taking place after Torin1 treatment. Ligated only glands revealed a high presence of all markers, with Atg5 significantly ($p<0.005$) increased in ligated glands in comparison to controls and Atg3 also significantly ($p<0.01$) increased in comparison to controls. LC3 western blots showed that in 3 day ligated glands the LC3-I to LC3-II ratio increased by 50%; normally such an LC3 blot cannot be used on it's own to interpret autophagy (Shvets et al., 2008), as the increased LC3 staining could possibly be an indication that autophagy is suppressed, resulting in decreased lysosomal degradation of LC3 and consequently increase of LC3 in immunoblots (Mizushima et al., 2010). However when viewing the LC3 blots in the context of the Atg3 and Atg5 blots, we can reach the conclusion that autophagy was active in ligated glands, which coincides with the activation of mTOR (Silver et al., 2010).

Although 3 days of Torin1 treatment did inhibit mTOR activity as discussed earlier, it did not reduce the presence of the autophagy markers Atg3, Atg5 and LC3 as indicated in immunoblots. Although Atg5 bands were reduced in comparison to ligation only, a clear visible presence of Atg5 remained following 3 days of Torin1 treatment. Atg3 was significantly ($p<0.01$) higher than controls and it was actually more present following Torin1 than it had been in ligated only samples. Furthermore, there was a 63% increase in the ratio of LC3-I to LC3-II following Torin1 treatment. The combination of these results, particularly the increases in LC3-II and Atg3, suggests that the inhibition of mTOR via 3days of Torin1 treatment increased autophagic activity, rather than decreasing it. This is in agreement with theories that inhibition of mTOR induces autophagy (Jung et al., 2010, Xie et al., 2013, Kapuy et al., 2014).

The treatment of Torin1 for 7 days following ligation significantly ($p<0.005$) reduced the presence of Atg5, in comparison to ligated only samples. Taken as a singularity, this would suggest that autophagic activity was inhibited by 7 days of Torin1 treatment, however when analysed in combination with Atg3 and LC3 this would appear to not be the case. Atg3's presence was at its highest levels following 7 days of

Torin1 treatment and was significantly (p=0.005) greater than ligation only. Immunoblotting analysis of LC3, which is considered a more reliable method for monitoring autophagy and autophagy-related processes, including autophagic cell death (Tanida et al., 2008), revealed that LC3 as a whole had been reduced greatly. Despite initial reactions however, reduction of total LC3 is paradoxically a good indicator of autophagic flux as LC3 is degraded by autophagy (Jung et al., 2010). This is because LC3-I was gradually reduced during autophagy due to it becoming covalently conjugated to phosphatidylethanolamine by Atg3 catalysis to form LC3-II (Silver et al., 2010) and LC3-II was reduced because LC3-II itself is degraded by autophagy (Mizushima and Yoshimori, 2007). Furthermore, the slight presence of LC3-II that remained in blots of 7 day ligated and Torin1 treated samples could be because LC3-II is more sensitive to immunoblotting than LC3-I (Klionsky, 2009).

Therefore, when evaluating all these immunoblots of the autophagy markers Atg3, Atg5 and LC3, it can be concluded that autophagy was active in all experimental groups. It became activated in ligated only glands, where its activation coincided with the activation of mTOR in submandibular gland atrophy, as previously shown by our group in rats

(Silver et al., 2010). Autophagic activity then became most prominent when mTOR was inhibited following 3 days of Torin1 treatment, where the inhibition of mTOR further induces autophagy (Jung et al., 2010, Xie et al., 2013, Kapuy et al., 2014). But in 7 days of Torin1 treatment following ligation, where mTOR activity had returned, autophagy was still present and autophagic flux was underway in full force, as indicated by the degradation of LC3.

Histological assessments of ligated only glands did not reveal any novel findings with shrunken acinar cells with loss of secretory granules, duct luminal dilation as they underwent degranulation and a general loss of cytoplasm in the duct cells of 3 day ligated glands, which are typical signs of salivary gland atrophy (Scott and Gunn, 1991). This was supported by the PAS gel staining of 3 day ligated glands which revealed that acinar mucins had been significantly reduced. 7 day ligated gland showed a complete loss of acini and increased amount of connective tissue filled with inflammatory cell infiltrates in the glandular histology, which are usually found in severely atrophic salivary glands (Scott et al., 1999), with the respective PAS gel staining experiments showing that acinar mucins had been lost to a significant extent which further backs up these histological results. All of which are similar to

previous findings of duct-ligation induced salivary gland atrophy in mice (Bozorgi et al., 2014).

However histological assessments of Torin1 treated ligated mice provided some compelling contradictory results between 3 day and 7 day experiments. 3 days of Torin1 treatment following submandibular gland ligation caused the ducts to display larger lumena in comparison controls and the presence of inflammatory cells, although acini had recovered from ligated only glands with a significant reduction in the area of acini. AB/PAS staining revealed that no granular ducts remained and that acini gylcoproteins were localised to mucous cells. This was further supported by PAS immunoblots that revealed recovery of acinar secretory gylcoproteins.

7 days of Torin1 treatment following ligation, however, showed signs of increasing atrophy in H&E results including morphological changes similar to ligation only samples, such as complete loss of serous and mucous cells. AB/PAS supported this by showing a complete lack of secretory granules and PAS immunoblots showed no acinar secretory glycoprotein, comparable to ligated only glands.

The tissue morphology of BEZ treated ligated glands revealed a significant increase of the mean acini area from the ligated state, unlike Torin1 treatment. Ductal structures experienced an apparent increase in quantity as well as increased ductal lumena, in comparison to controls, however granular convoluted tubules and striated duct cells had elongated to such an extent that they were degenerated. Furthermore, AB/PAS staining revealed that acini were intact and retained secretory granules and PAS gels further supported this by showing the presence of low molecular weight acinar mucins, similar to those from unoperated controls. These findings corroborate our previous suggestion that were it not for the BEZ-induced toxicity and bodily swelling that prevented a 7 day experiment of BEZ treatment following ligation, BEZ might have been able to fully recover glandular morphology to levels which would be comparable to controls by being able to fully inhibit mTOR even after 7 days of treatment following ligation unlike Torin1. However in such a scenario, although overall morphology may recover, GCT and striated ducts may remain degenerated as those have been identified as characteristics of apoptosis in rodent submandibular glands (Choi et al., 2009) and BEZ treatment has been shown to induce cell death and is associated with apoptosis (Li et al., 2013).

These results show that Torin1 is unable to fully inhibit the mTOR substrates 4E-BP1 and S6K, and BEZ is unable to fully inhibit S6K, during submandibular gland atrophy, similar to rapamycin (Bozorgi et al., 2014). This raises the question of why this occurs, as previously we concluded that it might be as a result of the negative feedback loop re-activating mTOR, however Torin1 and BEZ should effectively block this loop. With other studies, not in submandibular glandular atrophy, suggesting that Torin1 and BEZ do fully inhibit mTOR and/or the negative feedback loop (Thoreen et al., 2009, Dufour et al., 2011, Lee et al., 2011, Moon du et al., 2014), the question is raised of what is reactivating mTOR independently of mTOR inhibitors? In order to discover what kinase or pathway is rescuing the effects of mTOR substrates despite the presence of mTOR inhibitors, DNA microarray and LC-MS/MS protein identification was performed on rapamycin treated ligated samples and ligated only samples, in order to identify the gene changes, protein changes and phosphorylate protein changes that occur in submandibular gland atrophy in the presence of mTOR inhibitors.

A number of previous investigations, using a combination of 2-DE, MS and LC-MS/MS, have been carried out for the study of proteins in

normal, injured and recovering salivary glands (Ghafouri et al., 2003, Walz et al., 2006, Sawaki et al., 2011, Misuno et al., 2014). Even though an impressive number of over 300 total protein changes have been identified in this present study, it was possible to compare these results to those of previous studies to comprehensively determine their relevance to atrophic and/or regenerating submandibular glands. The results show that most components can be explained by mixed contributions of various bodily functions or glandular functions of the major salivary glands with only few components remaining that may be derived from the treatment of rapamycin to the atrophic salivary glands. Submandibular gland protein C was identified at 74.3 kDa and found to have a 16 fold increase in quantity. It is of note because protein C is a major product of the neonatal type I cells and is either absent or present at greatly diminished levels in normal adult glands (Ball et al., 1988, Mirels and Girard, 1993, Zinzen et al., 2004). Nidogen-1 was identified at 136.5 kDa and found to have a 2.7 fold increase. Nidogen-1 is an extracellular matrix component that is normally absent in adult submandibular glands but present in embryonic salivary glands (Miosge et al., 2000, Tucker and Miletich, 2010). The presence of these embryonic specific proteins in the rapamycin treated glands may suggest that these glands are regenerating in the presence of

rapamycin, as salivary gland regeneration following ligation retraces an embryonic-like state (Carpenter and Cotroneo, 2010, Cotroneo et al., 2010).

Furthermore some phosphorylated spots were upregulated in rapamycin treated glandular samples that are associated with the mTOR pathway. The BCKD mouse kinase and programmed cell death protein 4 (Pdcd4) were both upregulated in rapamycin treated ligated mice submandibular glands in comparison to ligated only glands. The BCKD mouse kinase that was activated, more specifically 3-methyl-2-oxobutanoate dehydrogenase kinase, is a key enzyme involved in regulating the activity state of the BCKD complex (Garcia-Cazorla et al., 2014). The phosphorylation of the BCKD complex has been proven to have links to mTOR activation via leucine (Lynch et al., 2003, Schaffer and Suleiman, 2007). BCKD has been delineated as reacting with α-ketoisocaproate acid (Dakshinamurti and Zempleni, 2005), this complex interaction (Figure 4.16) may be required for leucine activation of mTOR (McDaniel et al., 2002).

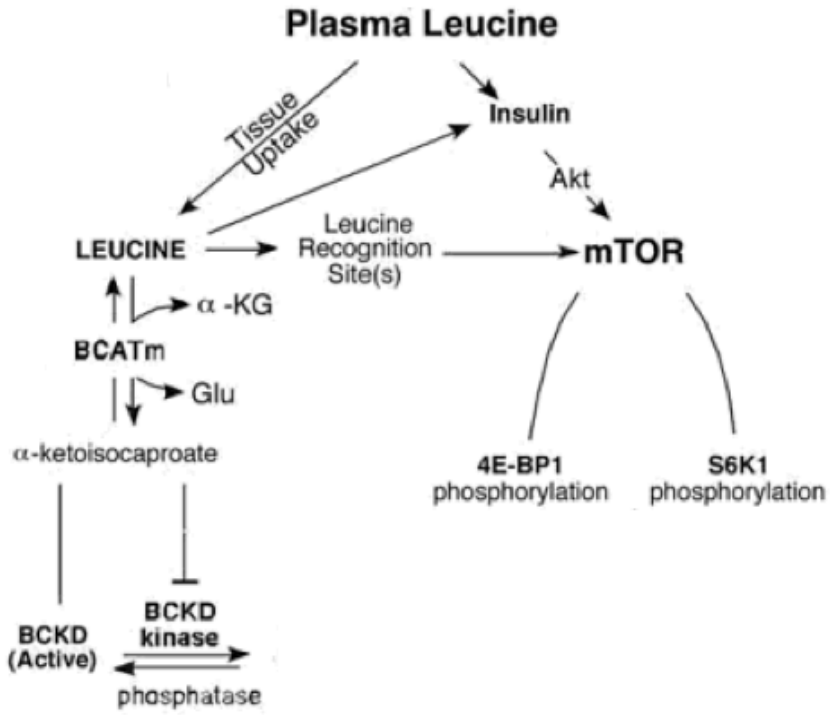

Figure 4.16 Schematic representation of the Leucine-BCKD-mTOR interaction. Figure altered from (Dakshinamurti and Zempleni, 2005)

Programmed cell death protein 4 is an inhibitor of translation initiation and cap-dependent translation (Yang et al., 2003, Parsyan, 2014). Pdcd4 does this by binding with the eIF4F complex (eIF4A, eIF4E, and eIF4G) and limiting the activity of free eIF4A (Waters et al., 2011). Previous studies have found links between the sequential engagement of the mTOR pathway and downstream suppression of Pdcd4 expression (Carayol et al., 2008), discovered that Akt phosphorylates Pdcd4 (Palamarchuk et al., 2005) and identified S6K as the mediator in phosphorylating Pdcd4 (Dennis et al., 2012).

The findings that both BCKD mouse kinase and Pdcd4 had been significantly upregulated following rapamycin treatment in atrophic submandibular glands are distinctive. The upregulation of Pdcd4 suggests that Akt / mTOR were active despite the presence of rapamycin and the upregulation of BCKD suggests that it may be the interactions of leucine that are causing the activation of Akt, which in turn activates mTOR. This is because it has been previously demonstrated that leucine levels are involved in regulating the activity of S6K1 and 4E-BP1 (Lynch et al., 2000, Xu et al., 2001) and that they also affect mTOR's interactions with the protein rictor (rapamycin-insensitive companion of mTOR) (Sarbassov et al., 2004).

DNA microarray analysis attempted to identify the genes of the pathways involved in reactivating mTOR irrespective of rapamycin's presence. One point of note is that out of over twenty thousand changed genes, only 3 genes were protein encoding genes for proteins that were also identified from our proteomic analysis of phospho-proteins. They were StarD10, which is closely related to breast cancer (Hoffmann et al., 2005), PPP1R16B, which is a subunit of the regulator of protein phosphatase 1 (PP1) (Kim et al., 2005), and IQGAP2, which is a Ras GTPase activator (Brill et al., 1996). The genes of interest (Table 4.6)

were particularly interesting as they presented many differing possibilities that might explain the re-activation in 7 day ligated glands despite the presence of rapamycin. Deptor, who's gene was upregulated more than 2 fold, has been shown to activate mTORC2 and Akt during its overexpression (Lamming and Sabatini, 2010), which may be reactivating mTORC1 again through the negative feedback loop (Efeyan and Sabatini, 2010). Lamtor2, a gene that had been upregulated more than 2 fold, directly activates mTORC1 via the receptor tyrosine kinase Flt3 (Scheffler et al., 2014).

Several genes of the Mitogen-activated protein kinases (MAPK) family were also significantly upregulated, including Map2k6, Mapk7, PDE6G and SGK1. These are of particular significance as the combination of these genes show that Map2k6 might be activating MAPK in response to the environmental stress (Koffel et al., 2014), in this case the stress being ligation. MAPK activity itself is kickstarted by PDE6G (Wan et al., 2001) and Mapk7 is activating SGK1 (Hayashi et al., 2001). SGK1 itself was upregulated more than 2 fold and this gene encodes a kinase that interacts with MAPK and is also phosphorylated by mTORC2 (Roux and Topisirovic, 2012). The interactions of this particular kinase family with mTOR is still highly debated, as a previous study states that mTOR

inhibition activates MAPK (Carracedo et al., 2008), whilst a differing study states that the MAPK and mTOR pathways are differentially activated (Rios-Moreno et al., 2011) and a contradictory study says that MAPK activates mTOR via Raptor (Carriere et al., 2011).

Based on the results obtained in this experiment, Torin1 treatment is not believed to be effective in longer periods of administration. Previously it was suggested that rapamycin may not be effective in longer periods of administration, such as for 7 days, because rapamycin is not a full inhibitor of mTOR, owing to the PI3K-negative feedback mechanism (which re-activates mTORC1 via the TSC1/2 complex) (Guertin and Sabatini, 2009, Bozorgi et al., 2014). However using a second generation mTOR inhibitor, Torin1, which is thought to inhibit all kinase-dependent functions of mTOR (Thoreen et al., 2009), we obtained essentially identical results to rapamycin. Therefore it may be possible that both rapamycin and Torin1 had been effective in mTOR inhibition, yet S6K1 and 4E-BP1 were activated via mTOR-independent phosphorylation of S6K1 and 4E-BP1, a mechanism suggested by other studies (Liu et al., 2013), perhaps via PI3K.

However using BEZ, a dual inhibitor of both mTOR and PI3K, provided promising results after 3 days, although S6K immunoblots had high variance between the highest and lowest expression levels. However 7 day experiments involving BEZ were unmanageable in this experiment, due to toxicity and swelling as discussed earlier. The reasoning for this could be that BEZ has different maximum drug concentrations in different models (Cao et al., 2009), which can therefore cause an accumulation of BEZ over time until it reaches a maximum concentration, causing toxicity issues.

Proteomic and Microarray analysis could not fully answer the question of just why BEZ could not completely inhibit S6K or why Torin1 could not fully inhibit mTOR. But they did give rise to a further path of enquiry into whether or not the MAP kinase or interactions with leucine are re-activating mTOR or its substrates.

CHAPTER 5

INFLUENCE OF mTOR DURING SALIVARY GLAND REGENERATION

5.1 Introduction

The development of our understanding of the morphological changes following ligation of the main excretory ducts (Carpenter et al., 2007a, Correia et al., 2008, Carpenter et al., 2009), has been followed up with a natural progression to examining the morphological and cellular effects during the regeneration of glands (Cotroneo et al., 2008a). This has led to uncovering that both intra-oral duct ligation and extra-oral duct ligation are completely reversible, due to the gland's ability to recover its functionality (Osailan et al., 2006, Carpenter et al., 2009).

Studies have attempted to draft a template for salivary gland regeneration by observing salivary gland development (Patel and Hoffman, 2014), however some controversy remains within literature about the developmental origin of the epithelium of major salivary glands. While the submandibular, parotid and sublingual glands are known to be derived from the oral epithelium (Myers and Ferris, 2007), it remains unclear which part of the epithelium they arise from (Patel and Hoffman, 2014).

Others have taken a more clinical approach to salivary gland regeneration, such as the potential use of bone marrow derived stem

cells in order to regenerate salivary glands (Lombaert et al., 2006, Yoo et al., 2014) or the substitution of salivary glands with bioengineered artificial salivary glands that closely resemble the native organ in both structure and function (Kagami et al., 2008, Nelson et al., 2013).

Gene therapy and gene transfer techniques have also shown promising futures in regards to salivary gland functional recovery (Delporte et al., 1997, Shan et al., 2005).

Other alternative approaches have appeared with slightly more exploratory results, such as the induction of proliferation, migration and differentiation of residual cells in damaged salivary glands to promote tissue regeneration (Kagami et al., 2008) or the possibility of using bioengineered organ germs, rather than entirely artificial salivary glands, for transplants as an alternative to regeneration (Ogawa et al., 2013).

However, some of the biochemical exchanges which occur as a result of regeneration are hitherto underexposed, particularly regarding the role of mTOR in salivary gland regeneration following de-ligation and the

characterisation of the early stages of glandular regeneration, which can be crucial in order to fully understand the mechanisms of recovery.

Therefore the aim of this study is to identify the key time points of the early stages of regeneration and the function of mTOR during glandular recovery by examining the regeneration of salivary glands after de-ligation following a period of ductal ligation in the presence of an mTOR inhibitor at different stages: during ligation only, de-ligation only or both during ligation and de-ligation.

5.2 Materials and Methods

5.2.1 Experimental design

26 adult ICR mice, weighing an average of 20-25g, were designated into control, ligation and de-ligation groups, as previously described in chapter 2.2 The control group (n=4) were unoperated controls and the ligation group (n=4) underwent submandibular main excretory duct ligation for 7 days. The de-ligation group consisted of 4 branches (Table 5.1).

The first branch consisted of 6 mice that underwent 7 days duct ligation followed by 7 days de-ligation. The second branch consisted of the aforementioned branch, 4 mice that underwent 7 days duct ligation followed by 7 days de-ligation, whilst receiving rapamycin treatment throughout the entire experiment, however one of said mice only survived until Day 8 of procedures due to death. The third branch had 4 mice that underwent 7 days duct ligation followed by 7 days de-ligation, whilst receiving no drug treatment for the first 7 days of the experiment but rapamycin treatment for the last 7 days. The final branch consisted of 4 mice that underwent 7 days duct ligation

followed by 7 days de-ligation, whilst receiving rapamycin treatment only for the first 7 days of the experiment.

For each individual mouse, glands were harvested and gland weights recorded. Half of the gland was fixed in 4% formalin for histological sections. The other half was snap frozen in liquid nitrogen and then used for gland homogenates for the purposes of PAS staining and western blotting.

Table 5.1

The experimental design of the de-ligation group and its 4 branches.

	Day 1	2	3	4	5	6	7	8	9	10	11	12	13	14
Branch 1	Ligation	Ligation	Ligation	Ligation	Ligation	Ligation	Ligation	De-ligation	De-ligation	De-ligation	De-ligation	De-ligation	De-ligation	De-ligation
Branch 2	Ligation & Rapamycin	Ligation & Rapamycin	Ligation & Rapamycin	Ligation & Rapamycin	Ligation & Rapamycin	Ligation & Rapamycin	Ligation & Rapamycin	De-ligation & Rapamycin	De-ligation & Rapamycin	De-ligation & Rapamycin	De-ligation & Rapamycin	De-ligation & Rapamycin	De-ligation & Rapamycin	De-ligation & Rapamycin
Branch 3	Ligation	Ligation	Ligation	Ligation	Ligation	Ligation	Ligation	De-ligation & Rapamycin	De-ligation & Rapamycin	De-ligation & Rapamycin	De-ligation & Rapamycin	De-ligation & Rapamycin	De-ligation & Rapamycin	De-ligation & Rapamycin
Branch 4	Ligation & Rapamycin	Ligation & Rapamycin	Ligation & Rapamycin	Ligation & Rapamycin	Ligation & Rapamycin	Ligation & Rapamycin	Ligation & Rapamycin	De-ligation	De-ligation	De-ligation	De-ligation	De-ligation	De-ligation	De-ligation

5.2.2 Protein Detection

SDS-PAGE was performed on tissue homogenates, in preparation for protein detection, as described in chapter 2.9. PAS of glandular homogenates was used to assess glycoproteins, as previously described in chapter 2.11. Western blotting was performed to visually analyse the specific proteins of total mTOR, pS6rp and p4-EBP1, as described in chapter 2.12.

5.2.3 Histology

General morphology of the tissue sections was assessed by haematoxylin and eosin staining. For this method, tissue sections were stained with Mayer's Haematoxylin for 3-5 minutes, washed in running water (2 minutes), differentiated (de-stain) with 1% acid alcohol and then stained with 1% Eosin for 1 to 3 minutes (H& E staining). The secretory granules inside acinar cells were identified by AB/PAS staining, as previously described in chapter 2.6.2.

5.2.4 Statistical

Data is expressed as mean $\pm$ S.E.M with $p<0.05$ being considered statistically significant. Statistical analyses were conducted using student's t-test; unless where stated via a one-way analysis of variance (ANOVA) using Prism version 5.00 (GraphPad Software, California USA) and Microsoft Excel 2011 (Microsoft, Redmond, WA).

5.3 Results

5.3.1 Gland weights

Mean submandibular gland weights were significantly ($p<0.005$) decreased in all groups in comparison to control. De-ligated mice experienced no significant change in gland weights in comparison to ligated only mice (Branch 1). Rapamycin treatment, no matter how it was administered in Branch 2, 3 or 4, also caused no significant change in gland weights in comparison to ligated only or de-ligated mice.

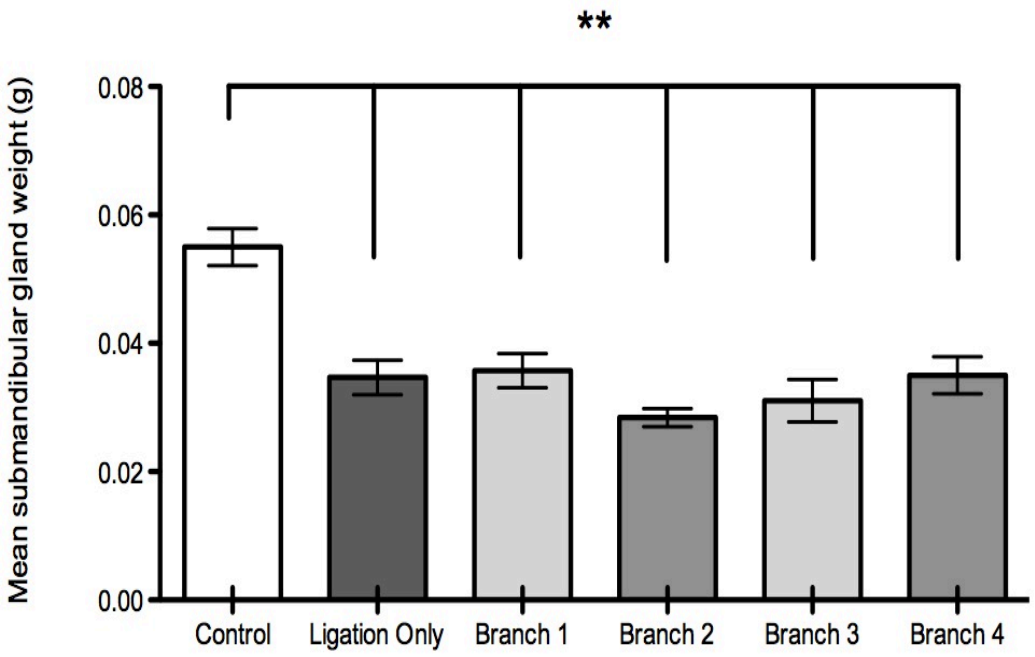

Figure 5.1 Mean submandibular gland weights for unoperated control, 7 days ligation only, ligated and de-ligated (Branch 1), de-ligated with rapamycin treatment throughout (Branch 2), de-ligated with rapamycin treatment for last 7 days (Branch 3) and de-ligated mice with rapamycin treatment for the first 7 days (Branch 4). In comparison to unoperated control, all other groups' mean gland weights were significantly ($p<0.005$) reduced. Rapamycin treatment did not significantly alter gland weights in comparison to ligation only group. Data is expressed as mean $\pm$ SEM.

5.3.2 Immunoprobing of mTOR Status

Western blots of the mTOR substrates, p4E-BP1 (Figure 5.2) and pS6rp (Figure 5.3), as well as total mTOR (Figure 5.4), in unoperated controls, 7 days ligation, ligated and de-ligated (Branch 1), de-ligated with rapamycin treatment throughout (Branch 2), de-ligated with rapamycin treatment for last 7 days (Branch 3) and de-ligated mice with rapamycin treatment for the first 7 days (Branch 4).

Unoperated controls displayed an inactivate state of the p4E-BP1 protein and similarly a small presence of total mTOR but with no pS6rp activity. 7 days of ligation caused the phosphorylation of 4E-BP1 protein, expressed as the activation of its higher molecular weight band, which was also visible in the p4E-BP1 positive control – muscle tissue. Ligation was the only experimental group to show presence of pS6rp.

Minimal expression of mTOR activity occurred throughout all Branch 1 tests, showing complete inactivity of mTOR despite no use of mTOR inhibitors. Whereas rapamycin treatment, on Branches 2, 3 and 4, expressed greater quantities, of both p4E-BP1 and total mTOR, than Branch 1 which had received no mTOR inhibitors.

Densitometric analysis showed pS6rp, p4E-BP1 and total mTOR, in all experiment groups, as a ratio of β-actin. The control's p4E-BP1 expression was significantly different from ligation only($p=0.0185$) and Branch 1 ($p=0.0245$). p4E-BP1 expression of ligation only was statistically significant in comparison to branches 1, 3 and 4 ($p<0.01$). pS6rp expression in regards to actin, only showed a statistically significant change in ligation only ($p=0.0129$), whilst total mTOR showed no statistically significant change throughout.

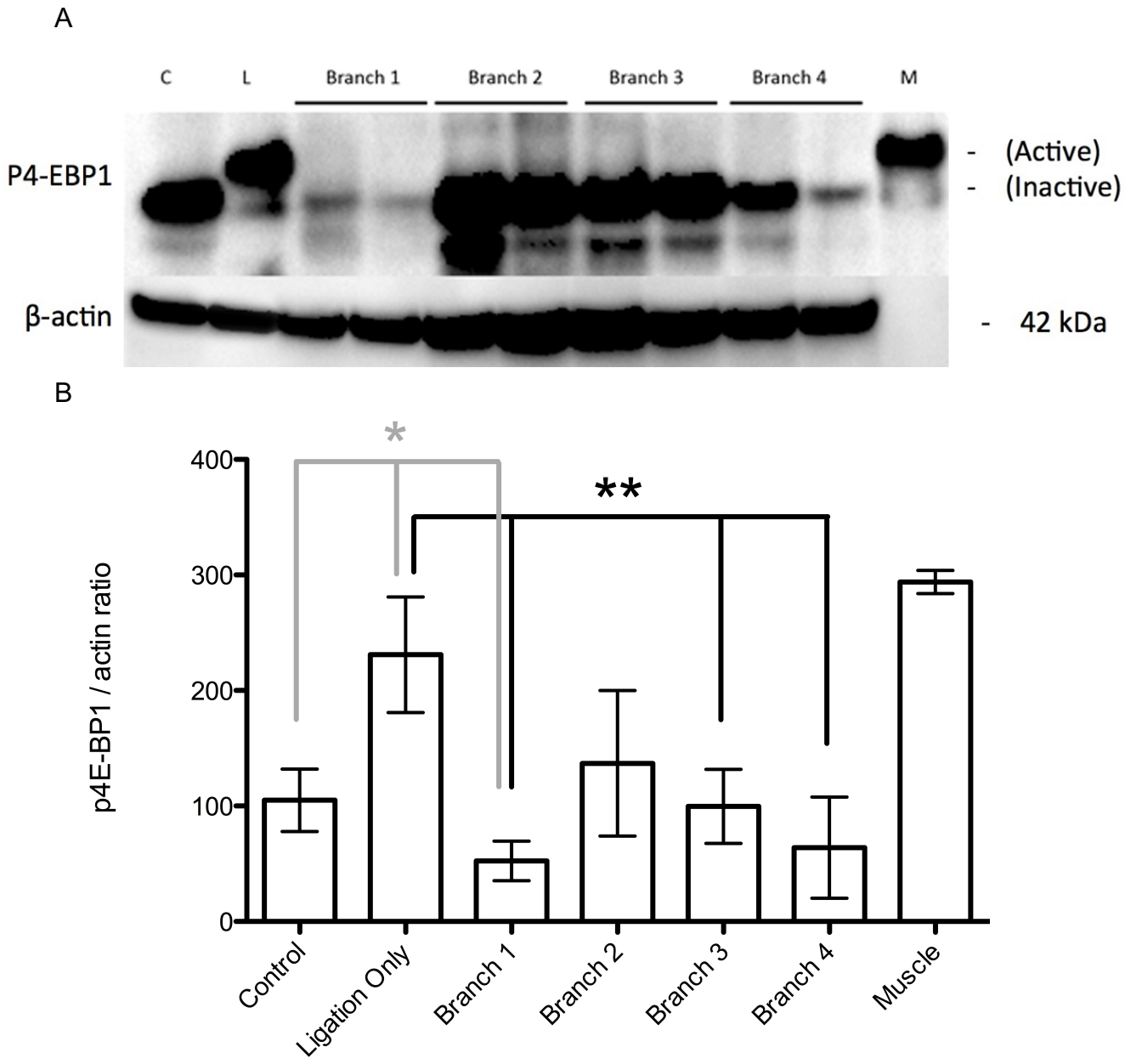

Figure 5.2 Immunoblotting of phospho-4EBP1 protein (A) and it's expression in comparison to β-actin in mouse submandibular glandular homogenates (B), showing unoperated control, 7 days ligation only, ligated and de-ligated (Branch 1), de-ligated with rapamycin treatment throughout (Branch 2), de-ligated with rapamycin treatment for last 7 days (Branch 3) and de-ligated mice with rapamycin treatment for the first 7 days (Branch 4). Low expression of 4E-BP1 (lower band) was visible in unoperated controls as well as branches 1 to 4. 7 day ligation only increased p4EBP1 phosphorylation (active isoform). Muscle homogenates (M) used as a positive control. Beta actin (β-actin) was used as a loading control, however muscle homogenates showed absence of beta actin (β-actin) as muscle expresses α-smooth muscle actin (α-SMA). Data represent results from at least three different experiments.

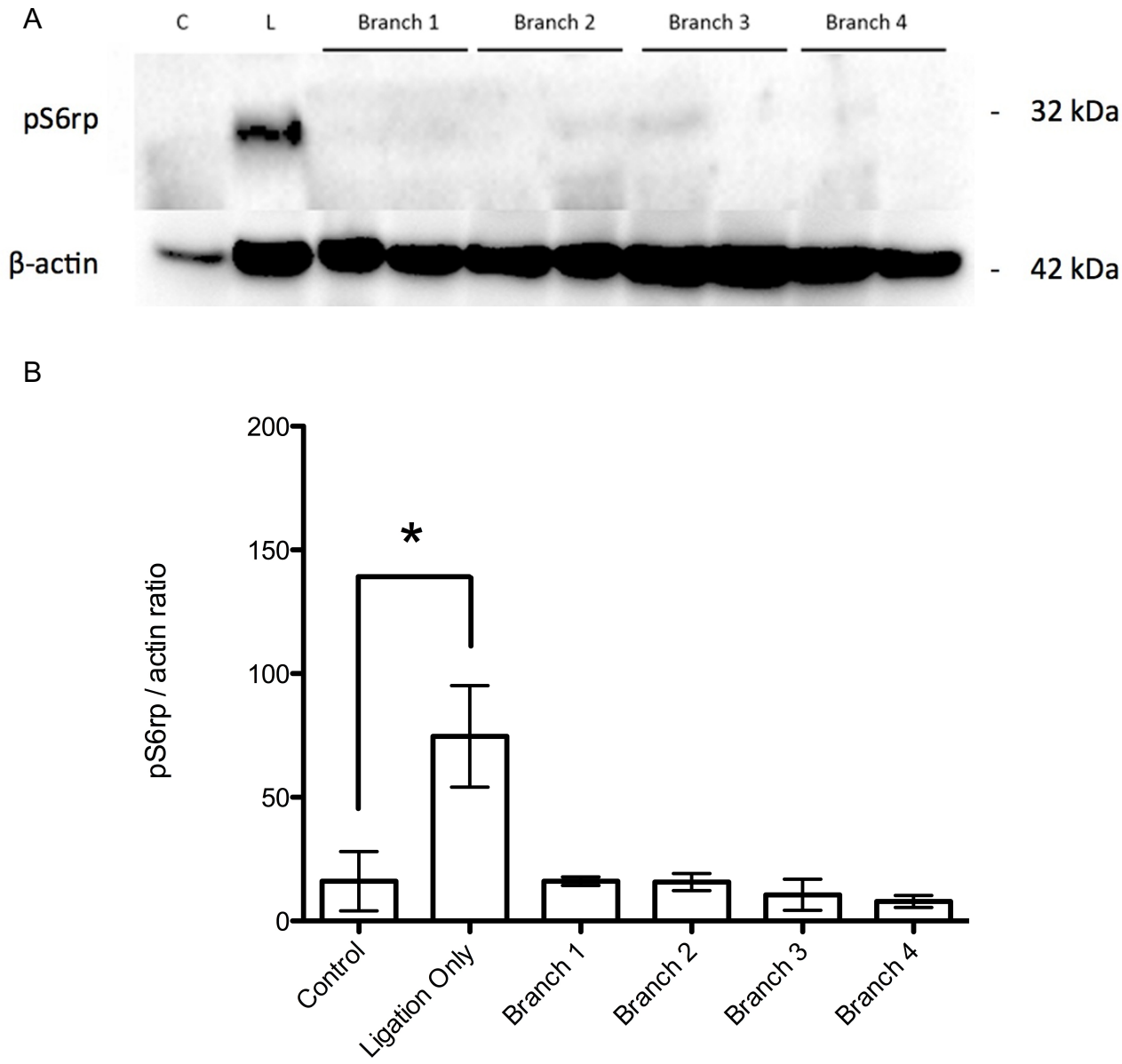

Figure 5.3 Immunoblotting of phospho-s6 ribosomal protein (A) and it's expression in comparison to β-actin in mouse submandibular glandular homogenates (B), showing unoperated control, 7 days ligation only, ligated and de-ligated (Branch 1), de-ligated with rapamycin treatment throughout (Branch 2), de-ligated with rapamycin treatment for last 7 days (Branch 3) and de-ligated mice with rapamycin treatment for the first 7 days (Branch 4). No expression of pS6rp was visible in unoperated controls, whereas ligation revealed activation of S6rp after 7 days of ligation only. Branch 1 showed absence of pS6rp protein band indicating no activation of mTOR during deligation. Rapamycin treatment, in branches 2 through 4, completely abolished pS6rp activation. Beta actin (β-actin) was used as a loading control. Data represent results from at least three different experiments.

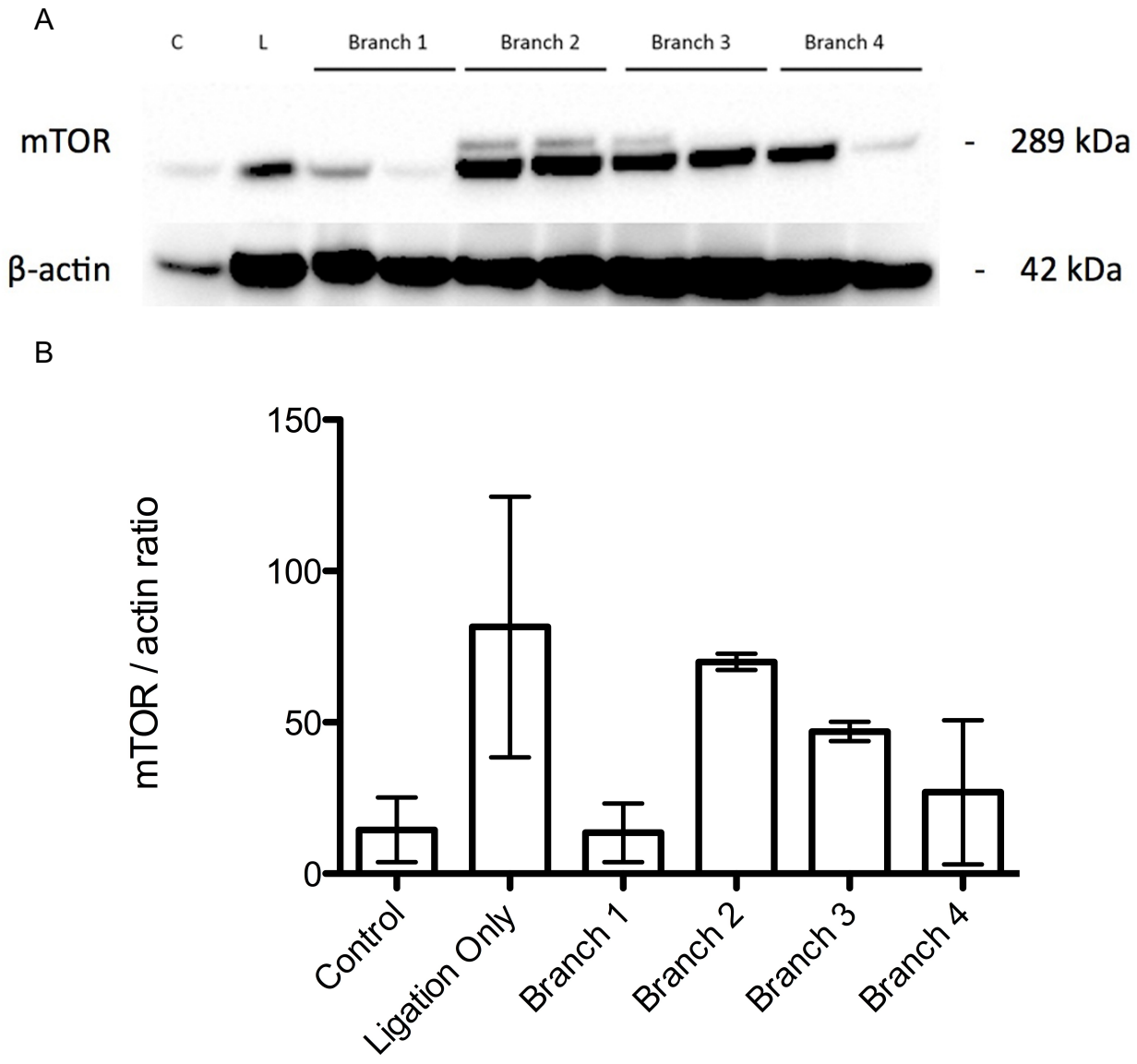

Figure 5.4 Immunoblotting of total mTOR expression (A) and a comparison of it's expression in relation to β-actin in mouse submandibular glandular homogenates (B), showing unoperated control, 7 days ligation only, ligated and de-ligated (Branch 1), de-ligated with rapamycin treatment throughout (Branch 2), de-ligated with rapamycin treatment for last 7 days (Branch 3) and de-ligated mice with rapamycin treatment for the first 7 days (Branch 4). No expression of mTOR was visible in unoperated controls, whereas ligation revealed increased mTOR presence and deligated glands. Rapamycin treatment at different time points (branches 2-4) also compounded total mTOR, showing an increase in comparison to control and branch 1. None of the groups were not of statistically significant difference to one another. Beta actin (β-actin) was used as a loading control. Data represent results from at least three different experiments.

5.3.3 Biochemical analysis of glycoprotein content

Periodic acid-Schiff's staining was used to identify the presence of acinar mucins in the gland homogenates of unoperated controls, ligated, branch 1, branch 2, branch 3 and branch 4 mice. Ligation resulted in significant loss ($p<0.0001$) of secretory glycoprotein content as shown by PAS staining and de-ligation without drug treatment did not cause a statistically significant recovery in the expression of this mucin, as branch 1 was still significantly lower ($p<0.0001$) than unoperated controls (Figure 5.5 A).

However a visibly progressive recovery in the expression of mucins was identified following rapamycin treatment, as shown by branches 2, 3 & 4. However their recovery rate was variable, where branch 3 (Figure 5.5 B) showed a recovery that was still significantly less ($p<0.01$) than unoperated controls and branch 4 (Figure 5.5 C) revealed a full recovery.

One-way ANOVA analysis between the 4 branches revealed that the different treatments of rapamycin at different stages of ligation and de-ligation causes a significant variation ($p = 0.0087$) of acinar mucin content between the samples, further corroborating our individual

analysis results. With the mean acinar mucin content (as a percentage of control) for branch 1 being 38.22%, branch 2 being 77.57%, branch 3 being 51.00% and branch 4 being 101.6%.

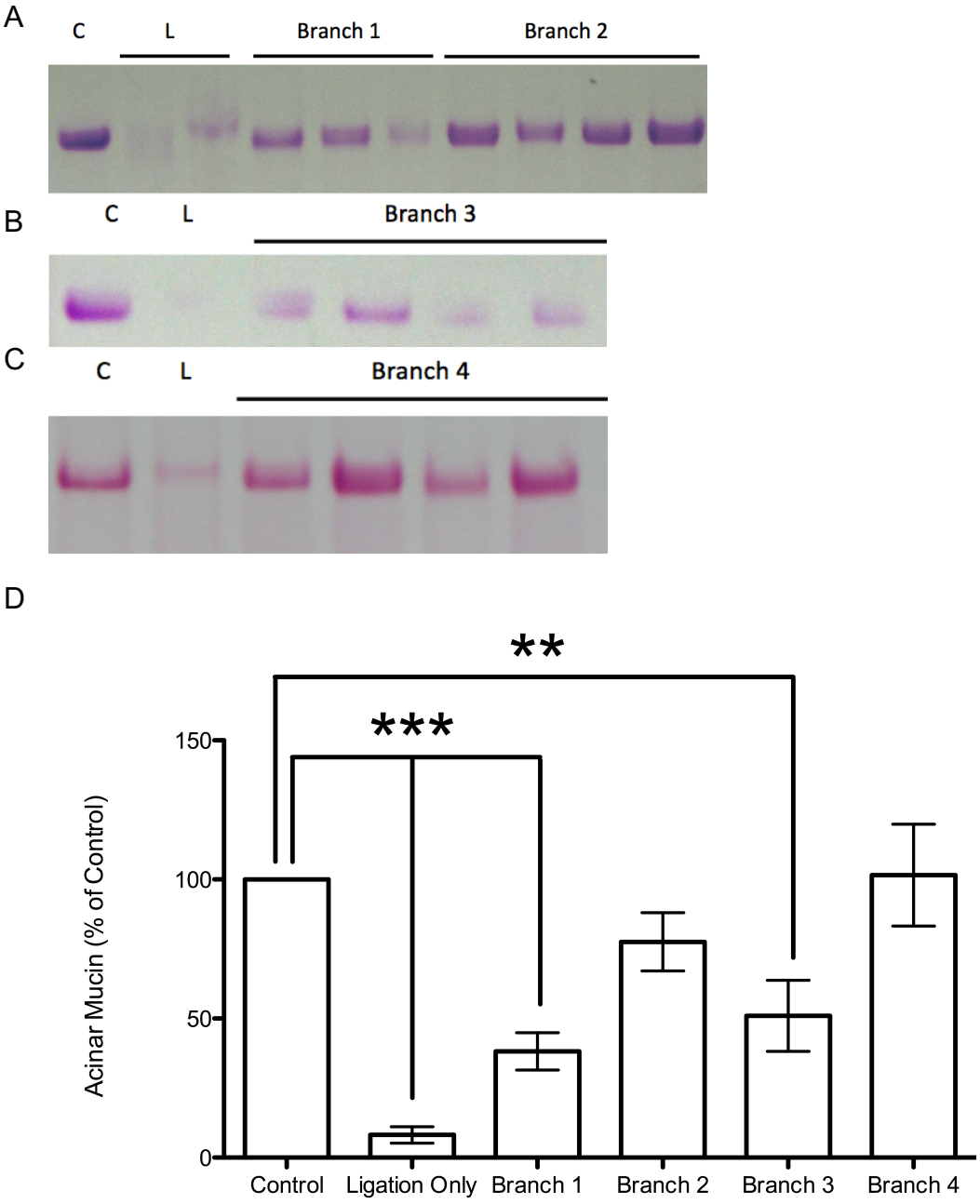

Figure 5.5 Periodic acid-Schiff's staining of glandular homogenates of unoperated control, 7 days ligation only, ligated and de-ligated (Branch 1), de-ligated with rapamycin treatment throughout (Branch 2), de-ligated with rapamycin treatment for last 7 days (Branch 3) and de-ligated mice with rapamycin treatment for the first 7 days (Branch 4). Ligation resulted in significant loss of mucins, branch 1 showed a visible recovery, yet this recovery was not statistically significant. Branches 2, 3, 4 all had visibly significant recoveries, however densiometric analysis of submandibular acinar mucin as a ratio of control (D), showed that branch 3's recovery was still significantly lower than controls. The bars represent the mean + SEM. Data represents results from at least three independent experiments.

5.3.4 Morphological changes

H&E staining of submandibular gland samples from unoperated controls (Figure 5.6 A), ligated (Figure 5.6 B), branch 1 (Figure 5.7), branch 2 (Figure 5.8), branch 3 (Figure 5.9) and branch 4 (Figure 5.10) all, to a certain extent, revealed presence of inflammatory cell infiltration composed mainly of neutrophils and macrophages, in the connective tissue between the lobules and among the parenchymal elements, in comparison to control adult submandibular glands.

Ligated gland acini displayed a loss of secretory granules and were generally reduced in both quantity and area, as evidenced by morphometric analysis (Figure 5.11) that revealed on average acini area were significantly ($p=0.0002$) decreased in comparison to unoperated controls. Yet remaining ducts displayed considerable duct luminal dilation in comparison to control, as they underwent degranulation. Cells also appeared less densely packed as the volume of interlobular space increased.

Deligation following ligation caused recovery of acini and ductal cell size, and AB/PAS revealed that the acini had also recovered some of their glycoprotein content to a minimal extent.

Rapamycin treatment in branch 2 caused ductal and acini cell structures to be comparable to normal glands, despite a demonstrable quantity of infiltrates and minimal fat cells and predominantly serous acini with scattered mucous cells.

Branch 3, demonstrated acini similar to branch 2, but ductal cells had visibly small lumena, suggesting a recovery of duct cell cytoplasm. Furthermore, the presence of inflammatory cells was minimal.

Branch 4 revealed a full recovery of acini & ductal cells and AB/PAS showed a restoration of glycoprotein content. Yet atrophic remnants remained such as minimal inflammatory cell infiltration and only the occasional abnormal acini with duct characteristics.

Morphometric analysis of the H&E stainings (Figure 5.11) indicated that ligation caused a significant decrease ($p=0.0002$) of the size of the acini in comparison with controls. All de-ligation groups caused a significant recovery ($p<0.005$).

A

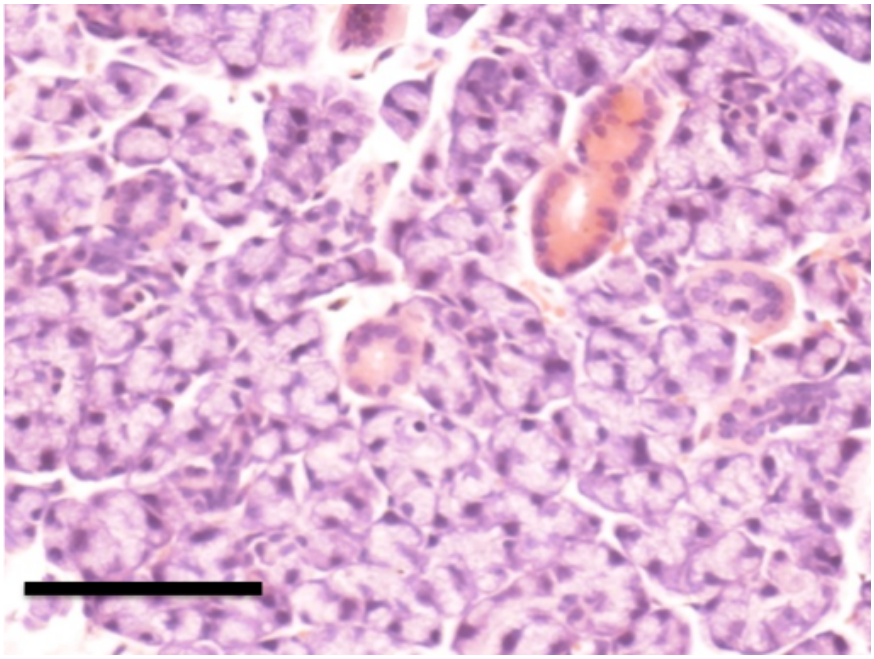

B

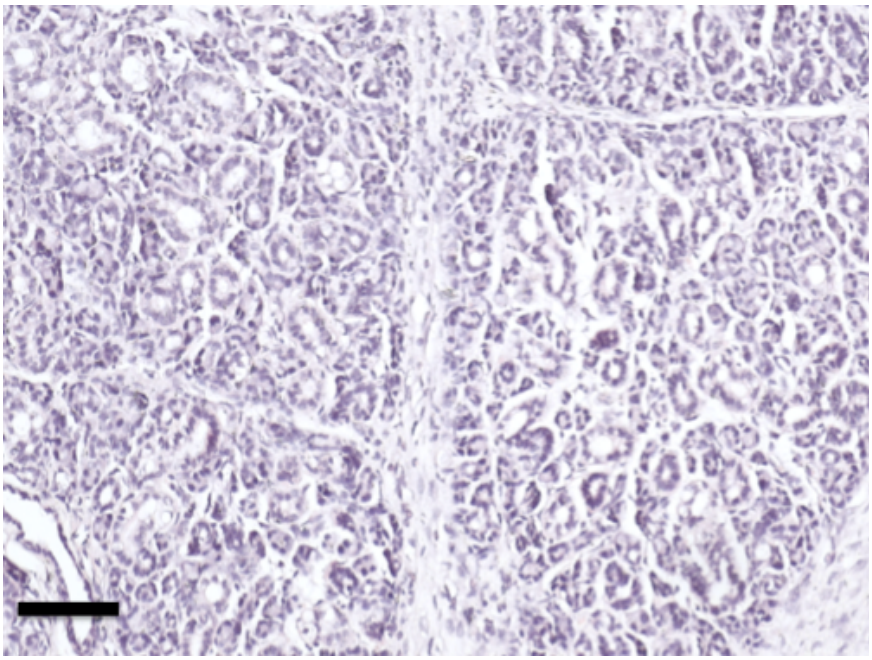

Figure 5.6 Comparison of morphological changes among unoperated controls (A) and 7 days ligation only (B). Controls showed typical appearance of acinar and ductal cells. Ligated glands displayed ductal lumen dilation, shrunken acini and extensive inflammatory cell infiltration. Results are representative of each experiment group. Scale bar represents 100 μm.

A

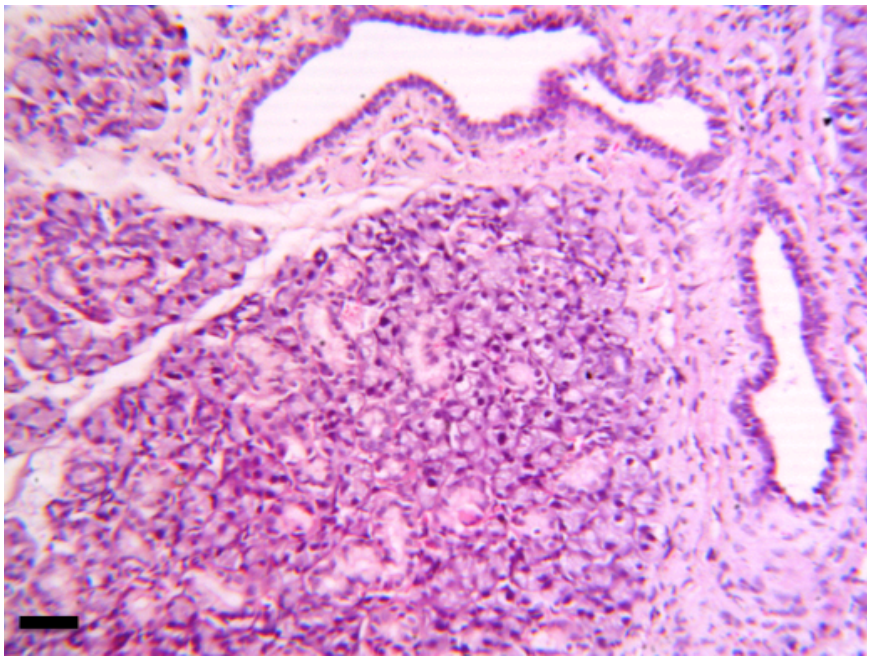

B

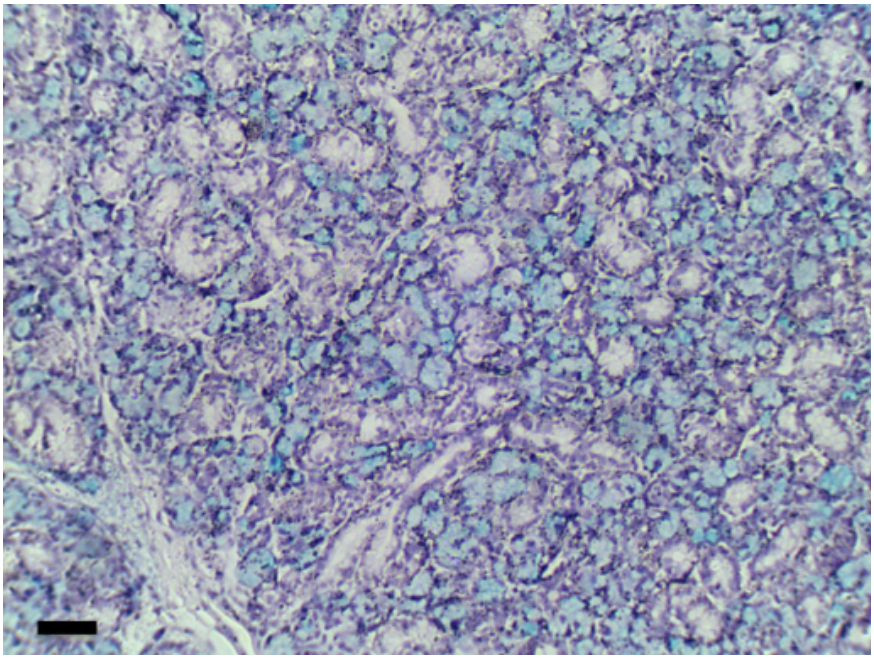

Figure 5.7 Morphological changes of mice that were only ligated and de-ligated (branch 1) H&E and AB/PAS (A and B respectively). Branch 1 exhibited recovery of acini and ductal cell size, acini-duct branched structures are often visible and several normal-like acinar are now present. AB/PAS revealed that de-ligation had minimal recovery of glycoprotein content. Results are representative of each experiment group. Scale bar represents 100 μm.

A

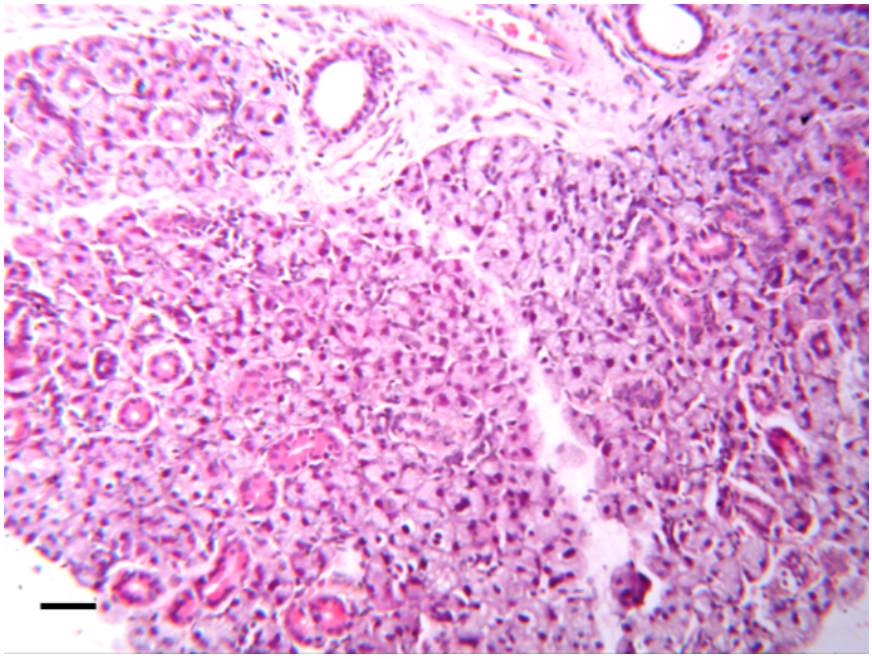

B

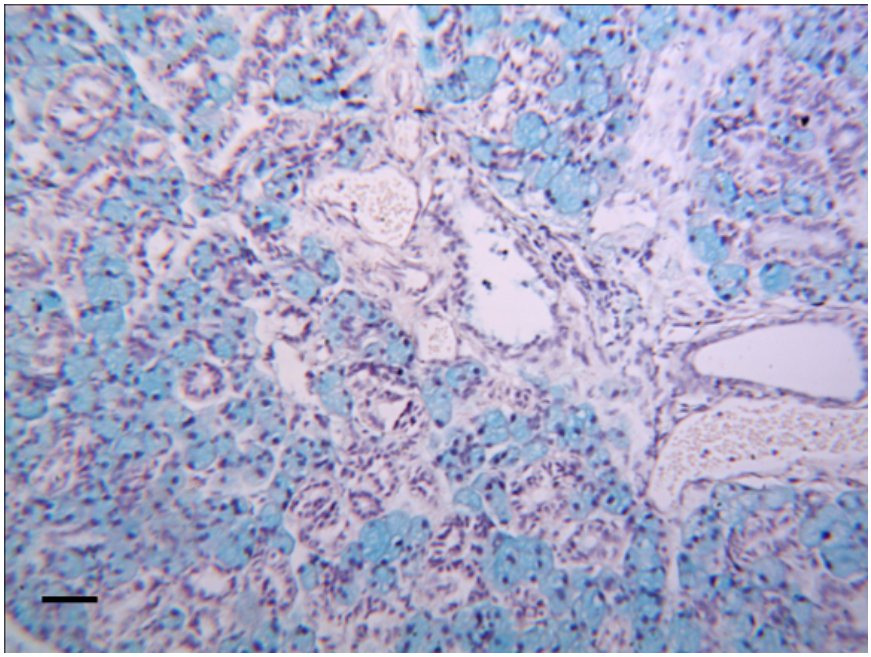

Figure 5.8 Morphological changes of de-ligated submandibular glands with rapamycin treatment throughout (Branch 2) H&E and AB/PAS (A and B respectively). Generally cell structures were comparable to normal glands, despite fibrosis and the associated presence of inflammatory cells. The interlobule space is filled by emerging acini. Results are representative of each experiment group. Scale bar represents 100μm.

A

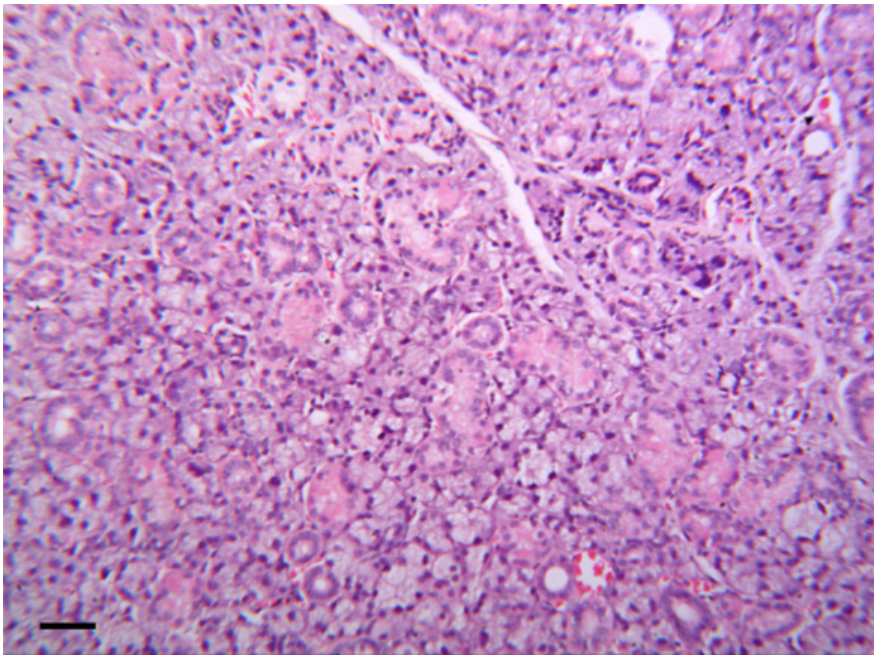

B

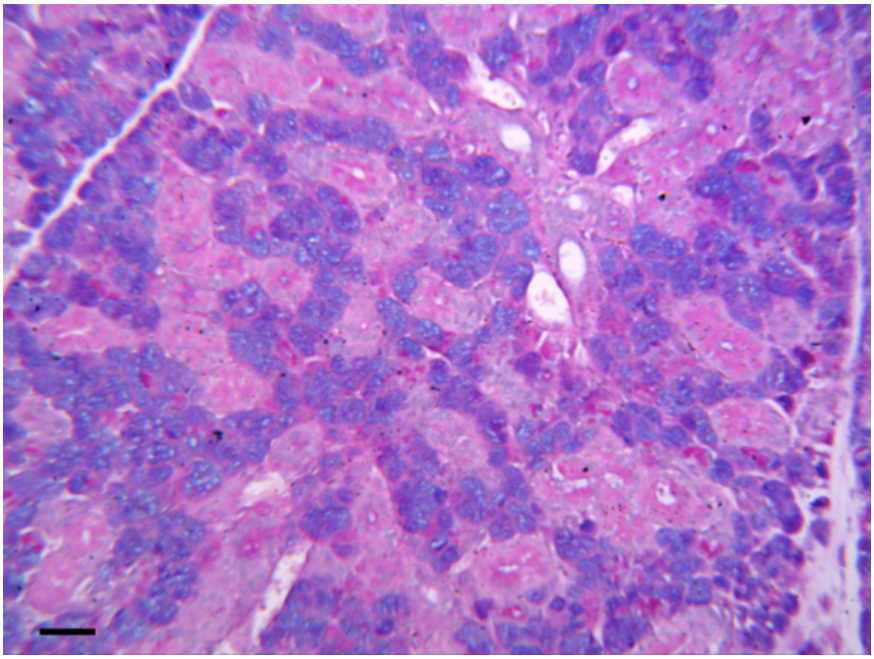

Figure 5.9 Morphological changes of de-ligated submandibular glands with rapamycin treatment for the last 7 days (branch 3) H&E and AB/PAS (A and B respectively). AB/PAS revealed recovery of glycoprotein content which also appeared in some acini to a certain extent. Furthermore some acini appeared similar to duct-like structure. Results are representative of each experiment group. Scale bar represents 100 μm.

A

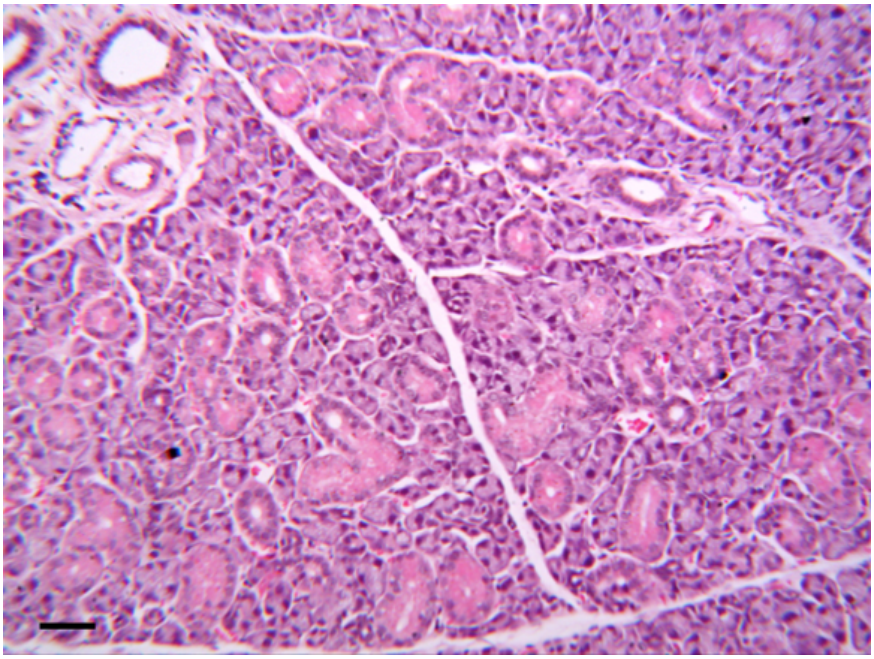

B

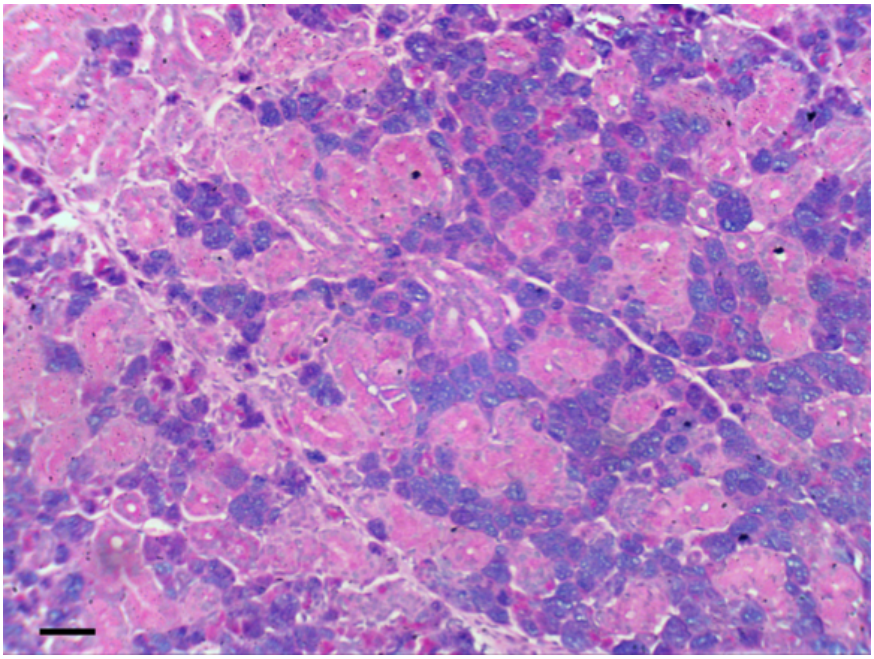

Figure 5.10 Morphological changes of de-ligated submandibular glands with rapamycin treatment for the first 7 days (Branch 4) H&E and AB/PAS (A and B respectively). Tissue morphology revealed a full recovery of acini & glycoprotein content, and ducts recovered from atrophy as evidenced by no luminal dilation. Remnants of previous atrophy remained in inflammatory cells. Results are representative of each experiment group. Scale bar represents 100 μm.

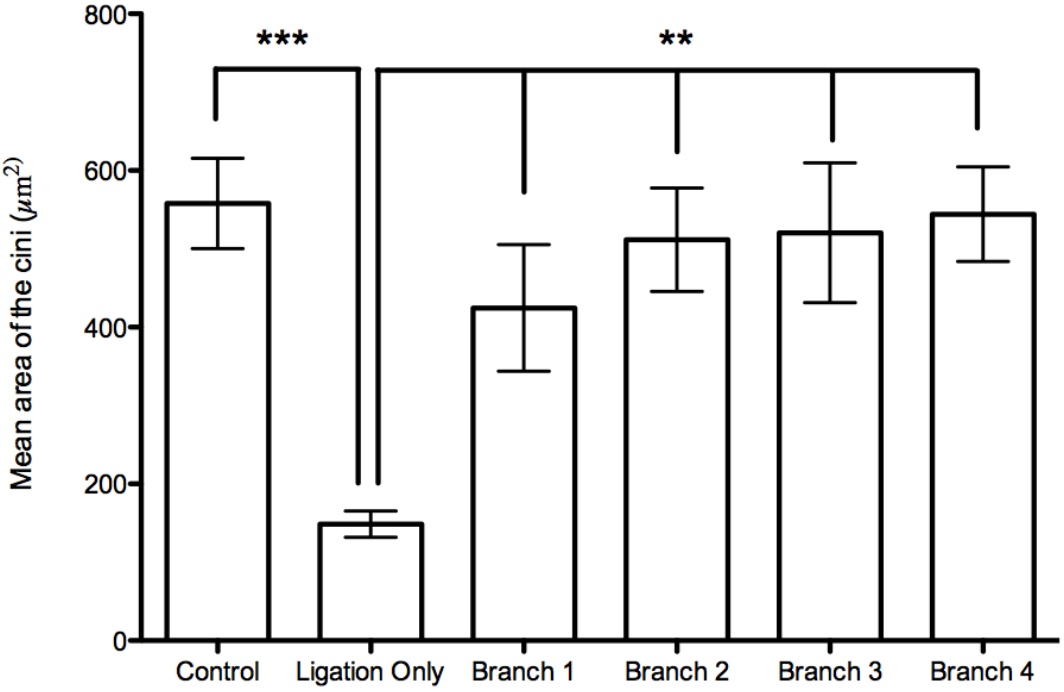

Figure 5.11 Morphometric analysis of the H&E-stained samples.
The mean area of acini from the control, 7 days ligation only, ligated and de-ligated (Branch 1), de-ligated with rapamycin treatment throughout (Branch 2), de-ligated with rapamycin treatment for last 7 days (Branch 3) and de-ligated mice with rapamycin treatment for the first 7 days (Branch 4) were compared. Ligation significantly decreased the size of the acini (P=0.0002) in comparison with control. De-ligation caused a significant increase in acini area (P<0.005). Data is based on 20 observations from at least 3 samples for each experimental group and is expressed as mean±S.E.M

5.4 Discussion

Previous progress has been made in the development of tissue regeneration strategies for a vast variety of tissues, including skin (Ma et al., 2003), corneal (Mimura et al., 2013), cartilage (Oldershaw, 2012), lacrimal (Hirayama et al., 2013) and cardiac tissue (Sapir et al., 2011). Determining the capacity of mTOR and the underlying mechanisms of de-ligation, in this study, should provide a novel insight to improving regenerative approaches for salivary glandular tissue.

Previously ductal ligation has been used as a prelude to investigate salivary gland regeneration (Carpenter et al., 2007b, Cotroneo et al., 2008b, Carpenter et al., 2009). This study observed the glandular regeneration ensuing de-ligation following 7 days of ligation of the submandibular gland main excretory duct in the presence of, the mTOR inhibitor, rapamycin to provide a clear insight into the role of mTOR during salivary gland regeneration.

As a contrast to ligation/de-ligation model of previous studies, which primarily observed de-ligation without the use of drug treatments, here an mTOR inhibitor – rapamycin was administered at differing time points in order to identify the most efficacious format of mTOR

inhibition, as well as identify the time points of the key interactions of the mTOR pathway in regeneration. This is because although it has been shown that mTOR inhibition during glandular development, specifically branching morphogenesis, can halt submandibular gland development (Larsen et al., 2003), it has also been shown that mTOR inhibition during ligation can help alleviate the effects of atrophy, as previously shown in Chapter 3. Raising the question of whether or not mTOR inhibition will help glandular regeneration or decelerate it.

Other studies observing the effects of mTOR in regeneration have taken differing stances regarding the role that mTOR has. Several studies have observed central nervous system injuries and found that the activation of mTOR is sufficient to promote axon regeneration (Park et al., 2008, Yang et al., 2014) and this theory was further developed by establishing that mTORC1 is necessary for axon regeneration (Hu, 2015). This theory would suggest that mTOR inhibition can possibily harm regeneration in submandibular glands as well, whereas another study suggests that the mTORC1 substrate S6 kinase inhibits instrinsic axon regeneration capacity and therefore inhibition can help regeneration (Hubert et al., 2014). A recent Nature study, which observed tissue regeneration, tied these theories all together by suggesting that

mTORC1-mediated translation limits tissue growth however s6k deletion decreases regeneration (Faller et al., 2015). These findings combined with this very study's methods could suggest that perhaps a combination of inhibiting mTORC1 during periods that need growth and translation (such as atrophy), and the stopping of mTORC1 inhibition during periods that need regeneration, is a treatment method which could be of importance.

The histological findings of this study showed that in regards to morphology, the most efficacious format of treatment is rapamycin treatment during 7 days of ligation while excluding during de-ligation (Branch 4). All samples, to a certain extent, experienced the presence of inflammatory cell infiltration, composed mainly of neutrophils and macrophages, in the connective tissue between the lobules and among the parenchymal elements, in comparison to control adult submandibular glands. However, branch 4's H&E revealed a full recovery of acini, ducts recovered from atrophy as evidenced by no luminal dilation and AB/PAS showed a restoration of glycoprotein content, whereas the recovery of other branches were still limited to some extents.

Branch 1 exhibited recovery of acini and ductal cell size, intriguing acini-duct branched structures were often visible and AB/PAS revealed that de-ligation had some recovery of glycoprotein content. This is keeping in line with previous research which has found that although ligation causes a reduction in the size and quantity of acinar cells to occur after ligation of main excretory duct as well as in the acini's mucin content (Matsumoto et al., 2007), de-ligation causes acini and ductal cells to recover some of their size (Cotroneo et al., 2010).

Rapamycin treatment in branches 2 & 3 caused acini cell structures to be comparable to normal glands, despite a demonstrable quantity of infiltrates and minimal fat cells and predominantly serous acini with scattered mucous cells, however glycoprotein content was not fully restored and ducts were still reminiscent of their atrophic counterparts. These findings are reaffirmed by the previous findings that inhibition of mTOR can affect the ligation-induced atrophy of salivary glands, however only affecting acinar, but not ductal atrophic processes (Bozorgi et al., 2014).

Morphological findings help to establish a theory that mTOR inhibition can help to speed up the recovery of tissue morphology if rapamycin is

administered during the ligation period, as evidenced by a comparison of the results of branches 4 & 1.

Morphometric analysis of the mean area of acini also supported the theory that the most efficacious format of administration is rapamycin treatment during 7 days of ligation, but not during de-ligation, by demonstrating that the order of efficacy from best to worst, in regards to acini recovery, is branch 4, branch 3, branch 2 and branch 1, respectively. The fact that de-ligation alone produced a statistically significant increase in acini area from ligation only, but the morphological improvements from rapamycin treatment, at any time point, were not statistically significant from de-ligation perhaps showcases one of the limitations of the animal ligation/de-ligation model. When using radiation on mice to cause functional salivary gland atrophy, rather than the ligation model, mTOR inhibition has been proven to be successful in improving both glandular functions and morphology (Morgan-Bathke et al., 2014). ANOVA did not produce any statistically significant results in mean area of the acini between Branches 1 to 4. Therefore data obtained were not computed as the overall ANOVA effect was deemed insignificant, indicating no variance between the branches.

The reduction in submandibular gland weight following atrophy has been well established (Walker and Gobe, 1987) and more recently a detailed understanding has been gained regarding the recovery process of submandibular gland weight following de-ligation only (Cotroneo et al., 2008b) or rapamycin treatment without de-ligation (Bozorgi et al., 2014). This study takes those foundations and concludes that rapamycin cannot help speed up the recovery of critical weights, as evidenced by the fact that no gland weights, no matter how rapamycin was administered, recovered any more beyond that of just ligation only.

In addition to the study of critical gland weights and glandular tissue morphology, the role of mTOR itself must be evaluated and the simplest way to do this was by analysis of mTOR itself, as well as it's substrates S6rp and 4E-BP1 in glandular homogenates. Previously we had established that mTOR and its substrates are activated during ligation (Silver et al., 2010) and that rapamycin treatment can reduce total mTOR protein expression, correlating with S6rp and 4E-BP1 proteins expression, but that rapamycin does not completely inhibit mTOR following ligation (Bozorgi et al., 2014).

One of the main findings of the current study was that mTOR activity is fully de-activated following de-ligation. Minimal expression of mTOR activity was observed in all branch 1 tests, including western blots of pS6rp and p4-EBP1, showing complete inactivity of mTOR despite no use of mTOR inhibitors. Densitometric analysis showed that pS6rp, p4E-BP1 and total mTOR phosphorylation for de-ligated glands were comparable to that of unoperated control mice. Suggesting that despite ligation causing phosphorylation of mTOR (Silver et al., 2010), this activation is fully reversible by de-ligation. This is of particular interest as the branches which received rapamycin treatment for different time periods (branches 2, 3 & 4) still exhibited remains of mTOR (and the 4E-BP1 substrate), to levels that were even higher than non rapamycin treated de-ligated mice (branch 1).

This is in contrast to the PAS staining which revealed that de-ligation without drug treatment did not cause a statistically significant recovery in the expression of the secretory glycoprotein content, as branch 1 was still significantly lower than unoperated controls and comparable to ligated glands, which had experienced a significant loss of the presence of acinar mucins. Nevertheless rapamycin treatment caused a visibly progressive recovery in the expression of mucins, as shown by the PAS

of branches 2, 3 & 4. Although densiometric analysis revealed that the recovery of branch 3, despite being visible, was still significantly lower than controls. This supports the theory that the best recovery is seen when rapamycin is administered during the ligation period. Furthermore, one-way ANOVA between the 4 branches revealed that different treatments of rapamycin at different stages of ligation and de-ligation caused a significant variation ($p = 0.0087$) of acinar mucin content between the samples, further corroborating our individual analysis results. ANOVA was performed to calculate variance here, as multiple student's t-test lead to high error rates when $n<15$ in sample groups (Ramsey, 1980).

This study has exposed some of the biochemical exchanges which occur as a possible result of regeneration, particularly regarding the role of mTOR in salivary gland regeneration following de-ligation and the characterisation of the early stages of glandular regeneration, which can be crucial in order to fully understand the mechanisms of recovery. It has identified the key time points for the early stages of regeneration as during the atrophic period itself, as demonstrated by the improved results for tissue morphology, glycoprotein content and gland weights when rapamycin was administered during only the 7 days ligation

period, but not during the de-ligation regeneration period. This is keeping in line with previous studies performed for observing the recovery aspects of rapamycin on other bodily organs. A renal transplant experiment found rapamycin to be an ideal immunosuppressive agent in the setting of delayed graft function (DGF) after renal transplantation, but found that continuing rapamycin treatment during the recovery phase after transplantation caused recipients to be twice as likely to remain on dialysis as those recipients without rapamycin (McTaggart et al., 2003). A study on regeneration after pancreatic ischemia-reperfusion injury found that rapamycin improves early microcirculation, but impairs longer term regeneration (Serr et al., 2007). Such findings are effectively agreeing with our conclusions that the best form of treatment for recovery is rapamycin treatment during atrophy but then left untreated during regeneration to help speed up recovery. This is likely as a result of rapamycin's immunosuppressive functions, which can inhibit a wide spectrum of T- and B-cell activities (Chen et al., 1994).

Understanding that the most effective format of treatment is mTOR inhibition during atrophy demonstrates a need to examine this process itself, in order to identify potential uses for regenerative strategies for

salivary glands damaged in human autoimmune disease or as unintended side effects of radiation treatments for head and neck cancers.

CHAPTER 6

EVIDENCE OF mTOR ACTIVITY DURING HUMAN SALIVARY GLAND ATROPHY

6.1 Introduction

In previous chapters of this thesis, the role of mTOR in morphological and biochemical changes during salivary gland atrophy and regeneration in mice was examined. Whilst it is important to study and identify the factors involved in this process in mice, it is also noteworthy that the ligation / de-ligation model of rodent salivary gland atrophy and regeneration is not identical to effects seen in humans. For example, rodent salivary glands enter an embryonic-like state following de-ligation with branched structures forming (Cotroneo et al., 2010) that have been hypothesized to play a critical role in regeneration (Cotroneo et al., 2008, Cotroneo et al., 2010) and as an alternative, some have utilised animal models that investigate radiation induced salivary gland atrophy (Hill et al., 2014). Therefore, due to these differences between the de-ligation animal models and the radiation induced damaged in humans, it can be crucial to understand how the processes of the mTOR pathway during salivary gland atrophy are driven in humans by studying the role of mTOR in atrophic human salivary glands.

Previous studies on atrophic human submandibular glands have focused on the repair (Coppes and Stokman, 2011) and long term regeneration (Braam et al., 2005) of glands following atrophy. These have shown how salivary gland functions can return following regeneration (Zhang et al., 2013) but were typically linked to stem cell transplantation (Feng et al., 2009) or the region-dependent radiosensitivity of irradiation (Konings et al., 2005). The role of mTOR in human salivary gland atrophy still remains unclear.

Salivary gland atrophy can be recreated experimentally in rodents via ligation of the main excretory duct of the submandibular gland. This creates a histological appearance involving deletion of acinar cells through apoptosis (Takahashi et al., 2000) and autophagy (Harrison et al., 2000), revealing characteristic autophagic vacuoles in ligation-induced atrophy (Tamarin, 1971b). The molecular processes involved in autophagy are only beginning to be unravelled (Silver et al., 2010), but it is believed that autophagy related (ATG) protein 5 may play a dual role in autophagy and autophagic cell death (Pyo et al., 2005).

Other markers of autophagy include the Microtubule-associated protein 1A/1B-light chain 3 (LC3) which conjugates to phosphatidylethanolamine (PE) to form LC3-II (Tanida et al., 2008). Thus, conversion of LC3-I to LC3-II via Atg3 is a useful marker for autophagy (Silver et al., 2010).

In chapter 3, rapamycin treatment following ligation was used to determine that mTOR mediates ligation-induced atrophy of salivary glands, however only affecting acinar, but not ductal, atrophic processes, in mice. However it was also observed that it is possible that the mTOR pathway can re-activate itself, even when inhibited, due to the PI3K negative feedback mechanism (which re-activates mTORC1 via the TSC1/2 complex) (Guertin and Sabatini, 2009).

In chapter 4, using second generation mTOR inhibitors, Torin1 and BEZ, despite their complexation to inhibit both mTOR and PI3K pathways, revealed similar results to rapamycin. This inability to fully inhibit mTOR during long-term ligation further establishes that the activation of mTOR as being an important mechanism during salivary gland atrophy and autophagic processes (Silver et al., 2010).

6.1.1 Salivary Markers of secretory function

The salivary film which covers all oral surfaces, get its physical properties from salivary proteins (Gibbins and Carpenter, 2013), including proline-rich proteins (PRPs), statherin, histatin, carbonic anhydrase VI (CA VI), mucins and amylase. The most important glycoproteins found in saliva are the secreted salivary mucins, MUC5B and MUC7 (Gibbins et al., 2014). Therefore in order to better grasp an understanding of human salivary gland atrophy with or without the presence of mTOR, it is important to analyse what is contained in the saliva of atrophic glands, or more specifically, their salivary secretory proteins. These salivary proteins can act as markers and be used to identify the functionality of atrophic salivary glands in this study.

Table 6.1 Major salivary markers and their respective functions

Salivary Marker	Function
MUC5B & MUC7	Anti-bacterial (Levine, 1993) Anti-viral (Bergey et al., 1994) Bond formation (Tabak, 1995) Rheological behaviour (Takehara et al., 2013)
CA VI	pH homeostasis (Kivela et al., 1999)
Statherin	Lubrication (Douglas et al., 1991) Mineralisation (Schlesinger et al., 1989)
Cystatin S	Protease inhibitor (Bobek et al., 1991)
TC-1	Carrier protein (Stupperich and Nexo, 1991)
PIP	Function unknown (Gallo et al., 2013)

6.1.2 Aims

The aim of this study was to better understand the role of mTOR in human salivary gland atrophy by determining if mTOR activation occurs during atrophy and whether its role is still a contributing factor in the process of ageing-related atrophy. In order to perform this study, salivary protein markers were analysed, alongside morphological analysis of submandibular gland tissue sections, whilst accommodating for the atrophic processes reported for age-related volumetric tissue changes in human submandibular salivary glands (Scott, 1977).

6.2 Materials & Methods

6.2.1 Human Submandibular Gland Biopsy

10 human submandibular gland samples were obtained with consent from King's College London's Dental Institute Biobank, from patients aged between 44 to 80 years suffering from a varying range of diseases from Tongue Squamous Cell Carcinoma (SCC) to Laryngeal SCC, as described in further detail in the supplementary appendix 8.1. With submandibular glands incurring atrophy ranging from minimal/none to severe atrophy. Samples excluded diseased areas and were chosen with varying levels of fibrosis and fat replacement of parenchymal tissue. The specimens were pre-prepared into $5mm^2$ tissues frozen in optimal cutting temperature medium (OCT) and slides with paraffin-embedded sections at 5-µm thickness.

6.2.2 Protein Detection

The human tissues were homogenised, as previously described in chapter 2.9, with the addition of phosphatase inhibitor (New England Biolabs, MA, USA) Protein loading on gels was normalised using BCA Assay (Thermo Scientific, IL, USA), as detailed in chapter 2.10.

Membranes were blocked in TBS-T for 60 minutes or PBS-T with 10% milk power (Marvel) overnight at 4°C. Membranes were immunoprobed for salivary protein markers, mTOR and autophagy status using the antibodies shown in Table 6.2.

In order to be used as positive control for immunoprobing of salivary protein markers, unstimulated whole mouth saliva was collected from normal, healthy controls by passive drooling into universal tubes. The samples were kept on ice in order to prevent degradation and then centrifuged at 13,000 × g for 2 minutes at 4°C to remove debris. Also used as positive controls were mouse gastrocnemius muscle tissue homogenates and 7 days ligated mice submandibular glands for mTOR substrates and autophagy markers Atg 3 and Atg5. A 100 uL solution of $1x10^5$ cells of human LC3B/293T suspended in Laemmli's sample buffer was used as positive control for LC3.

Table 6.2 Antibodies and their respective concentrations in immunoblotting protocol

Primary Antibodies	Concentration
Rabbit Anti-human / mouse p4E-BP1	1 : 1000
Rabbit Anti-human / mouse pS6RP	1 : 1000
Rabbit Anti-human / mouse mTOR	1 : 1000
Mouse Anti-human MUC5B	1 : 100
Mouse Anti-human MUC7	1 : 100
Rabbit Anti-human Statherin	1 : 2000
Mouse Anti-human Cystatin S	1 : 1000
Goat Anti-human CA VI	1 : 1000
Rabbit Anti-human TC-1	1 : 1000
Rabbit Anti-human PIP	1 : 100
Rabbit Anti-human LC3	1 : 1000
Rabbit Anti-human / mouse ATG3	1 : 1000
Rabbit Anti-human / mouse ATG5	1 : 1000
Mouse Anti-human / mouse β-actin	1 : 4000

Secondary Antibodies	Concentration
Horseradish peroxide (HRP) Goat Anti-rabbit	1 : 2000
Horseradish peroxide (HRP) Goat Anti-mouse	1 : 1000
Horseradish peroxide (HRP) Mouse Anti-goat	1 : 1000

6.2.4 Histology

The pre-cut tissue samples were treated with 3% hydrogen peroxide, in order to aide the inhibition of endogenous peroxidase. Then treated for prevention of non-specific binding of the primary antibody was carried out as previously described in chapter 2.7. The primary antibody, Rabbit Anti-Human PS6 (Cell Signalling, Hertfordshire, UK) at 1:250, was used and incubated overnight at 4˚C. Slides were then incubated for 1 hour at room temperature with appropriate secondary HRP polyclonal antibodies at 1:200 dillution (DAKO, Ely, Uk).

Tonsil tissue sections were used as positive control for mTOR, due to their positive mTOR expression in immunohistochemical studies (Brown et al., 2006), and negative controls were performed by incubating supplementary slides with bovine serum albumin (BSA) as a substitute for Rabbit Anti-Human PS6.

In order to analyse general tissue morphology, slides were also stained with H&E (see chapter 2.6.1). H&E slides were analysed by a clinical pathologist by the King's Health Partner Cancer Biobank at Guy's and St Thomas' trust, as well as the author.

6.2.5 Morphometric Analysis

The mean acini area (μm^2) was measured using Leica TCS SP2 confocal microscope software version 2.1 (Leica Microsystems, Germany) from the human submandibular gland H&E stained slides, by selecting 20 acini per sample.

6.2.6 Densitometric Analysis

The immunoblotting band intensities were quantified and displayed as a ratio of β-actin using Image J version 1.46 (NIH, MD, USA), as previously explained in 2.13.

6.2.7 Statistical Analysis

Experiments were repeated three times and data is represented by the average of three experiments. The significance of these morphometric and densitometric analyses was compared by student's t-test and expressed as mean $\pm$ S.E.M with $p<0.05$ being considered statistically significant.

The relationship between age and mean acini area was analysed using exponential regression models of plateau following one phase decay using Prism version 5.00 (GraphPad Software, California USA). Comparisons between age and salivary protein expression were explored using a linear regression analysis using Prism version 5.00 (GraphPad Software, California USA).

6.3 Results

6.3.1 Histological Assessment (General Morphology)

H&E staining of most of the human submandibular glands (Figure 6.1 A - F) revealed the presence of inflammatory cell infiltration, composed mainly of neutrophils and macrophages, in the connective tissue between the lobules and among the parenchymal elements. Whereas the control adult submandibular glands, with the exception of the none / minimally atrophic glands, displayed relatively normal lobular histology with only occasional infiltrates, minimal fat cells and predominantly serous acini with scattered mucous cells.

The acini, which displayed fewer secretory granules, were generally reduced in both quantity and area, as morphometric analysis revealed that on average acini area had significantly ($p = 0.01$) decreased by mild atrophy in comparison to control by 51.6 % $\pm$ SEM. Mean acini area was also significantly ($p < 0.001$) reduced by 75 % between control and severe atrophy (Figure 6.2). Regression analysis of mean acini area in comparison to the age of each sample at the time of biopsy revealed that

as the age increased, the mean acini area decreased sharply causing a significant ($p<0.001$) drop after the age of 50 years and eventually reaching a plateau.

Atrophic acini had more visible duct-like structures in more progressive cases of atrophy. This resulted in a 54 % $\pm$ SEM increase in the proportion of ducts between control and severe atrophy (Figure 6.1 – F & G). The residual duct-like structures displayed considerable ductal luminal dilation in comparison to control, presumably as a result of degranulation. This trend of morphological results also showed that as atrophy intensified, cells appeared less densely packed as the volume of interlobular space increased.

More advanced cases of atrophy demonstrated fat infiltration between serous and mucous acinar cells as well as replacement of parenchymal cells with fat. In most severe cases, serous and mucous cells were absent and had been substituted by fibrous and adipose tissue, as only duct-like structures had abided.

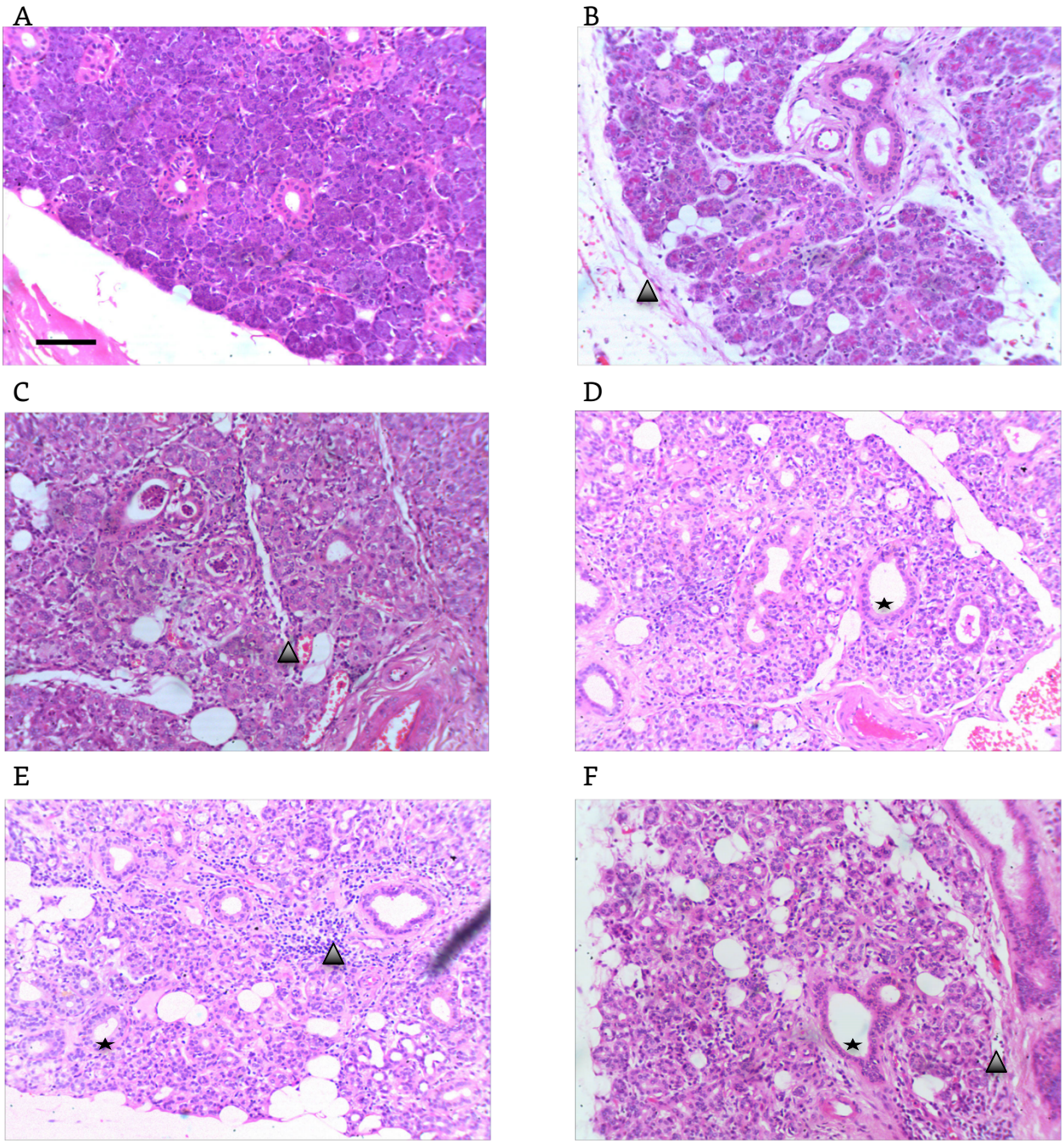

Figure 6.1 H&E staining of none or minimal atrophic (A), mildly atrophic (B) (C), moderately atrophic (D) (E), severely atrophic (F) and control (G) human submandibular glands. Samples showed signs of atrophy including reduced acinar area, fat displacement, dilated ducts (star), inflammatory infiltrates (arrowhead), even in minimally atrophic samples. Photos (A – F) are representative of all samples (n=10). Scale *bar* represents 100 µm.

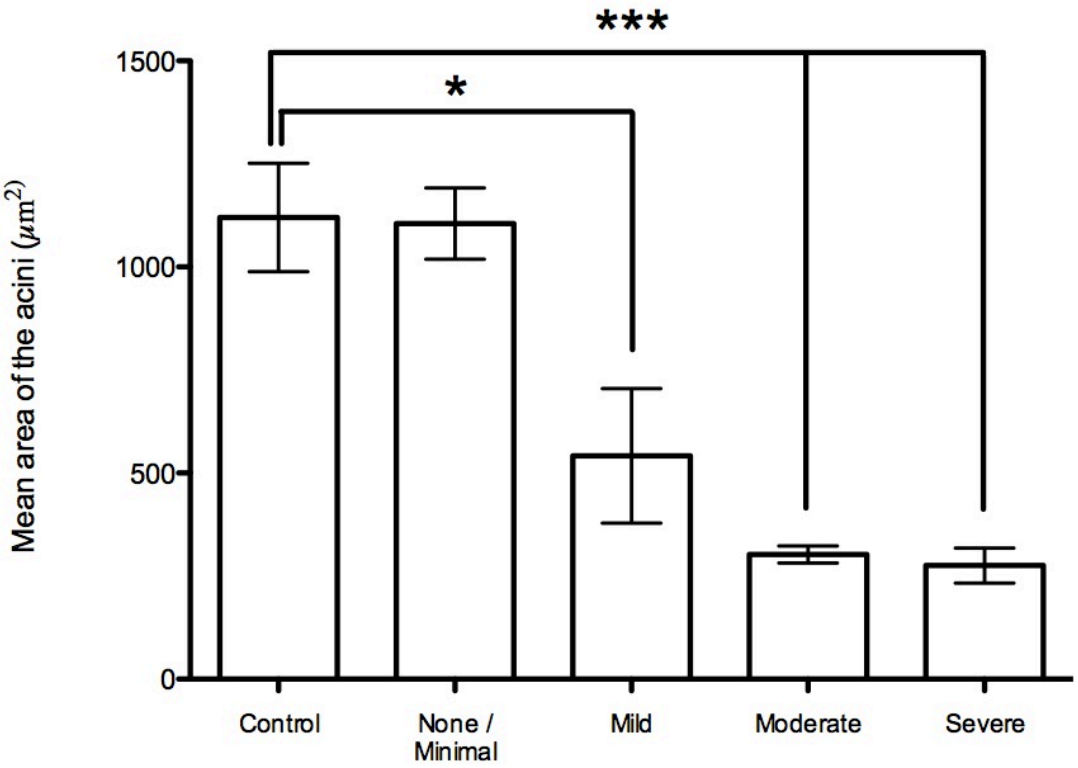

Figure 6.2 Morphometric analysis of the H&E stained samples from Figure 6.1. indicated the mean area of the acini in submandibular glands of control, none/ minimal, mild, moderate and severe atrophy. Mean acini area, in comparison to control, was significantly decreased ($p = 0.01$) as a result of mild atrophy. Moderate and severe atrophy reduced mean acini area significantly ($p < 0.0001$) in comparison with control. Data is based on 20 randomly selected observations per sample. Data is expressed as mean + S.E.M.

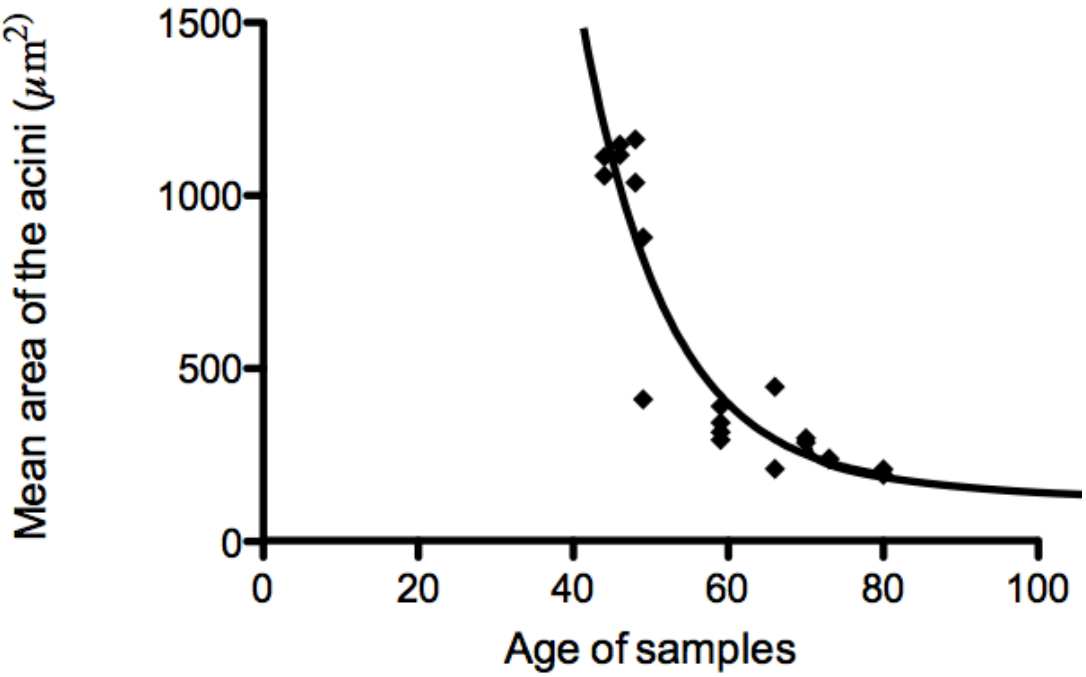

Figure 6.3 Regression analysis of the correlation between the mean acini area in atrophic submandibular glands and the age of each respective sample at the time of biopsy, revealing that as the age increased, the mean acini area decreased. This is indicated by a plateau following a one phase decay. The time of graph decay begins at 38.97 years at which point the mean acini is 1620 (hypothetical), the acini span is 1508 and the plateau mean area of the acini reached is 112, data expressed at 95% confidence levels (sequence p = 0.05).

6.3.2 Immunohistochemistry

The localisation of mTOR substrate expression was evaluated in human submandibular glands with varying degrees of atrophy, using pS6rp antibody (Figure 6.4).

Phospho-S6rp was expressed in all cases to various degrees. Minimal atrophy (A & B) exhibited signs of early stages of atrophy, including shrunken acini, fat displacement and basolateral acinar membrane positive staining for pS6rp but no positive ductal staining.

Mild and moderate cases of atrophy (C & D) showed that mTOR substrate expression was evident in acini, alongside signs of more advanced atrophy such as increased inflammatory cell infiltration.

Cases with more advanced atrophy (E & F) exhibited the most deterioration, with no 'normal' acini remaining as all had shrunk. mTOR positive staining was visible in the shrunken acini as well as ducts, alongside the presence of abnormal branched entities characterised by short duct-like structures ending with small acini.

The secondary antibody controls (Figure 6.5 A) were used as a negative control and showed no mTOR substrate staining. Tonsil tissue showed interfollicular space and lymphocytes indicating positive mTOR staining (B) was used as positive control.

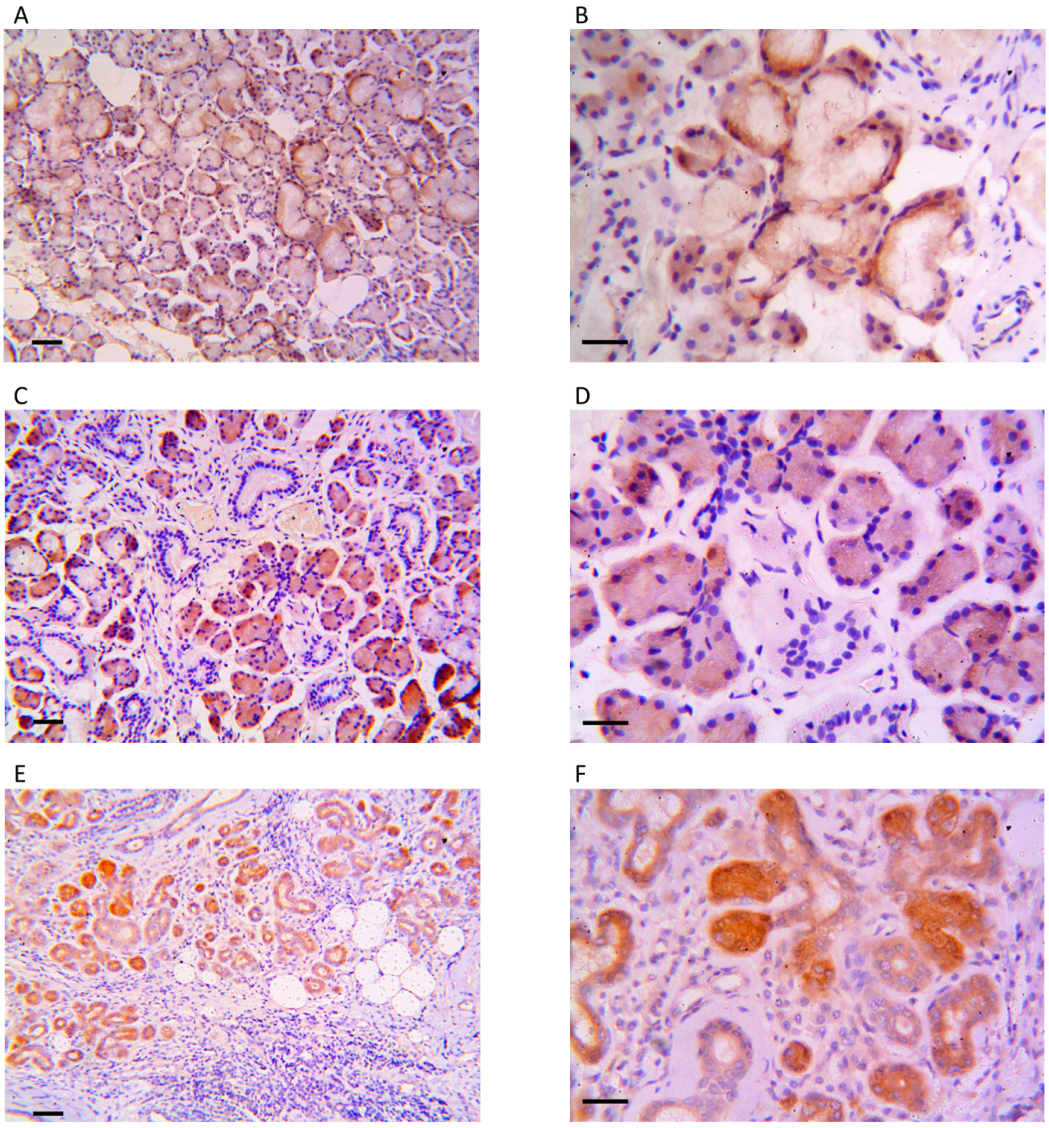

Figure 6.4 Immunostaining of pS6rp (counter-stained with H&E) in minimally to mildly atrophic (A , B), moderately atrophic (C , D) and severely atrophic (E , F) submandibular gland tissue. mTOR substrate expression was evident in all samples in the acini, with the exception of more severe cases of atrophy (E , F) which showed positive staining in duct-like structures as well as acini. Scale bars: A, C & E represent 50 µm; B, D, & F represent 100 µm.

A

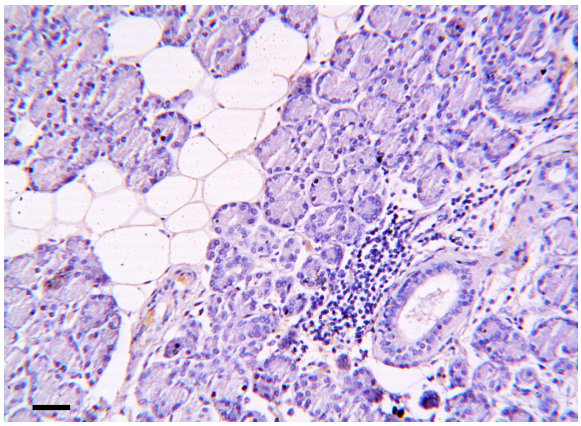

B

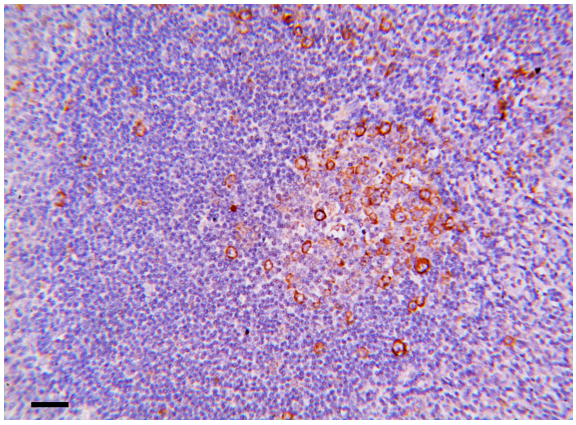

Figure 6.5 Immunostaining of negative and positive controls for mTOR substrates, with secondary antibody control (A) and tonsil tissue (B). Secondary antibody control showed no mTOR staining (A) whereas tonsil tissue showed positive mTOR staining in interfollicular space and lymphocytes. Scale bars represent 100 µm.

6.3.3 mTOR status

Western blots of total mTOR and the mTOR substrates, pS6rp and p4E-BP1, in human submandibular glands of 10 patients, were analysed in two sets (Figure 6.6 A & B).

Total mTOR was present in all cases of atrophy, however there was a notable reduction with severe atrophy. Human whole mouth saliva was used as negative control for total mTOR measurements and the first blot of p4E-BP1, and thus showed no presence of total mTOR (Figure 6.6 A). Whereas mouse muscle tissue and 7 day ligated mouse submandibular gland homogenates were used as positive control for all other blots, since the antibodies were reactive to both mouse & human proteins.

Anti-phospho-4E-BP1 antibody was used to show the phosphorylated isoform in various cases of atrophy, which signified mTOR substrate activity in all cases of atrophy to varying degrees. Whereas, phospho-S6 ribosomal protein exhibited a limited presence only in cases of no atrophy or minimal atrophy, with the exception of one set of analysis which revealed pS6rp expression in all but mild atrophy.

A

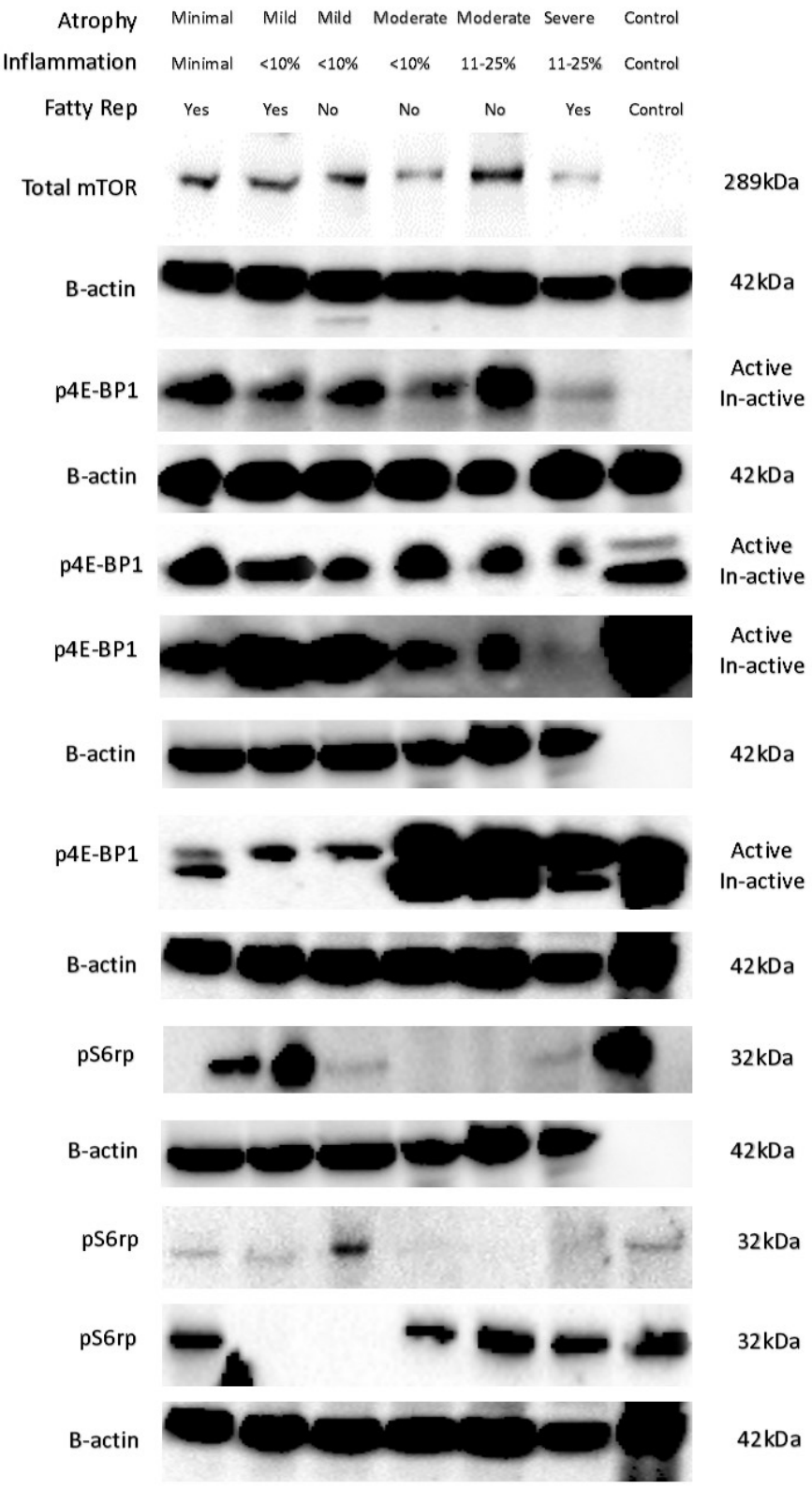
Atrophy
Minimal
Mild
Mild
Moderate
Moderate
Severe
Control
Inflammation
Minimal
<10%
<10%
<10%
11-25%
11-25%
Control
Fatty Rep
Yes
Yes
No
No
No
Yes
Control
Total mTOR
289kDa
B-actin
42kDa
p4E-BP1
Active
In-active
B-actin
42kDa
p4E-BP1
Active
In-active
p4E-BP1
Active
In-active
B-actin
42kDa
p4E-BP1
Active
In-active
B-actin
42kDa
pS6rp
32kDa
B-actin
42kDa
pS6rp
32kDa
pS6rp
32kDa
B-actin
42kDa

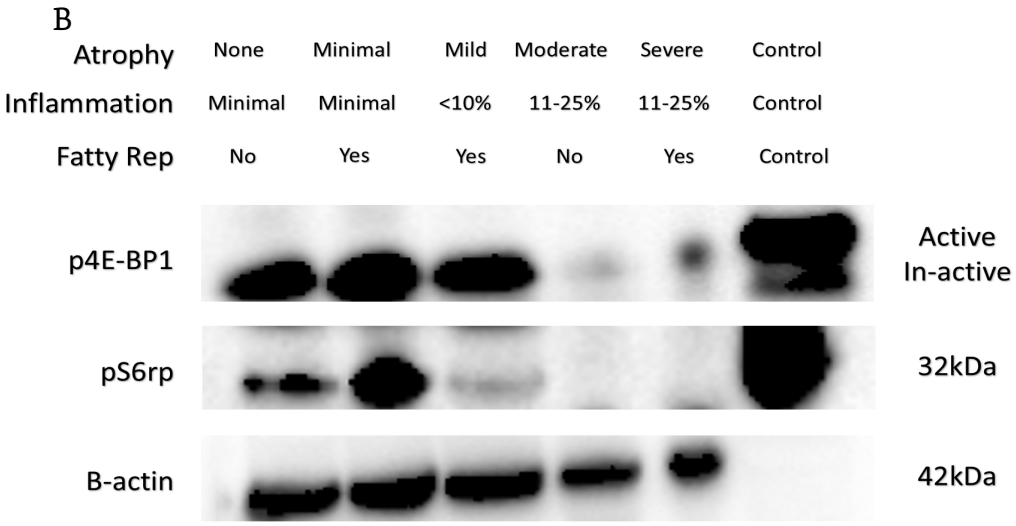

Figure 6.6 Immunoblotting of total mTOR and the mTOR substrates - phospho-S6 ribosomal protein (pS6rp) and phospho-4E-BP1 protein (p4E-BP1) in human submandibular gland homogenates of patients with varying degrees of atrophy, ranging from minimal to severe (A) or no atrophy to severe (B). Total mTOR was apparent in all samples with a visible reduction in the case of severe atrophy. Substrates of the mTOR kinase (phosphorylated 4E-BP1 and S6rp) were greatest in samples that showed mild atrophy and least in the most atrophic samples. Beta actin (β-actin) was used as a loading control. Human whole mouth saliva was used as negative control for total mTOR and the first row of p4E-BP1. Mouse muscle tissue and 7 day ligated mouse submandibular gland homogenates were used as positive control, however muscle homogenates show absence of β-actin, as muscle expresses α-smooth muscle actin (α-SMA).

6.3.4 Biochemical analysis of autophagy

In order to determine presence of autophagy, immunoblotting analysis was performed on submandibular glands of 10 patients, probing for the autophagy markers that are Atg3, Atg5 and LC3 (Figure 6.7).

The Atg3 and Atg5 immunoblots indicated that autophagic activity was virtually consistent at all stages of atrophy (A & B). Levels of the autophagy markers LC3-I (18 kDa) and LC3-II (16 kDa) showed that autophagy was greatest in none atrophic or minimally atrophic samples and progressively reduced in each succeeding stage of atrophy until only a singular isoform of LC3-II was visible in severely atrophic samples.

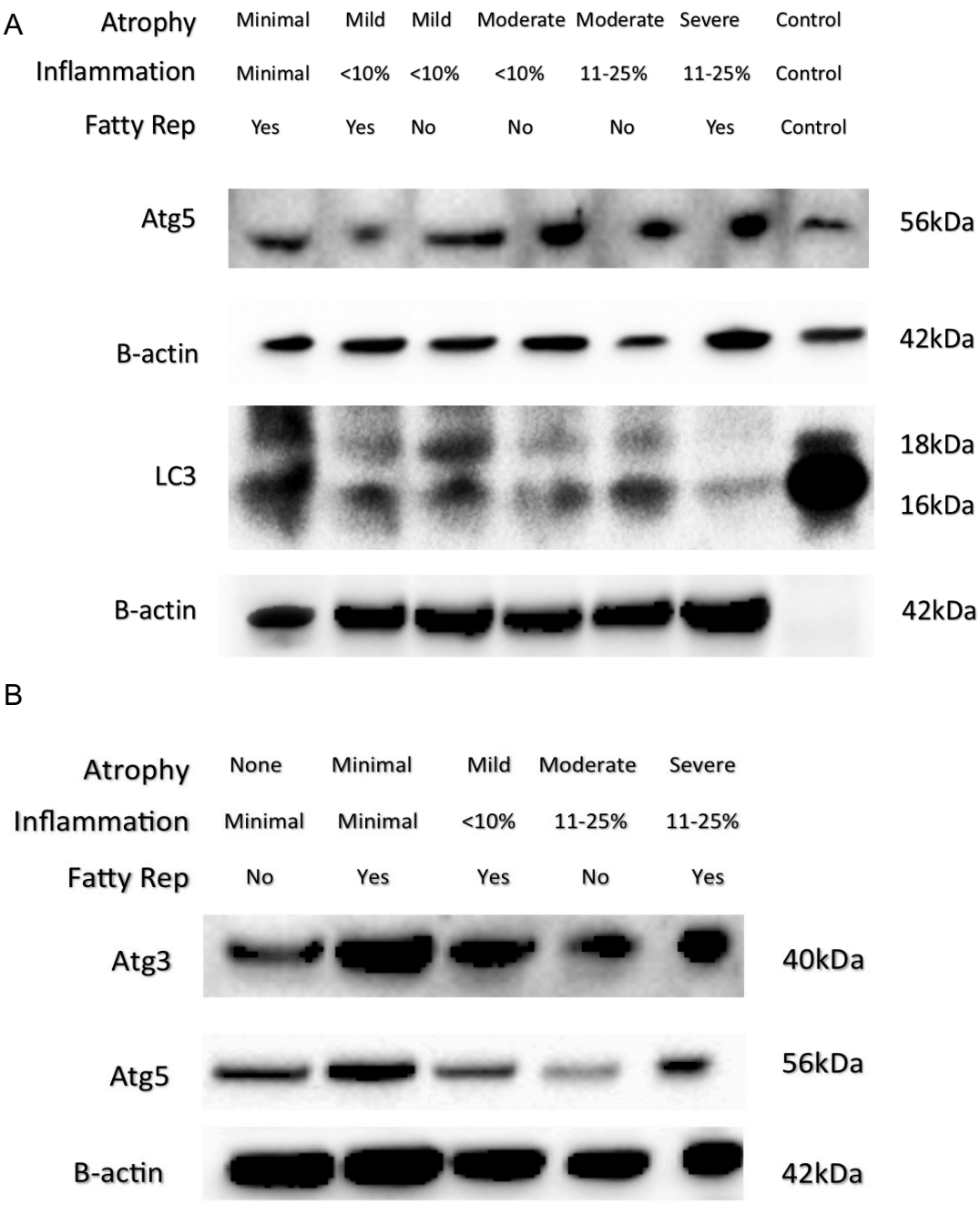

Figure 6.7 Immunoblotting of autophagy markers Atg3, Atg 5 and LC3 in human submandibular gland homogenates of patients with varying degrees of atrophy ranging from minimal to severe (A). Alongside, Immunoblotting of the autophagy markers Atg3 and Atg5 in human submandibular gland homogenates of patients with varying degrees of atrophy ranging from no atrophy to severe (B). Levels of the autophagy markers were greatest in none or minimally atrophic samples and least in severely atrophic samples. Anti-beta actin (β-actin) was used as a loading control. Human LC3B/293T cells served as positive control for LC3 and 7 day ligated mouse submandibular gland homogenates were used as positive control for Atg5.

6.3.5 Biochemical analysis of salivary proteins

Immunoblotting demonstrated presence of specific salivary proteins in human submandibular glands of patients with varying degrees of atrophy, ranging from minimal to severe. This revealed that the presence of the two salivary mucins, MUC5B and MUC7, were minimal throughout, with MUC7 visible bands present only in minimal cases of atrophy (Figure 6.8).

On the other hand, western blots of the levels of salivary proteins such as cystatin, statherin and CA 6 revealed their existence only in mild or minimal atrophy, but exhibited no staining in the more severe cases of human submandibular gland atrophy. Furthermore, PIP was only present in minimal cases of atrophy and the salivary glycoprotein transcobalamin 1 was not present in any atrophic glands, it only revealed itself in control whole mouth saliva.

Statistical analysis of the band intensity of the western blots of the salivary proteins Cystatin S, Statherin and CA VI to β-actin ratio using linear regression analysis in comparison to the age of the samples, revealed that as the age increases, protein expression decreases in a

uniform manner, to the extent that their regression lines appeared to be almost identical (Figure 6.9).

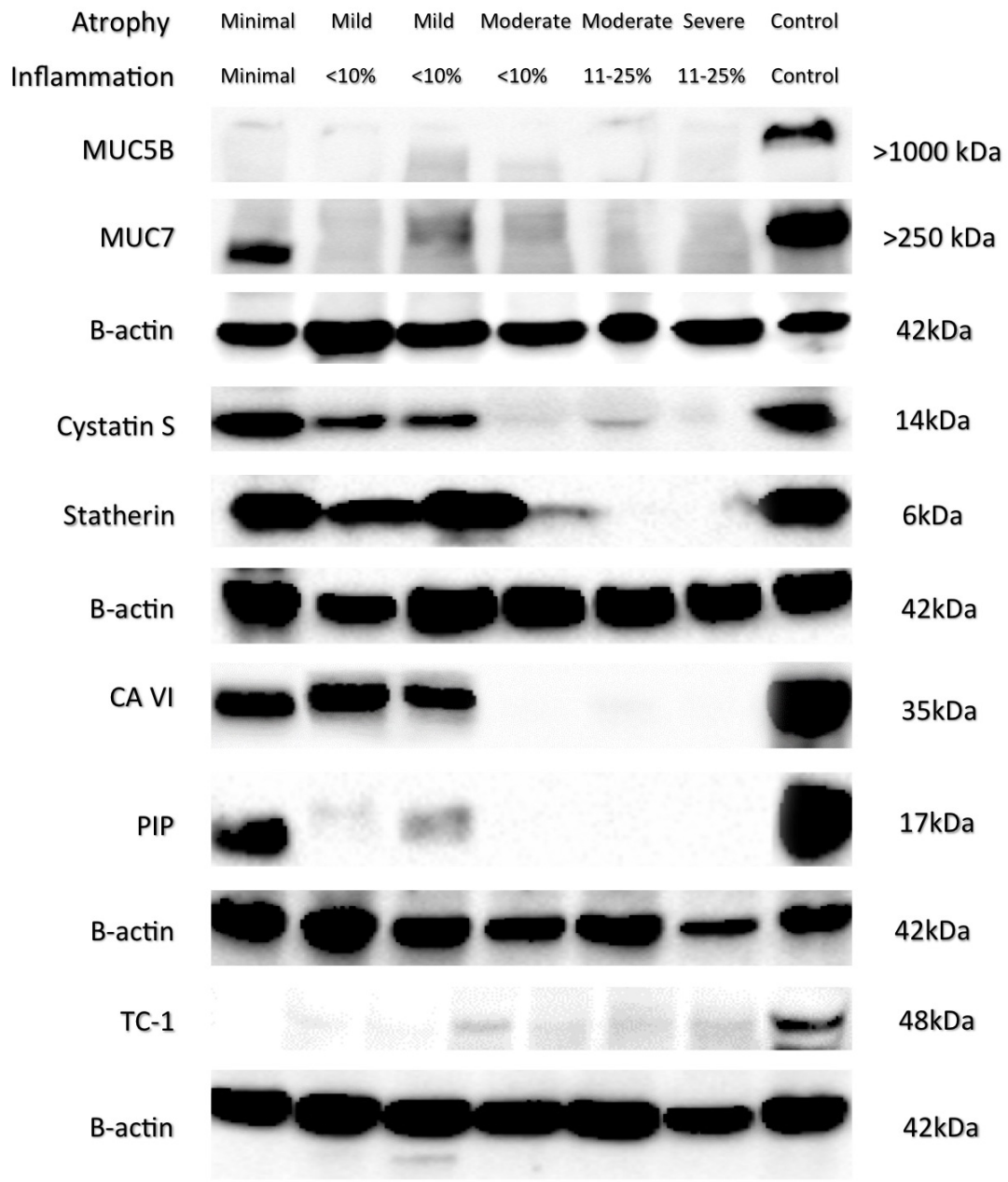

Figure 6.8 Immunoblotting demonstrated presence of specific salivary proteins in human submandibular glands of patients with varying degrees of atrophy, ranging from minimal to severe. Presence of mucins, such as MUC5B and MUC7, as well as Transcobalamin I (TC-1), were minimal throughout. Whereas, levels of proteins such as cystatin, statherin, prolactin-inducible protein (PIP) and carbonic anhydrase 6 (CA VI) were present in glands with minimal salivary gland atrophy but not detected in the severely

atrophic samples. Human whole mouth saliva was used as positive control. Anti-beta actin (β-actin) was used as a loading control.

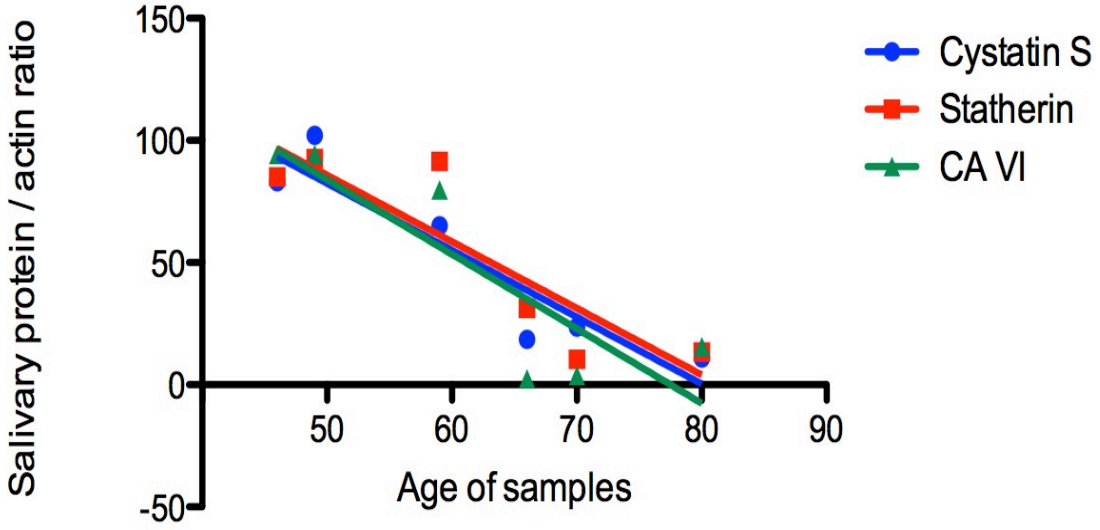

Figure 6.9 Correlation between the salivary proteins Cystatin S, Statherin and CA VI to actin ratio and the age of the human patient of each respective sample at the time of biopsy shown via linear regression analysis. Western blot band intensity levels of the proteins decreased as age increased. Cystatin S constant is 219.3 and formula is Y=-2.737X+219.3 where r^2 is 0.8652. Statherin constant is 221.1 and formula is Y=-2.725X+221.1 where r^2 is 0.7850. CA VI constant is 236.5 and formula is Y=-3.051X+236.5 where r^2 is 0.7515.

6.4 Discussion

Our previous study found that inhibition of mTOR can delay ligation-induced atrophy of salivary glands, however only affecting acinar, but not ductal, atrophic processes (Bozorgi et al., 2014) and the previous chapters have suggested how the mTOR pathway can be associated with the process of autophagy. However this study underlines the complexity of *in vivo* analysis of mTOR on human salivary glands and hints at its interaction with other glandular processes by studying mTOR activity as well as gland function, morphology and biochemistry.

The salivary gland atrophy that is induced by old age, cancer treatment or other diseases, can lead to morphological, cellular and microscopic changes (Bozorgi et al., 2014). Typically the changes, which occur as a result of atrophy, include decreased acinar cells volume and size (Harrison and Garrett, 1976), acinar & ductal degranulation (Osailan et al., 2006, Norberg et al., 1988) and interlobular duct dilation (Scott, 1977). These same findings were observed via H&E staining (Figure 6.1) in atrophic glands in comparison with controls.

One possible theory arising for the significant ($p < 0.001$) reduction in mean acini area, which was reduced by 75 % between control and

severe atrophy, is that acini are linked to ageing in submandibular glands, evidenced by Figure 6.3, whereby regression analysis of mean acini area in correlation to the age of the patients at the time of biopsy revealed that as the age increased, the mean acini area decreased sharply. The derivation of simple regression estimators show that derivatives diverge at the age of 50 years, causing a significant ($p<0.001$) drop in mean acini area after this age.

From the morphological assessments, other changes observed include accumulation of intracellular fat and adipose tissue and increasing fibrosis. As previously established by (Hamperl, 1931, Waterhouse et al., 1973) as signs of ageing in human salivary glands (Scott, 1977), however the pathogenesis of fibrosis in unhealthy glands is mostly unknown (Teymoortash et al., 2003)

As the atrophy progressively increased, these morphological changes observed by H&E staining findings intensified to the extent of reduced acini but a vast increase in duct-like structure. This appears to be evidence of ductal metaplasia (Azevedo et al., 2005), which Scott considers to be an interdependent morphological change from acinar atrophy (Scott, 1980) resulting in a significantly higher than normal

duct-to-acinar ratio (Scott et al., 1999). This may also be linked to ageing (Scott, 1977), as Scott shows how the percentage of acini continuously depletes throughout adult life to a statistically significant extent whilst ductal proportion increases gradually. However, it should be noted that although morphology may be associated with age, it has been suggested that salivary gland function in healthy individuals does not decrease with age (Pedersen et al., 1999).

Immunohistochemistry revealed S6 kinase expression, suggesting mTOR pathway activation, in all cases of atrophy. This is similar to previous studies which have shown salivary gland tumours exhibit strong activation of the mTOR pathway (Diegel et al., 2010).

However as the atrophy worsened, S6 immunohistochemical results became more evident, with the placement of S6 having shifted from from only on acinar cells to both acini and ducts in advanced atrophic glands. This reflects the differences of species, as mice atrophic glands without treatment showed an absence of mTOR in ducts, as shown in Chapter 4. Furthermore this progression of S6 immunohistochemistry with worsening of atrophy is similar to previous findings, whereby patients with head and neck SCC had activated and overexpressed

phosphorylated ribosomal S6 kinase as their disease metastised (Kang et al., 2010).

These findings were further supported by immunoblotting results that revealed mTOR was active during all stages of atrophy. This was shown in blots of the mTOR substrates, S6k and 4E-BP1, whereby Phospho-4E-BP1 protein was in its phosphorylated isoform in various cases of atrophy, and S6 revealed inconsistent findings including one set of analysis which revealed pS6rp expression in all but mild atrophy. Total mTOR kinase was also present in all cases of atrophy, however there was a visible reduction in severe atrophy, probably related to most acinar cells being displaced by fat cells and fibrotic deposits, similar to previous western blot experiments which found total mTOR to be abundant in muscular atrophy despite fluctuating reductions in 4E-BP1 and S6K1 (Dreyer et al., 2008).

These findings, which signified mTOR substrate activity in all cases of atrophy to varying degrees, coincided with the highest levels of autophagy as evidenced by the immunoprobing for the autophagy markers, Atg3 and Atg5. Immunoblotting analysis of the markers for Atg3 and Atg5 indicated that autophagic activity was virtually present

at all stages of atrophy, similar to the varying degrees of pS6k and p4E-BP1 that were expressed in western blots of all stages of atrophy. These findings further supports the theory that activation of mTOR coincides with autophagy in submandibular gland atrophy (Silver et al., 2010). Immunohistochemistry for autophagy was not attempted as it would be expected that autophagy occurs in both acinar and ductal cells.

Another autophagic marker - LC3, is considered a more reliable method for monitoring autophagy and autophagy-related processes, including autophagic cell death (Tanida et al., 2008). Thus immunoblotting analysis was performed on submandibular glands of 10 patients in order to probe for LC3. Unlike Atg3 and Atg5, LC3 was not present in all variances of atrophy, as levels of the autophagy markers LC3-I and LC3-II were greatest in minimally atrophic samples and progressively reduced in each succeeding stage of atrophy until only a singular isoform of LC3-II was visible in severely atrophic samples. Despite these findings, this does not indicate that autophagic processes had terminated during severe atrophy, as LC3-I is gradually reduced during autophagy because it becomes covalently conjugated to phosphatidylethanolamine by Atg3 catalysis to form LC3-II (Silver et al., 2010) and LC3-II was reduced because LC3-II itself is degraded by

autophagy (Mizushima and Yoshimori, 2007). Furthermore, the slight presence of LC3-II that remained in blots of severely atrophic samples could be because LC3-II is more sensitive to immunoblotting than LC3-I (Klionsky, 2009). The result of these factors is that interpretation of the results from LC3 immunoblotting alone can be problematic. Therefore it may be more appropriate to observe the conversion of LC3-I to LC3-II relative to immunoblotting of its catalyst Atg 3 (Silver et al., 2010), or the levels of LC3-II relative to actin for autophagy assays (Klionsky et al., 2008) or the summation of LC3-I and LC3-II for ratio determinations (Mizushima and Yoshimori, 2007). When evaluating the immunoblots of autophagy markers Atg3, Atg5 and LC3 with these considerations in mind, it can still be concluded here that autophagy has coincided with the activation of mTOR in human submandibular gland atrophy, as previously shown by our group in rats (Silver et al., 2010).

The minimal presence of the salivary protein markers, or their lack thereof, indicated that salivary gland functions have been impaired as a result of atrophy. Despite recent literature suggesting that MUC7 is more susceptible to degradation and that MUC5B is more resistant to degradation (Takehara et al., 2013), our findings were contradictory, showing that despite the presence of the two salivary mucins, MUC5B

and MUC7, being quantifiably low throughout, MUC7 exhibited a visible presence in minimal cases of atrophy suggesting it was more resistant, which may be due to a lack of mucous acini which are sparse in submandibular glands. Furthermore, seromucous cells only accounts for 10% of cells in submandibular glands, so it maybe that the biopsies missed these acini.

Whilst the presence of PIP and TC-1 were minimal throughout and only exhibited a visible presence in very minimal cases of atrophy. This suggests that prolactin-inducible protein are very susceptible, to the extent that even the slightest atrophy can affect their secretory function. This theory is further supported because PIP is typically present at moderate levels in human submandibular and sublingual glands (Rathman et al., 1989, Schenkels et al., 1994, Mirels et al., 1998). Whereas TC-1, which is typically present in the secretory cells of human submandibular and parotid glands (Hurlimann and Zuber, 1969, Nexo et al., 1988), was not exhibited because this protein is detected in the mucous secretory acini and intercalated ducts (Nexo et al., 1985) however the tissue samples utilised in this study had a low quantity of mucous acini that were sparse in submandibular glands and the ducts had underwent degranulation during atrophy.

Immunoblots of the levels of cystatin, statherin and CA VI, revealed their presence in mild and minimal atrophy, perhaps because cystatin is less susceptible to autophagy during salivary gland atrophy, as shown by its increase during Sjögren's syndrome by van der Reijden (van der Reijden et al., 1996) or perhaps it could be because cystatin, statherin and CA VI, are predominantly found in serous cells (Isemura et al., 1984, Leinonen et al., 2001, Isola et al., 2008), of which there remained a continued presence during mild and minimal atrophy in our H&E staining.

An alternative theory for the diminishment of Cystatin S, Statherin and CA VI, could be that their secretion is possibly intrinsically linked to ageing, as shown by Figure 6.9, which shows an almost identical linear regression slope for each of the 3 proteins in correlation to the age of the patients at the time of biopsy.

The mere fact that these proteins diminished in older people does not necessarily constitute that ageing is the cause of the diminishment. For example, a recent study into mucosal lesions found that although mucosal lesions are more prevalent in older people, it was associated with environmental changes but not with age or gender (Lynge

Pedersen et al., 2015). mTOR itself has been proven to be integral to ageing and growth, whether it is the mTOR pathway stimulating hypertrophy, cellular growth and protein synthesis at young ages (Wullschleger et al., 2006, Blagosklonny, 2010), or whether it is mTOR being part responsible for mechanistically driving aging, as a continuation of growth (Blagosklonny and Hall, 2009). Furthermore, inhibiting mTOR, via rapamycin, late in life prolongs lifespan in mammals (Harrison et al., 2009) and confers protection against a growing list of age-related pathologies (Johnson et al., 2013). The mTOR pathway is also involved in human cancer (Sato et al., 2010), pulmonary atrophy (Razeghi et al., 2003), cardiovascular diseases (Mueller et al., 2008), osteoporosis (Chen et al., 2014) and diabetes (Zoncu et al., 2011); solidifying mTOR as a key modulator of ageing and age-related disease (Johnson et al., 2013).

Interestingly, a recent multi-centric study reported that when mTOR inhibition started late in the life of mice, i.e. 600 days, which corresponds roughly to an age of 60 years in humans, it increased both maximal and median life span (Harrison et al., 2009, Miller et al., 2010). Although these results cannot be directly extrapolated to humans, they do corroborate with our findings, regarding mean acini area and the

diminishment of salivary proteins, which all appeared to decrease around a similar age range reported from that study.

The possible future of treating salivary gland atrophy in humans lies not only in artificial lubricants and drugs stimulating residual function, as their effects are at best transient (Pringle et al., 2013), but also in transplantation of cultured salivary gland cells into atrophic salivary glands (Sugito et al., 2004) and stem cell transplantation into impaired salivary glands (Lombaert et al., 2008). This study built upon these foundations, by basing rapamycin as another treatment therapy. Rapamycin's use in cancer treatment and as an immunosuppressant has already confirmed it to be suitable and safe (Martinez et al., 2010), and this study found evidence of mTOR activity during human salivary gland atrophy, although it has not conclusively uncovered the causation behind mTOR activity during human salivary gland atrophy. The causation behind it could be ageing or it could be each sample's disease e.g. SSC. mTOR's localisation during human salivary gland atrophy, found using immunohistochemistry, in acinar cells and then to ductal cells as atrophy worsens, suggests it is a druggable target, possibly by intraductal injection of rapamycin loaded nanoparticles to

get localised targeting whilst reducing whole body toxicity (Bibee et al., 2014).

CHAPTER 7

DISCUSSION

7.1 Conclusions

It has been shown here that the conditional inhibition of the mammalian target of rapamycin (mTOR) pathway, also known as the mechanistic target of rapamycin, in the salivary glands results in proliferation and recovery from atrophic processes, however only affecting acinar, but not ductal, atrophic processes. Various conditional inhibition models were created and studied, using rapamycin, Torin1 and BEZ. To the best of our knowledge, an *in vivo* study to determine the response of mTOR inhibition during salivary gland atrophy as well as it's recovery from atrophy has not been performed on mice prior to this study. However our group has previously looked into the activation of mTOR during autophagy and atrophy in rat salivary glands (Silver et al., 2010), as well as observing the gland's ability to recover its functionality following non-drug treated de-ligation in rats (Osailan et al., 2006, Carpenter et al., 2009).

Initially, all drug treated models significantly rescued glandular structure and morphology, in comparison to untreated atrophic glands. On the other hand, longer periods of mTOR inhibitor administration proved that the mTOR inhibition is conditional but the conditions are unknown. 7 days of treatment, whether by rapamycin or Torin1,

showed a loss of efficacy, with glands returning to a similar state to that of untreated atrophic glands. This suggested that inhibition of mTOR can delay ligation-induced atrophy of salivary glands, however only affecting acinar, but not ductal, atrophic processes.

The reasoning for this being that the main mechanism of salivary gland homeostasis is self-duplication of acinar cells and acinar cells that survive injury are involved in the regeneration of salivary glands (Aure et al., 2015). Furthermore, it is generally accepted that rapamycin's ability to regulate cap-dependant translation varies significantly among different cell types (Choo et al., 2008), whether they be acini or ductal affects such variations. These conditional mTOR inhibition results coincide with multiple studies defining a resistance to rapamycin (Brunn et al., 1996, Schmelzle and Hall, 2000, Gingras et al., 2001). The general consensus being that the PI3K negative feedback loop (Figure 7.1) can reactivate mTOR via the TSC1/2 complex (Guertin and Sabatini, 2009).

The hypothesis that rapamycin is ineffective against the negative feedback mechanism because rapamycin only inhibits mTORC1 (Zaytseva et al., 2012) was investigated via the use of second generation

mTOR inhibitors, Torin1 and BEZ, which in longer periods of administration provided similar results to rapamycin in this study.

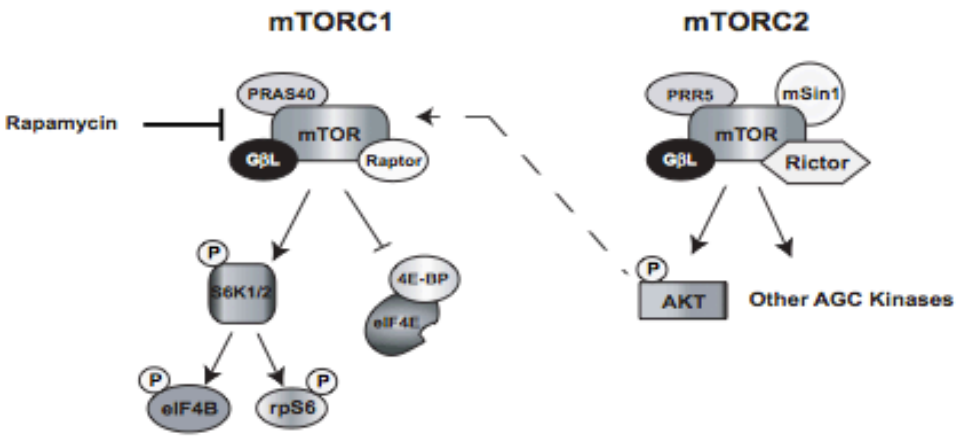

Figure 57.1 Diagram depicting mTORC1 and mTORC2 signalling, including the Akt feedback loop adapted from (Dowling et al., 2010)

Furthermore, there has been evidence which suggests that prolonged use of rapamycin inhibits mTORC2 assembly (Sarbassov et al., 2006), which along with the ineffectiveness of Torin1 and BEZ, helps to disprove the theory that rapamycin is ineffective against the negative feedback mechanism because rapamycin only inhibits mTORC1.

This gives rise to an alternate theory that rapamycin, as well as the second generation mTOR inhibitors, have been effective in mTOR inhibition and that the inhibition itself is conditional upon mTOR-

independent factors, such as S6K1 and 4E-BP1 possibly being activated via mTOR-independent phosphorylation of S6K1 and 4E-BP1, a mechanism suggested by other studies (Liu et al, 2013). An unknown mechanism that prevents the simultaneous activation of both mTORC1 and mTORC2 also adds weight to this theory (Efeyan and Sabatini, 2010). Although mTORC2's kinase activity can be partially positively regulated, via an unknown mechanism that is seemingly independent of the inhibition of mTORC1 (Huang et al., 2008). Furthermore, these loops all prevent the sustained activation of the PI3K pathway (Giaccone and Soria, 2014) because activation of S6K1 abrogates the activation of PI3K (Chandarlapaty et al., 2011).

As the PI3K pathway is highly interconnected with multiple feedback loops across other signalling networks, this presents us with an interesting strategy to observe in the future of dealing with salivary gland atrophy and whether combination therapy strategies could fully inhibit mTOR *in vivo,* with an example of this approach involving dual PI3K/mTOR inhibitors and the combination of everolimus with IGF-1R inhibitors to test this proof of concept (Ghigo et al., 2010, Giaccone and Soria, 2014) .

Furthermore, there appears to be a vast difference between *in vivo* and *in vitro* mTOR inhibition results. For example, BEZ treatment on cells fully inhibits mTOR and disables autophagy as a mechanism of self-preservation (Kim et al., 2014), whereas *in vivo* studies, including this study, have found BEZ to be not fully effective in fully blocking mTOR and recommend combination therapy of BEZ with the addition of chloroquine (CQ), a common clinical anti-cancer drug, that inhibits autophagy and counteracts the cytotoxic effect of BEZ (Li et al., 2013). This is in line with rapamycin experiments too, such as S6K activation in a T cell line being extremely sensitive to inhibition by rapamycin (Kuo et al., 1992), whereas in contrast mTORC1 kinase activity *in vivo* is much less sensitive to rapamycin (Abraham, 2004). The reasoning behind this apparent difference in mTORC1 sensitivity to inhibition *in vivo* and *in vitro* is not yet understood (Ballou and Lin, 2008).

Furthermore, mTORC1 substrates could be overcompensating for mTOR inhibition (Mendoza et al., 2011, Fruman and Rommel, 2014) which would explain why the presence of 4E-BP1 and S6k were actually greater in 7 day Torin1 treated ligated glands than in untreated ligated

only glands. This is because these kinases could accumulate across the 7days and Torin1 has been suggested as having only a limited ability to affect the long term accumulation of early or immediate proteins (Moorman and Shenk, 2010). Rapamycin also has little effect on the accumulation of immediate-early proteins, but can reduce the level of late proteins (Moorman and Shenk, 2010).

In comparing BEZ and Torin1 to rapamycin, in terms of inhibiting mTORC1 substrates, Torin1 was found to present very similar results to rapamycin whereby S6K was inhibited to varying degrees but 4E-BP1 could completely recover its activity in phosphorylation despite initial inhibition, in line with other studies that found some mTOR substrates to be rapamycin-resistant but still requiring mTOR, Raptor and mTORC1's activity (Choo et al., 2008). These results suggest that cap-dependent translation via mTORC1 can be maintained in the presence of mTOR inhibitors (Choo et al., 2008). Whereas BEZ proved to be more effective in comparison to Torin1 or rapamycin, proving that when administered with a dual inhibitor of PI3K/mTOR, BEZ was more effective than inhibition of mTORC1 along, as exhibited by the 3 day inhibition results, keeping in line with previous studies (Cho et al., 2010). However despite providing a promising path to follow up in

future studies, the cytotoxicity of BEZ prevented longer periods of administration in this study.

This leads to an interesting avenue of possibilities to explore regarding combination therapies, whereby the use of mTOR inhibitors is combined with an additional drug that improves efficacy, such as the recommended combination therapy of BEZ with the addition of CQ, a common clinical anti-cancer drug, that inhibits autophagy and counteracts the cytotoxic effect of BEZ (Li et al., 2013). Furthermore, a recent review concluded that combination therapies with other targeted agents may be needed to block negative feedback loops *in vivo* (Carneiro et al., 2015). This is in line with another recent study focused on cancer therapy which found that the use of chemotherapy or a dual mTOR/PI3K inhibitor alone provided limited functionality in comparison to combining gemcitabine (chemotherapy) with dual PI3K/mTOR inhibitors like NVP-BEZ2235 to obtain improved efficacy on growth inhibition in human pancreatic cell lines (Maute et al., 2015). Observing the regeneration and recovery of salivary glands from atrophy in the presence of mTOR inhibitors revealed some interesting findings which built upon our group's previously established detailed understanding regarding the recovery process of submandibular gland

weight following de-ligation (Cotroneo et al., 2008). Chapter 5 of this study took the previous foundations and built upon them, establishing that rapamycin can help to speed up the recovery of salivary glands from atrophy, especially if rapamycin is administered during the ligation period only but then left untreated to recover naturally during the regeneration phase.

This is in line with previous studies performed for examining the recovery aspects of rapamycin on other bodily parts, such as a renal transplant experiment which found rapamycin to be an ideal immunosuppressive agent in the setting of delayed graft function (DGF) after renal transplantation but found that continuing rapamycin treatment during the recovery phase after transplantation caused recipients to be twice as likely to remain on dialysis as recipients without rapamycin (McTaggart et al., 2003) effectively agreeing with our findings that the best form of treatment for recovery is rapamycin treatment during atrophy but then left untreated during regeneration to help speed up recovery. This is likely as a result of rapamycin's immunosuppressive functions, which can inhibit a wide spectrum of T- and B-cell activities (Chen et al., 1994).

Microarray experiments performed in order to identify the gene changes that occur in submandibular gland atrophy in the presence of mTOR inhibitors, led to uncovering many differing possibilities that might explain the re-activation of mTOR in 7 day ligated glands despite the presence of rapamycin. The most promising avenue to explore appears to be the Mitogen-activated protein kinases (MAPK) family, several genes of which were significantly upregulated following rapamycin treatment, including Map2k6, Mapk7, PDE6G and SGK1. Although the interactions of this particular kinase family with mTOR are still highly debated, a previous study has suggested that MAPK activates mTOR via Raptor (Carriere et al., 2011). Furthermore rapamycin is known to activate the MAP kinase-interacting kinase 2a (Mnk2a) (Stead and Proud, 2013), by blocking phosphorylation at Ser437 which elicits activation Mnk2a (Scheper et al., 2001, Stead and Proud, 2013). These findings interlink with the recent assertion that the Mnk pathway maintains mTORC1 activity in rapamycin treated tumours (Grzmil et al., 2014) and these findings can be related to our study as the MAPK and Mnk protein families could be the forces that are reactivating mTORC1 substrates in this study despite the presence of mTOR inhibitors.

LC-MS/MS protein identification attempted to identify the protein pathways involved in reactivating mTOR irrespective of rapamycin's presence. One point of note is that out of over 300 total protein changes identified in this study, a few were linked to neonatal or embryonic glands. The presence of such embryonic specific proteins in the adult rapamycin treated glands may suggest that these glands are regenerating in the presence of rapamycin, as salivary gland regeneration following ligation retraces an embryonic-like state (Carpenter and Cotroneo, 2010, Cotroneo et al., 2010). Furthermore, the BCKD mouse kinase phosphorylated protein was upregulated in rapamycin treated ligated mice submandibular glands in comparison to ligated only glands. The BCKD complex has been linked to mTOR activation via leucine (Lynch et al., 2003, Schaffer and Suleiman, 2007). BCKD phosphorylation has been delineated as reacting with α-ketoisocaproate acid (Dakshinamurti and Zempleni, 2005), this complex interaction (Figure 4.16) may be required for leucine activation of mTOR (McDaniel et al., 2002). As the mechanism of mTOR activation is different when leucine is regulatory (Lynch, 2001), this may explain why the mTOR substrates appear to be reactivating after 7 days in this study despite rapamycin's inhibition.

Human tissue observations revealed that human salivary gland atrophy, and the subsequent salivary gland atrophy on-set mTOR activity, is age associated. The regression analysis of mean acini area in correlation to the age of the patients at the time of biopsy revealed that as the age increased, the mean acini area decreased sharply. The derivation of simple regression estimators show that derivatives diverge at the age of 50 years, causing a significant ($p<0.001$) drop in mean acini area after this age. Furthermore the diminishment of Cystatin S, Statherin and CA VI were linked to ageing, as linear regression analysis revealed an almost identical linear regression slope for each of the 3 proteins in correlation to the age of the patients at the time of biopsy. As mTOR has been proven to be integral to ageing and growth, inhibiting mTOR via rapamycin late in life prolongs lifespan in mammals (Harrison et al., 2009) and confers protection against a growing list of age-related pathologies (Johnson et al., 2013).

Interestingly, a recent multi-centric study reported that when mTOR inhibition started late in the life of mice, i.e. 600 days, which corresponds roughly to an age of 60 years in humans, it expanded both maximal and median life span (Harrison et al., 2009, Miller et al., 2010). Although these results cannot be directly extrapolated to humans, they

do corroborate our findings, regarding mean acini area and the diminishment of salivary proteins, which all appeared to decrease around a similar age range reported from that study, presenting us with a novel approach to prolong salivary gland health in humans by attempting mTOR inhibition in patients with age associated atrophy.

Furthermore, the human study found that mTOR substrate activity coincided with the highest levels of autophagy. Immunoblotting analysis of the markers for Atg3 and Atg5 indicated that autophagic activity was virtually present at all stages of atrophy, similar to the varying degrees of pS6k and p4E-BP1 that were expressed in western blots of all stages of atrophy. Whilst probing for LC3, as discussed in Chapter 6.4, led to the conclusion that autophagy coincided with the activation of mTOR in human submandibular gland atrophy, as previously shown by our group in rats (Silver et al., 2010). This can be interpreted in two differing theories: Beugnet et al. find that it is autophagy which is regulating mTOR, as their study found that inhibition of autophagy impaired the ability of leucine levels, and other intracellular amino acid levels, to regulate 4E-BP1 or S6K1 (Beugnet et al., 2003); whilst an alternative school of thought is that mTOR is able to regulate both apoptosis and autophagy (Silver et al., 2010, Tucci, 2012).

The possible future of treating salivary gland atrophy may not only be in the form of artificial lubricants and drugs stimulating residual function, as their effects are at best transient (Pringle et al., 2013). It is possible that the future lies in transplantation of cultured salivary gland cells into atrophic salivary glands (Sugito et al., 2004), bioengineered salivary gland germ transplantation (Ogawa et al., 2013) and combination drug therapies such as a dual mTOR/PI3K inhibitor along with a supplementary treatment. There have also been recent positive signs of future avenues to explore in the field of repairing radiation damaged-salivary glands with stem cell transplantation (Feng et al., 2009), however it should be noted that the reported 4 phases of dysfunction caused in rodent salivary glands in response to irradiation (Coppes et al., 2001) has not been replicated in similar studies of humans (Zeilstra et al., 2000, Coppes et al., 2002, Vissink et al., 2010).

This study has built upon those previously established foundations by finding evidence of mTOR activity during human salivary gland atrophy and the best method of utilising mTOR inhibition to help with recovery from atrophy in mice. Although it has not yet conclusively uncovered the causation behind mTOR reactivation in salivary gland

atrophy despite the presence of inhibitors, it does suggest it to possibly be the Leucine-BCKD-mTOR or the MAPK-Mnk-mTOR interaction pathway that reactivate mTOR.

7.2 Future Plans

Although the results of this PhD study have provided some novel insights into the role of mTOR in salivary gland atrophy and regeneration, they also open up more avenues to explore in potential future studies in the field.

- **Functional Study**

  Previously our group has reviewed the fluid secretion of salivary glands and reported them to be stopped by duct ligation induced atrophy but reversible, provided that the automatic innervation remains intact (Proctor and Carpenter, 2007). A potential future study can look at the effects of mTOR inhibition on atrophic glands to observe their effects on function, in order to fully complete our understanding of the role of mTOR in salivary gland atrophy. The study can also look at the protein changes in saliva, as rapamycin has been shown to control certain protein levels (Wang et al., 2004).

- **Link between mTOR and autophagy**

  Our group has previously looked into the activation of mTOR during autophagy and atrophy in rat salivary glands (Silver et al., 2010) and this study has observed a similar link in mice atrophic glands. This potential avenue of exploration could be utilised by observing the genes and protein expression of Unc-51 like autophagy activating kinase 1 (ULK1), one of the ULK protein

kinases that play a play critical physiological roles in controlling autophagy (Kim et al., 2013).

- **Gene Expression study**

  Real-time PCR is a reliable tool which is used to measure mRNA transcripts, providing valuable information on gene expression profiles and has been previously utilised by our group to observe adult rat submandibular glands under atrophy and regeneration (Silver et al., 2008). In order to carry out more specific analysis and validate our theories, the genes of interest that were observed in this study's microarray analysis can be followed up on by performing real time PCR analysis.

- **Link between mTOR and MAPK**

  The microarray analysis of this study showed that several genes of the Mitogen-activated protein kinases (MAPK) family were significantly upregulated, including Map2k6, Mapk7, PDE6G and SGK1. This is of particular interest as previous studies have debated that mTOR inhibition activates MAPK (Carracedo et al., 2008) and that MAPK activates mTOR via Raptor (Carriere et al., 2011). With recent evidence indicating that Mnk inhibition presents attractive therapeutic potential (Hou et al., 2012), a future study could inhibit MAPK/Mnk pathways during rapamycin treatment to observe whether or not mTOR reactivates after 7 days as it did in this study.

8.0 Appendix

Table 8.1 Listing of human patients

Patient	Gender	Age	Reason for Dissection	Atrophy	Inflammation	Fatty Rep
7015	Male	70	Laryngeal SCC	Moderate	11-25%	No
3458	Male	49	Maxilla SCC	Mild	<10%	Yes
5185	Male	46	Tongue SCC	Mild	<10%	No
4497	Male	59	Tongue SCC	Moderate	11-25%	No
5434	Female	66	Retromolar SCC	Moderate	<10%	No
7493	Female	80	Tongue SCC	Severe	11-25%	Yes
478	Female	44	Tongue CIS	Minimal	Minimal	Yes
3096	Female	59	Mandible SCC	None	Minimal	No
1249	Male	73	Buccal Mucosa SCC	Severe	11-25%	Yes
713	Male	48	Mandible SCC	Mild	<10%	Yes

9.0 BIBLIOGRAPHY

ABRAHAM, R. T. 2004. PI 3-kinase related kinases: "big" players in stress-induced signaling pathways. *DNA repair,* 3, 883-887.

ANDING, A. L. & BAEHRECKE, E. H. 2015. Vps15 is required for stress induced and developmentally triggered autophagy and salivary gland protein secretion in Drosophila. *Cell Death Differ,* 22, 457-464.

ANTONIO TROCA-MARIN, J., JOSE CASANAS, J., BENITO, I. & LUZ MONTESINOS, M. 2014. The Akt-mTOR Pathway in Down's Syndrome: The Potential Use of Rapamycin/Rapalogs for Treating Cognitive Deficits. *CNS & Neurological Disorders-Drug Targets (Formerly Current Drug Targets-CNS & Neurological Disorders),* 13, 34-40.

ASANTE, C. O. & DICKENSON, A. H. 2010. Descending serotonergic facilitation mediated by spinal 5-HT3 receptors engages spinal rapamycin-sensitive pathways in the rat. *Neuroscience letters,* 484, 108-12.

ASKING, B. & EMMELIN, N. 1989. Secretion of amylase from the rat parotid salivary gland after degeneration of the auriculotemporal nerve. *Archives of oral biology,* 34, 863-5.

ATKINSON, J. C. & FOX, P. C. 1992. Salivary gland dysfunction. *Clinics in geriatric medicine,* 8, 499-511.

ATKINSON, J. C. & WU, A. J. 1994. Salivary gland dysfunction: causes, symptoms, treatment. *Journal of the American Dental Association,* 125, 409-16.

AURE, M. H., KONIECZNY, S. F. & OVITT, C. E. 2015. Salivary Gland Homeostasis Is Maintained through Acinar Cell Self-Duplication. *Developmental cell,* 33, 231-237.

AVRUCH, J., LONG, X., LIN, Y., ORTIZ-VEGA, S., RAPLEY, J., PAPAGEORGIOU, A., OSHIRO, N. & KIKKAWA, U. 2009. Activation of mTORC1 in two steps: Rheb-GTP activation of catalytic function and increased binding of substrates to raptor1. *Biochemical Society Transactions,* 37, 223.

AZEVEDO, L. R., DAMANTE, J. H., LARA, V. S. & LAURIS, J. R. 2005. Age-related changes in human sublingual glands: a post mortem study. *Archives of oral biology,* 50, 565-74.

BAEHRECKE, E. H. 2005. Autophagy: dual roles in life and death? *Nature reviews Molecular cell biology,* 6, 505-510.

BALL, W. D., HAND, A. R., MOREIRA, J. E. & JOHNSON, A. O. 1988. A secretory protein restricted to type I cells in neonatal rat submandibular glands. *Developmental biology,* 129, 464-75.

BALLOU, L. M. & LIN, R. Z. 2008. Rapamycin and mTOR kinase inhibitors. *Journal of chemical biology,* 1, 27-36.

BANASZYNSKI, L. A., LIU, C. W. & WANDLESS, T. J. 2005. Characterization of the FKBP.rapamycin.FRB ternary complex. *Journal of the American Chemical Society,* 127, 4715-21.

BARON, H. C. & OBER, W. B. 1962. Parotid gland atrophy: Observations after ligation of stenson's duct. *Archives of Surgery,* 85, 1042-1044.

BERGEY, E. J., CHO, M. I., BLUMBERG, B. M., HAMMARSKJOLD, M. L., REKOSH, D., EPSTEIN, L. G. & LEVINE, M. J. 1994. Interaction of HIV-1 and human salivary mucins. *Journal of acquired immune deficiency syndromes,* 7, 995-1002.

BERRY, D. L. & BAEHRECKE, E. H. 2008. Autophagy functions in programmed cell death. *Autophagy,* 4, 359-360.

BEUGNET, A., TEE, A., TAYLOR, P. & PROUD, C. 2003. Regulation of targets of mTOR (mammalian target of rapamycin) signalling by intracellular amino acid availability. *Biochem. J,* 372, 555-566.

BIBEE, K. P., CHENG, Y. J., CHING, J. K., MARSH, J. N., LI, A. J., KEELING, R. M., CONNOLLY, A. M., GOLUMBEK, P. T., MYERSON, J. W., HU, G., CHEN, J., SHANNON, W. D., LANZA, G. M., WEIHL, C. C. & WICKLINE, S. A. 2014. Rapamycin nanoparticles target defective autophagy in muscular dystrophy to enhance both strength and cardiac function. *FASEB J,* 28, 2047-61.

BLAGOSKLONNY, M. V. 2010. Why men age faster but reproduce longer than women: mTOR and evolutionary perspectives. *Aging,* 2, 265.

BLAGOSKLONNY, M. V. & HALL, M. N. 2009. Growth and aging: a common molecular mechanism. *Aging,* 1, 357-62.

BOBEK, L. A., AGUIRRE, A. & LEVINE, M. J. 1991. Human salivary cystatin S. Cloning, sequence analysis, hybridization in situ and immunocytochemistry. *The Biochemical journal,* 278 (Pt 3), 627-35.

BORGHESE, E. 1950. Explantation experiments on the influence of the connective tissue capsule on the development of the epithelial part of the submandibular gland of Mus musculus. *Journal of anatomy,* 84, 303.

BOYER, R., JAME, F. & ARANCIBIA, S. Une fonction non exocrine de la glande sous-maxilliaire. Annales d'endocrinologie, 1991. Masson, 307-322.

BOZE, H. L. N., MARLIN, T. R. S., DURAND, D., PEREZ, J., VERNHET, A., CANON, F., SARNI-MANCHADO, P., CHEYNIER, V. R. & CABANE, B. 2010. Proline-rich salivary proteins have extended conformations. *Biophysical journal,* 99, 656-665.

BOZORGI, S. S., PROCTOR, G. B. & CARPENTER, G. H. 2014. Rapamycin delays salivary gland atrophy following ductal ligation. *Cell Death Dis,* 5, e1146.

BRAAM, P. M., ROESINK, J. M., MOERLAND, M. A., RAAIJMAKERS, C. P., SCHIPPER, M. & TERHAARD, C. H. 2005. Long-term parotid gland function after radiotherapy. *International journal of radiation oncology, biology, physics,* 62, 659-64.

BRADLEY, R. M., FUKAMI, H. & SUWABE, T. 2005. Neurobiology of the gustatory-salivary reflex. *Chem Senses,* 30 Suppl 1, i70-1.

BRIAN, M., BILGEN, E. & DIANE, C. F. 2012. Regulation and function of ribosomal protein S6 kinase (S6K) within mTOR signalling networks. *Biochemical Journal,* 441, 1-21.

BRILL, S., LI, S., LYMAN, C. W., CHURCH, D. M., WASMUTH, J. J., WEISSBACH, L., BERNARDS, A. & SNIJDERS, A. J. 1996. The Ras GTPase-activating-protein-related human protein IQGAP2 harbors a potential actin binding domain and interacts with calmodulin and Rho family GTPases. *Molecular and cellular biology,* 16, 4869-4878.

BROSKY, M. E. 2007. The role of saliva in oral health: strategies for prevention and management of xerostomia. *The journal of supportive oncology,* 5, 215-25.

BROWN, R. E., ZHANG, P. L., LUN, M., ZHU, S., PELLITTERI, P. K., RIEFKOHL, W., LAW, A., WOOD, G. C. & KENNEDY, T. L. 2006. Morphoproteomic and pharmacoproteomic rationale for mTOR effectors as therapeutic targets in head and neck squamous cell carcinoma. *Annals of clinical and laboratory science,* 36, 273-82.

BRUNN, G. J., HUDSON, C. C., SEKULIĴÁ, A., WILLIAMS, J. M., HOSOI, H., HOUGHTON, P. J., LAWRENCE, J. C. & ABRAHAM, R. T. 1997. Phosphorylation of the translational repressor PHAS-I by the mammalian target of rapamycin. *Science,* 277, 99-101.

BRUNN, G. J., WILLIAMS, J., SABERS, C., WIEDERRECHT, G., LAWRENCE JR, J. & ABRAHAM, R. T. 1996. Direct inhibition of the signaling functions of the mammalian target of rapamycin by the phosphoinositide 3-kinase inhibitors, wortmannin and LY294002. *The EMBO journal,* 15, 5256.

BURGESS, K. L. & DARDICK, I. 1998. Cell population changes during atrophy and regeneration of rat parotid gland. *Oral surgery, oral*

medicine, oral pathology, oral radiology, and endodontics, 85, 699-706.

BURGESS, K. L., DARDICK, I., CUMMINS, M. M., BURFORD-MASON, A. P., BASSETT, R. & BROWN, D. H. 1996. Myoepithelial cells actively proliferate during atrophy of rat parotid gland. *Oral Surgery, Oral Medicine, Oral Pathology, Oral Radiology, and Endodontology,* 82, 674-680.

BURNETT, P. E., BARROW, R. K., COHEN, N. A., SNYDER, S. H. & SABATINI, D. M. 1998. RAFT1 phosphorylation of the translational regulators p70 S6 kinase and 4E-BP1. *Proceedings of the National Academy of Sciences,* 95, 1432-1437.

BYYNY, R., ORTH, D. & COHEN, S. 1972. Radioimmunoassay of epidermal growth factor. *Endocrinology,* 90, 1261-1266.

CAO, P., MAIRA, S.-M., GARCIA-ECHEVERRIA, C. & HEDLEY, D. 2009. Activity of a novel, dual PI3-kinase/mTor inhibitor NVP-BEZ235 against primary human pancreatic cancers grown as orthotopic xenografts. *British journal of cancer,* 100, 1267-1276.

CARAMIA, F. 1966. Ultrastructure of mouse submaxillary gland: I. Sexual differences. *Journal of ultrastructure research,* 16, 505-523.

CARAYOL, N., KATSOULIDIS, E., SASSANO, A., ALTMAN, J. K., DRUKER, B. J. & PLATANIAS, L. C. 2008. Suppression of programmed cell death 4 (PDCD4) protein expression by BCR-ABL-regulated engagement of the mTOR/p70 S6 kinase pathway. *The Journal of biological chemistry,* 283, 8601-10.

CARNEIRO, B. A., KAPLAN, J. B., ALTMAN, J. K., GILES, F. J. & PLATANIAS, L. C. 2015. Targeting mTOR signaling pathways and related negative feedback loops for the treatment of acute myeloid leukemia. *Cancer biology & therapy*, 00-00.

CARPENTER, G. 2014. *Dry mouth : a clinical guide on causes, effects and treatments,* New York, Springer.

CARPENTER, G. & COTRONEO, E. 2010. *Salivary Gland Regeneration in Tucker, A. S. Miletich, I. (ed) Salivary glands : development, adaptations, and disease,* Basel; New York, Karger.

CARPENTER, G. H. 2013. The Secretion, Components, and Properties of Saliva. *Annual Review of Food Science and Technology,* 4, 267-276.

CARPENTER, G. H., KHOSRAVANI, N., EKSTROM, J., OSAILAN, S. M., PATERSON, K. P. & PROCTOR, G. B. 2009a. Altered plasticity of the parasympathetic innervation in the recovering rat submandibular gland following extensive atrophy. *Experimental physiology,* 94, 213-9.

CARPENTER, G. H., KHOSRAVANI, N., EKSTRÖM, J., OSAILAN, S. M., PATERSON, K. P. & PROCTOR, G. B. 2009b. Altered plasticity of the parasympathetic innervation in the recovering rat submandibular gland following extensive atrophy. *Experimental physiology,* 94, 213-219.

CARPENTER, G. H., OSAILAN, S. M., CORREIA, P., PATERSON, K. P. & PROCTOR, G. B. 2007. Rat salivary gland ligation causes reversible secretory hypofunction. *Acta physiologica,* 189, 241-9.

CARRACEDO, A., MA, L., TERUYA-FELDSTEIN, J., ROJO, F., SALMENA, L., ALIMONTI, A., EGIA, A., SASAKI, A. T., THOMAS, G. & KOZMA, S. C. 2008. Inhibition of mTORC1 leads to MAPK pathway activation through a PI3K-dependent feedback loop in human cancer. *The Journal of clinical investigation,* 118, 3065.

CARRIERE, A., ROMEO, Y., ACOSTA-JAQUEZ, H. A., MOREAU, J., BONNEIL, E., THIBAULT, P., FINGAR, D. C. & ROUX, P. P. 2011. ERK1/2 phosphorylate Raptor to promote Ras-dependent activation of mTOR complex 1 (mTORC1). *The Journal of biological chemistry,* 286, 567-77.

CHAI, Y., KLAUSER, D. K., DENNY, P. A. & DENNY, P. C. 1993. Proliferative and structural differences between male and female mouse submandibular glands. *The Anatomical Record,* 235, 303-311.

CHANDARLAPATY, S., SAWAI, A., SCALTRITI, M., RODRIK-OUTMEZGUINE, V., GRBOVIC-HUEZO, O., SERRA, V., MAJUMDER, P. K., BASELGA, J. & ROSEN, N. 2011. AKT inhibition relieves feedback suppression of receptor tyrosine kinase expression and activity. *Cancer cell,* 19, 58-71.

CHEN, J., TU, X., ESEN, E., JOENG, K. S., LIN, C., ARBEIT, J. M., RUEGG, M. A., HALL, M. N., MA, L. & LONG, F. 2014. WNT7B promotes bone formation in part through mTORC1. *PLoS genetics,* 10, e1004145.

CHEN, Y., CHEN, H., RHOAD, A. E., WARNER, L., CAGGIANO, T. J., FAILLI, A., ZHANG, H., HSIAO, C. L., NAKANISHI, K. & MOLNAR-KIMBER, K. L. 1994. A putative sirolimus (rapamycin) effector protein. *Biochemical and biophysical research communications,* 203, 1-7.

CHEN, Y. & KLIONSKY, D. J. 2011. The regulation of autophagy - unanswered questions. *Journal of cell science,* 124, 161-170.

CHEN, Z., CHEN, L. & BLUMBERG, R. S. 2009. Editorial: CEACAM1: fine-tuned for fine-tuning. *Journal of leukocyte biology,* 86, 195-7.

CHO, D. C., COHEN, M. B., PANKA, D. J., COLLINS, M., GHEBREMICHAEL, M., ATKINS, M. B., SIGNORETTI, S. & MIER, J. W. 2010. The efficacy of the novel dual PI3-kinase/mTOR inhibitor NVP-

BEZ235 compared with rapamycin in renal cell carcinoma. *Clinical Cancer Research,* 16, 3628-3638.

CHOI, J. H., WU, H. G., JUNG, K. C., LEE, S. H. & KWON, E. K. 2009. Apoptosis and expression of AQP5 and TGF-beta in the irradiated rat submandibular gland. *Cancer research and treatment : official journal of Korean Cancer Association,* 41, 145-54.

CHOO, A. Y., YOON, S.-O., KIM, S. G., ROUX, P. P. & BLENIS, J. 2008. Rapamycin differentially inhibits S6Ks and 4E-BP1 to mediate cell-type-specific repression of mRNA translation. *Proceedings of the National Academy of Sciences,* 105, 17414-17419.

CHRETIEN, M. 1977. Action of testosterone on the differentiation and secretory activity of a target organ: the submaxillary gland of the mouse. *International review of cytology,* 50, 333-96.

COPPES, R. P. & STOKMAN, M. A. 2011. Stem cells and the repair of radiation-induced salivary gland damage. *Oral diseases,* 17, 143-53.

COPPES, R. P., VISSINK, A. & KONINGS, A. W. 2002. Comparison of radiosensitivity of rat parotid and submandibular glands after different radiation schedules. *Radiother Oncol,* 63, 321-8.

COPPES, R. P., ZEILSTRA, L. J., KAMPINGA, H. H. & KONINGS, A. W. 2001. Early to late sparing of radiation damage to the parotid gland by adrenergic and muscarinic receptor agonists. *British journal of cancer,* 85, 1055-63.

CORREIA, P. N., CARPENTER, G. H., OSAILAN, S. M., PATERSON, K. L. & PROCTOR, G. B. 2008. Acute salivary gland hypofunction in the duct ligation model in the absence of inflammation. *Oral diseases,* 14, 520-8.

COTRONEO, E., PROCTOR, G. B. & CARPENTER, G. H. 2010. Regeneration of acinar cells following ligation of rat submandibular gland retraces the embryonic-perinatal pathway of cytodifferentiation. *Differentiation,* 79, 120-30.

COTRONEO, E., PROCTOR, G. B., PATERSON, K. L. & CARPENTER, G. H. 2008. Early markers of regeneration following ductal ligation in rat submandibular gland. *Cell Tissue Res,* 332, 227-35.

CURTIS, R., FREEDMAN, D., RON, E., RIES, L., HACKER, D., EDWARDS, B., TUCKER, M. & FRAUMENI, J. 2006. New Malignancies Among Cancer Survivors. *SEER Cancer Registries,* 5.

CURTIS, R. E., FREEDMAN, D. M., RON, E., RIES, L. A., HACKER, D. G., EDWARDS, B. K., TUCKER, M. A. & FRAUMENI JR, J. F. 1973. New malignancies among cancer survivors. *SEER cancer registries,* 2000.

CUTLER, L. S. & CHAUDHRY, A. P. 1973. Intercellular contacts at the epithelial-mesenchymal interface during the prenatal development of the rat submandibular gland. *Developmental biology,* 33, 229-240.

DAKSHINAMURTI, K. & ZEMPLENI, J. 2005. *Nutrients and cell signaling,* Boca Raton, Taylor & Francis.

DANCEY, J. E. 2005. Inhibitors of the mammalian target of rapamycin. *Expert opinion on investigational drugs,* 14, 313-28.

DARBY, M. L. 2013. *Mosby's Comprehensive Review of Dental Hygiene*. St. Louis, Mo. Elsevier.

DAS, A., DURRANT, D., KOKA, S., SALLOUM, F. N., XI, L. & KUKREJA, R. C. 2014. Mammalian target of rapamycin (mTOR) inhibition with rapamycin improves cardiac function in type 2 diabetic mice: potential role of attenuated oxidative stress and altered contractile protein expression. *The Journal of biological chemistry,* 289, 4145-60.

DATAN, E., SHIRAZIAN, A., BENJAMIN, S., MATASSOV, D., TINARI, A., MALORNI, W., LOCKSHIN, R. A., GARCIA-SASTRE, A. & ZAKERI, Z. 2014. mTOR/p70S6K signaling distinguishes routine, maintenance-level autophagy from autophagic cell death during influenza A infection. *Virology,* 452-453, 175-90.

DAVIES, A. N. 2000. A comparison of artificial saliva and chewing gum in the management of xerostomia in patients with advanced cancer. *Palliative medicine,* 14, 197-203.

DAVIES, J. A. 2002. Do different branching epithelia use a conserved developmental mechanism? *Bioessays,* 24, 937-948.

DAVOODI, J., MARKERT, C. D., VOELKER, K. A., HUTSON, S. M. & GRANGE, R. W. 2012. Nutrition strategies to improve physical capabilities in Duchenne muscular dystrophy. *Physical medicine and rehabilitation clinics of North America,* 23, 187-99, xii-xiii.

DAWES, C. 2008. Salivary flow patterns and the health of hard and soft oral tissues. *Journal of the American Dental Association,* 139 Suppl, 18S-24S.

DAZERT, E. & HALL, M. N. 2011. mTOR signaling in disease. *Current opinion in cell biology,* 23, 744-55.

DE MOERLOOZE, L., SPENCER-DENE, B., REVEST, J., HAJIHOSSEINI, M., ROSEWELL, I. & DICKSON, C. 2000. An important role for the IIIb isoform of fibroblast growth factor receptor 2 (FGFR2) in mesenchymal-epithelial signalling during mouse organogenesis. *Development,* 127, 483-492.

DELPORTE, C., O'CONNELL, B. C., HE, X., LANCASTER, H. E., O'CONNELL, A. C., AGRE, P. & BAUM, B. J. 1997. Increased fluid

secretion after adenoviral-mediated transfer of the aquaporin-1 cDNA to irradiated rat salivary glands. *Proceedings of the National Academy of Sciences of the United States of America,* 94, 3268-73.

DENNIS, M. D., JEFFERSON, L. S. & KIMBALL, S. R. 2012. Role of p70S6K1-mediated phosphorylation of eIF4B and PDCD4 proteins in the regulation of protein synthesis. *The Journal of biological chemistry,* 287, 42890-9.

DENNY, P., BALL, W. & REDMAN, R. 1997. Salivary glands: a paradigm for diversity of gland development. *Critical Reviews in Oral Biology & Medicine,* 8, 51-75.

DENNY, P. A., PIMPRAPAIPORN, W., KIM, M. S. & DENNY, P. C. 1988. Quantitation and localization of acinar cell-specific mucin in submandibular glands of mice during postnatal development. *Cell and tissue research,* 251, 381-386.

DENTON, D., NICOLSON, S. & KUMAR, S. 2012. Cell death by autophagy: facts and apparent artefacts. *Cell Death & Differentiation,* 19, 87-95.

DESAI, B. N., MYERS, B. R. & SCHREIBER, S. L. 2002. FKBP12-rapamycin-associated protein associates with mitochondria and senses osmotic stress via mitochondrial dysfunction. *Proceedings of the National Academy of Sciences,* 99, 4319-4324.

DIEGEL, C. R., CHO, K. R., EL-NAGGAR, A. K., WILLIAMS, B. O. & LINDVALL, C. 2010. Mammalian target of rapamycin-dependent acinar cell neoplasia after inactivation of Apc and Pten in the mouse salivary gland: implications for human acinic cell carcinoma. *Cancer research,* 70, 9143-52.

DORLAND, W. A. N. 2007. *Dorland's illustrated medical dictionary,* Philadelphia, PA, Saunders.

DOUGLAS, W. H., REEH, E. S., RAMASUBBU, N., RAJ, P. A., BHANDARY, K. K. & LEVINE, M. J. 1991. Statherin: a major boundary lubricant of human saliva. *Biochemical and biophysical research communications,* 180, 91-7.

DOWLING, R. J., TOPISIROVIC, I., FONSECA, B. D. & SONENBERG, N. 2010. Dissecting the role of mTOR: lessons from mTOR inhibitors. *Biochimica et Biophysica Acta (BBA)-Proteins and Proteomics,* 1804, 433-439.

DOWNEY, T., PEVSNER, J., JEON, O.-H., MURILLO, F.M., AND SPITZNAGEL, E.L. 2004. Estimating and removing batch effects from microarray data. *7th International Meeting of the Microarray Gene Expression Data Society.* Toronto, Canada.

DRENAN, R. M., LIU, X., BERTRAM, P. G. & ZHENG, X. S. 2004. FKBP12-rapamycin-associated protein or mammalian target of rapamycin (FRAP/mTOR) localization in the endoplasmic reticulum and the Golgi apparatus. *Journal of Biological Chemistry,* 279, 772-778.

DREYER, H. C., GLYNN, E. L., LUJAN, H. L., FRY, C. S., DICARLO, S. E. & RASMUSSEN, B. B. 2008. Chronic paraplegia-induced muscle atrophy downregulates the mTOR/S6K1 signaling pathway. *Journal of applied physiology,* 104, 27-33.

DU, K. & MONTMINY, M. 1998. CREB is a regulatory target for the protein kinase Akt/PKB. *Journal of Biological Chemistry,* 273, 32377-32379.

DUFOUR, M., DORMOND-MEUWLY, A., DEMARTINES, N. & DORMOND, O. 2011. Targeting the Mammalian Target of Rapamycin (mTOR) in Cancer Therapy: Lessons from Past and Future Perspectives. *Cancers,* 3, 2478-500.

DUNN, J. D., REID, G. E. & BRUENING, M. L. 2010. Techniques for phosphopeptide enrichment prior to analysis by mass spectrometry. *Mass spectrometry reviews,* 29, 29-54.

EDGAR, W. M., DAWES, C. & O'MULLANE, D. M. 2004. *Saliva and oral health* [Online]. London: British Dental Association.

EFEYAN, A. & SABATINI, D. M. 2010. mTOR and cancer: many loops in one pathway. *Current opinion in cell biology,* 22, 169-76.

EMMELIN, N., GARRETT, J. & OHLIN, P. 1974. Secretory activity and the myoepithelial cells of salivary glands after duct ligation in cats. *Archives of oral biology,* 19, 275-283.

ENGELEN, L., VAN DEN KEYBUS, P. A., DE WIJK, R. A., VEERMAN, E. C., AMERONGEN, A. V. N., BOSMAN, F., PRINZ, J. F. & VAN DER BILT, A. 2007. The effect of saliva composition on texture perception of semi-solids. *Archives of oral biology,* 52, 518-525.

ENTESARIAN, M., MATSSON, H., KLAR, J., BERGENDAL, B., OLSON, L., ARAKAKI, R., HAYASHI, Y., OHUCHI, H., FALAHAT, B. & BOLSTAD, A. I. 2005. Mutations in the gene encoding fibroblast growth factor 10 are associated with aplasia of lacrimal and salivary glands. *Nature genetics,* 37, 125-128.

EPSTEIN, J. B. & HUHMANN, M. B. 2011. Dietary and nutritional needs of patients undergoing therapy for head and neck cancer. *Journal of the American Dental Association,* 142, 1163-7.

ETTL, T., SCHWARZ-FURLAN, S., HAUBNER, F., MULLER, S., ZENK, J., GOSAU, M., REICHERT, T. E. & ZEITLER, K. 2012. The PI3K/AKT/mTOR signalling pathway is active in salivary gland cancer and implies different functions and prognoses depending on cell localisation. *Oral oncology,* 48, 822-30.

FALLER, W. J., JACKSON, T. J., KNIGHT, J. R., RIDGWAY, R. A., JAMIESON, T., KARIM, S. A., JONES, C., RADULESCU, S., HUELS, D. J., MYANT, K. B., DUDEK, K. M., CASEY, H. A., SCOPELLITI, A., CORDERO, J. B., VIDAL, M., PENDE, M., RYAZANOV, A. G., SONENBERG, N., MEYUHAS, O., HALL, M. N., BUSHELL, M., WILLIS, A. E. & SANSOM, O. J. 2015. mTORC1-mediated translational elongation limits intestinal tumour initiation and growth. *Nature,* 517**,** 497-500.

FASOLD, M. & BINDER, H. 2012. Estimating RNA-quality using GeneChip microarrays. *BMC genomics,* 13**,** 186.

FEKETE, E. 1941. Histology In: Biology of the laboratory mouse. By Clarence C. Little, Director, George D. Snell, Editor, J. J. Bittner, A. M. Cloudman, E. Fekete, W. E. Heston, W. L. Russell, and G. W. Woolley 497 pages, 172 illustration. *The Anatomical Record,* 81**,** 137-141.

FELDMAN, M. E., APSEL, B., UOTILA, A., LOEWITH, R., KNIGHT, Z. A., RUGGERO, D. & SHOKAT, K. M. 2009. Active-site inhibitors of mTOR target rapamycin-resistant outputs of mTORC1 and mTORC2. *PLoS biology,* 7**,** e38.

FENG, J., VAN DER ZWAAG, M., STOKMAN, M. A., VAN OS, R. & COPPES, R. P. 2009. Isolation and characterization of human salivary gland cells for stem cell transplantation to reduce radiation-induced hyposalivation. *Radiotherapy and oncology : journal of the European Society for Therapeutic Radiology and Oncology,* 92**,** 466-71.

FERREIRA, T. & RASBAND, W. 2012. ImageJ User Guide.[online] 198 pp. *available at address:* http://rsbweb*.nih.gov/ij/docs/guide/user-guide. pdf.[7. 6. 2013]*.

FINGAR, D. C. & BLENIS, J. 2004. Target of rapamycin (TOR): an integrator of nutrient and growth factor signals and coordinator of cell growth and cell cycle progression. *Oncogene,* 23**,** 3151-71.

FINKEL, T. 2012. Relief with Rapamycin: mTOR Inhibition Protects against Radiation-Induced Mucositis. *Cell Stem Cell,* 11**,** 287-288.

FINN, R. D., BATEMAN, A., CLEMENTS, J., COGGILL, P., EBERHARDT, R. Y., EDDY, S. R., HEGER, A., HETHERINGTON, K., HOLM, L., MISTRY, J., SONNHAMMER, E. L., TATE, J. & PUNTA, M. 2014. Pfam: the protein families database. *Nucleic acids research,* 42**,** D222-30.

FOX, P. C. 1998. Acquired salivary dysfunction. Drugs and radiation. *Annals of the New York Academy of Sciences,* 842**,** 132-7.

FOX, P. C. 2003. Salivary enhancement therapies. *Caries research,* 38**,** 241-246.

FRUMAN, D. A. & ROMMEL, C. 2014. PI3K and cancer: lessons, challenges and opportunities. *Nature reviews. Drug discovery,* 13, 140-56.

GALLAGHER, M. P., KELLY, P. J., JARDINE, M., PERKOVIC, V., CASS, A., CRAIG, J. C., ERIS, J. & WEBSTER, A. C. 2010. Long-term cancer risk of immunosuppressive regimens after kidney transplantation. *Journal of the American Society of Nephrology : JASN,* 21, 852-8.

GALLO, A., MARTINI, D., SERNISSI, F., GIACOMELLI, C., PEPE, P., ROSSI, C., RIVEROS, P., MOSCA, M., ALEVIZOS, I. & BALDINI, C. 2013. Gross Cystic Disease Fluid Protein-15(GCDFP-15)/Prolactin-Inducible Protein (PIP) as Functional Salivary Biomarker for Primary Sjogren's Syndrome. *Journal of genetic syndromes & gene therapy,* 4.

GANGLOFF, Y.-G. L., MUELLER, M., DANN, S. G., SVOBODA, P., STICKER, M., SPETZ, J.-F., UM, S. H., BROWN, E. J., CEREGHINI, S. & THOMAS, G. 2004. Disruption of the mouse mTOR gene leads to early postimplantation lethality and prohibits embryonic stem cell development. *Molecular and cellular biology,* 24, 9508-9516.

GARCIA-CAZORLA, A., OYARZABAL, A., FORT, J., ROBLES, C., CASTEJON, E., RUIZ-SALA, P., BODOY, S., MERINERO, B., LOPEZ-SALA, A., DOPAZO, J., NUNES, V., UGARTE, M., ARTUCH, R., PALACIN, M., RODRIGUEZ-POMBO, P., ALCAIDE, P., NAVARRETE, R., SANZ, P., FONT-LLITJOS, M., VILASECA, M. A., ORMAIZABAL, A., PRISTOUPILOVA, A. & AGULLO, S. B. 2014. Two novel mutations in the BCKDK (branched-chain keto-acid dehydrogenase kinase) gene are responsible for a neurobehavioral deficit in two pediatric unrelated patients. *Human mutation,* 35, 470-7.

GARRETT, J. R., EKSTRÖM, J. & ANDERSON, L. C. 1999. *Neural mechanisms of salivary gland secretion,* Basel ; London, Karger.

GHAFOURI, B., TAGESSON, C. & LINDAHL, M. 2003. Mapping of proteins in human saliva using two,Äêdimensional gel electrophoresis and peptide mass fingerprinting. *Proteomics,* 3, 1003-1015.

GHARAGOZLOO, M., JAVID, E. N., REZAEI, A. & MOUSAVIZADEH, K. 2013. Silymarin inhibits cell cycle progression and mTOR activity in activated human T cells: therapeutic implications for autoimmune diseases. *Basic & clinical pharmacology & toxicology,* 112, 251-6.

GHIGO, A., DAMILANO, F., BRACCINI, L. & HIRSCH, E. 2010. PI3K inhibition in inflammation: Toward tailored therapies for specific diseases. *Bioessays,* 32, 185-196.

GIACCONE, G. & SORIA, J.-C. 2014. *Targeted therapies in oncology,* New York, Informa health care.

GIBBINS, H. & CARPENTER, G. 2013. Alternative mechanisms of astringency - What is the role of saliva? *Journal of Texture Studies,* 44, 364-375.

GIBBINS, H. L., PROCTOR, G. B., YAKUBOV, G. E., WILSON, S. & CARPENTER, G. H. 2014. Concentration of salivary protective proteins within the bound oral mucosal pellicle. *Oral diseases,* 20, 707-13.

GINGRAS, A.-C., GYGI, S. P., RAUGHT, B., POLAKIEWICZ, R. D., ABRAHAM, R. T., HOEKSTRA, M. F., AEBERSOLD, R. & SONENBERG, N. 1999a. Regulation of 4E-BP1 phosphorylation: a novel two-step mechanism. *Genes & development,* 13, 1422-1437.

GINGRAS, A.-C., RAUGHT, B. & SONENBERG, N. 2001a. Regulation of translation initiation by FRAP/mTOR. *Genes & development,* 15, 807-826.

GINGRAS, A. C., RAUGHT, B., GYGI, S. P., NIEDZWIECKA, A., MIRON, M., BURLEY, S. K., POLAKIEWICZ, R. D., WYSLOUCH-CIESZYNSKA, A., AEBERSOLD, R. & SONENBERG, N. 2001b. Hierarchical phosphorylation of the translation inhibitor 4E-BP1. *Genes & development,* 15, 2852-64.

GINGRAS, A. C., RAUGHT, B. & SONENBERG, N. 1999b. eIF4 initiation factors: effectors of mRNA recruitment to ribosomes and regulators of translation. *Annual review of biochemistry,* 68, 913-63.

GRESIK, E. W. 1994. The granular convoluted tubule (GCT) cell of rodent submandibular glands. *Microscopy research and technique,* 27, 1-24.

GRESIK, E. W. & MACRAE, E. K. 1975. The postnatal development of the sexually dimorphic duct system and of amylase activity in the submandibular glands of mice. *Cell and tissue research,* 157, 411-422.

GRZMIL, M., HUBER, R. M., HESS, D., FRANK, S., HYNX, D., MONCAYO, G., KLEIN, D., MERLO, A. & HEMMINGS, B. A. 2014. MNK1 pathway activity maintains protein synthesis in rapalog-treated gliomas. *The Journal of clinical investigation,* 124, 742.

GUERTIN, D. A. & SABATINI, D. M. 2005. An expanding role for mTOR in cancer. *Trends in molecular medicine,* 11, 353-61.

GUERTIN, D. A. & SABATINI, D. M. 2007. Defining the role of mTOR in cancer. *Cancer cell,* 12, 9-22.

GUERTIN, D. A. & SABATINI, D. M. 2009. The pharmacology of mTOR inhibition. *Science signaling,* 2, pe24.

GUERTIN, D. A., STEVENS, D. M., SAITOH, M., KINKEL, S., CROSBY, K., SHEEN, J.-H., MULLHOLLAND, D. J., MAGNUSON, M. A., WU, H. & SABATINI, D. M. 2009. mTOR complex 2 is required for the development of prostate cancer induced by Pten loss in mice. *Cancer cell,* 15, 148-159.

GUERTIN, D. A., STEVENS, D. M., THOREEN, C. C., BURDS, A. A., KALAANY, N. Y., MOFFAT, J., BROWN, M., FITZGERALD, K. J. & SABATINI, D. M. 2006. Ablation in mice of the mTORC components raptor, rictor, or mLST8 reveals that mTORC2 is required for signaling to Akt-FOXO and PKCalpha, but not S6K1. *Developmental cell,* 11, 859-871.

GUYTON, A. & HALL, J. 2006. Textbook of medical physiology, 11th.

HALL, E. J. & WUU, C. S. 2003. Radiation-induced second cancers: the impact of 3D-CRT and IMRT. *International journal of radiation oncology, biology, physics,* 56, 83-8.

HAMILTON, W. J., BOYD, J. D. & MOSSMAN, H. W. 1945. Human embryology (prenatal development of form and function). *Human embryology (prenatal development of form and function).*

HAMPERL, H. 1931. Beitrage zur normalen und pathologischen Histologie menschlicher Speicheldrusen. *Z Mikrosk Anat Forsch,* 27.

HANDS, S. L., PROUD, C. G. & WYTTENBACH, A. 2009. mTOR's role in ageing: protein synthesis or autophagy? *Aging,* 1, 586-97.

HANNAN, K. M., BRANDENBURGER, Y., JENKINS, A., SHARKEY, K., CAVANAUGH, A., ROTHBLUM, L., MOSS, T., POORTINGA, G., MCARTHUR, G. A. & PEARSON, R. B. 2003. mTOR-dependent regulation of ribosomal gene transcription requires S6K1 and is mediated by phosphorylation of the carboxy-terminal activation domain of the nucleolar transcription factor UBF. *Molecular and cellular biology,* 23, 8862-8877.

HARRINGTON, L. S., FINDLAY, G. M., GRAY, A., TOLKACHEVA, T., WIGFIELD, S., REBHOLZ, H., BARNETT, J., LESLIE, N. R., CHENG, S., SHEPHERD, P. R., GOUT, I., DOWNES, C. P. & LAMB, R. F. 2004. The TSC1-2 tumor suppressor controls insulin-PI3K signaling via regulation of IRS proteins. *The Journal of cell biology,* 166, 213-23.

HARRISON, D. E., STRONG, R., SHARP, Z. D., NELSON, J. F., ASTLE, C. M., FLURKEY, K., NADON, N. L., WILKINSON, J. E., FRENKEL, K., CARTER, C. S., PAHOR, M., JAVORS, M. A., FERNANDEZ, E. &

MILLER, R. A. 2009. Rapamycin fed late in life extends lifespan in genetically heterogeneous mice. *Nature,* 460, 392-5.
HARRISON, J., FOUAD, H. & GARRETT, J. 2001. Variation in the response to ductal obstruction of feline submandibular and sublingual salivary glands and the importance of the innervation. *Journal of oral pathology & medicine,* 30, 29-34.
HARRISON, J. & GARRETT, J. 1976. Histological effects of ductal ligation of salivary glands of the cat. *The Journal of pathology,* 118, 245-254.
HARRISON, J. D., FOUAD, H. M. & GARRETT, J. R. 2000. The effects of ductal obstruction on the acinar cells of the parotid of cat. *Archives of oral biology,* 45, 945-9.
HARTLEY, D. & COOPER, G. M. 2002. Role of mTOR in the degradation of IRS-1: regulation of PP2A activity. *Journal of cellular biochemistry,* 85, 304-14.
HAY, N. & SONENBERG, N. 2004. Upstream and downstream of mTOR. *Genes & development,* 18, 1926-45.
HAYASHI, M., TAPPING, R. I., CHAO, T.-H., LO, J.-F., KING, C. C., YANG, Y. & LEE, J.-D. 2001. BMK1 mediates growth factor-induced cell proliferation through direct cellular activation of serum and glucocorticoid-inducible kinase. *Journal of Biological Chemistry,* 276, 8631-8634.
HE, C. & KLIONSKY, D. J. 2009. Regulation mechanisms and signaling pathways of autophagy. *Annual review of genetics,* 43, 67.
HILL, G., HEADON, D., HARRIS, Z. I., HUTTNER, K. & LIMESAND, K. H. 2014. Pharmacological activation of the EDA/EDAR signaling pathway restores salivary gland function following radiation-induced damage. *PloS one,* 9, e112840.
HIRAMATSU, M., KASHIMATA, M., TAKAYAMA, F. & MINAMI, N. 1994. Developmental changes in and hormonal modulation of epidermal growth factor concentration in the rat submandibular gland. *Journal of endocrinology,* 140, 357-363.
HIRAYAMA, M., OGAWA, M., OSHIMA, M., SEKINE, Y., ISHIDA, K., YAMASHITA, K., IKEDA, K., SHIMMURA, S., KAWAKITA, T., TSUBOTA, K. & TSUJI, T. 2013. Functional lacrimal gland regeneration by transplantation of a bioengineered organ germ. *Nature communications,* 4, 2497.
HOFFMAN, M. P., KIDDER, B. L., STEINBERG, Z. L., LAKHANI, S., HO, S., KLEINMAN, H. K. & LARSEN, M. 2002. Gene expression profiles of mouse submandibular gland development: FGFR1 regulates branching morphogenesis in vitro through BMP-and FGF-dependent mechanisms. *Development,* 129, 5767-5778.

HOFFMANN, P., OLAYIOYE, M. A., MORITZ, R. L., LINDEMAN, G. J., VISVADER, J. E., SIMPSON, R. J. & KEMP, B. E. 2005. Breast cancer protein StarD10 identified by three-dimensional separation using free-flow electrophoresis, reversed-phase high-performance liquid chromatography, and sodium dodecyl sulfate-polyacrylamide gel electrophoresis. *Electrophoresis,* 26, 1029-1037.

HOGAN, B. L. 1999. Morphogenesis. *Cell,* 96, 225-233.

HOLLINSHEAD, W. H. 1982. *Anatomy for surgeons. 1, 1,* New York u.a., Harper & Row.

HOSOI, K., KOBAYASHI, S. & UEHA, T. 1978. Sex difference in L-glutamine D-fructose-6-phosphate aminotransferase activity of mouse submandibular gland. *Biochimica et biophysica acta,* 543, 283-92.

HOSOKAWA, N., HARA, T., KAIZUKA, T., KISHI, C., TAKAMURA, A., MIURA, Y., IEMURA, S.-I., NATSUME, T., TAKEHANA, K. & YAMADA, N. 2009. Nutrient-dependent mTORC1 Association with the ULK1–Atg13–FIP200 Complex Required for Autophagy. *Molecular biology of the cell,* 20, 1981-1991.

HOU, J., LAM, F., PROUD, C. & WANG, S. 2012. Targeting Mnks for cancer therapy. *Oncotarget,* 3, 118.

HU, L., HOFMANN, J., LU, Y., MILLS, G. B. & JAFFE, R. B. 2002. Inhibition of phosphatidylinositol 3'-kinase increases efficacy of paclitaxel in in vitro and in vivo ovarian cancer models. *Cancer research,* 62, 1087-92.

HU, Y. 2015. The necessary role of mTORC1 in central nervous system axon regeneration. *Neural Regen Res,* 10, 186-8.

HUANG, J., DIBBLE, C. C., MATSUZAKI, M. & MANNING, B. D. 2008. The TSC1-TSC2 complex is required for proper activation of mTOR complex 2. *Molecular and cellular biology,* 28, 4104-4115.

HUANG, S. & HOUGHTON, P. J. 2001. Mechanisms of resistance to rapamycins. *Drug Resistance Updates,* 4, 378-391.

HUBERT, T., WU, Z., CHISHOLM, A. D. & JIN, Y. 2014. S6 kinase inhibits intrinsic axon regeneration capacity via AMP kinase in Caenorhabditis elegans. *J Neurosci,* 34, 758-63.

HUMPHREY, S. P. & WILLIAMSON, R. T. 2001. A review of saliva: normal composition, flow, and function. *The Journal of prosthetic dentistry,* 85, 162-9.

HURLIMANN, J. & ZUBER, C. 1969. Vitamin B12-binders in human body fluids. I. Antigenic and physico-chemical characteristics. *Clinical and experimental immunology,* 4, 125-40.

IGLESIAS-BARTOLOME, R., PATEL, V., COTRIM, A., LEELAHAVANICHKUL, K., MOLINOLO, A. A., MITCHELL, J. B. & GUTKIND, J. S. 2012. mTOR inhibition prevents epithelial stem cell senescence and protects from radiation-induced mucositis. *Cell Stem Cell,* 11, 401-414.

IMANGULI, M. M., ATKINSON, J. C., HARVEY, K. E., HOEHN, G. T., RYU, O. H., WU, T., KINGMAN, A., BARRETT, A. J., BISHOP, M. R., CHILDS, R. W., FOWLER, D. H., PAVLETIC, S. Z. & HART, T. C. 2007. Changes in salivary proteome following allogeneic hematopoietic stem cell transplantation. *Experimental hematology,* 35, 184-92.

INOKI, K., CORRADETTI, M. N. & GUAN, K. L. 2005. Dysregulation of the TSC-mTOR pathway in human disease. *Nature genetics,* 37, 19-24.

INOKI, K., LI, Y., XU, T. & GUAN, K.-L. 2003. Rheb GTPase is a direct target of TSC2 GAP activity and regulates mTOR signaling. *Genes & development,* 17, 1829-1834.

INOKI, K., LI, Y., ZHU, T., WU, J. & GUAN, K.-L. 2002. TSC2 is phosphorylated and inhibited by Akt and suppresses mTOR signalling. *Nature cell biology,* 4, 648-657.

INOKI, K., OUYANG, H., ZHU, T., LINDVALL, C., WANG, Y., ZHANG, X., YANG, Q., BENNETT, C., HARADA, Y., STANKUNAS, K., WANG, C. Y., HE, X., MACDOUGALD, O. A., YOU, M., WILLIAMS, B. O. & GUAN, K. L. 2006. TSC2 integrates Wnt and energy signals via a coordinated phosphorylation by AMPK and GSK3 to regulate cell growth. *Cell,* 126, 955-68.

INOUE, H., ONO, K., MASUDA, W., INAGAKI, T., YOKOTA, M. & INENAGA, K. 2008. Rheological properties of human saliva and salivary mucins. *Journal of Oral Biosciences,* 50, 134-141.

ISEMURA, S., SAITOH, E., ITO, S., ISEMURA, M. & SANADA, K. 1984. Cystatin S: a cysteine proteinase inhibitor of human saliva. *Journal of biochemistry,* 96, 1311-4.

ISOLA, M., CABRAS, T., INZITARI, R., LANTINI, M. S., PROTO, E., COSSU, M. & RIVA, A. 2008. Electron microscopic detection of statherin in secretory granules of human major salivary glands. *Journal of anatomy,* 212, 664-8.

ISOTANI, S., HARA, K., TOKUNAGA, C., INOUE, H., AVRUCH, J. & YONEZAWA, K. 1999. Immunopurified mammalian target of rapamycin phosphorylates and activates p70 S6 kinase Œ± in vitro. *Journal of Biological Chemistry,* 274, 34493-34498.

JANSMA, J., VISSINK, A., SPIJKERVET, F. K., ROODENBURG, J. L., PANDERS, A. K., VERMEY, A., SZABO, B. G. & GRAVENMADE, E. J.

1992. Protocol for the prevention and treatment of oral sequelae resulting from head and neck radiation therapy. *Cancer,* 70, 2171-80.

JASKOLL, T., ABICHAKER, G., WITCHER, D., SALA, F. G., BELLUSCI, S., HAJIHOSSEINI, M. K. & MELNICK, M. 2005. FGF10/FGFR2b signaling plays essential roles during in vivo embryonic submandibular salivary gland morphogenesis. *BMC developmental biology,* 5, 11.

JASKOLL, T., ZHOU, Y. M., CHAI, Y., MAKARENKOVA, H. P., COLLINSON, J. M., WEST, J. D., HAJIHOSSEINI, M. K., LEE, J. & MELNICK, M. 2002. Embryonic submandibular gland morphogenesis: stage-specific protein localization of FGFs, BMPs, Pax6 and Pax9 in normal mice and abnormal SMG phenotypes in FgfR2-IIIc(+/Delta), BMP7(-/-) and Pax6(-/-) mice. *Cells, tissues, organs,* 170, 83-98.

JEMAL, A., BRAY, F., CENTER, M. M., FERLAY, J., WARD, E. & FORMAN, D. 2011. Global cancer statistics. *CA: a cancer journal for clinicians,* 61, 69-90.

JENSEN, S. B., PEDERSEN, A. M., VISSINK, A., ANDERSEN, E., BROWN, C. G., DAVIES, A. N., DUTILH, J., FULTON, J. S., JANKOVIC, L., LOPES, N. N., MELLO, A. L., MUNIZ, L. V., MURDOCH-KINCH, C. A., NAIR, R. G., NAPENAS, J. J., NOGUEIRA-RODRIGUES, A., SAUNDERS, D., STIRLING, B., VON BULTZINGSLOWEN, I., WEIKEL, D. S., ELTING, L. S., SPIJKERVET, F. K. & BRENNAN, M. T. 2010. A systematic review of salivary gland hypofunction and xerostomia induced by cancer therapies: management strategies and economic impact. *Supportive care in cancer : official journal of the Multinational Association of Supportive Care in Cancer,* 18, 1061-79.

JOHNSON, R. A., WANG, X., MA, X. L., HUONG, S. M. & HUANG, E. S. 2001. Human cytomegalovirus up-regulates the phosphatidylinositol 3-kinase (PI3-K) pathway: inhibition of PI3-K activity inhibits viral replication and virus-induced signaling. *Journal of virology,* 75, 6022-32.

JOHNSON, S. C., RABINOVITCH, P. S. & KAEBERLEIN, M. 2013. mTOR is a key modulator of ageing and age-related disease. *Nature,* 493, 338-345.

JUNG, C. H., JUN, C. B., RO, S.-H., KIM, Y.-M., OTTO, N. M., CAO, J., KUNDU, M. & KIM, D.-H. 2009. ULK-Atg13-FIP200 complexes mediate mTOR signaling to the autophagy machinery. *Molecular biology of the cell,* 20, 1992-2003.

JUNG, C. H., RO, S. H., CAO, J., OTTO, N. M. & KIM, D. H. 2010. mTOR regulation of autophagy. *FEBS letters,* 584, 1287-95.

KAIZUKA, T., HARA, T., OSHIRO, N., KIKKAWA, U., YONEZAWA, K., TAKEHANA, K., IEMURA, S., NATSUME, T. & MIZUSHIMA, N. 2010. Tti1 and Tel2 are critical factors in mammalian target of rapamycin complex assembly. *The Journal of biological chemistry,* 285, 20109-16.

KAMADA, Y., SEKITO, T. & OHSUMI, Y. 2004. Autophagy in Yeast: ATOR-Mediated Response to Nutrient Starvation. *TOR.* Springer.

KANG, S., ELF, S., LYTHGOE, K., HITOSUGI, T., TAUNTON, J., ZHOU, W., XIONG, L., WANG, D., MULLER, S., FAN, S., SUN, S. Y., MARCUS, A. I., GU, T. L., POLAKIEWICZ, R. D., CHEN, Z. G., KHURI, F. R., SHIN, D. M. & CHEN, J. 2010. p90 ribosomal S6 kinase 2 promotes invasion and metastasis of human head and neck squamous cell carcinoma cells. *The Journal of clinical investigation,* 120, 1165-77.

KAPUY, O., VINOD, P. K. & BANHEGYI, G. 2014. mTOR inhibition increases cell viability via autophagy induction during endoplasmic reticulum stress - An experimental and modeling study. *FEBS open bio,* 4, 704-13.

KIM, K., LI, L., KOZLOWSKI, K., SUH, H.-S., CAO, W. & BALLERMANN, B. J. 2005. The protein phosphatase-1 targeting subunit TIMAP regulates LAMR1 phosphorylation. *Biochemical and biophysical research communications,* 338, 1327-1334.

KIM, K. W., MYERS, C. J., JUNG, D. K. & LU, B. 2014. NVP-BEZ-235 enhances radiosensitization via blockade of the PI3K/mTOR pathway in cisplatin-resistant non-small cell lung carcinoma. *Genes & cancer,* 5, 293.

KIM, M., PARK, H. L., PARK, H.-W., RO, S.-H., NAM, S. G., REED, J. M., GUAN, J.-L. & LEE, J. H. 2013. Drosophila Fip200 is an essential regulator of autophagy that attenuates both growth and aging. *Autophagy,* 9, 1201-1213.

KIVELA, J., PARKKILA, S., PARKKILA, A. K., LEINONEN, J. & RAJANIEMI, H. 1999. Salivary carbonic anhydrase isoenzyme VI. *The Journal of physiology,* 520 Pt 2, 315-20.

KLIONSKY, D. J. 2003. *Autophagy,* Georgetown, Landes Bioscience.

KLIONSKY, D. J. 2009. *Autophagy in disease and clinical applications. Part C Part C,* Amsterdam, Elsevier/Academic Press.

KLIONSKY, D. J., ABDALLA, F. C., ABELIOVICH, H., ABRAHAM, R. T., ACEVEDO-AROZENA, A., ADELI, K., AGHOLME, L., AGNELLO, M., AGOSTINIS, P. & AGUIRRE-GHISO, J. A. 2012. Guidelines for the use and interpretation of assays for monitoring autophagy. *Autophagy,* 8, 445-544.

KLIONSKY, D. J., ABDALLA FC FAU - ABELIOVICH, H., ABELIOVICH H FAU - ABRAHAM, R. T., ABRAHAM RT FAU - ACEVEDO-AROZENA, A., ACEVEDO-AROZENA A FAU - ADELI, K., ADELI K FAU - AGHOLME, L., AGHOLME L FAU - AGNELLO, M., AGNELLO M FAU - AGOSTINIS, P., AGOSTINIS P FAU - AGUIRRE-GHISO, J. A., AGUIRRE-GHISO JA FAU - AHN, H. J., AHN HJ FAU - AIT-MOHAMED, O., AIT-MOHAMED O FAU - AIT-SI-ALI, S., AIT-SI-ALI S FAU - AKEMATSU, T., AKEMATSU T FAU - AKIRA, S., AKIRA S FAU - AL-YOUNES, H. M., AL-YOUNES HM FAU - AL-ZEER, M. A., AL-ZEER MA FAU - ALBERT, M. L., ALBERT ML FAU - ALBIN, R. L., ALBIN RL FAU - ALEGRE-ABARRATEGUI, J., ALEGRE-ABARRATEGUI J FAU - ALEO, M. F., ALEO MF FAU - ALIREZAEI, M., ALIREZAEI M FAU - ALMASAN, A., ALMASAN A FAU - ALMONTE-BECERRIL, M., ALMONTE-BECERRIL M FAU - AMANO, A., AMANO A FAU - AMARAVADI, R., AMARAVADI R FAU - AMARNATH, S., AMARNATH S FAU - AMER, A. O., AMER AO FAU - ANDRIEU-ABADIE, N., ANDRIEU-ABADIE N FAU - ANANTHARAM, V., ANANTHARAM V FAU - ANN, D. K., ANN DK FAU - ANOOPKUMAR-DUKIE, S., ANOOPKUMAR-DUKIE S FAU - AOKI, H., AOKI H FAU - APOSTOLOVA, N., APOSTOLOVA N FAU - ARANCIA, G., ARANCIA G FAU - ARIS, J. P., ARIS JP FAU - ASANUMA, K., ASANUMA K FAU - ASARE, N. Y. O., ASARE NY FAU - ASHIDA, H., ASHIDA H FAU - ASKANAS, V., ASKANAS V FAU - ASKEW, D. S., ASKEW DS FAU - AUBERGER, P., AUBERGER P FAU - BABA, M., BABA M FAU - BACKUES, S. K., BACKUES SK FAU - BAEHRECKE, E. H., BAEHRECKE EH FAU - BAHR, B. A., BAHR BA FAU - BAI, X.-Y., BAI XY FAU - BAILLY, Y., BAILLY Y FAU - BAIOCCHI, R., BAIOCCHI R FAU - BALDINI, G., BALDINI G FAU - BALDUINI, W., BALDUINI W FAU - BALLABIO, A., BALLABIO A FAU - BAMBER, B. A., BAMBER BA FAU - BAMPTON, E. T. W., BAMPTON ET FAU - BANHEGYI, G., BANHEGYI G FAU - BARTHOLOMEW, C. R., BARTHOLOMEW CR FAU - BASSHAM, D. C., BASSHAM DC FAU - BAST, R. C., JR., BAST RC JR FAU - BATOKO, H., BATOKO H FAU - BAY, B.-H., BAY BH FAU - BEAU, I., BEAU I FAU - BECHET, D. M., BECHET DM FAU - BEGLEY, T. J., BEGLEY TJ FAU - BEHL, C., BEHL C FAU - BEHRENDS, C., BEHRENDS C FAU - BEKRI, S., BEKRI S FAU - BELLAIRE, B., BELLAIRE B FAU - BENDALL, L. J., BENDALL LJ FAU - BENETTI, L., BENETTI L FAU - BERLIOCCHI, L., BERLIOCCHI L FAU - BERNARDI, H., BERNARDI H FAU - BERNASSOLA, F., BERNASSOLA F FAU - BESTEIRO, S., BESTEIRO S FAU - BHATIA-KISSOVA, I., BHATIA-KISSOVA I FAU - BI, X., BI X FAU - BIARD-PIECHACZYK, M., BIARD-PIECHACZYK M

FAU - BLUM, J. S., BLUM JS FAU - BOISE, L. H., BOISE LH FAU - BONALDO, P., BONALDO P FAU - BOONE, D. L., BOONE DL FAU - BORNHAUSER, B. C., BORNHAUSER BC FAU - BORTOLUCI, K. R., BORTOLUCI KR FAU - BOSSIS, I., BOSSIS I FAU - BOST, F., BOST F FAU - BOURQUIN, J.-P., BOURQUIN JP FAU - BOYA, P., BOYA P FAU - BOYER-GUITTAUT, M., BOYER-GUITTAUT M FAU - BOZHKOV, P. V., BOZHKOV PV FAU - BRADY, N. R., BRADY NR FAU - BRANCOLINI, C., BRANCOLINI C FAU - BRECH, A., BRECH A FAU - BRENMAN, J. E., BRENMAN JE FAU - BRENNAND, A., BRENNAND A FAU - BRESNICK, E. H., BRESNICK EH FAU - BREST, P., BREST P FAU - BRIDGES, D., BRIDGES D FAU - BRISTOL, M. L., BRISTOL ML FAU - BROOKES, P. S., BROOKES PS FAU - BROWN, E. J., BROWN EJ FAU - BRUMELL, J. H., BRUMELL JH FAU - BRUNETTI-PIERRI, N., et al. 2008. Guidelines for the use and interpretation of assays for monitoring autophagy in higher eukaryotes. *Autophagy,* 4**,** 151-175.

KOFFEL, R., MESHCHERYAKOVA, A., WARSZAWSKA, J., HENNIG, A., WAGNER, K., JORGL, A., GUBI, D., MOSER, D., HLADIK, A., HOFFMANN, U., FISCHER, M. B., VAN DEN BERG, W., KOENDERS, M., SCHEINECKER, C., GESSLBAUER, B., KNAPP, S. & STROBL, H. 2014. Monocytic cell differentiation from band-stage neutrophils under inflammatory conditions via MKK6 activation. *Blood,* 124**,** 2713-24.

KOJIMA, T., KANEMARU, S., HIRANO, S., TATEYA, I., OHNO, S., NAKAMURA, T. & ITO, J. 2011. Regeneration of radiation damaged salivary glands with adipose-derived stromal cells. *The Laryngoscope,* 121**,** 1864-9.

KONINGS, A. W., COTTELEER, F., FABER, H., VAN LUIJK, P., MEERTENS, H. & COPPES, R. P. 2005. Volume effects and region-dependent radiosensitivity of the parotid gland. *International journal of radiation oncology, biology, physics,* 62**,** 1090-5.

KROEMER, G., MARINO, G. & LEVINE, B. 2010. Autophagy and the integrated stress response. *Molecular cell,* 40**,** 280-293.

KUDCHODKAR, S. B., YU, Y., MAGUIRE, T. G. & ALWINE, J. C. 2004. Human cytomegalovirus infection induces rapamycin-insensitive phosphorylation of downstream effectors of mTOR kinase. *Journal of virology,* 78**,** 11030-9.

KUO, C. J., CHUNG, J., FIORENTINO, D. F., FLANAGAN, W. M., BLENIS, J. & CRABTREE, G. R. 1992. Rapamycin selectively inhibits interleukin-2 activation of p70 S6 kinase. *Nature,* 358**,** 70-73.

LAMBOTTE, L., SALIEZ, A., TRIEST, S., MAITER, D., BARANSKI, A., BARKER, A. & LI, B. 1997. Effect of sialoadenectomy and

epidermal growth factor administration on liver regeneration after partial hepatectomy. *Hepatology,* 25, 607-612.
LAMMING, D. W. & SABATINI, D. M. 2010. *The Enzymes*
Chapter 2 – Regulation of TOR Signaling in Mammals.
LAPLANTE, M. & SABATINI, D. M. 2009. An emerging role of mTOR in lipid biosynthesis. *Current biology : CB,* 19, R1046-52.
LAPLANTE, M. & SABATINI, D. M. 2012. mTOR signaling in growth control and disease. *Cell,* 149, 274-93.
LARSEN, M., HOFFMAN, M. P., SAKAI, T., NEIBAUR, J. C., MITCHELL, J. M. & YAMADA, K. M. 2003. Role of PI 3-kinase and PIP3 in submandibular gland branching morphogenesis. *Dev Biol,* 255, 178-91.
LEE, C. C., HUANG, C. C., WU, M. Y. & HSU, K. S. 2005. Insulin stimulates postsynaptic density-95 protein translation via the phosphoinositide 3-kinase-Akt-mammalian target of rapamycin signaling pathway. *The Journal of biological chemistry,* 280, 18543-50.
LEE, M., THEODOROPOULOU, M., GRAW, J., RONCAROLI, F., ZATELLI, M. C. & PELLEGATA, N. S. 2011. Levels of p27 sensitize to dual PI3K/mTOR inhibition. *Molecular cancer therapeutics,* 10, 1450-9.
LEINONEN, J., PARKKILA, S., KAUNISTO, K., KOIVUNEN, P. & RAJANIEMI, H. 2001. Secretion of carbonic anhydrase isoenzyme VI (CA VI) from human and rat lingual serous von Ebner's glands. *The journal of histochemistry and cytochemistry : official journal of the Histochemistry Society,* 49, 657-62.
LEONE, M., CROWELL, K. J., CHEN, J., JUNG, D., CHIANG, G. G., SARETH, S., ABRAHAM, R. T. & PELLECCHIA, M. 2006. The FRB domain of mTOR: NMR solution structure and inhibitor design. *Biochemistry,* 45, 10294-302.
LEVI-MONTALCINI, R. & ANGELETTI, P. U. 1964. Hormonal Control of the Ngf Content in the Submaxillary Glands of Mice. *International series of monographs on oral biology,* 3, 129-41.
LEVINE, M. J. 1993. Salivary macromolecules. A structure/function synopsis. *Annals of the New York Academy of Sciences,* 694, 11-6.
LI, C. & WONG, W. H. 2001. Model-based analysis of oligonucleotide arrays: expression index computation and outlier detection. *Proceedings of the National Academy of Sciences of the United States of America,* 98, 31-6.
LI, J.-R., CHENG, C.-L., YANG, C.-R., OU, Y.-C., WU, M.-J. & KO, J.-L. 2013. Dual inhibitor of phosphoinositide 3-kinase/mammalian target of rapamycin NVP-BEZ235 effectively inhibits cisplatin-resistant

urothelial cancer cell growth through autophagic flux. *Toxicology letters,* 220, 267-276.

LIGTENBERG, A. J. M. & VEERMAN, E. C. I. 2014. *Saliva : secretion and functions,* Amsterdam, Karger.

LIM, J. Y., YI, T., CHOI, J. S., JANG, Y. H., LEE, S., KIM, H. J., SONG, S. U. & KIM, Y. M. 2013. Intraglandular transplantation of bone marrow-derived clonal mesenchymal stem cells for amelioration of post-irradiation salivary gland damage. *Oral oncology,* 49, 136-43.

LIU, Q., CHANG, J. W., WANG, J., KANG, S. A., THOREEN, C. C., MARKHARD, A., HUR, W., ZHANG, J., SIM, T. & SABATINI, D. M. 2010. Discovery of 1-(4-(4-propionylpiperazin-1-yl)-3-(trifluoromethyl) phenyl)-9-(quinolin-3-yl) benzo [h][1, 6] naphthyridin-2 (1 H)-one as a highly potent, selective mammalian target of rapamycin (mTOR) inhibitor for the treatment of cancer. *Journal of medicinal chemistry,* 53, 7146-7155.

LIU, X. & ZHENG, X. S. 2007. Endoplasmic reticulum and Golgi localization sequences for mammalian target of rapamycin. *Molecular biology of the cell,* 18, 1073-1082.

LIU, Y., VERTOMMEN, D., RIDER, M. H. & LAI, Y. C. 2013. Mammalian target of rapamycin-independent S6K1 and 4E-BP1 phosphorylation during contraction in rat skeletal muscle. *Cellular signalling,* 25, 1877-86.

LOMBAERT, I. M., BRUNSTING, J. F., WIERENGA, P. K., FABER, H., STOKMAN, M. A., KOK, T., VISSER, W. H., KAMPINGA, H. H., DE HAAN, G. & COPPES, R. P. 2008. Rescue of salivary gland function after stem cell transplantation in irradiated glands. *PloS one,* 3, e2063.

LOMBAERT, I. M., KNOX, S. M. & HOFFMAN, M. P. 2011. Salivary gland progenitor cell biology provides a rationale for therapeutic salivary gland regeneration. *Oral diseases,* 17, 445-9.

LOO, B. B., DARWISH, K. K., VAINIKKA, S. S., SAARIKETTU, J. J., VIHKO, P. P., HERMONEN, J. J., GOLDMAN, A. A., ALITALO, K. K. & JALKANEN, M. M. 2000. Production and characterization of the extracellular domain of recombinant human fibroblast growth factor receptor 4. *The international journal of biochemistry & cell biology,* 32, 489-97.

LYNCH, C. J. 2001. Role of leucine in the regulation of mTOR by amino acids: revelations from structure,Äìactivity studies. *The Journal of nutrition,* 131, 861S-865S.

LYNCH, C. J., FOX, H. L., VARY, T. C., JEFFERSON, L. S. & KIMBALL, S. R. 2000. Regulation of amino acid-sensitive TOR signaling by

leucine analogues in adipocytes. *Journal of cellular biochemistry,* 77, 234-51.

LYNCH, C. J., HALLE, B., FUJII, H., VARY, T. C., WALLIN, R., DAMUNI, Z. & HUTSON, S. M. 2003. Potential role of leucine metabolism in the leucine-signaling pathway involving mTOR. *American journal of physiology. Endocrinology and metabolism,* 285, E854-63.

LYNGE PEDERSEN, A. M., NAUNTOFTE, B., SMIDT, D. & TORPET, L. A. 2015. Oral mucosal lesions in older people: relation to salivary secretion, systemic diseases and medications. *Oral Diseases,* 21, 721-729.

MA, L., GAO, C., MAO, Z., ZHOU, J., SHEN, J., HU, X. & HAN, C. 2003. Collagen/chitosan porous scaffolds with improved biostability for skin tissue engineering. *Biomaterials,* 24, 4833-41.

MAIRA, S. M., STAUFFER, F., BRUEGGEN, J., FURET, P., SCHNELL, C., FRITSCH, C., BRACHMANN, S., CHENE, P., DE POVER, A., SCHOEMAKER, K., FABBRO, D., GABRIEL, D., SIMONEN, M., MURPHY, L., FINAN, P., SELLERS, W. & GARCIA-ECHEVERRIA, C. 2008. Identification and characterization of NVP-BEZ235, a new orally available dual phosphatidylinositol 3-kinase/mammalian target of rapamycin inhibitor with potent in vivo antitumor activity. *Molecular cancer therapeutics,* 7, 1851-63.

MAJESKI, A. E. & DICE, J. F. 2004. Mechanisms of chaperone-mediated autophagy. *The international journal of biochemistry & cell biology,* 36, 2435-2444.

MARTELLI, A. M., EVANGELISTI, C., CHAPPELL, W., ABRAMS, S. L., BASECKE, J., STIVALA, F., DONIA, M., FAGONE, P., NICOLETTI, F., LIBRA, M., RUVOLO, V., RUVOLO, P., KEMPF, C. R., STEELMAN, L. S. & MCCUBREY, J. A. 2011. Targeting the translational apparatus to improve leukemia therapy: roles of the PI3K/PTEN/Akt/mTOR pathway. *Leukemia,* 25, 1064-79.

MARTINEZ, J., BYLUND, D. & CASSITY, N. 1982. Progressive secretory dysfunction in the rat submandibular gland after excretory duct ligation. *Archives of oral biology,* 27, 443-450.

MARTINEZ, J. M., PULIDO, L. B., BELLIDO, C. B., USERO, D. D., AGUILAR, L. T., MORENO, J. L., ARTACHO, G. S., DIEZ-CANEDO, J. S., GOMEZ, L. M. & BRAVO, M. A. 2010. Rescue immunosuppression with mammalian target of rapamycin inhibitor drugs in liver transplantation. *Transplant Proc,* 42, 641-3.

MATHISON, R., DAVISON, J. S. & BEFUS, A. D. 1994. Neuroendocrine regulation of inflammation and tissue repair by submandibular gland factors. *Immunology today,* 15, 527-532.

MATSUMOTO, S., OKUMURA, K., OGATA, A., HISATOMI, Y., SATO, A., HATTORI, K., MATSUMOTO, M., KAJI, Y., TAKAHASHI, M., YAMAMOTO, T., NAKAMURA, K. & ENDO, F. 2007. Isolation of tissue progenitor cells from duct-ligated salivary glands of swine. *Cloning Stem Cells,* 9, 176-90.

MATSUO, R., YAMAUCHI, Y. & MORIMOTO, T. 1997. Role of submandibular and sublingual saliva in maintenance of taste sensitivity recorded in the chorda tympani of rats. *The Journal of physiology,* 498 (Pt 3), 797-807.

MAUTE, L., WICHT, J. & BERGMANN, L. 2015. The Dual PI3K/mTOR Inhibitor NVP-BEZ235 Enhances the Antitumoral Activity of Gemcitabine in Human Pancreatic Cancer Cell Lines. *J Integr Oncol,* 4, 2.

MCCARTNEY-FRANCIS, N. L., MIZEL, D. E., REDMAN, R. S., FRAZIER-JESSEN, M., PANEK, R. B., KULKARNI, A. B., WARD, J. M., MCCARTHY, J. B. & WAHL, S. M. 1996. Autoimmune Sjogren's-like lesions in salivary glands of TGF-beta1-deficient mice are inhibited by adhesion-blocking peptides. *Journal of immunology,* 157, 1306-12.

MCDANIEL, M. L., MARSHALL, C. A., PAPPAN, K. L. & KWON, G. 2002. Metabolic and autocrine regulation of the mammalian target of rapamycin by pancreatic beta-cells. *Diabetes,* 51, 2877-85.

MCKENNA, R. J. 1984. Tumors of the Major and Minor Salivary Glands. *CA A Cancer Journal for Clinicians, 34, 24-39.*

MCTAGGART, R. A., GOTTLIEB, D., BROOKS, J., BACCHETTI, P., ROBERTS, J. P., TOMLANOVICH, S. & FENG, S. 2003. Sirolimus prolongs recovery from delayed graft function after cadaveric renal transplantation. *American Journal of Transplantation,* 3, 416-423.

MENDOZA, M. C., ER, E. E. & BLENIS, J. 2011. The Ras-ERK and PI3K-mTOR pathways: cross-talk and compensation. *Trends in biochemical sciences,* 36, 320-8.

MIGUEL, M. C., ANDRADE, E. S., TAGA, R., PINTO, L. P. & SOUZA, L. B. 2002. Hyperplasia of myoepithelial cells expressing calponin during atrophy of the rat parotid gland induced by duct ligation. *Histochem J,* 34, 499-506.

MILLER, R. A., HARRISON, D. E., ASTLE, C., BAUR, J. A., BOYD, A. R., DE CABO, R., FERNANDEZ, E., FLURKEY, K., JAVORS, M. A. & NELSON, J. F. 2010. Rapamycin, but not resveratrol or simvastatin, extends life span of genetically heterogeneous mice. *The Journals of Gerontology Series A: Biological Sciences and Medical Sciences*, glq178.

MIMURA, T., YAMAGAMI, S. & AMANO, S. 2013. Corneal endothelial regeneration and tissue engineering. *Progress in retinal and eye research,* 35, 1-17.

MIOSGE, N., QUONDAMATTEO, F., KLENCZAR, C. & HERKEN, R. 2000. Nidogen-1. Expression and ultrastructural localization during the onset of mesoderm formation in the early mouse embryo. *The journal of histochemistry and cytochemistry : official journal of the Histochemistry Society,* 48, 229-38.

MIRELS, L. & GIRARD, L. R. 1993. Molecular cloning of developmentally regulated neonatal rat submandibular gland proteins. *Critical reviews in oral biology and medicine : an official publication of the American Association of Oral Biologists,* 4, 525-30.

MIRELS, L., HAND, A. R. & BRANIN, H. J. 1998. Expression of gross cystic disease fluid protein-15/prolactininducible protein in rat salivary glands. *Journal of Histochemistry & Cytochemistry,* 46, 1061-1071.

MISUNO, K., TRAN, S. D., KHALILI, S., HUANG, J., LIU, Y. & HU, S. 2014. Quantitative analysis of protein and gene expression in salivary glands of Sjogren's-like disease NOD mice treated by bone marrow soup. *PloS one,* 9, e87158.

MIZUSHIMA, N. & YOSHIMORI, T. 2007. How to interpret LC3 immunoblotting. *Autophagy,* 3, 542-545.

MIZUSHIMA, N., YOSHIMORI, T. & LEVINE, B. 2010. Methods in mammalian autophagy research. *Cell,* 140, 313-26.

MOHAMMADI, M., SCHLESSINGER, J. & HUBBARD, S. R. 1996. Structure of the FGF receptor tyrosine kinase domain reveals a novel autoinhibitory mechanism. *Cell,* 86, 577-87.

MONTERO, J. C., CHEN, X., OCANA, A. & PANDIELLA, A. 2012. Predominance of mTORC1 over mTORC2 in the regulation of proliferation of ovarian cancer cells: therapeutic implications. *Molecular cancer therapeutics,* 11, 1342-1352.

MOON DU, G., LEE, S. E., OH, M. M., LEE, S. C., JEONG, S. J., HONG, S. K., YOON, C. Y., BYUN, S. S., PARK, H. S. & CHEON, J. 2014. NVP-BEZ235, a dual PI3K/mTOR inhibitor synergistically potentiates the antitumor effects of cisplatin in bladder cancer cells. *International journal of oncology,* 45, 1027-35.

MOORMAN, N. J. & SHENK, T. 2010. Rapamycin-resistant mTORC1 kinase activity is required for herpesvirus replication. *Journal of virology,* 84, 5260-5269.

MORGAN-BATHKE, M., HARRIS, Z. I., ARNETT, D. G., KLEIN, R. R., BURD, R., ANN, D. K. & LIMESAND, K. H. 2014. The Rapalogue, CCI-779,

improves salivary gland function following radiation. *PloS one,* 9, e113183.
MOSLEY, J. D., POIRIER, J. T., SEACHRIST, D. D., LANDIS, M. D. & KERI, R. A. 2007. Rapamycin inhibits multiple stages of c-Neu/ErbB2 induced tumor progression in a transgenic mouse model of HER2-positive breast cancer. *Molecular cancer therapeutics,* 6, 2188-97.
MOTHE-SATNEY, I., BRUNN, G. J., MCMAHON, L. P., CAPALDO, C. T., ABRAHAM, R. T. & LAWRENCE, J. C. 2000. Mammalian target of rapamycin-dependent phosphorylation of PHAS-I in four (S/T) P sites detected by phospho-specific antibodies. *Journal of Biological Chemistry,* 275, 33836-33843.
MUELLER, M. A., BEUTNER, F., TEUPSER, D., CEGLAREK, U. & THIERY, J. 2008. Prevention of atherosclerosis by the mTOR inhibitor everolimus in LDLR-/- mice despite severe hypercholesterolemia. *Atherosclerosis,* 198, 39-48.
MUNGER, B. L. 1964. Histochemical studies on seromucous and mucous secreting cells of human salivary glands. *American Journal of Anatomy,* 115, 411-429.
MURAKAMI, M., ICHISAKA, T., MAEDA, M., OSHIRO, N., HARA, K., EDENHOFER, F., KIYAMA, H., YONEZAWA, K. & YAMANAKA, S. 2004. mTOR is essential for growth and proliferation in early mouse embryos and embryonic stem cells. *Molecular and cellular biology,* 24, 6710-6718.
MYERS, E. N. & FERRIS, R. L. 2007. *Salivary gland disorders,* Berlin ; [London], Springer.
NAGLER, R., MARMARY, Y., KRAUSZ, Y., CHISIN, R., MARKITZIU, A. & NAGLER, A. 1996. Major salivary gland dysfunction in human acute and chronic graft-versus-host disease (GVHD). *Bone marrow transplantation,* 17, 219-24.
NAGLER, R. M. 2004. Salivary glands and the aging process: mechanistic aspects, health-status and medicinal-efficacy monitoring. *Biogerontology,* 5, 223-33.
NAKASHIMA, A., TANIMURA-ITO, K., OSHIRO, N., EGUCHI, S., MIYAMOTO, T., MOMONAMI, A., KAMADA, S., YONEZAWA, K. & KIKKAWA, U. 2013. A positive role of mammalian Tip41-like protein, TIPRL, in the amino-acid dependent mTORC1-signaling pathway through interaction with PP2A. *FEBS letters,* 587, 2924-2929.
NANCI, A. & TEN CATE, A. R. 2012. *Ten Cate's oral histology : development, structure, and function,* St. Louis, Mo., Mosby Elsevier.

NASHIDA, T., YOSHIE, S., HAGA-TSUJIMURA, M., IMAI, A. & SHIMOMURA, H. 2013. Atrophy of myoepithelial cells in parotid glands of diabetic mice; detection using skeletal muscle actin, a novel marker. *FEBS open bio,* 3, 130-4.

NELSON, J., MANZELLA, K. & BAKER, O. J. 2013. Current cell models for bioengineering a salivary gland: a mini-review of emerging technologies. *Oral diseases,* 19, 236-44.

NESHAT, M. S., MELLINGHOFF, I. K., TRAN, C., STILES, B., THOMAS, G., PETERSEN, R., FROST, P., GIBBONS, J. J., WU, H. & SAWYERS, C. L. 2001. Enhanced sensitivity of PTEN-deficient tumors to inhibition of FRAP/mTOR. *Proceedings of the National Academy of Sciences of the United States of America,* 98, 10314-9.

NEXO, E., HANSEN, M. & KONRADSEN, L. 1988. Human salivary epidermal growth factor, haptocorrin and amylase before and after prolonged exercise. *Scandinavian journal of clinical & laboratory investigation,* 48, 269-273.

NEXO, E., HANSEN, M., POULSEN, S. S. & OLSEN, P. S. 1985. Characterization and immunohistochemical localization of rat salivary cobalamin-binding protein and comparison with human salivary haptocorrin. *Biochimica et biophysica acta,* 838, 264-9.

NODA, T. & OHSUMI, Y. 1998. Tor, a phosphatidylinositol kinase homologue, controls autophagy in yeast. *Journal of Biological Chemistry,* 273, 3963-3966.

NORBERG, L. E., ABOK, K. & LUNDQUIST, P. G. 1988. Effects of ligation and irradiation on the submaxillary glands in rats. *Acta oto-laryngologica,* 105, 181-92.

NUTTING, C. M., MORDEN, J. P., HARRINGTON, K. J., URBANO, T. G., BHIDE, S. A., CLARK, C., MILES, E. A., MIAH, A. B., NEWBOLD, K., TANAY, M., ADAB, F., JEFFERIES, S. J., SCRASE, C., YAP, B. K., A'HERN, R. P., SYDENHAM, M. A., EMSON, M. & HALL, E. 2011. Parotid-sparing intensity modulated versus conventional radiotherapy in head and neck cancer (PARSPORT): a phase 3 multicentre randomised controlled trial. *The Lancet. Oncology,* 12, 127-36.

NYFELER, B., BERGMAN, P., TRIANTAFELLOW, E., WILSON, C. J., ZHU, Y., RADETICH, B., FINAN, P. M., KLIONSKY, D. J. & MURPHY, L. O. 2011. Relieving autophagy and 4EBP1 from rapamycin resistance. *Molecular and cellular biology,* 31, 2867-76.

OHSAKI, Y., SUZUKI, M., SHINOHARA, Y. & FUJIMOTO, T. 2010. Lysosomal accumulation of mTOR is enhanced by rapamycin. *Histochemistry and cell biology,* 134, 537-544.

OLDERSHAW, R. A. 2012. Cell sources for the regeneration of articular cartilage: the past, the horizon and the future. *International journal of experimental pathology,* 93, 389-400.

OLIVER, C., AUTH, R. E. & HAND, A. R. 1979. Formation and fate of ethionine-induced cytoplasmic crystalloids in rat parotid acinar cells. *Am J Anat,* 155, 185-99.

OLSEN, J. V., ONG, S. E. & MANN, M. 2004. Trypsin cleaves exclusively C-terminal to arginine and lysine residues. *Molecular & cellular proteomics : MCP,* 3, 608-14.

OSAILAN, S. M., PROCTOR, G. B., CARPENTER, G. H., PATERSON, K. L. & MCGURK, M. 2006a. Recovery of rat submandibular salivary gland function following removal of obstruction: a sialometrical and sialochemical study. *International journal of experimental pathology,* 87, 411-23.

OSAILAN, S. M., PROCTOR, G. B., MCGURK, M. & PATERSON, K. L. 2006b. Intraoral duct ligation without inclusion of the parasympathetic nerve supply induces rat submandibular gland atrophy. *International journal of experimental pathology,* 87, 41-48.

OSTERBERG, T., BIRKHED, D., JOHANSSON, C. & SVANBORG, A. 1992. Longitudinal study of stimulated whole saliva in an elderly population. *Scandinavian journal of dental research,* 100, 340-5.

PALAMARCHUK, A., EFANOV, A., MAXIMOV, V., AQEILAN, R. I., CROCE, C. M. & PEKARSKY, Y. 2005. Akt phosphorylates and regulates Pdcd4 tumor suppressor protein. *Cancer research,* 65, 11282-6.

PAN, Y., BAI, C. B., JOYNER, A. L. & WANG, B. 2006. Sonic hedgehog signaling regulates Gli2 transcriptional activity by suppressing its processing and degradation. *Molecular and cellular biology,* 26, 3365-77.

PARK, K. K., LIU, K., HU, Y., SMITH, P. D., WANG, C., CAI, B., XU, B., CONNOLLY, L., KRAMVIS, I., SAHIN, M. & HE, Z. 2008. Promoting axon regeneration in the adult CNS by modulation of the PTEN/mTOR pathway. *Science,* 322, 963-6.

PARSYAN, A. 2014. *Translation and its regulation in cancer biology and medicine,* Amsterdam, Springer.

PATEL, V. N., REBUSTINI, I. T. & HOFFMAN, M. P. 2006. Salivary gland branching morphogenesis. *Differentiation; research in biological diversity,* 74, 349-64.

PATURSKY-POLISCHUK, I., STOLOVICH-RAIN, M., HAUSNER-HANOCHI, M., KASIR, J., CYBULSKI, N., AVRUCH, J., RUEGG, M. A., HALL, M. N. & MEYUHAS, O. 2009. The TSC-mTOR pathway mediates translational activation of TOP mRNAs by insulin

largely in a raptor-or rictor-independent manner. *Molecular and cellular biology,* 29, 640-649.

PAUSE, A., BELSHAM, G. J., GINGRAS, A. C., DONZE, O., LIN, T. A., LAWRENCE, J. C., JR. & SONENBERG, N. 1994. Insulin-dependent stimulation of protein synthesis by phosphorylation of a regulator of 5'-cap function. *Nature,* 371, 762-7.

PAZDUR, R., WAGMAN, L. D. & CAMPHAUSEN, K. A. 2010. *Cancer management a multidisciplinary approach : medical, surgical & radiation oncology,* Lawrence, KS, CMPMedica.

PEDERSEN, A. M., REIBEL, J., NORDGARDEN, H., BERGEM, H. O., JENSEN, J. L. & NAUNTOFTE, B. 1999. Primary Sjogren's syndrome: salivary gland function and clinical oral findings. *Oral Dis,* 5, 128-38.

PERRY, J. & KLECKNER, N. 2003. The ATRs, ATMs, and TORs are giant HEAT repeat proteins. *Cell,* 112, 151-5.

PETERSON, R. T. & SCHREIBER, S. L. 1998. Translation control: connecting mitogens and the ribosome. *Current biology : CB,* 8, R248-50.

PFESTROFF, A., MULLER, F., LIBRIZZI, D., EIVAZI, B., BEHE, M., HOEFFKEN, H., BEHR, T. M. & TEYMOORTASH, A. 2010. Scintigraphic assessment of salivary gland function in a rat model. *In vivo,* 24, 681-5.

PHAM, F. H., SUGDEN, P. H. & CLERK, A. 2000. Regulation of protein kinase B and 4E-BP1 by oxidative stress in cardiac myocytes. *Circulation research,* 86, 1252-1258.

PIHA-PAUL, S. A., COHEN, P. R. & KURZROCK, R. 2011. Salivary duct carcinoma: targeting the phosphatidylinositol 3-kinase pathway by blocking mammalian target of rapamycin with temsirolimus. *Journal of clinical oncology : official journal of the American Society of Clinical Oncology,* 29, e727-30.

PINKSTAFF, C. A. 1993. Serous, seromucous, and special serous cells in salivary glands. *Microscopy research and technique,* 26, 21-31.

PRINGLE, S., VAN OS, R. & COPPES, R. P. 2013. Concise review: Adult salivary gland stem cells and a potential therapy for xerostomia. *Stem cells,* 31, 613-9.

PROCTOR, G. B. & CARPENTER, G. H. 2007. Regulation of salivary gland function by autonomic nerves. *Autonomic neuroscience : basic & clinical,* 133, 3-18.

PULLEN, N., DENNIS, P. B., ANDJELKOVIC, M., DUFNER, A., KOZMA, S. C., HEMMINGS, B. A. & THOMAS, G. 1998. Phosphorylation and activation of p70s6k by PDK1. *Science,* 279, 707-10.

PYO, J. O., JANG, M. H., KWON, Y. K., LEE, H. J., JUN, J. I., WOO, H. N., CHO, D. H., CHOI, B., LEE, H., KIM, J. H., MIZUSHIMA, N., OSHUMI, Y. & JUNG, Y. K. 2005. Essential roles of Atg5 and FADD in autophagic cell death: dissection of autophagic cell death into vacuole formation and cell death. *The Journal of biological chemistry,* 280, 20722-9.

QWARNSTRÖM, E. & HAND, A. 1983. A granular cell at the acinar-intercalated duct junction of the rat submandibular gland. *The Anatomical Record,* 206, 181-187.

RAMSEY, P. H. 1980. Exact Type 1 Error Rates for Robustness of Student's t Test with Unequal Variances. *Journal of Educational Statistics,* 5, 337-349.

RATHMAN, W. M., VAN ZEYL, M. J., VAN DEN KEYBUS, P. A., BANK, R. A., VEERMAN, E. C. & NIEUW AMERONGEN, A. V. 1989. Isolation and characterization of three non-mucinous human salivary proteins with affinity for hydroxyapatite. *Journal de biologie buccale,* 17, 199-208.

RAUNIYAR, N., GAO, B., MCCLATCHY, D. B. & YATES, J. R., 3RD 2013. Comparison of protein expression ratios observed by sixplex and duplex TMT labeling method. *Journal of proteome research,* 12, 1031-9.

RAYNAUD, J. 1964. [Sexual Dimorphism of the Submaxillary Gland of the Shrew-Mouse (Crocidura)]. *Comptes rendus des seances de la Societe de biologie et de ses filiales,* 158, 942-7.

RAZ, E., SABA, L., HAGIWARA, M., HYGINO DE CRUZ, L. C., JR., SOM, P. M. & FATTERPEKAR, G. M. 2013. Parotid gland atrophy in patients with chronic trigeminal nerve denervation. *AJNR. American journal of neuroradiology,* 34, 860-3.

RAZEGHI, P., SHARMA, S., YING, J., LI, Y. P., STEPKOWSKI, S., REID, M. B. & TAEGTMEYER, H. 2003. Atrophic remodeling of the heart in vivo simultaneously activates pathways of protein synthesis and degradation. *Circulation,* 108, 2536-41.

RIOS-MORENO, M. J., JARAMILLO, S., DIAZ-DELGADO, M., SANCHEZ-LEON, M., TRIGO-SANCHEZ, I., PADILLO, J. P., AMERIGO, J. & GONZALEZ-CAMPORA, R. 2011. Differential activation of MAPK and PI3K/AKT/mTOR pathways and IGF1R expression in gastrointestinal stromal tumors. *Anticancer research,* 31, 3019-25.

ROUX, P. P. & TOPISIROVIC, I. 2012. Regulation of mRNA translation by signaling pathways. *Cold Spring Harbor perspectives in biology,* 4, a012252.

SABATINI, D. M., BARROW, R. K., BLACKSHAW, S., BURNETT, P. E., LAI, M. M., FIELD, M. E., BAHR, B. A., KIRSCH, J., BETZ, H. & SNYDER, S. H. 1999. Interaction of RAFT1 with gephyrin required for rapamycin-sensitive signaling. *Science,* 284**,** 1161-1164.

SAITOH, M., PULLEN, N., BRENNAN, P., CANTRELL, D., DENNIS, P. B. & THOMAS, G. 2002. Regulation of an activated S6 kinase 1 variant reveals a novel mammalian target of rapamycin phosphorylation site. *The Journal of biological chemistry,* 277**,** 20104-12.

SANTOS, R. X., CORREIA, S. C., CARDOSO, S., CARVALHO, C., SANTOS, M. S. & MOREIRA, P. I. 2011. Effects of rapamycin and TOR on aging and memory: implications for Alzheimer's disease. *Journal of neurochemistry,* 117**,** 927-36.

SAPIR, Y., KRYUKOV, O. & COHEN, S. 2011. Integration of multiple cell-matrix interactions into alginate scaffolds for promoting cardiac tissue regeneration. *Biomaterials,* 32**,** 1838-1847.

SARBASSOV, D. D., ALI, S. M., KIM, D.-H., GUERTIN, D. A., LATEK, R. R., ERDJUMENT-BROMAGE, H., TEMPST, P. & SABATINI, D. M. 2004. Rictor, a novel binding partner of mTOR, defines a rapamycin-insensitive and raptor-independent pathway that regulates the cytoskeleton. *Current Biology,* 14**,** 1296-1302.

SARBASSOV, D. D., ALI, S. M., SENGUPTA, S., SHEEN, J. H., HSU, P. P., BAGLEY, A. F., MARKHARD, A. L. & SABATINI, D. M. 2006. Prolonged rapamycin treatment inhibits mTORC2 assembly and Akt/PKB. *Molecular cell,* 22**,** 159-68.

SARBASSOV, D. D., GUERTIN, D. A., ALI, S. M. & SABATINI, D. M. 2005. Phosphorylation and regulation of Akt/PKB by the rictor-mTOR complex. *Science,* 307**,** 1098-101.

SATO, T., NAKASHIMA, A., GUO, L., COFFMAN, K. & TAMANOI, F. 2010. Single amino-acid changes that confer constitutive activation of mTOR are discovered in human cancer. *Oncogene,* 29**,** 2746-2752.

SAWAKI, K., SHINOMIYA, T., OKUBO, M., TSUKAGOSHI, E., OGANE, M., MATSUURA, M., YOSHIKAWA, M. & KAWAGUCHI, M. 2011. Proteomic analysis of lipopolysaccharide-treated submandibular gland in rat. *The Bulletin of Tokyo Dental College,* 52**,** 31-7.

SCHAFFER, S. W. & SULEIMAN, M. S. 2007. *Mitochondria the dynamic organelle,* New York, Springer.

SCHEFFLER, J. M., SPARBER, F., TRIPP, C. H., HERRMANN, C., HUMENBERGER, A., BLITZ, J., ROMANI, N., STOITZNER, P. & HUBER, L. A. 2014. LAMTOR2 regulates dendritic cell homeostasis through FLT3-dependent mTOR signalling. *Nature communications,* 5.

SCHENKELS, L. C., SCHALLER, J., WALGREEN-WETERINGS, E., SCHADEE-EESTERMANS, I. L., VEERMAN, E. C. & NIEUW AMERONGEN, A. V. 1994. Identity of human extra parotid glycoprotein (EP-GP) with secretory actin binding protein (SABP) and its biological properties. *Biological chemistry Hoppe-Seyler,* 375, 609-15.

SCHEPER, G. C., MORRICE, N. A., KLEIJN, M. & PROUD, C. G. 2001. The mitogen-activated protein kinase signal-integrating kinase Mnk2 is a eukaryotic initiation factor 4E kinase with high levels of basal activity in mammalian cells. *Molecular and cellular biology,* 21, 743-754.

SCHLESINGER, D. H., HAY, D. I. & LEVINE, M. J. 1989. Complete primary structure of statherin, a potent inhibitor of calcium phosphate precipitation, from the saliva of the monkey, Macaca arctoides. *International journal of peptide and protein research,* 34, 374-80.

SCHMELZLE, T. & HALL, M. N. 2000. TOR, a central controller of cell growth. *Cell,* 103, 253-62.

SCOTT, J. 1977. Quantitative age changes in the histological structure of human submandibular salivary glands. *Archives of oral biology,* 22, 221-227.

SCOTT, J. 1980. Qualitative and quantitative observations on the histology of human labial salivary glands obtained post mortem. *Journal de biologie buccale,* 8, 187-200.

SCOTT, J. & GUNN, D. L. 1991. A comparative quantitative histological investigation of atrophic changes in the major salivary glands of liquid-fed rats. *Archives of oral biology,* 36, 855-7.

SCOTT, J., LIU, P. & SMITH, P. 1999. Morphological and functional characteristics of acinar atrophy and recovery in the duct-ligated parotid gland of the rat. *Journal of dental research,* 78, 1711-1719.

SERR, F., LAUER, H., ARMANN, B., LUDWIG, S., THIERY, J., FIEDLER, M., CEGLAREK, U., TANNAPFEL, A., UHLMANN, D., HAUSS, J. & WITZIGMANN, H. 2007. Sirolimus improves early microcirculation, but impairs regeneration after pancreatic ischemia-reperfusion injury. *Am J Transplant,* 7, 48-56.

SERRA, V., MARKMAN, B., SCALTRITI, M., EICHHORN, P. J., VALERO, V., GUZMAN, M., BOTERO, M. L., LLONCH, E., ATZORI, F., DI COSIMO, S., MAIRA, M., GARCIA-ECHEVERRIA, C., PARRA, J. L., ARRIBAS, J. & BASELGA, J. 2008. NVP-BEZ235, a dual PI3K/mTOR inhibitor, prevents PI3K signaling and inhibits the growth of cancer cells with activating PI3K mutations. *Cancer research,* 68, 8022-30.

SHAN, Z., LI, J., ZHENG, C., LIU, X., FAN, Z., ZHANG, C., GOLDSMITH, C. M., WELLNER, R. B., BAUM, B. J. & WANG, S. 2005. Increased fluid secretion after adenoviral-mediated transfer of the human aquaporin-1 cDNA to irradiated miniature pig parotid glands. *Molecular therapy : the journal of the American Society of Gene Therapy,* 11, 444-51.

SHEN, S., KEPP, O., MICHAUD, M., MARTINS, I., MINOUX, H., METIVIER, D., MAIURI, M., KROEMER, R. & KROEMER, G. 2011. Association and dissociation of autophagy, apoptosis and necrosis by systematic chemical study. *Oncogene,* 30, 4544-4556.

SHIBA, R., HAMADA, T. & KAWAKATSU, K. 1972. Histochemical and electron microscopical studies on the effect of duct ligation of rat salivary glands. *Archives of oral biology,* 17, 299-309.

SHIMA, H., PENDE, M., CHEN, Y., FUMAGALLI, S., THOMAS, G. & KOZMA, S. C. 1998. Disruption of the p70s6k/p85s6k gene reveals a small mouse phenotype and a new functional S6 kinase. *The EMBO journal,* 17, 6649-6659.

SHINTANI, T. & KLIONSKY, D. J. 2004. Autophagy in health and disease: a double-edged sword. *Science,* 306, 990-995.

SHVETS, E., FASS, E. & ELAZAR, Z. 2008. Utilizing flow cytometry to monitor autophagy in living mammalian cells. *Autophagy,* 4, 621-8.

SILVER, N., COTRONEO, E., PROCTOR, G., OSAILAN, S., PATERSON, K. L. & CARPENTER, G. H. 2008. Selection of housekeeping genes for gene expression studies in the adult rat submandibular gland under normal, inflamed, atrophic and regenerative states. *BMC molecular biology,* 9, 64.

SILVER, N., PROCTOR, G. B., ARNO, M. & CARPENTER, G. H. 2010. Activation of mTOR coincides with autophagy during ligation-induced atrophy in the rat submandibular gland. *Cell death & disease,* 1, e14.

SOEFJE, S. A., KARNAD, A. & BRENNER, A. J. 2011. Common toxicities of mammalian target of rapamycin inhibitors. *Targeted oncology,* 6, 125-9.

SREEBNY, L. M. & SCHWARTZ, S. S. 1997. A reference guide to drugs and dry mouth – 2nd edition. *Gerodontology,* 14, 33-47.

STEAD, R. L. & PROUD, C. G. 2013. Rapamycin enhances eIF4E phosphorylation by activating MAP kinase-interacting kinase 2a (Mnk2a). *FEBS letters,* 587, 2623-2628.

STEINBERG, Z., MYERS, C., HEIM, V. M., LATHROP, C. A., REBUSTINI, I. T., STEWART, J. S., LARSEN, M. & HOFFMAN, M. P. 2005. FGFR2b signaling regulates ex vivo submandibular gland epithelial cell

proliferation and branching morphogenesis. *Development,* 132, 1223-1234.

STUPPERICH, E. & NEXO, E. 1991. Effect of the cobalt-N coordination on the cobamide recognition by the human vitamin B12 binding proteins intrinsic factor, transcobalamin and haptocorrin. *European journal of biochemistry / FEBS,* 199, 299-303.

SUGITO, T., KAGAMI, H., HATA, K., NISHIGUCHI, H. & UEDA, M. 2004. Transplantation of cultured salivary gland cells into an atrophic salivary gland. *Cell transplantation,* 13, 691-699.

SUMI, M., IZUMI, M., YONETSU, K. & NAKAMURA, T. 1999. The MR imaging assessment of submandibular gland sialoadenitis secondary to sialolithiasis: correlation with CT and histopathologic findings. *AJNR. American journal of neuroradiology,* 20, 1737-43.

SUMITA, Y., LIU, Y., KHALILI, S., MARIA, O. M., XIA, D., KEY, S., COTRIM, A. P., MEZEY, E. & TRAN, S. D. 2011. Bone marrow-derived cells rescue salivary gland function in mice with head and neck irradiation. *The international journal of biochemistry & cell biology,* 43, 80-7.

SUZUKI, K., MATSUMOTO, M., NAKASHIMA, M., TAKADA, K., NAKANISHI, T., OKADA, M. & OHSUZU, F. 2005. Effect of cevimeline on salivary components in patients with Sjogren syndrome. *Pharmacology,* 74, 100-5.

TABAK, L. A. 1995. In defense of the oral cavity: structure, biosynthesis, and function of salivary mucins. *Annual review of physiology,* 57, 547-64.

TAKAHASHI, S., DOMON, T., YAMAMOTO, T. & WAKITA, M. 1997. Regeneration of myoepithelial cells in rat submandibular glands after yttrium aluminium garnett laser irradiation. *International journal of experimental pathology,* 78, 91-99.

TAKAHASHI, S., GOBE, G. C., YOSHIMURA, Y., KOHGO, T., YAMAMOTO, T. & WAKITA, M. 2007. Participation of the Fas and Fas ligand systems in apoptosis during atrophy of the rat submandibular glands. *International journal of experimental pathology,* 88, 9-17.

TAKAHASHI, S., NAKAMURA, S., DOMON, T., YAMAMOTO, T. & WAKITA, M. 2005. Active participation of apoptosis and mitosis in sublingual gland regeneration of the rat following release from duct ligation. *Journal of molecular histology,* 36, 199-205.

TAKAHASHI, S., NAKAMURA, S., SHINZATO, K., DOMON, T., YAMAMOTO, T. & WAKITA, M. 2001. Apoptosis and proliferation of myoepithelial cells in atrophic rat submandibular glands. *Journal of Histochemistry & Cytochemistry,* 49, 1557-1563.

TAKAHASHI, S., NAKAMURA, S., SUZUKI, R., DOMON, T., YAMAMOTO, T. & WAKITA, M. 1999. Changing myoepithelial cell distribution during regeneration of rat parotid glands. *International journal of experimental pathology,* 80, 283-290.

TAKAHASHI, S., NAKAMURA, S., SUZUKI, R., ISLAM, N., DOMON, T., YAMAMOTO, T. & WAKITA, M. 2000. Apoptosis and mitosis of parenchymal cells in the duct-ligated rat submandibular gland. *Tissue & cell,* 32, 457-63.

TAKAHASHI, S., SCHOCH, E. & WALKER, N. I. 1998. Origin of acinar cell regeneration after atrophy of the rat parotid induced by duct obstruction. *International journal of experimental pathology,* 79, 293-301.

TAKAHASHI, S., SHINZATO, K., DOMON, T., YAMAMOTO, T. & WAKITA, M. 2003. Proliferation and distribution of myoepithelial cells during atrophy of the rat sublingual gland. *Journal of oral pathology & medicine,* 32, 90-94.

TAKAHASHI, S., SHINZATO, K., NAKAMURA, S., DOMON, T., YAMAMOTO, T. & WAKITA, M. 2004. Cell death and cell proliferation in the regeneration of atrophied rat submandibular glands after duct ligation. *Journal of oral pathology & medicine,* 33, 23-29.

TAKAI, Y., NODA, Y., SUMITOMOS, S., HIKOSAKA, N. & MORI, M. 1986. Immunohistochemical demonstration of keratin proteins in duct-ligated salivary glands of mice and rats. *Journal of oral pathology,* 15, 16-20.

TAKANO, A., USUI, I., HARUTA, T., KAWAHARA, J., UNO, T., IWATA, M. & KOBAYASHI, M. 2001. Mammalian target of rapamycin pathway regulates insulin signaling via subcellular redistribution of insulin receptor substrate 1 and integrates nutritional signals and metabolic signals of insulin. *Molecular and cellular biology,* 21, 5050-62.

TAKAYAMA, K., KAWAKAMI, Y., KOBAYASHI, M., GRECO, N., CUMMINS, J. H., MATSUSHITA, T., KURODA, R., KUROSAKA, M., FU, F. H. & HUARD, J. 2014. Local intra-articular injection of rapamycin delays articular cartilage degeneration in a murine model of osteoarthritis. *Arthritis Res Ther,* 16, 482.

TAKEHARA, S., YANAGISHITA, M., PODYMA-INOUE, K. A. & KAWAGUCHI, Y. 2013. Degradation of MUC7 and MUC5B in human saliva. *PloS one,* 8, e69059.

TAMARIN, A. 1971a. Submaxillary gland recovery from obstruction. I. Overall changes and electron microscopic alterations of granular duct cells. *Journal of ultrastructure research,* 34, 276-87.

TAMARIN, A. 1971b. Submaxillary gland recovery from obstruction. II. Electron microscopic alterations of acinar cells. *Journal of ultrastructure research,* 34, 288-302.

TANG, K. & LING, M.-T. 2014. Targeting drug-resistant prostate cancer with dual PI3K/MTOR inhibition. *Current medicinal chemistry,* 21, 3048-3056.

TANIDA, I., UENO, T. & KOMINAMI, E. 2008. LC3 and Autophagy. *Methods in molecular biology,* 445, 77-88.

TEE, A. R., MANNING, B. D., ROUX, P. P., CANTLEY, L. C. & BLENIS, J. 2003. Tuberous sclerosis complex gene products, Tuberin and Hamartin, control mTOR signaling by acting as a GTPase-activating protein complex toward Rheb. *Current Biology,* 13, 1259-1268.

TENNANT, D. A., DURAN, R. V. & GOTTLIEB, E. 2010. Targeting metabolic transformation for cancer therapy. *Nature reviews. Cancer,* 10, 267-77.

TEYMOORTASH, A., TIEMANN, M., SCHRADER, C., HARTMANN, O. & WERNER, J. A. 2003. Transforming growth factor beta in chronic obstructive sialadenitis of human submandibular gland. *Archives of oral biology,* 48, 111-6.

THOMSON, A. W., TURNQUIST, H. R. & RAIMONDI, G. 2009. Immunoregulatory functions of mTOR inhibition. *Nature reviews. Immunology,* 9, 324-37.

THOREEN, C. C., CHANTRANUPONG, L., KEYS, H. R., WANG, T., GRAY, N. S. & SABATINI, D. M. 2012. A unifying model for mTORC1-mediated regulation of mRNA translation. *Nature,* 485, 109-113.

THOREEN, C. C., KANG, S. A., CHANG, J. W., LIU, Q., ZHANG, J., GAO, Y., REICHLING, L. J., SIM, T., SABATINI, D. M. & GRAY, N. S. 2009. An ATP-competitive mammalian target of rapamycin inhibitor reveals rapamycin-resistant functions of mTORC1. *The Journal of biological chemistry,* 284, 8023-32.

THOREEN, C. C. & SABATINI, D. M. 2009. Rapamycin inhibits mTORC1, but not completely. *Autophagy,* 5, 725-726.

TIRADO, O. M., MATEO-LOZANO, S., SANDERS, S., DETTIN, L. E. & NOTARIO, V. 2003. The PCPH oncoprotein antagonizes the proapoptotic role of the mammalian target of rapamycin in the response of normal fibroblasts to ionizing radiation. *Cancer research,* 63, 6290-6298.

TUCCI, P. 2012. Caloric restriction: is mammalian life extension linked to p53? *Aging (Albany NY),* 4, 525.

TUCKER, A. S. 2007. Salivary gland development. *Seminars in cell & developmental biology,* 18, 237-44.

TUCKER, A. S. & MILETICH, I. 2010. *Salivary glands : development, adaptations, and disease,* Basel; New York, Karger.

UM, S. H., FRIGERIO, F., WATANABE, M., PICARD, F. D. R., JOAQUIN, M., STICKER, M., FUMAGALLI, S., ALLEGRINI, P. R., KOZMA, S. C. & AUWERX, J. 2004. Absence of S6K1 protects against age-and diet-induced obesity while enhancing insulin sensitivity. *Nature,* 431, 200-205.

VAN DER REIJDEN, W. A., VAN DER KWAAK, J. S., VEERMAN, E. C. & NIEUW AMERONGEN, A. V. 1996. Analysis of the concentration and output of whole salivary constituents in patients with Sjogren's syndrome. *European journal of oral sciences,* 104, 335-40.

VAN VALCKENBORGH, I C. 2005 Salivary and mammary gland tumorigenesis in PLAG1 transgenic mice. Leuven, Leuven University Press.

VISSINK, A., JANSMA, J., SPIJKERVET, F. K., BURLAGE, F. R. & COPPES, R. P. 2003. Oral sequelae of head and neck radiotherapy. *Critical reviews in oral biology and medicine : an official publication of the American Association of Oral Biologists,* 14, 199-212.

VISSINK, A., MITCHELL, J. B., BAUM, B. J., LIMESAND, K. H., JENSEN, S. B., FOX, P. C., ELTING, L. S., LANGENDIJK, J. A., COPPES, R. P. & REYLAND, M. E. 2010. Clinical management of salivary gland hypofunction and xerostomia in head-and-neck cancer patients: successes and barriers. *Int J Radiat Oncol Biol Phys,* 78, 983-91.

VISSINK, A., SPIJKERVET, F. K. & VAN NIEUW AMERONGEN, A. 1996. Aging and saliva: a review of the literature. *Special care in dentistry : official publication of the American Association of Hospital Dentists, the Academy of Dentistry for the Handicapped, and the American Society for Geriatric Dentistry,* 16, 95-103.

WALKER, N. I. & GOBE, G. C. 1987. Cell death and cell proliferation during atrophy of the rat parotid gland induced by duct obstruction. *The Journal of pathology,* 153, 333-44.

WALSH, D., PEREZ, C., NOTARY, J. & MOHR, I. 2005. Regulation of the translation initiation factor eIF4F by multiple mechanisms in human cytomegalovirus-infected cells. *Journal of virology,* 79, 8057-64.

WALZ, A., STUHLER, K., WATTENBERG, A., HAWRANKE, E., MEYER, H. E., SCHMALZ, G., BLUGGEL, M. & RUHL, S. 2006. Proteome analysis of glandular parotid and submandibular-sublingual saliva in comparison to whole human saliva by two-dimensional gel electrophoresis. *Proteomics,* 6, 1631-9.

WAN, K. F., SAMBI, B. S., FRAME, M., TATE, R. & PYNE, N. J. 2001. The inhibitory gamma subunit of the type 6 retinal cyclic guanosine monophosphate phosphodiesterase is a novel intermediate regulating p42/p44 mitogen-activated protein kinase signaling in human embryonic kidney 293 cells. *Journal of Biological Chemistry,* 276, 37802-37808.

WANG, H., ZHANG, Q., WEN, Q., ZHENG, Y., LAZAROVICI, P., JIANG, H., LIN, J. & ZHENG, W. 2012. Proline-rich Akt substrate of 40kDa (PRAS40): a novel downstream target of PI3k/Akt signaling pathway. *Cellular signalling,* 24, 17-24.

WANG, J., VOUTETAKIS, A., ZHENG, C. & BAUM, B. 2004. Rapamycin control of exocrine protein levels in saliva after adenoviral vector-mediated gene transfer. *Gene therapy,* 11, 729-733.

WANG, X. & PROUD, C. G. 2006. The mTOR pathway in the control of protein synthesis. *Physiology,* 21, 362-9.

WATERHOUSE, J. P., CHISHOLM, D. M., WINTER, R. B., PATEL, M. & YALE, R. S. 1973. Replacement of functional parenchymal cells by fat and connective tissue in human submandibular salivary glands: an age-related change. *Journal of oral pathology,* 2, 16-27.

WATERS, L. C., STRONG, S. L., FERLEMANN, E., OKA, O., MUSKETT, F. W., VEVERKA, V., BANERJEE, S., SCHMEDT, T., HENRY, A. J., KLEMPNAUER, K. H. & CARR, M. D. 2011. Structure of the tandem MA-3 region of Pdcd4 protein and characterization of its interactions with eIF4A and eIF4G: molecular mechanisms of a tumor suppressor. *The Journal of biological chemistry,* 286, 17270-80.

WITHERS, D. J., OUWENS, D. M., NAVE, B. T., VAN DER ZON, G. C., ALARCON, C. M., CARDENAS, M. E., HEITMAN, J., MAASSEN, J. A. & SHEPHERD, P. R. 1997. Expression, enzyme activity, and subcellular localization of mammalian target of rapamycin in insulin-responsive cells. *Biochemical and biophysical research communications,* 241, 704-709.

WITT, R. L. 2005. *Salivary gland diseases : surgical and medical management,* New York, Thieme.

WU, L., BIRLE, D. C. & TANNOCK, I. F. 2005. Effects of the mammalian target of rapamycin inhibitor CCI-779 used alone or with chemotherapy on human prostate cancer cells and xenografts. *Cancer Research,* 65, 2825-2831.

WULLSCHLEGER, S., LOEWITH, R. & HALL, M. N. 2006. TOR signaling in growth and metabolism. *Cell,* 124, 471-84.

XI, L., ZHU, S. G., HOBBS, D. C. & KUKREJA, R. C. 2011. Identification of protein targets underlying dietary nitrate-induced protection

against doxorubicin cardiotoxicity. *Journal of cellular and molecular medicine,* 15, 2512-24.

XIE, X., WHITE, E. P. & MEHNERT, J. M. 2013. Coordinate autophagy and mTOR pathway inhibition enhances cell death in melanoma. *PloS one,* 8, e55096.

XU, G., KWON, G., CRUZ, W. S., MARSHALL, C. A. & MCDANIEL, M. L. 2001. Metabolic regulation by leucine of translation initiation through the mTOR-signaling pathway by pancreatic Œ≤-cells. *Diabetes,* 50, 353-360.

YANG, H.-S., JANSEN, A. P., KOMAR, A. A., ZHENG, X., MERRICK, W. C., COSTES, S., LOCKETT, S. J., SONENBERG, N. & COLBURN, N. H. 2003. The transformation suppressor Pdcd4 is a novel eukaryotic translation initiation factor 4A binding protein that inhibits translation. *Molecular and cellular biology,* 23, 26-37.

YANG, L., MIAO, L., LIANG, F., HUANG, H., TENG, X., LI, S., NURIDDINOV, J., SELZER, M. E. & HU, Y. 2014. The mTORC1 effectors S6K1 and 4E-BP play different roles in CNS axon regeneration. *Nat Commun,* 5, 5416.

YANG, Q., INOKI, K., IKENOUE, T. & GUAN, K.-L. 2006. Identification of Sin1 as an essential TORC2 component required for complex formation and kinase activity. *Genes & development,* 20, 2820-2832.

YASUMIZU, Y., MIYAJIMA, A., KOSAKA, T., MIYAZAKI, Y., KIKUCHI, E. & OYA, M. 2014. Dual PI3K/mTOR inhibitor NVP-BEZ235 sensitizes docetaxel in castration resistant prostate cancer. *The Journal of urology,* 191, 227-34.

YOO, C., VINES, J. B., ALEXANDER, G., MURDOCK, K., HWANG, P. & JUN, H.-W. 2014. Adult stem cells and tissue engineering strategies for salivary gland regeneration: a review. *Biomaterials Research,* 18, 9.

YU, G. T., BU, L. L., ZHAO, Y. Y., LIU, B., ZHANG, W. F., ZHAO, Y. F., ZHANG, L. & SUN, Z. J. 2014. Inhibition of mTOR reduce Stat3 and PAI related angiogenesis in salivary gland adenoid cystic carcinoma. *American journal of cancer research,* 4, 764-75.

ZAYTSEVA, Y. Y., VALENTINO, J. D., GULHATI, P. & EVERS, B. M. 2012. mTOR inhibitors in cancer therapy. *Cancer letters,* 319, 1-7.

ZEILSTRA, L. J., VISSINK, A., KONINGS, A. W. & COPPES, R. P. 2000. Radiation induced cell loss in rat submandibular gland and its relation to gland function. *Int J Radiat Biol,* 76, 419-29.

ZHANG, H., BAJRASZEWSKI, N., WU, E., WANG, H., MOSEMAN, A. P., DABORA, S. L., GRIFFIN, J. D. & KWIATKOWSKI, D. J. 2007.

PDGFRs are critical for PI3K/Akt activation and negatively regulated by mTOR. *Journal of Clinical Investigation,* 117, 730.
ZHANG, J. & ROKOSH, G. 2007. *Cardiac gene expression methods and protocols,* Totowa, N.J., Humana Press.
ZHANG, N. N., HUANG, G. L., HAN, Q. B., HU, X., YI, J., YAO, L. & HE, Y. 2013. Functional regeneration of irradiated salivary glands with human amniotic epithelial cells transplantation. *International journal of clinical and experimental pathology,* 6, 2039-47.
ZINZEN, K. M., HAND, A. R., YANKOVA, M., BALL, W. D. & MIRELS, L. 2004. Molecular cloning and characterization of the neonatal rat and mouse submandibular gland protein SMGC. *Gene,* 334, 23-33.
ZONCU, R., EFEYAN, A. & SABATINI, D. M. 2011. mTOR: from growth signal integration to cancer, diabetes and ageing. *Nature reviews. Molecular cell biology,* 12, 21-35.